

**PREPARATION AND CHARACTERIZATION OF  
HEMODIALYSIS MEMBRANES WITH  
IMPROVED BIOCOMPATIBILITY THROUGH  
ANTICOAGULANT, ANTIOXIDANT AND  
ENZYME IMMOBILIZATION**

**A Thesis Submitted to  
the Graduate School of Engineering and Sciences of  
İzmir Institute of Technology  
in Partial Fulfillment of the Requirements for the Degree of**

**DOCTOR OF PHILOSOPHY**

**in Chemical Engineering**

**by  
Filiz YAŞAR MAHLIÇLI**

**December, 2012  
İZMİR**

We approve the thesis of **Filiz YAŞAR MAHLIÇLI**

**Examining Committee Members:**

---

**Prof. Dr. Sacide ALSOY ALTINKAYA**

Department of Chemical Engineering, İzmir Institute of Technology

---

**Prof. Dr. Serdar ÖZÇELİK**

Department of Chemistry İzmir Institute of Technology

---

**Prof. Dr. Mehmet Şengün ÖZSÖZ**

Department of Biomedical Engineering, Katip Çelebi University

---

**Assoc. Prof. Dr. Erol ŞEKER**

Department of Chemical Engineering, İzmir Institute of Technology

---

**Assoc. Prof. Dr. Volga Esmâ BULMUŞ ZAREİRE**

Department of Chemical Engineering, İzmir Institute of Technology

31 January 2013

---

**Prof. Dr. Sacide ALSOY ALTINKAYA**

Supervisor, Department of Chemical Engineering,  
İzmir Institute of Technology

---

**Prof. Dr. Fehime ÖZKAN**

Head of the Department of  
Chemical Engineering

---

**Prof. Dr. R. Tuğrul ŞENGER**

Dean of the Graduate School of  
Engineering and Sciences

## ACKNOWLEDGMENTS

At the end of my thesis, I would like to thank all those people who made this thesis possible and an unforgettable experience for me. It is difficult to overstate my gratitude to my Ph.D. supervisor, Prof. Dr. Sacide Alsoy Altinkaya, who offered her continuous advice and encouragement throughout this thesis. I express my deepest appreciation to her for the systematic guidance and great effort she put into training me in the scientific field and life as well. Like a mentor!

I want to thank my committee members, Assoc. Prof. Dr. Erol ŐEKER, Prof. Dr. Serdar ŐZŐELİK, Assoc. Prof. Dr. Volga Esmā BulmuŐ Zareie and Prof Dr. Mehmet Őengün ŐZSŐZ for their insightful comments and constructive criticism, which helped to improve the overall quality of my thesis.

I am indebted to my many student colleagues for providing a stimulating and fun environment in which to learn and grow. I am especially grateful to Senem YETGİN, Metin UZ, Őefika ŐAĐLA GÜNDOĐAN, Melda BÜYÜKŐZ, Pelin OYMACI, Bahar BaŐak PEKŐEN, Dr. Yılmaz YÜREKLİ, Őzgür YILMAZER, Paptya KANER, Őzgün DELİİSMAİL, Ferit Deniz GÜNER, Ekrem ŐZER, Bengisu MIZRAPOĐLU, Elif GÜNGÖRMÜŐ, Serenay AYTAŐ and Dr. Yasemin ERTEN KAYA.

I would like to thank Selahattin UMDU who is the donor for *in vitro* hemocompatibility tests.

Also, I would like to take this opportunity to thank Izmir Institute of Technology, Biotechnology and Bioengineering Research and Application Center, Material Research Center and specialists to provide facilities for performing the *in vitro* blood compatibility tests and SEM and AFM analyses. I also acknowledge Prof. Dr. Erhan SÜLEYMANOĐLU and Pelin TŐREN from Gazi University, Faculty of Pharmacy for XPS analysis.

I wish to thank my entire extended family for providing a loving environment for me.

Lastly, and most importantly, I wish to thank my husband, Berkan MAHLIŐLI who blessed me with a life of joy. He raised me, supported me, taught me, and loved me. To him I dedicate this thesis...

...dedicated to  
Berkan MAHLIÇLI

## ABSTRACT

### PREPARATION AND CHARACTERIZATION OF HEMODIALYSIS MEMBRANES WITH IMPROVED BIOCOMPATIBILITY THROUGH ANTICOAGULANT, ANTIOXIDANT AND ENZYME IMMOBILIZATION

The objective of this thesis is to improve blood compatibility of polysulfone (PSF) based hemodialysis membranes through generating thromboresistant and/or antioxidative surfaces with biomolecule immobilization. To create a nonthrombogenic surface, support membrane was modified with layer by layer (LBL) deposition of polyethyleneimine (PEI) and alginate (ALG) and heparin (HEP) was immobilized on the outermost surface of the assembly by blending with ALG.  $\alpha$ -lipoic acid (ALA) and superoxide dismutase (SOD)/catalase (CAT) enzyme couple were chosen to provide antioxidative properties. ALA was immobilized site-specifically to PEI deposited support membrane while SOD/CAT enzyme couple were attached both covalently and ionically on the plasma treated and PEI deposited membranes, respectively. Blending a small amount of HEP with alginate remarkably prolonged the coagulation time (APTT) of HEP free membranes. The stability of ALA under typical hemodialysis conditions was improved by immobilization, and the greatest enhancement was achieved when it was sandwiched between two PEI layers. *In vitro* studies showed that all ALA or SOD/CAT coated PSF membranes are capable of reducing reactive oxygen species levels in blood, furthermore, they can significantly prolong APTT. The hemocompatibility results also demonstrated that the adsorption of human plasma proteins, platelet and cell activation on all modified membranes decreased significantly compared with the unmodified PSF membranes due to the change in surface properties such as hydrophilicity, surface charge and roughness upon immobilization of the biomolecules. The modification methods proposed in this study did not change high permeability, mechanical strength and nontoxic property of the PSF membranes.

## ÖZET

### ANTİKOAGÜLAN, ANTİOKSİDAN ve ENZİM İMMOBİLİZASYONU YÖNTEMLERİ ile BİYOUYUMLULUĞU İYİLEŞTİRİLMİŞ HEMODİYALİZ MEMBRANLARININ HAZIRLANMASI ve KARAKTERİZE EDİLMESİ

Bu tezin amacı biyomolekül tutturma yöntemi ile pıhtılaşmaya karşı dirençli ve/veya antioksidatif yüzeyler yaratarak polisülfon bazlı hemodiyaliz membranlarının kan uyumluluklarını iyileştirmektir. Nontrombojenik yüzey yaratmak için, destek membranı polietilenimin (PEI) ve alginat (ALG) ile kendi kendine katman oluşturma (LBL) metodu ile modifiye edilmiş ve heparin (HEP) ALG ile harmanlanarak LBL yapının en üst katmanına tutturulmuştur. Antioksidatif özellik kazandırmak için ise, alfa-lipoik asit (ALA) ve superoksit dismutaz (SOD)/katalaz (CAT) enzim çifti seçilmiştir. ALA, negatif yüklü destek membran üzerine adsorplanan PEI katman üzerine elektrostatik etkileşimler ile aktif kısmını açıkta bırakacak biçimde tutturulmuştur. SOD/CAT enzim çifti ise plazma modifiye edilmiş ve PEI kaplanmış destek membranları üzerine kovalent ve iyonik olarak tutturulmuştur. ALG içerisine az miktarda heparinin eklenmesi ile pıhtılaşma süresinin (APTT) ciddi biçimde uzadığı gözlemlenmiştir. Alfa-lipoik asitin tipik hemodiyaliz koşulları altında stabilitesinin iyileştiği gözlenmiş, en fazla iyileşme iki PEI katmanı arasına sandviç formda tutturulduğu durumda elde edilmiştir. CAT aktivitesi kovalent veya iyonik olarak tutturulduğu durumlarda aynı iken, SOD kovalent bağ ile tutturulduğunda daha iyi performans göstermiştir. *In vitro* çalışmalar ALA veya SOD/CAT kaplı tüm membranların kanın reaktif oksijen bileşenlerinin seviyesini düşürdüğünü, buna ek olarak pıhtılaşma süresini de önemli oranda uzattığını göstermiştir. Modifiye edilen tüm membranların yüzeyinde plazma protein adsorpsiyonu ile platelet ve hücre aktivasyonunun azaldığı gözlenmiştir. Membranın hidrofilitesinin, yüzey yükünün ve pürüzlülüğünün protein adsorpsiyonu, platelet aktivasyonu ve yüzeye tutunan enzimin konformasyonu üzerinde etkili parametreler olduğu bulunmuştur.

# TABLE OF CONTENTS

LIST OF FIGURES .....	xi
LIST OF TABLES .....	xvii
CHAPTER 1. INTRODUCTION .....	1
CHAPTER 2. BIOCOMPATIBILITY OF HEMODIALYSIS MEMBRANES .....	7
2.1. Protein Adsorption .....	8
2.1.1. Coagulation .....	9
2.1.2. Kallikrein–kinin Pathways (Contact Phase) .....	9
2.1.3. Complement Activation .....	9
2.1.4. Stimulation of Cells .....	10
2.2. Methods for Controlling Protein Fouling .....	11
2.2.1. Cleaning and Regeneration of Membranes .....	12
2.2.2. Using Asymmetric Membrane .....	12
2.2.3. Modification of Membrane Surfaces for Antifouling .....	13
2.2.3.1. Introduction of Negatively Charged Surface Groups ....	13
2.2.3.2. Increasing Hydrophilicity .....	14
2.3. Oxidative Stress .....	17
2.4. Methods to Prevent Oxidative Stress .....	18
CHAPTER 3. IMMOBILIZATION OF BIOMOLECULES .....	22
3.1. Chemical Methods .....	22
3.2. Physical Methods .....	27
3.2.1. Physical Adsorption .....	27
3.2.2. Ionic Binding .....	27
CHAPTER 4. EXPERIMENTAL .....	32
4.1. Materials .....	32
4.2. Preparation of the Membranes .....	33
4.2.1. Preparation of Support Membranes .....	33

4.2.2. Preparation of Heparin Immobilized Polysulfone Membrane ....	34
4.2.3. Preparation of Alpha-Lipoic Acid Immobilized Polysulfone Membrane .....	35
4.2.4. Preparation of Superoxide Dismutase-Catalase Immobilized Polysulfone Membrane .....	36
4.2.4.1. SOD-CAT Immobilization onto the PEI Deposited PSF-SPSF Membranes.....	36
4.2.4.2. SOD-CAT Immobilization onto the Plasma Treated PSF Membranes .....	37
4.3. Surface Characterization.....	38
4.4. Measurement of Alpha-Lipoic Acid Activity.....	40
4.5. Measurement of Superoxide Dismutase (SOD) Activity .....	41
4.6. Measurement of Catalase (CAT) Activity .....	42
4.7. Determination of Operational Stability of the Immobilized Enzymes .	43
4.8. <i>In vitro</i> Hemocompatibility .....	43
4.8.1. Protein Adsorption Experiments.....	43
4.8.2. Platelet and Blood Cell Adhesion and Activation .....	44
4.8.3. Blood Coagulation Time.....	44
4.8.4. ROS Levels in Plasma .....	45
4.8.5. Cell Viability Assay.....	45
4.9. Permeation Experiments .....	46
4.10. Mechanical Analysis.....	47
4.11. Data Analysis .....	47
 CHAPTER 5. RESULTS AND DISCUSSION.....	 48
5.1. Surface Modification of Polysulfone Based Hemodialysis Membranes with Layer by Layer Self Assembly of Polyethyleneimine/Alginate-Heparin .....	  48
5.1.1. Surface Characterization of the Heparin Immobilized Membranes.....	 49
5.1.2. <i>In vitro</i> Hemocompatibility of Heparin Immobilized Membranes.....	 60
5.1.2.1. Protein Adsorption Capacity.....	60
5.1.2.2. Platelet and Blood Cell Activation .....	62



5.1.2.3. Activated Partial Thromboplastin Time (APTT).....	71
5.1.2.4. Cytotoxicities .....	73
5.1.3. Transport and Mechanical Properties of the Heparin Immobilized Membranes .....	75
5.2. Immobilization of Alpha Lipoic Acid onto Polysulfone Membranes to Suppress Hemodialysis Induced Oxidative Stress.....	77
5.2.1. Quantification of Amount of ALA in the Membrane and Release of ALA from the Membranes .....	78
5.2.2. Surface Characterization of ALA Immobilized Membranes .....	80
5.2.3. The Antioxidant Activity of Free $\alpha$ -Lipoic Acid and $\alpha$ -Lipoic Acid Immobilized Membranes .....	90
5.2.4. Determination of Immobilized ALA Stability in Buffer .....	91
5.2.5. <i>In vitro</i> Hemocompatibility of ALA Immobilized PSF Membranes.....	92
5.2.5.1. Protein Adsorption Capacity.....	92
5.2.5.2. Platelet Adhesion and Activation .....	94
5.2.5.3. Activated Partial Thromboplastin Time .....	96
5.2.5.4. Inhibition of Reactive Oxidant Species in Plasma.....	97
5.2.5.5. Cytotoxicity .....	98
5.2.6. Transport and Mechanical Properties of the ALA Immobilized Membranes.....	99
5.3. Immobilization of Superoxide Dismutase and Catalase onto Polysulfone Membranes to Suppress Hemodialysis Induced Oxidative Stress .....	101
5.3.1. Optimization Conditions for SOD/CAT Immobilization .....	102
5.3.2. Surface Characterization of SOD/CAT Immobilized Membranes.....	107
5.3.3. Stability of Immobilized SOD/CAT .....	121
5.3.4. Kinetic Study of Immobilized SOD/CAT .....	124
5.3.5. <i>In vitro</i> Hemocompatibility of SOD/CAT Immobilized PSF Membranes.....	134
5.3.5.1. Protein Adsorption Capacity.....	134
5.3.5.2. Platelet Adhesion and Activation .....	136
5.3.5.3. Inhibition of Reactive Oxidant Species in Plasma.....	139

5.3.5.4. Activated Partial Thromboplastin Time .....	141
5.3.5.5. Cytotoxicity .....	142
5.3.6. Transport and Mechanical Properties of the SOD/CAT Immobilized Membranes .....	143
CHAPTER 6. CONCLUSION .....	146
REFERENCES .....	149
APPENDIX A. CALIBRATION CURVES and EXTINCTION COEFFICIENTS ....	159

# LIST OF FIGURES

<b><u>Figure</u></b>	<b><u>Page</u></b>
Figure 2.1. Important activation pathways of blood in contact with foreign surface (Source: Deppisch et al. 1998) .....	8
Figure 2.2. Visual inspection by light microscopy and SEM of isolated mononuclear blood cells cultivated in contact with polycarbonate/polyether (left) and Cuprophan (right) dialysis membranes (Source: Deppisch et al. 1998).....	11
Figure 2.3. Schematic diagram of the filtration behavior of (a) an asymmetric and (b) a symmetric membrane (Source: Sun et al. 2003). .....	13
Figure 2.4. The change of concentration of urea in donor compartment with respect to time. The symbols denote experimental data and lines correspond to model predictions (CAI: unmodified cellulose acetate membrane, CAI-U: urease immobilized cellulose acetate membrane) (Source: Mahlicli and Altinkaya 2009) .....	17
Figure 3.1. The reaction schemes for esterification of conjugated linoleic acid to CA membranes. (Source: Kung and Yang 2006-a) .....	22
Figure 3.2. XPS spectra of CA and CA-CLA membranes. (Source: Kung and Yang 2006-a).....	23
Figure 3.3. FT-IR spectra of unmodified PSF and modified PSF membranes (Source: Kung et al. 2007).....	24
Figure 3.4. The platelet adhesion of unmodified PSF and modified PSF membranes (Source: Kung et al. 2007) .....	25
Figure 3.5. Synthesis route for chloromethylation of PSf and the formation of PSf-g-PEG. (Source: Park et al. 2006) .....	26
Figure 3.6. Effect of ionic strength on layer thickness and polymer orientation at the substrate surface; (A) at low ionic strength, and (B) at high ionic strength (Source: Guzey et al. 2006) .....	29
Figure 3. 7. Schematic representation of the mechanism of adsorption of the PEI intermediate layer and immobilization of enzyme and heparin (Source: Nguyen et al. 2003).....	30
Figure 4. 1. Sulfonation of polysulfone (Blanco et al. 2002) . .....	33

Figure 4. 2. Structures of PEI and ALA and their possible ionic complexation .....	35
Figure 4.3. Schematic representation of ionic bonding between negatively charged carboxylic groups of enzymes and protonated amine groups of polyethyleneimine.....	37
Figure 4.4. Schematic representation of amide bond between carboxylic groups of enzymes and amine groups of plasma treated polysulfone membrane.....	38
Figure 4.5. Chemical structure of alpha-lipoic acid (ALA) and dihydrolipoic acid (DHLA).....	40
Figure 4.6. Experimental set-up used for permeation experiments.....	46
Figure 5.1. Water contact angles of the unmodified and modified PSF membranes layer by layer self assembly of polyethyleneimine/alginate-heparin.....	50
Figure 5.2. Intensity of colours of Toluidine Blue O and Congo Red dyes adsorbed on the unmodified and modified PSF membranes layer by layer self assembly of polyethyleneimine/alginate-heparin.....	51
Figure 5.3. Representative FTIR-ATR spectra of (a) PEI/ALG-HEP or PEI/ALG multilayers on the ZnSe substrate and (b) an example of a peak fitting result for the 1 bilayer PEI/ALG-HEP multilayers.....	533
Figure 5.4. AFM images of (a) PSF (b) PSF-SPSF and (c) PSF-SPSF-PEI-ALG/HEP-15-1b membranes.....	565
Figure 5.5. Surface roughness of unmodified and modified PSF membranes with layer by layer self assembly of polyethyleneimine/alginate-heparin.....	57
Figure 5.6. Surface SEM pictures of (a-c) dense skin (b-d) porous layer of PSF. Cross section SEM pictures of (e) PSF (f) PSF-SPSF (g) PSF-SPSF-PEI-ALG/HEP-15-1b (h) PSF-SPSF-PEI-ALG/HEP-45-5b membranes. Magnification x 2000 (a-b; e-f); x 40000 (c-d). *PEI/ALG-5b magnification x 5000 (i) 10000 (j). * 5 bilayer PEI/ALG coating was prepared from a solution containing 1M NaCl and each polyelectrolyte with a concentration of 10 mg.ml <sup>-1</sup> .....	59
Figure 5.7. Amount of BSA adsorbed onto the unmodified and modified PSF membranes with layer by layer self assembly of polyethyleneimine/alginate-heparin.....	61
Figure 5.8. Amount of blood plasma proteins adsorbed on the unmodified and modified PSF membranes with layer by layer self assembly of polyethyleneimine/alginate-heparin.....	62

Figure 5.9. Amount of platelet activation on the unmodified and modified PSF membranes with layer by layer self assembly of polyethyleneimine/alginate-heparin.....	64
Figure 5.10. FTIR-ATR spectra of PSF-SPSF membrane before blood plasma protein adsorption and PSF, PSF-SPSF and PSF-SPSF-PEI-ALG/HEP-15-1b membranes after blood plasma proteins in a region (a) 650-4000 cm <sup>-1</sup> (b) 1500-1700 cm <sup>-1</sup> . Deconvoluted spectra in the chosen band (1600-1700 cm <sup>-1</sup> ) of blood plasma protein adsorbed (c) PSF (d) PSF-SPSF (e) PSF-SPSF-PEI-ALG/HEP-15-1b membranes....	676
Figure 5.11. The SEM pictures of unmodified and modified PSF membranes after incubating with PRP for 25 minutes (a) PSF (b) PSF-SPSF (c) PSF-SPSF-PEI-ALG/HEP-15-1b (d) PSF-SPSF-PEI-ALG/HEP-45-5b, magnification x2000.....	70
Figure 5.12. The SEM pictures of (a-b) PSF-SPSF and (c-d) PSF-SPSF-PEI-ALG/HEP-15-1b membranes after incubating in whole blood for 15 minutes. Magnification (a-c) x1000 and (b-d) x 5000. ....	71
Figure 5.13. Live and dead cells labeled with TO and PI after incubating PMBCs with (a) Control (b) PSF (c) PSF-SPSF (d) PSF-SPSF-PEI-ALG/HEP-15-1b membranes. ....	74
Figure 5.14. The permeation coefficient of urea, vitamin B <sub>12</sub> and lysozyme through the unmodified and modified PSF membranes with layer by layer self assembly of polyethyleneimine/alginate-heparin. ....	76
Figure 5.15. (a) UV-Spectrum of ALA (b) Amount of immobilized and released ALA. Immobilized amount of ALA for PSF-SPSF-PEI-ALA-III membrane is statistically different that of PSF-SPSF-PEI-ALA-I and PSF-SPSF-PEI-ALA-II membranes (p<0.05). Released amounts of ALA for each membrane are statistically different from each other (p<0.05). ....	800
Figure 5.16. Water contact angle of PSF membranes. *Contact angle of PEI-ALA-II membrane is statistically different from that of PSF-SPSF membrane (p<0.05) .....	81
Figure 5.17. XPS Spectra of PSF-SPSF-PEI-ALA-I membrane for (a) survey at 45° (b) N 1s (c) S 2p (d) C 1s and (e) O 1s peaks at 15°.....	83

Figure 5.18. AFM images of (a) PSF-SPSF-PEI-ALA-I (b) PSF-SPSF-PEI-ALA-II membranes. ....	888
Figure 5.19. Surface roughness of unmodified and modified PSF membranes with ALA immobilization. ....	89
Figure 5.20. SEM pictures of (a) PSF-SPSF and (b) PSF-SPSF-PEI-ALA-I .....	90
Figure 5.21. % RSA of free and immobilized ALA. *RSA (%) values at 240th minute of immobilized ALA for each membranes are statistically different from each other and also that of same amount of free ALA (p<0.05) .....	91
Figure 5.22. The effect of storing time on the relative antioxidant activity of $\alpha$ -lipoic acid immobilized on PSF membranes. Membranes were stored in phosphate buffer solution at pH=7.4, T=37°C for 4 hours. *RSA (%) value of PSF-SPSF-PEI-ALA-II membrane is statistically different from PSF-SPSF-PEI-ALA-I and PSF-SPSF-PEI-ALA-III membranes after treatment.(p<0.05) .....	92
Figure 5.23. The amount of blood plasma proteins adsorbed onto ALA coated PSF membranes.....	93
Figure 5.24. Amount of platelet activation on the unmodified and modified PSF membranes with ALA immobilization.....	95
Figure 5.25. The SEM pictures of (a) PSF-SPSF (b) PSF-SPSF-PEI-ALA-I membranes after incubating with PRP for 25 minutes, magnification x2000.....	96
Figure 5.26. The SEM pictures of (a) PSF-SPSF (b) PSF-SPSF-PEI-ALA-I membranes after incubating with whole blood for 15 minutes, magnification x1000.....	96
Figure 5.27. The inhibition HOCl in blood by unmodified and modified PSF membranes with ALA immobilization.....	98
Figure 5.28. The permeation coefficient of urea, vitamin B12, lysozyme through unmodified and modified PSF membranes with ALA immobilization. * Permeation coefficients of all the solutes though each membrane are not statistically different (p>0.05).....	100
Figure 5.29. Immobilized activities of SOD and CAT vs initial PEI concentration. Experiments were conducted with CCAT-initial: 0.25 mg.ml <sup>-1</sup> and C <sub>H2O2</sub> : 30 mM, C <sub>SOD-initial</sub> : 0.25 mg.ml <sup>-1</sup> and C <sub>Riboflavin</sub> : 2 $\mu$ M.....	103

Figure 5.30. Immobilized amount of CAT and immobilized activity vs initial CAT concentration. CAT was immobilized with layer by layer self-assembly method (a) and plasma treatment method (b). Experiments were conducted with $C_{PEI-initial}$ : $0.1 \text{ mg.ml}^{-1}$ and $C_{H_2O_2}$ : $30 \text{ mM}$ .....	104
Figure 5.31. Immobilized amount of SOD and immobilized activity vs initial SOD concentration. SOD was immobilized with layer by layer self-assembly (a) and plasma treatment (b) method. Analyses were conducted with $C_{PEI-initial}$ : $0.1 \text{ mg.ml}^{-1}$ and $C_{Riboflavin}$ : $2\mu\text{M}$ . ....	105
Figure 5.32. Stability of immobilized CAT vs initial enzyme concentration.....	106
Figure 5.33. Water contact angle of unmodified and modified PSF membranes with SOD/CAT immobilization. ....	108
Figure 5.34. AFM images of (a) PSF-PLS (b) PSF-PLS-SOD/CAT and (c) PSF-SPSF-PEI-SOD/CAT membranes. ....	1110
Figure 5.35. Surface roughness of unmodified and modified PSF membranes with SOD/CAT immobilization.....	112
Figure 5.36. Cross section SEM pictures of (a) PSF (b) PSF-PLS (c) PSF-PLS-SOD/CAT .....	113
Figure 5.37. FTIR-ATR spectra of (a) native SOD/CAT (b) PSF-SPSF-PEI and PSF-SPSF-PEI-SOD/CAT (c) PSF-PLS and PSF-PLS-SOD/CAT Deconvoluted spectra in the chosen band ( $1600-1700 \text{ cm}^{-1}$ ) of (d) native SOD/CAT (e) PSF-SPSF-PEI-SOD/CAT (f) PSF-PLS-SOD/CAT .....	116
Figure 5.38. Stability of immobilized CAT at operating conditions ( $T=37 \text{ C}$ and $\text{pH}:7.4$ ). CAT was immobilized by layer by layer self-assembly of polyelectrolytes and plasma treatment method. Analysis were conducted with $C_{PEI-initial}$ : $0.1 \text{ mg.ml}^{-1}$ ; $C_{CAT-initial}$ : $0.25 \text{ mg.ml}^{-1}$ ; $C_{H_2O_2}$ : $30 \text{ mM}$ . ....	122
Figure 5.39. Stability of immobilized SOD at operating conditions ( $T=37 \text{ C}$ and $\text{pH}:7.4$ ). CAT was immobilized by layer by layer self-assembly of polyelectrolytes and plasma treatment method. Analysis were conducted with $C_{PEI-initial}$ : $0.1 \text{ mg.m}^{-1}$ ; $C_{enzyme-initial}$ : $0.25 \text{ mg.ml}^{-1}$ ; $C_{Riboflavin}$ : $2 \mu\text{M}$ . ....	123
Figure 5.40. Amount of released SOD and CAT at operating conditions ( $T=37 \text{ }^\circ\text{C}$ and $\text{pH}:7.4$ ). ....	124

Figure 5.41. Substrate Concentration vs. rate of free CAT (a), immobilized CAT with self assembly of PEI (b) and plasma treatment method (c). Analysis were conducted with $C_{PEI-initial}: 0.1 \text{ mg.ml}^{-1}$ ; $C_{enzyme-initial}: 0.25 \text{ mg.ml}^{-1}$ and $C_{H_2O_2}: 30 \text{ mM}$ .....	127
Figure 5.42. Substrate concentration vs rate of free SOD (a), immobilized SOD with self-assembly of polyelectrolytes (b) and plasma treatment method (c). Analysis were conducted with $C_{PEI-initial}: 0.1 \text{ mg.ml}^{-1}$ ; $C_{enzyme-initial}: 0.25 \text{ mg.m}^{-1}$ and $C_{Riboflavin}: 2 \text{ }\mu\text{M}$ . ....	130
Figure 5.43. The amount of blood plasma proteins adsorbed onto unmodified and modified PSF membranes with SOD/CAT immobilization.....	136
Figure 5.44. Amount of platelet activation on the unmodified and modified PSF membranes with SOD/CAT immobilization. ....	137
Figure 5.45. The SEM pictures of (a) PSF-SPSF-PEI-SOD/CAT and (b) PSF-PLS-SOD/CAT membranes after incubating with PRP for 25 minutes, magnification x 2000. ....	138
Figure 5.46. SEM pictures of (a) PSF-SPSF (b) PSF-PLS (c) PSF-PLS-SOD/CAT and (d) PSF-SPSF-PEI-SOD/CAT membranes after incubating with whole blood for 15 minutes, magnification x 1000.....	139
Figure 5.47. The inhibition HOCl in blood by unmodified and modified membranes with SOD/CAT immobilization. ....	141
Figure 5.48. The permeation coefficient of urea, vitamin B <sub>12</sub> , lysozyme through unmodified and modified PSF membranes with SOD/CAT immobilization. * Permeation coefficients of each membrane are not statistically different from each other for each solute ( $p>0.05$ ) .....	144



## LIST OF TABLES

<u>Table</u>	<u>Page</u>
Table 5.1. Codes of the unmodified and modified PSF membranes with layer by layer self assembly of polyethyleneimine/alginate-heparin. ....	49
Table 5.2. Secondary Structure of Adsorbed Blood Plasma Proteins on the Unmodified and Modified PSF Membranes Estimated from the Deconvolved FTIR Spectroscopy.....	68
Table 5.3. APTT values of the unmodified and modified PSF membranes. ....	73
Table 5.4. % of live cells after incubating PMBCs with the unmodified and modified PSF membranes with layer by layer self assembly of polyethyleneimine/alginate-heparin for 4 hours.....	74
Table 5.5. Mechanical properties of the unmodified and modified PSF membranes.....	77
Table 5.6. Codes of the unmodified and modified PSF membranes with ALA immobilization.....	78
Table 5.7. The ratio of calculated peak areas of the PSF-SPSF-PEI-ALA-I membrane to those of PSF-SPSF-PEI-ALA-II membrane.....	85
Table 5.8. The APTT values for unmodified PSF and modified membranes with with ALA immobilization .....	97
Table 5.9. % live peripheral mononuclear blood cells after 4 hours treatment with modified and unmodified PSF membranes .....	99
Table 5.10. Mechanical properties of the unmodified and modified PSF membranes.....	101
Table 5.11. Codes of the unmodified and modified PSF membranes with SOD/CAT immobilization.....	102
Table 5.12. Specific activities of immobilized SOD and CAT .....	107
Table 5.13. Secondary Structure of Native and Immobilized SOD and CAT Estimated from the Deconvolved FTIR Spectroscopy .....	120
Table 5. 14. Michealis-Menten kinetic parameters of native and immobilized CAT ..	129
Table 5.15. Michealis-Menten kinetic parameters for native and immobilized SOD ..	132
Table 5.16. The change in Damköhler numbers with respect to stirring rate for the native and immobilized CAT. ....	133

Table 5.17. The change in Damköhler numbers with respect to stirring rate for the native and immobilized SOD. ....	134
Table 5.18. APTT Values for SOD/CAT Immobilized Membranes .....	142
Table 5.19. % Live peripheral mononuclear blood cells after 4 hours treatment with unmodified and modified PSF membranes with SOD/CAT immobilization.....	143
Table 5.20. Mechanical properties of the unmodified and modified PSF membranes with SOD/CAT immobilization. ....	145

# CHAPTER 1

## INTRODUCTION

Hemodialysis operation is an important clinical therapy to remove toxic metabolites from the blood of a patient with end-stage renal disease. By the end of 2008, approximately 2.3 million patients received treatment for end-stage renal disease throughout the world. The most important element of the hemodialysis operation is the semipermeable membrane which allows the selective removal of low to medium molecular weight biological metabolites from the blood. The clinical use of hemodialysis membranes started in 1960, and in 1992 more than 400 dialyzers produced from different polymers with different pore size and surface area were listed by the European Dialysis Transplant Association-European Renal Association (Morti et al. 2003).

High mass transfer rate through the membrane is usually desired in order to keep treatment time to a minimum. In addition, membrane must have high blood compatibility to prevent undesirable reaction of blood components at the membrane surface. Most of the hemodialysis membrane materials are hydrophobic in nature and allow easily protein adsorption on the surface due to hydrophobic interaction between membrane surface and protein molecules when these membranes contact with blood. It is generally accepted that protein adsorption depends on surface characteristics, including degree of hydrophilicity/hydrophobicity and degree of charge (Sperling et al. 2009). Surface modification is a commonly used approach to create surfaces of biomedical devices which resist to protein adsorption. Numerous surface modification methods which can be summarized as blending hydrophilic polymers into the membrane forming solution; grafting hydrophilic groups by UV-irradiation or low temperature plasma technique; graft copolymerization of monomers and coating with hydrophilic polymers or copolymers have been suggested (Sun et al. 2003). Protein adsorption does not only cause reductions in solutes permeation characteristics but can also be followed by the activation of different defense systems in blood. (Sun et al. 2003, Blitz et al. 2006) Adsorbed proteins can affect platelet and leukocyte adhesion that results in thrombogenic formation, response of immune system or other tissues.

Leukocyte adhesion and then activation during the blood-membrane interaction causes generation of free radicals. Reaction of these radicals with the proteins and lipids in blood is the main reason of a problem called hemodialysis induced oxidative stress. Over the last ten years, researchers focused on developing hemodialysis membranes with antioxidative properties to suppress hemodialysis-induced oxidative stress. The most commonly used approach is to immobilize antioxidants such as vitamin E (Mydlik et al., 2001; Clermont et al., 2001, Yamamoto et al., 2007), linoleic acid (Kung and Yang, 2006<sup>a,b,c</sup>, 2007) and soybean-derived phytochemical, genistein on the blood contacting surfaces of the membranes (Neelakandan et al., 2011). Vitamin E coated dialyzer provided more effective antioxidant defense than peroral administration of vitamin E in hemodialysis patients (Mydlik et al., 2001). On the other hand, it has been observed that vitamin C administration increased antioxidant activity of the vitamin-E coated membrane (Yamamoto et al., 2007). Antioxidant immobilization not only allowed to inhibit production of reactive oxygen species (ROS) but also reduced platelet adhesion, protein adsorption and prolonged blood coagulation time (Kung and Yang, 2006<sup>a,b,c</sup>, 2007).

Extracorporeal thrombosis is another important problem of hemodialysis operation leading to embolism and infarction. To prevent this problem, blood anticoagulant heparin is usually injected during hemodialysis. However, using large amount of heparin can increase the risk of abnormal bleeding and heparin induced thrombocytopenia. To provide heparin-free hemodialysis, the attempts have concentrated on producing nonthrombogenic materials by mimicking endothelial cell layer through heparin immobilization. *In vitro* studies have shown that heparin or endothelial cell surface heparin sulfate immobilized on the membranes can modulate complement and intrinsic coagulation activation (Cheung et al., 1992), generate surfaces resistant to platelet adhesion, (Baumann and Kokott, 2000; Yang and Lin, 2002, 2003; Lin et al., 2004) plasma protein adsorption and prolong the coagulation time (Yang and Lin, 2002, 2003; Lin et al., 2004). *In vivo* tests carried out with commercial hemodialysis membranes, AN69 ST, HEMOPHAN and EVODIAL, have demonstrated that it is possible to reduce systemic administration of heparin through its immobilization on these membranes (Lavaud et al., 2003, 2005; Lee et al., 2004; Chanard et al., 2005, 2008; Morena et al., 2010) although one clinical study have reported that heparin coated AN69 ST membrane does not reduce clotting during hemodialysis when compared to a conventional polysulfone filter (Sagedal et al., 2011).

Various types of dialyzers are currently available in the market, on the other hand, the clinical studies have suggested that there is still a need for developing membranes with improved biocompatibilities. It is clearly noted that the biocompatibility of the hemodialysis membranes have a significant effect on mortality rate of the dialysis patients. The motivation of this work comes from this fact and the main objective is to prepare polysulfone (PSF) based hemodialysis membranes with improved hemocompatibility. PSF is successfully applied as membrane material in biomedical application due to its excellent properties such as chemical inertness, thermal stability, and mechanical strength. In addition, PSF has good permeability for solutes including low-molecular-weight ( $< 2 \times 10^4$ ) proteins. However, the hydrophobic nature of PSF is undesirable in hemodialysis applications. In this thesis, two main strategies have been utilized for increasing biocompatibility of PSF based hemodialysis membranes. First one is to create nonfouling surfaces by increasing hydrophilic character of the surface and the second strategy is to generate antithrombogenic and antioxidative surfaces by immobilizing bioactive agents on the PSF membranes.

Covalent attachment is commonly used for immobilizing biomolecules on the blood contacting surfaces. Although the method provides good stability of the molecules over long-term, it involves a complicated chemistry with the use of various toxic chemicals and causes significant activity loss due to attachment of the active sides of the molecules. Recently, the layer by layer self-assembly (LBL) technique has emerged as a versatile, gentle and easy surface modification method for immobilization of functional molecules. The assembly process can be conducted in an aqueous solution under mild ambient conditions which minimize the loss in the activity of biological agents due to attachment on a surface. Electrostatic interactions are most often used to drive multilayer assembly, however, other interactions such as hydrogen bonding, hydrophobic interactions and molecular recognition can also be applied for constructing the assembly (Quinn et al., 2007). The strength of interactions between interacting species can be easily adjusted to minimize desorption of the functional molecules on the surface of the assembly. The layer by layer self-assembly (LBL) technique was used for attaching bioactive molecules such as drugs, enzymes, DNA or proteins on various support (Thierry et al. 2003). The advantage of this method in the modification of the hemodialysis membranes was illustrated only in a few study (Gong et al., 2011; Yu et al., 2007, Lavaud et al., 2003, 2005, Chanard et al., 2005, 2008)

In this study, the biomolecules were noncovalently attached by modifying the surface of the support membrane with a single or multilayer assembly of the polyelectrolytes. The studies in this thesis have been discussed in 3 parts each containing the influence of a different biomolecule immobilization on the biocompatibility of the PSF membranes.

In the first part of this study, it is intended to create nonthrombogenic surfaces through heparin (HEP) immobilization on the PSF membranes. For immobilization, first PSF was modified by sulfonation to induce negatively charged groups and the support membrane was prepared from a blend of PSF and sulfonated PSF (SPSF). Next, positively charged, hydrophilic polyelectrolyte, polyethyleneimine (PEI), was adsorbed on the negatively charged support membrane. To construct the layer by layer self assembly of the polyelectrolytes, alginate (ALG), was chosen as negatively charged polyelectrolyte due to its hydrophilic, biocompatible, immunoprotective and bioadhesive properties. Heparin was immobilized only on the outermost surface of the LBL assembly by blending with ALG. In previous studies, heparin was used alone to adsorb on positively charged polyelectrolytes for each alternating layer. In this study, small amount of HEP was blended with another polyanion, ALG, to form the outermost layer of the assembly. The intermediate layers were prepared with the alternate deposition of the PEI and heparin free ALG. The scientific motivation of this part of the thesis was to investigate the anticoagulant activity and biological properties of HEP when blended with another polyanion, ALG, as the outermost layer of layer by layer deposition.

In the second part of this study, the PSF membranes were modified with an antioxidant alpha lipoic acid (ALA) through an intermediate PEI layer to prevent hemodialysis induced oxidative stress formation. Unlike other antioxidants, alpha-lipoic acid (ALA) and its reduced form dihydrolipoic acid (DHLA) effectively quench a number of free radicals in both lipid and aqueous media. ALA and DHLA together have metal-chelating activity which may have effects on regulatory proteins and on genes involved in normal growth and metabolism (Packer et al., 1995). Therefore, ALA is widely used as a drug for preventing various chronic diseases associated with oxidative stress and is administered as a daily supplement for dietary purposes, antiageing, diabetes, and cardiovascular disease. In recent years, some clinical studies showed that administration of ALA therapy could decrease the biomarkers of oxidative stress in end-stage renal disease patients under hemodialysis (Chang et al., 2007) and

prolong clotting time via inhibition of the intrinsic coagulation pathway (Ford et al., 2001; Marsh et al., 2006). To the best knowledge, this is the first study that suggests immobilization of ALA onto hemodialysis membranes to suppress hemodialysis induced oxidative stress. Furthermore, the immobilization method used in this study is unique in that antioxidant isn't attached on the membranes covalently through a complex chemistry. The method is based on adsorbing PEI on the support membrane and then site-specifically binding a carboxylic group of ALA to an amine group of PEI through electrostatic interactions. Thus, the cyclic disulphide bond that forms the active site of ALA becomes available on the surface of the membrane to scavenge ROS.

In the third part of the thesis, immobilization of superoxide dismutase (SOD) - catalase (CAT) enzymatic antioxidant couple was proposed as a second alternative to generate PSF membranes that are capable of suppressing oxidative stress. The motivation for selecting SOD and CAT enzymes is to mimic the antioxidant properties of blood since they are known as the most important antioxidant couple in the blood that can eliminate the most harmful free radical in biological systems-superoxide anions ( $O_2^-$ ). Encapsulation or immobilization of individual SOD or CAT was tried for use in drug delivery (Giovagnoli et al. 2004) and biosensor applications (Pastor et al. 2010). However, there are limited studies about SOD-CAT multienzyme immobilization (Villalong et al. 2005). To the best knowledge, in previous studies the SOD-CAT enzymes together were not used for improving biocompatibility of hemodialysis membranes. The enzymes were immobilized onto plasma modified and PEI deposited PSF membranes through covalent and ionic bonding, respectively. In order to compare two enzyme immobilization methods, kinetics were determined with Michaelis-Menten kinetic equation which is one of the simplest and best-known models of enzyme kinetics. The optimization of the immobilization conditions of CAT was also carried.

The blood compatibilities of the all fabricated membranes were evaluated in terms of the inhibition of ROS in blood plasma, the amount of adsorbed plasma proteins, the activated partial thromboplastin time (APTT), platelet adhesion, activation and cytotoxicity on blood cells. In addition, the transport, structural and mechanical properties of the membranes were also characterized.

This thesis consists of six chapters. After the introduction, in the second chapter, a review of the strategies which were developed to improve hemocompatibility of blood contacting membranes is explained. Chapter 3 gives detailed information about the biomacromolecule immobilization onto hemodialysis membranes. In the fourth chapter,

the detailed experimental methods for preparing unmodified and modified membranes are presented. In addition, all the methods used for characterizing the prepared membranes are explained. Chapter 5 includes discussion of all experimental results. In Chapter 6, brief summary of the study and possible suggestions for further research are presented.



## CHAPTER 2

# BIOCOMPATIBILITY OF HEMODIALYSIS MEMBRANES

The clinical performance of a hemodialyzer is an important issue for the patient. The selection of the membrane should be carefully done assuring the safety and effectiveness during the application. There is growing evidence that long term complications in end-stage renal failure may be attributed to bioincompatibility of these membranes (Deppisch et al. 1998). To ensure a successful hemodialysis operation the membrane used in the dialyzer should have some properties. First of all, high mass transfer rate through the membrane is necessary in order to shorten the treatment time. The other important demand is hemocompatibility of the membrane. Contacting of blood with a foreign surface causes activation of the blood components which results in the formation of macromolecular complexes (Deppisch et al. 1998).

In order to obtain high permeability and blood compatibility, the selected membrane should have some properties which are listed below.

- a. The pore size should have a definite size.
- b. The porosity of should be high to provide high flux.
- c. The tortuosity should be low.
- d. The pore size distribution should be narrow to obtain sharp molecular weight cut-off (MWCO).
- e. The diffusion coefficient of middle-molecular weight solutes in the membrane should be high.
- f. The smallest sized pores should be on the blood contacting surface to prevent plugging of pores.
- g. The resistance of the membrane to protein adsorption should be high.
- h. The active membrane layer (skin) should be as thin as possible to provide high permeability of solutes. (Deppisch et al. 1998).
- i. Surface roughness should be minimum to reduce interaction with proteins and cells in blood.
- j. Mechanical strength should be high to hold the required pressure limits

(maximum 500 mm Hg). (Stamatialis et al. 2008)

A further demand on the membrane is blood compatibility that is assessed via five sets of parameters by Stamatialis et al. (2008). The material should have:

- k. Low thrombogenicity and coagulation potential.
- l. Low complement or cell activation potential.
- m. No hemodynamic effects (“contact phase” coagulation).
- n. No allergic or hypersensitivity reaction.
- o. No interaction with administrated drugs.

## 2.1. Protein Adsorption

Protein adsorption is a major problem in hemodialysis membranes, as it changes membrane selectivity and causes series of undesired reaction with blood. Protein deposition on dialysis membranes can change the transport characteristics of the membranes. Furthermore, adsorption of proteins during contacting blood with artificial surfaces also causes activation of several cascades of proteolytic systems in the plasma, e.g. complement, contact phase, coagulation pathway, fibrinolytic pathway, etc. as seen in Figure 2.1. In addition, cellular interactions with artificial surfaces are induced by adsorbed proteins (Deppisch et al. 1998).

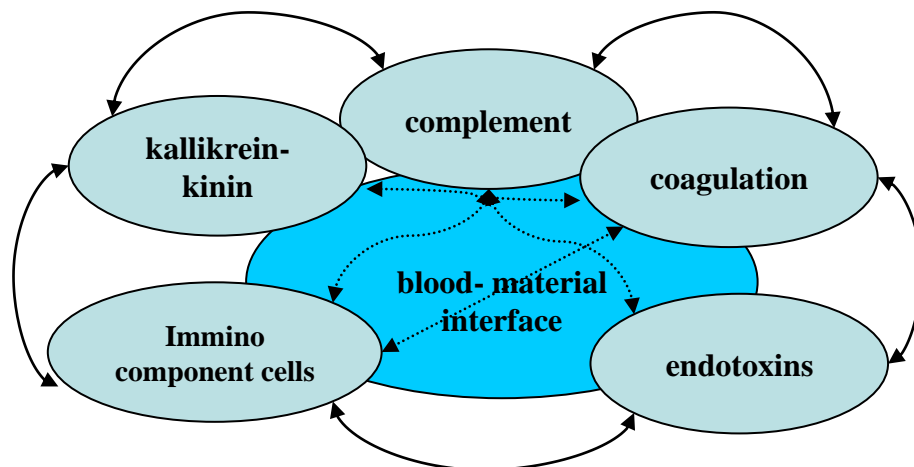


Figure 2.1. Important activation pathways of blood in contact with foreign surface

(Source: Deppisch et al., 1998)

### **2.1.1. Coagulation**

Extracorporeal thrombogenesis is a major problem of hemodialysis operation. When blood interacts with membrane, adsorption of plasma protein onto the membrane is followed by platelet adhesion and activation which are the initial step of clotting cascade. The level of coagulation during hemodialysis is investigated by measuring the formation of thrombin-antithrombin III complex and platelet adhesion (Deppisch et al. 1998).

### **2.1.2. Kallikrein–kinin Pathways (Contact Phase)**

The kinin-kallikrein system is a system of blood proteins that plays a role in inflammation, blood pressure control, coagulation and pain. In extracorporeal circuits, when the kinin-kallikrein system has been activated, factor XIIa is generated which increases the formation of kallikrein from prekallikrein. Then, kallikrein increases the cleavage of high-molecular weight kininogen and causes release of bradykinin, which is a potent vasodilator. Thus, the activation of the kallikrein pathways by dialysis membranes induces severe hypersensitivity reactions such as dialysis hypotension and also coagulation. Kallikrein generation is measured as kallikrein-like activity in plasma supernatant in contact with biomaterial. Surfaces with high streaming potentials, e.g. glass, sulfonated membranes, polystyrene membranes activates kinin-kallikrein system (Deppisch et al. 1998)

### **2.1.3. Complement Activation**

The complement system is part of the innate immune system that comprises the cells and mechanisms and defend the host from infection by other organisms, in a non-specific manner. All surfaces foreign to blood cause the complement activation which represents recognizing and responding to pathogens. The reaction is initiated by direct chemical interaction of complement protein C3 with the foreign surface, followed by activation of C5 and assembling terminal complement complex (TCC). Then, the cationic polypeptides C3a and C5a are released and initiated a series of consecutive reactions such as stimulation of cells and the release of oxygen radical species etc.

(Deppisch et al. 1998). The recurrent activation of complement may cause oxidative stress (Floccari et al. 2005) which induces tissue destruction, organ dysfunction and a decreased response to further stimuli. In biocompatibility studies, the level of C3 and C5 are measured as indicator of complement activation. The complement activation significantly depends on the number of reactive groups of material surface, especially OH groups (Deppisch et al. 1998).

#### **2.1.4. Stimulation of Cells**

When blood contacts with a foreign material (hemodialyzer membrane), cells are also activated by adhesion onto membrane and stimulation in addition to the protein-mediated activation. In Figure 2.2, it can be seen that peripheral blood mononuclear cells (PMBCs) change their morphology (bottom electron micrograph) and start spreading (top micrograph) after adhesion to the homogeneous hydrogel surface of regenerated cellulose. On the other hand, with polycarbonate/polyether membrane fewer adhered cells (top left micrograph) and no sign of a morphology change (bottom left micrograph) are detected. Due to the difference in cell repulsion potential of the surfaces, the density of adhered mononuclear cells was found significantly lower on polycarbonate/polyether membranes than on the surfaces of hydrogel regenerated cellulose membranes which is bioincompatible one (Deppisch et al. 1998).

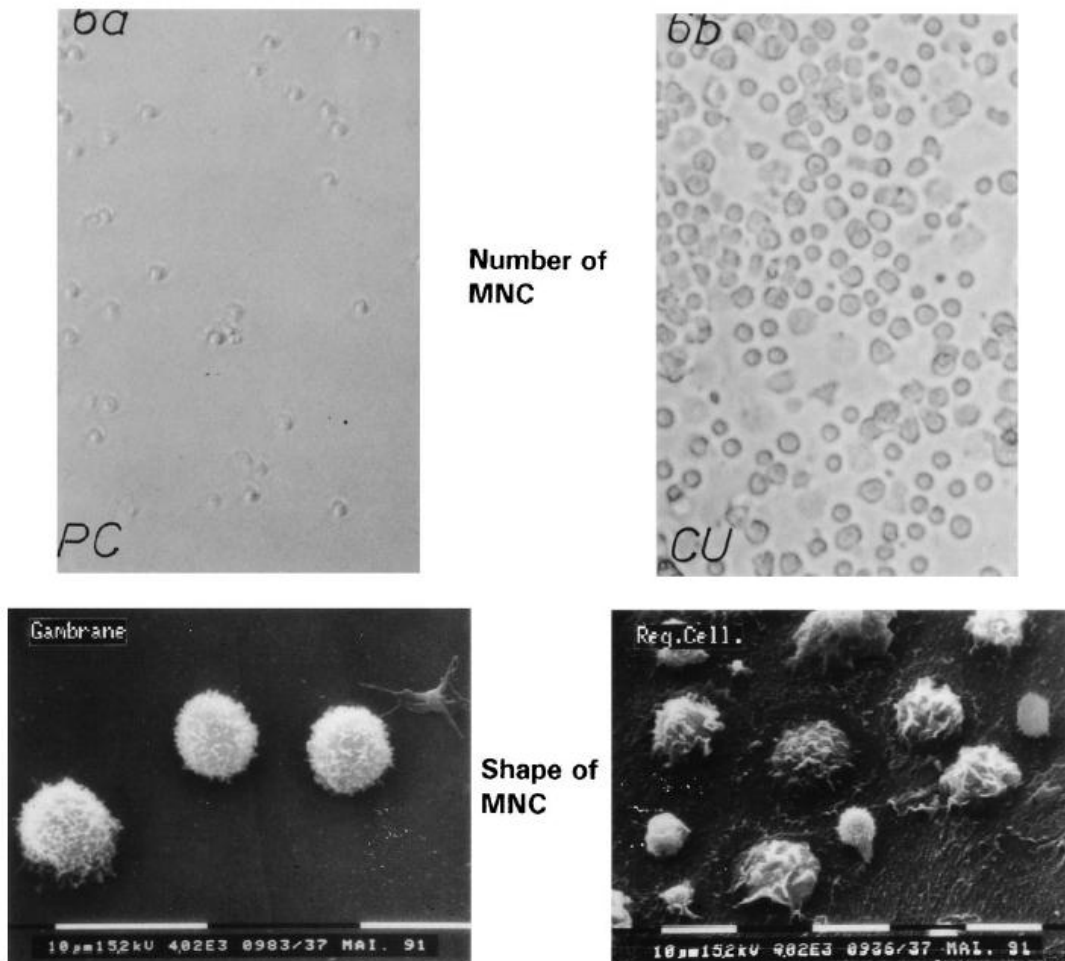


Figure 2.2. Visual inspection by light microscopy and SEM of isolated mononuclear blood cells cultivated in contact with polycarbonate/polyether (left) and Cuprophan (right) dialysis membranes (Source: Deppisch et al., 1998).

Apart from surface adhesion, the activation of proinflammatory cytokines (immunocytes) cells by bioincompatible membranes leads to an attenuation of the ability to respond to phagocytic stimuli (e.g. infectious pathogens) and with that to a weakening of immune defense system of the patient.

## 2.2. Methods for Controlling Protein Fouling

Protein adsorption on membranes is a complex process and still not completely understood. It is controlled by the physico-chemical properties, microstructure and morphology of the surface. Thermodynamics and kinetics of adsorption are dependent on properties of protein molecules such as size, shape, stability, charge and charge

distribution; the solution properties such as protein concentration, pH, and ionic strength; and the physical nature of membrane such as its hydrophobicity, charge, and charge density. The interplay between the factors is complex; however, electrostatic, hydrophobic, and entropic effects are often regarded as the main driving forces for surface adsorption (Deppisch et al. 1998, Wang et al. 2007). Researchers have been applying different strategies to control the protein adsorption on the surface of blood-contact membranes by focusing on its type and morphology, hydrophilicity and operating conditions. In a review paper by Sun et al. (2003) these strategies are classified in detail as discussed below.

### **2.2.1. Cleaning and Regeneration of Membranes**

Since mid-1970s, some scientists recommended the reuse of hemodialyzers, because of its excessive cost even though these devices were designed for disposable using. While the practice of reusing dialyzers has become common in the United States, it is forbidden in West European countries, Japan and France. It is claimed that the relatively high mortality reported for patients receiving dialysis in the United States is associated with the reuse of the dialyzers. Cleaning and regeneration methods currently arranged in clinical use of dialyzers are performed off-line to permit reuse (Sun et al. 2003).

### **2.2.2. Using Asymmetric Membrane**

An asymmetric membrane includes a very thin skin layer which determines the permeability for solutes and highly porous and relatively thick sublayer as a support. The size of the pores in the skin layer is very small compared to that in the sublayer. Conventional symmetric membranes are depth filters and retain most particles within their internal structure, as shown in Figure 2.3. These trapped particles cause fouling easily. On the other hand, asymmetric membranes are surface filters leaving all rejected materials on the surface. Consequently, the use of asymmetric membranes, rather than symmetric ones can partially prevent the protein fouling (Sun et al. 2003).

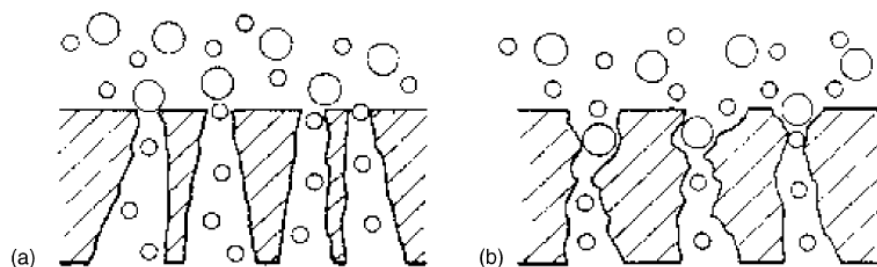


Figure 2.3. Schematic diagram of the filtration behavior of (a) an asymmetric and (b) a symmetric membrane (Source: Sun et al., 2003).

### 2.2.3. Modification of Membrane Surfaces for Antifouling

Surface modification is the most effective method against protein adsorption. In this approach, only the surface characteristic of the membranes is modified, thus the original characteristics such as mechanical strength and thermal stability are kept. Surface modification on the surface of hydrophobic membranes introduces hydrophilic segments only on the surface, thus resulting membrane presents the advantages of both hydrophilic and hydrophobic membranes. A variety of surface modification methods have been reported, which can be mainly classified into four distinct categories as follows (Sun et al. 2003):

- a. Introduction of negatively charged surface groups
- b. Increasing hydrophilicity
- c. Introduction of steric hindrance
- d. Biomimetic modifications

#### 2.2.3.1. Introduction of Negatively Charged Surface Groups

It is usually claimed that the introduction of negative charges on the membrane surface should decrease protein fouling by increasing the electrostatic repulsion between the membrane surface and mostly negatively charged proteins and cells in blood. Chen et al. (1992) treated an ultrafiltration membrane with anionic surfactants to reduce the adsorption of proteins. They found that small anionic surfactant reduced protein adsorption by changing electrostatic interactions between proteins and membrane surface. Higuchi and Nakagawa (1990) chemically modified both the inner and the

outer surfaces of PSF hollow fibers with some hydrophilic components such as propane sulfone and some Friedel-Crafts catalysts. Their results indicated that the modified fibers with hydrophilic surfaces showed better antifouling property compared with the unmodified ones. Lin et al. (2004) covalently immobilized chitosan (CS)/heparin (HEP) onto the surface of the polyacrylonitrile (PAN). The influence of surface modification on the protein adsorption and platelet adhesion, metabolites permeation and anticoagulation activity of resulting membrane was investigated. The immobilization of polyelectrolyte complex (PEC) caused the water contact angle to reduce that showed an increase in the hydrophilicity. Protein adsorption, platelet adhesion, and thrombus formation were all reduced by the immobilization of HEP (Lin et al. 2004).

### **2.2.3.2. Increasing Hydrophilicity**

It is commonly accepted that the driving force for adsorption of proteins onto the surfaces is primarily via hydrophobic interactions. Hydrophobic interactions are mainly entropic interactions and caused by minimized surface area of water droplets surrounding the protein via the reduced mobility of water molecules. Similarly, hydrophobic amino acid side chains are also oriented away from water, which in turn minimizes their interaction with water (Jahnig, 1983). Consequently, interaction of a hydrophobic patch on the surface of the protein and a hydrophobic region on the surface is followed by adsorption. It is hypothesized that hydrogen bond formed between the hydrophilic surface and water may decrease protein adsorption since proteins must first displace water molecules on the surface which requires significant amount of energy, thus, it does not occur instantaneously. Various studies exist in the literature which concentrated on the strategies to increase the hydrophilic character of the surfaces. For example, Woffinfin and Hoenich (1988) decreased the degree of complement activation and leukopenia in blood associated with the use of cellulosic membranes by adjusting the ratio of hydrophobic segments. Nie et al. (2004) improved the anti-fouling properties and blood compatibility of poly(acrylonitrile-co-maleic acid) (PANCMA) membranes by the immobilization of poly(ethylene glycol)s (PEG) on the membrane surface. They found that the reactive carboxyl groups on PANCMA membrane surface could be conveniently conserved into anhydride groups then esterified with PEG. The hydrophilicity and blood compatibility of the acrylonitrile-based copolymer membranes



were improved with the immobilization of PEG. Compared with the original PANcMA membrane, the membrane immobilized with PEG showed a three-fold increase in a bovine serum albumin (BSA) solution flux, a 40.4% reduction in total fouling, and a 57.9% decrease in BSA adsorption (Nie et al. 2004).

Coating, blending, grafting techniques were commonly used to introduce a hydrophilic character into traditional hydrophobic membranes. These techniques are discussed below.

**Physical Coating** is the oldest and simplest method for improving the surface properties of a membrane. In this technique, a hydrophobic membrane is coated with a hydrophilic polymer. For example, in the study Brink's et al. (1993), PSF ultrafiltration (UF) and microfiltration (MF) membranes were coated with two water-soluble polymers. Protein adsorption at the pore walls of the UF membranes was prevented, however, coating of the surface could not stop the plugging of the pores by the proteins. Ye et al. (2005) modified cellulose acetate membrane with the water-soluble amphiphilic 2-methacryloyloxyethyl phosphorylcholine (MPC) and its copolymer butyl methacrylate (BMA). PMB80 (MPC: BMA=80:20 mol %) was coated on the cellulose acetate (CA) hollow fiber membrane surface during the phase inversion of the dope solution by using a PMB 80 solution as inner coagulant. The CA/PMB80 coated hollow fiber membrane showed low membrane fouling property compared with the unmodified CA hollow fiber membrane, due to the low protein adsorption property of the PMB80. Modification of the surfaces by coating with hydrophilic polymers has generally been found not a successful approach due to desorption of the coating easily in a short period of time after its initial use (Sun et al. 2003).

**Blending** is another simple modification technique used to increase hydrophilic character of the hydrophobic membranes. In this technique, a hydrophilic polymer is directly added into the casting solution and it is distributed evenly both on the membrane surface and within the matrix. Many studies exist in the literature which utilizes this approach for modifying membrane surfaces (Sun et al. 2003). Ward et al. (1998) modified the hydrophobic PSF membrane by blending it with polyvinyl pyrrolidone (PVP). They found that surface hydrophilicity increased with the increased PVP content in the solution. Hasegawa et al. (2001) prepared a polymer blend composed of polysulfone and MPC polymer (PSF/MPC polymer) and obtained asymmetric porous membrane by the dry/wet phase inversion technique. It was found that amount of protein adsorbed on the PSF membrane from plasma was reduced by the

addition of the MPC polymer and platelet adhesion was also effectively suppressed on the PSF/MPC polymer membrane. In addition, the reduction in permeabilities due to protein fouling was found to be smaller with blend membranes. Ye et al. (2002) improved the blood compatibility of CA by blending it with PMB30 (MPC and its copolymer BMA). Both the original CA and the blend membrane had an asymmetric and porous structure. The mechanical properties and solute permeability of the CA/PMB30 blended membrane were controlled by preparation conditions. These membranes showed good permeabilities for water and solutes in comparison with the original CA membrane. Mahlicli and Altinkaya (2009) prepared urease immobilized cellulose acetate (CA) membranes by directly blending urease into the casting solution. The effects of enzyme on the protein adsorption, solute transport rates and mechanical properties were investigated through static adsorption and permeation experiments, mechanical tests and structural characterization by scanning electron microscope. It was found that the urease immobilization improved transport rates for all model solutes, uric acid, creatinine and urea, over the regular CA membrane as seen Figure 2.4. In addition, the decrease in the transport rates due to the protein fouling was found lower. This was attributed to reduced protein adsorption capacity of urease immobilized CA membrane compared with that of the regular CA membrane.

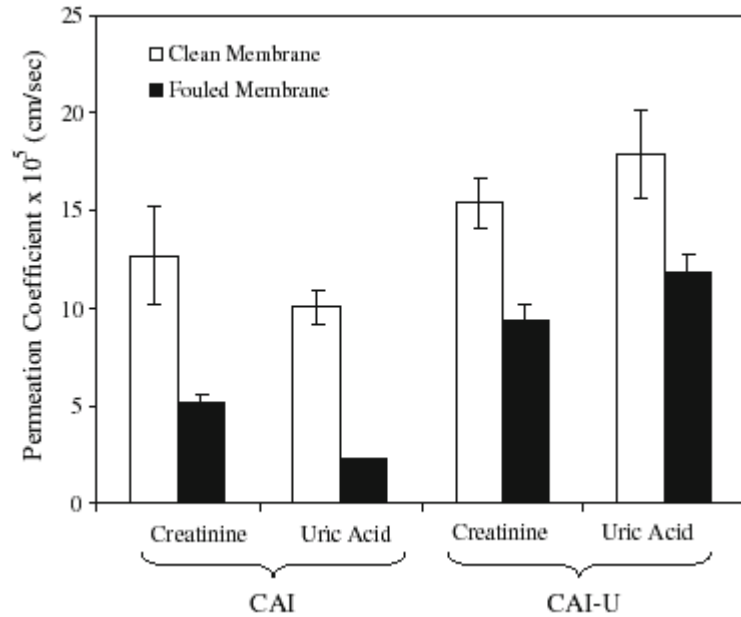
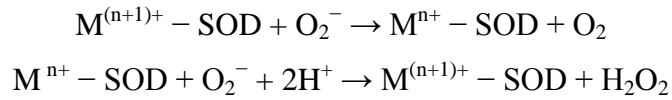


Figure 2.4. The change of concentration of urea in donor compartment with respect to time. The symbols denote experimental data and lines correspond to model predictions (CAI: unmodified cellulose acetate membrane, CAI-U: urease immobilized cellulose acetate membrane) (Source: Mahlicli and Altinkaya, 2009)

### 2.3. Oxidative Stress

In human body, there is an oxidative balance between the antioxidant defence and free radicals. Antioxidants react with reactive oxygen species (ROS) in biological systems and prevent their harmful effects on the cells. During hemodialysis, significant amount of reactive oxygen species is generated due to leukocyte activation (Deppich et al., 1998). These free radicals react with the proteins and lipids in blood causing oxidative stress.

Superoxide anion is the most effective radical in the biological system and causes cell damage. It is converted to H<sub>2</sub>O<sub>2</sub> which is less harmful than O<sub>2</sub><sup>·-</sup> by superoxide dismutase (SOD) enzyme and catalase (CAT) enzyme deactivates the hydrogen peroxide (H<sub>2</sub>O<sub>2</sub>) by converting to water and oxygen. Therefore, SOD is the most potential antioxidant enzyme in spite of its short plasma half life of 6 minute (Çelik et al. 2007). The SOD-catalysed dismutation of superoxide anion into oxygen and hydrogen peroxide may be written with the following half-reactions:



Oxidative stress causes a harmful effect on the biochemical components in blood such as lipids, proteins, carbohydrates and nucleic acids (Floccari et al. 2003). Lipids are the most important biochemical component of the blood cell membrane and they are degraded by oxidative action of ROS. These degraded lipids release malondialdehyde (MDA) which is the end product of lipid peroxidation. MDA reacts with deoxyadenosine and deoxyguanosine in deoxyribonucleic acid (DNA). Therefore, the level of 8-hydroxy-2-deoxyguanosine on DNA of leukocytes of uremic patients is higher than healthy population (Floccari et al. 2003). Proteins are also susceptible to the oxidative action of ROS. Oxidation of proteins caused forming high molecular weight oxidation protein products that reduced the hemodialysis clearance (Floccari et al. 2003).

## 2.4. Methods to Prevent Oxidative Stress

Complications caused by hemodialysis induced oxidative stress motivate the researchers working in this field to further improve the biocompatibility of the membranes. The techniques proposed for this purpose are to blend, coat or immobilize antioxidants into/onto the membranes. Vitamin E is the most commonly used natural agent with anti-oxidative and anti-inflammatory properties to decrease the oxidative stress in uremic patients during hemodialysis (Clermont et al. 2001, Reno et al. 2005, Yamamoto et al. 2007). For instance, Clermont et al. (2001) searched if the vitamin E coated synthetic hemodialysis membrane, AN69, protect the hemodialysis patient against oxidative stress. They measured the level of vitamin C and ascorbyl free radical (AFR)/vitamin C ratio as an indicator for oxidative stress and found a decrease in vitamin C and AFR/vitamin C ratio as a result of coating the membrane with vitamin E. Yamamoto et al. (2007) used vitamin E coated polysulfone dialysis membrane and measured the level of 2-methyl-6-p-methoxyphenylethynylimidazopyrazinone (MPEC) as superoxide anion probe. They found that for decreasing the MPEC level, a large amount of vitamin E should be coated onto PSF membrane. They also examined the possibility of using vitamin E coated PSf membrane where vitamin C is administrated to

uremic patient during hemodialysis treatment. They obtained higher antioxidant property with a smaller amount of vitamin E coating by administrating vitamin C.

In another study by Reno et al. (2005), vitamin E was used to improve the surface properties of poly (D,L)-lactic membrane by blending into the polymer. They found that blending vitamin E increases the hydrophilicity of the membranes.

Kung and Yang (2006-a,b,c, 2007) used conjugated linoleic acid (CLA) which is found in dairy products and ruminant meats and can scavenge free radicals, inhibit both platelet aggregation and blood coagulation. They immobilized CLA onto some industrial hemodialysis membranes such as CA, PAN, PSF and investigated the influence of CLA on hemocompatibility of the membranes. In the case of CA membrane, they investigated the covalent attachment of CLA on protein (BSA) adsorption, hematological parameters, blood coagulation time and the level of reactive oxidants in plasma. The results have shown that platelet adhesion and protein adsorption were reduced, coagulation time was prolonged and production of ROS decreased (Kung and Yang 2006-a). Similar results were obtained when they grafted CLA onto PAN (Kung and Yang 2006-b) or when CLA was covalently immobilized onto PSF membranes (Kung and Yang 2006-c, Kung et al. 2007). CLA immobilization onto PSF membrane inhibited not only production of ROS, but it also reduced endotoxin production measured with enzyme-linked immunosorbent assay (ELISA). Neelakandan et al. (2011) have chosen genistein as the modifying agent due its antioxidant and anti-inflammatory properties to modify poly(amide):poly(vinyl pyrrolidone) (PA:PVP/G) hemodialysis membranes. They pointed out that genistein-modified PA:PVP raised intracellular reactive oxygen species (ROS) levels and ROS level can be controlled by the immobilized genistein dosage.

There has also been interest in clinical methods such as administration of antioxidants by orally and intravenously to hemodialysis patient. For instance, Ferretti et al. (2008) studied intravenous administration of vitamin C to the hemodialysis patient. They compared plasma paraoxonase (PON1) activity, the levels of lipid hydroperoxides and AGE adducts in plasma of 42 hemodialysis patients before and after administration of vitamin C and found that vitamin C administration increases PON1 activity and decreases AGE and lipid hydroperoxides levels. Delfino et al. (2007) studied the effect of folic acid treatment to hemodialysis patients on the level of Homocysteine (Hcy) which is an indicator of oxidative stress, as increasing Hcy level in blood increases the oxidative stress. They found that folic acid treatment has significant

effect on adjusting plasma homocysteine levels and increasing total plasma antioxidant capacity. Candan et al. (2002) investigated the influences vitamin C and zinc administration on lipid peroxidation of erythrocytes and found that the lipid peroxidation decreased significantly with vitamin C and zinc administration. Stepniewska et al. (2006) searched the influence of glucose present in dialysate on antioxidant defense system. A group of hemodialysis patient was treated with regular dialyzing fluid and the other group was treated with the modified dialyzing fluid by adding glucose. It was found that modified dialysate solution improves the glutathione system reactions and antioxidant defence of erythrocytes.

The clinical studies have suggested that there is still a need for developing membranes with improved biocompatibilities. Poor biocompatibility causes 37% of the total mortality of dialysis patients (more than 1.5 million patients). In addition, modification method should be cost-effective since the reuse of hemodialysis membranes is forbidden in most countries (10 million \$/year in USA). Therefore, this thesis have proposed two strategies to improve biocompatibility of the PSF membranes through immobilization of three different biomolecules on the surface of these membranes. Heparin was selected for generating thromboresistant surfaces and immobilized through layer by layer deposition of polyethyleneimine (PEI) and alginate (ALG) layers on the support membrane. In previous studies, heparin was used alone to adsorb on positively charged polyelectrolytes for each alternating layer, on the other hand in this study , it was immobilized on the outermost surface of the assembly by blending with ALG. The scientific motivation of immobilizing HEP was to investigate its anticoagulant activity and biological properties when blended with another polyanion, ALG, as the outermost layer of layer by layer deposition.  $\alpha$ -lipoic acid (ALA) and superoxide dismutase (SOD)/catalase (CAT) enzyme couple were chosen as the other modifying agents to provide antioxidative properties to the PSF membranes. Both of these antioxidants have been used for the first time in order to improve biocompatibility of hemodialysis membranes. The motivation for selecting ALA is its excellent antioxidant capacity in quenching a number of free radicals in both lipid and aqueous media (superoxide, singlet oxygen, hypochlorous acid, hydrogen peroxide, piperonylpicrylhydrazyl (DPPH)) and regenerating other antioxidants as well as its metal-chelating activity. SOD-CAT enzymes are known as the most important antioxidants in blood, they scavenge superoxide, the most harmful radical in blood,

thus, they were selected for the modification of PSF membranes with a biomimetic approach.

## CHAPTER 3

### IMMOBILIZATION OF BIOMOLECULES

Introduction of biomacromolecules into membranes may impart not only the hydrophilicity but also new functions. A critical review of the literature indicates that a variety of methods reported for biomolecule immobilization may be subdivided into two general classes as chemical where covalent bonds are formed with the biomolecule, and physical methods where weaker interactions with the biomolecules are involved (Bailey and Ollis 1986) .

#### 3.1. Chemical Methods

In chemical immobilization methods, biomolecules are attached to the membrane by covalent bonding which is sufficiently strong that bonded molecule can not easily desorb. However, the procedure is usually complicated and relatively expensive (Sun et al. 2003). Kung et al. (2006-a,b,c, 2007) covalently bonded conjugated linoleic acid (CLA) onto cellulose acetate (CA), polyacrylonitrile (PAN) and PSF for decreasing oxidative stress and blood coagulation. For immobilization the CLA first activated with 1-ethyl-3-(3-di-methylaminopropyl) carbodiimide (EDC) was covalently bonded with the -OH group of CA membrane as seen in Figure 3.1. The surface density of CLA attained was determined as  $17.9 \text{ nmol.cm}^{-2}$

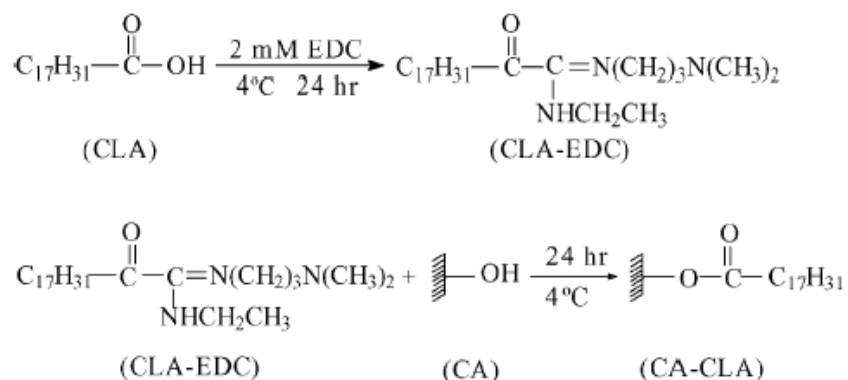


Figure 3.1. The reaction schemes for esterification of conjugated linoleic acid to CA membranes. (Source: Kung and Yang, 2006-a)



The comparison of XPS spectra of CA and CA-CLA membranes indicated the attachment of CLA onto CA membrane as shown in Figure 3.2. (Kung and Yang 2006-a)

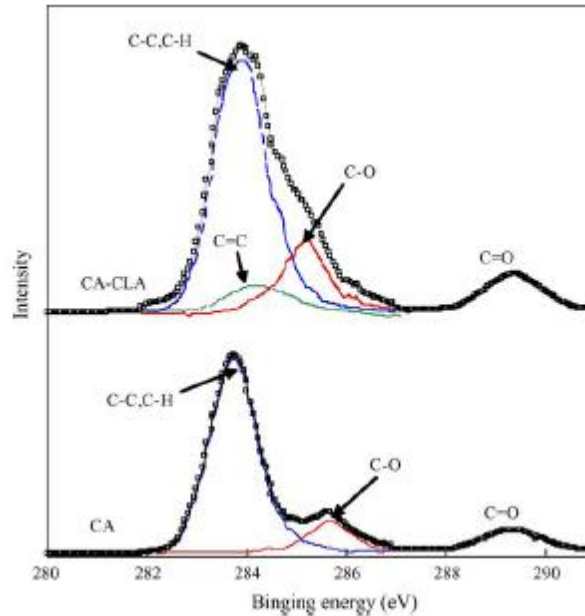
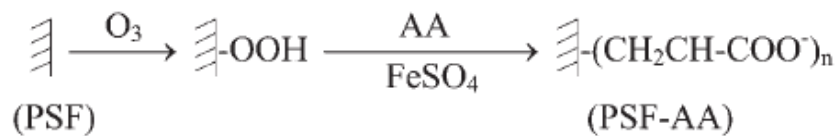


Figure 3.2. XPS spectra of CA and CA-CLA membranes  
(Source: Kung and Yang, 2006-a)

To attach CLA onto PSF membranes, PSF surface was first activated with ozonation treatment and grafting of acrylic acid (AA) as shown below (Kung and Yang 2006-c, Kung et al. 2007).



Then, CLA was grafted onto modified PSF (PSF-AA) membrane using 1,3 propanedial as a crosslinking agent.

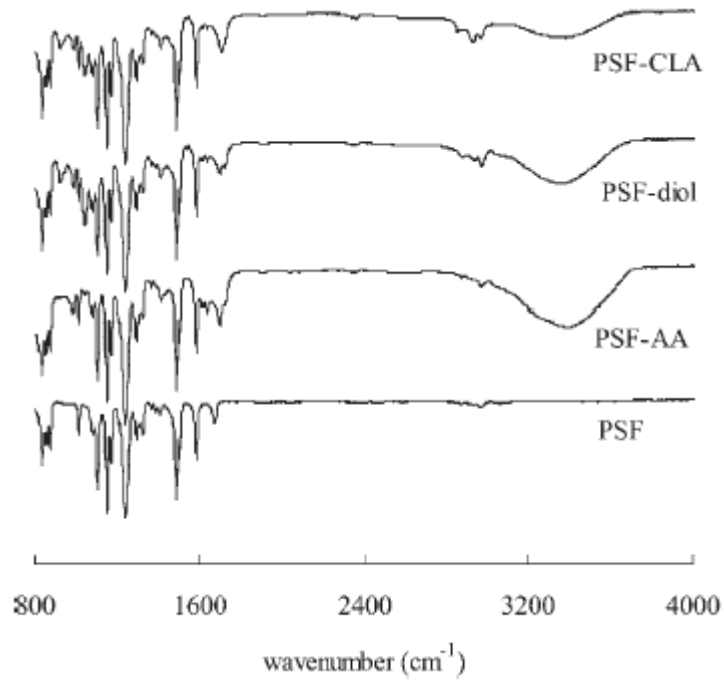
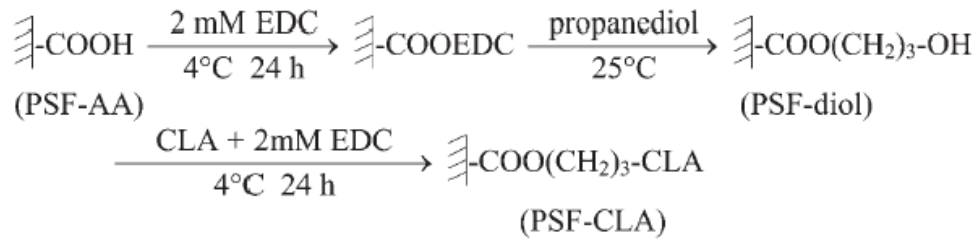


Figure 3.3. FT-IR spectra of unmodified PSF and modified PSF membranes  
(Source: Kung et al., 2007)

Each modification step was followed with the FTIR spectra as demonstrated in Figure 3.3. Figure 3.4 shows that platelet adhesion on the CLA immobilized PSF was lower than that of CLA adsorbed and unmodified PSF.

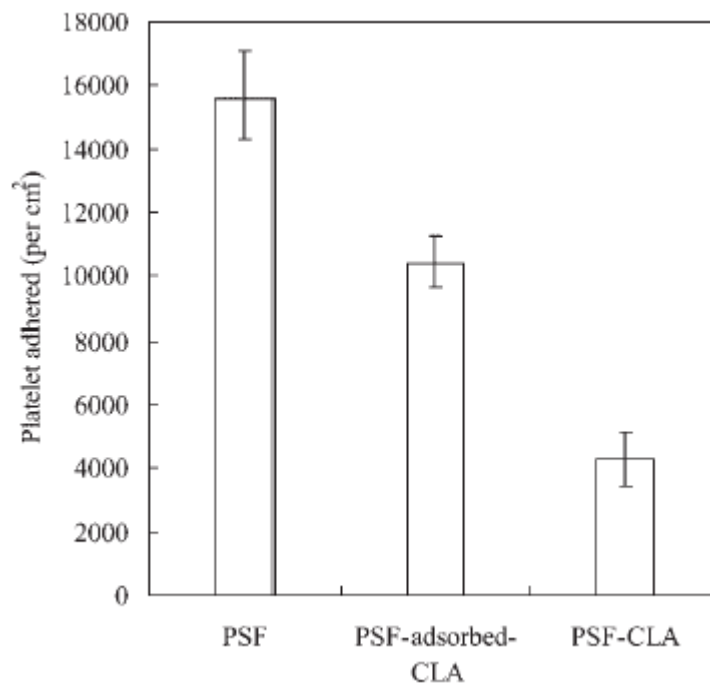


Figure 3.4. The platelet adhesion of unmodified PSF and modified PSF membranes  
(Source: Kung et al., 2007)

In another study of Kung and Yang (2006-b), PAN membrane was grafted with CLA via esterification with 1,3-propanediol in order to increase the hemocompatibility of the membrane. Using FTIR and XPS they discerned that only PAN-CLA showed C=C peak which was from CLA.

Park et al. (2006) modified the PSF by grafting PEG onto the membrane. They used chloromethylation method to create functional groups on PSF as shown in Figure 3.5.

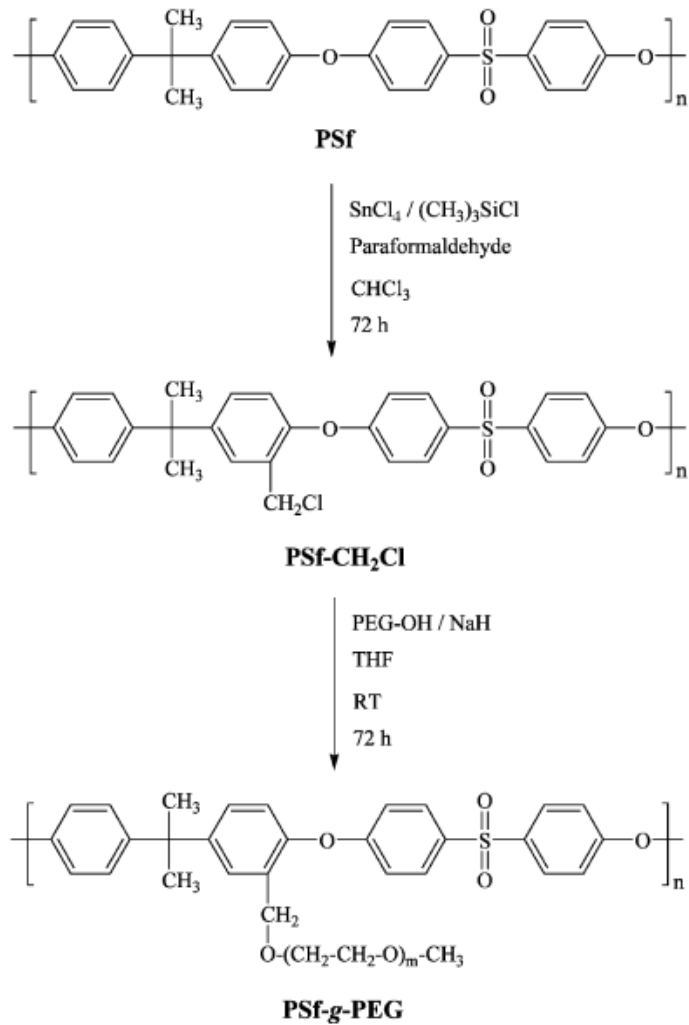


Figure 3.5. Synthesis route for chloromethylation of PSf and the formation of PSf-g-PEG. (Source: Park et al., 2006)

Ulbricht et al. (1996) functionalized the surface of PSF membrane for covalent immobilization of biomolecules via heterogeneous photoinitiated graft polymerization with acrylic acid (AA) as a carrier of reactive groups. They used the modified PSF surface for attachment of protein (BSA), enzyme (invertase), antibody-enzyme conjugate and a peptide and found high binding capacities, up to 40 fold compared with unmodified PSF.

Miyata et al. (1996) activated ethylene-vinyl alcohol copolymer (EVA) membrane with cyanuric acid for covalent immobilization of urease. Yang and Lin (2001) also covalently bonded the urease onto the PAN hollow fiber dialyzer by using glutaraldehyde and found that urease immobilized PAN dialyzer increased the permeation of urea.

## **3.2. Physical Methods**

Biomolecule immobilization by physical methods has the benefit of applicability to many biomolecules with high loading. Since, no reagents and only a minimum of activation steps are required, this method may provide relatively small perturbation of biomolecule (especially if biomolecule is enzyme) native structure or function. Physical methods may be subdivided into two general classes i) physical adsorption and ii) ionic binding due to the interaction between biomolecule and support.

### **3.2.1. Physical Adsorption**

In this method, biomolecules bond to the support with the attractive Van Der Waals forces. Despite the physical adsorption has the weakest binding force, it is the easiest preparation method, and thus used for immobilization of biomolecules onto hemodialysis membranes. For instance, Yamamoto et al. (2007) used four vitamin E-coated polysulfone (PSF) dialysis membrane containing 0, 26, 74, 160 mg.m<sup>-2</sup> amounts of vitamin E in order to see its effect on decreasing oxidative stress. Vitamin E coated membranes were prepared by Asahi Kasei Medical using the following method: The hollow part of the membranes was filled with dilute vitamin E alcoholic water solution. After removing the remaining solution, the membranes were dried by air. They measured the level of oxidative stress by using a superoxide probe of 2-methyl-6-p-methoxyphenylethynylimidazopyrazinone (MPEC) by the optical fiber method and found that vitamin E coating density must be over 74 mg.m<sup>-2</sup> to eliminate O<sub>2</sub><sup>-</sup>.

Reno et al. (2004) coated polystyrene (PS) surface with Vitamin E in order to see the effect on granulocyte adhesion and protease (MMP-9) release that are the indicators of oxidative stress. Using optical microscopy, flow cytometry, respiratory burst and substrate zymography they determined that vitamin E coated PS induced an increase in granulocyte adhesion and protease (MMP-9) release.

### **3.2.2. Ionic Binding**

In this method; the biomacromolecule is attached to the surface by ionic interactions. The method simply consists of depositing a layer of a charged

biomacromolecule by sorption from an aqueous solution onto a support membrane which should have opposite charge on its surface with the charge of biomacromolecules.

Recently, layer by layer (LBL) self-assembly method has been used for immobilizing biomacromolecules by ionic interactions. The principle of this method is the charge inversion of a polymeric surface by immersing the surface in a solution of oppositely charged polyelectrolytes (Yu et al. 2007). The layer of adsorbed macromolecules serves at the same time as an anchoring material on the surface and as an active component for the biomacromolecule capture by charge interactions. For the immobilization, the modified support is put into contact with a solution containing the bio-macromolecule (proteins, their fragments, or any bio-active species) that has charges opposite to those of the adsorbed macromolecule layer. This leads to an immobilization of the proteins by charge interactions, as there are always both types of charges on protein molecules. The support membrane does not need to be made of polyelectrolytes since limited number of charges are required on the membrane (or pore) surfaces. Most of the membranes have negative surface charges, therefore, a hydrophilic polymer containing protonated or/and quaternized ammonium groups are chosen as the polycationic macromolecule for the anchoring to the membrane surface. The polycations that can be commercially available are polyethyleneimine, polyvinylamine, polyallylamine, polyvinylbenzyl trimethyl ammonium chloride, polyacrylamide with quaternary amine groups, polyvinyl-4 pyridine, diethylaminoethyl polysaccharides or chitosan. Among them, polyethyleneimine is the most convenient one due to its availability and well-controlled quality.

The formation and properties of polyelectrolyte multilayer are strongly influenced by pH of the solution since it determines the ionization of surface groups and therefore the final surface charge density (Guzey et al. 2006). The ionic strength of the solution also influences the strength and range of intra- and inter-molecular electrostatic interactions and hence multilayer film formation, structure and thickness. The magnitude and range of electrostatic interactions between a polyelectrolyte and a support decrease as the ionic strength of the solution increases because of the accumulation of counter-ions around the surfaces. The presence of salt during multilayer buildup can affect the composition, structure and thickness of the adsorbed polymer layers. In the presence of salt, polyelectrolytes often form thicker layers because they have a more compact chain conformation in solution (due to weaker intra-

molecular repulsion) and because the weaker electrostatic attraction between charged polyelectrolyte and surface groups allows post-adsorption molecular rearrangements as seen in Figure 3.6. The chain length, charge density, charge distribution, rigidity, and degree of branching of polyelectrolytes are other factors that influence their tendency to adsorb on the surfaces and the characteristics of the adsorbed layers formed, such as thickness, structure, porosity and environmental sensitivity. It is important to use a polyelectrolyte concentration that is high enough to completely saturate the surface of the charged particles, and that will reverse the surface charge of the previous layer. The amount of polyelectrolyte needed to saturate the surface and the final charge on the surface depends on the molecular characteristics of the polyelectrolyte used such as chain length, conformation, charge density, and flexibility.

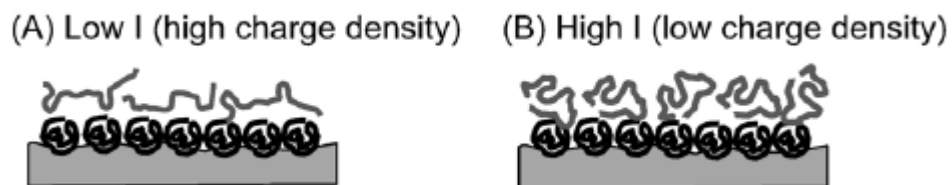


Figure 3.6. Effect of ionic strength on layer thickness and polymer orientation at the substrate surface; (A) at low ionic strength, and (B) at high ionic strength (Source: Guzey et al., 2006)

The layer by-layer self-assembly of polyelectrolytes first studied experimentally by Decher (1997) is an easy method and allows to develop biologically active surfaces by attaching bioactive molecules, such as drugs, enzymes, DNA, or proteins on various supports. For example, Zhang et al. (2008) immobilized model protein fibrinogen onto the brushed surfaces by self-assembly-monolayer (SAM) in order increase the blood compatibility. They compared the effect of 5 types of SAM on the protein adsorption from blood plasma, platelet adhesion, and blood clotting. Nguyen et al. (2003) used this method for immobilizing the bio-macromolecules onto the surface of PSF membrane and different industrial hemodialysis membranes. The PAN membrane that was used in that work is an industrial hemodialysis membrane, AN69, and has slight negative charges. As PSF membrane doesn't have any charges on its surface, it was first sulphonated to generate negative charges ( $\text{SO}_3^-$ ) on the membrane. Negatively charged membrane was immersed into a polycation solution, polyethylenimine (PEI), at the pH

8.0 in order to obtain a positively charged layer on the membrane as seen in Figure 3.7. The glucose oxidase and heparin were immobilized onto PEI layer for improving the performances of glucose biosensor and hemodialysis membrane, respectively. The results have shown that this enzyme immobilized membrane had high enzyme activity which was explained by the fact that high amount of enzyme was bonded on the intermediate PEI layer. The good properties of the immobilized enzyme were explained by the hydrophilicity of the intermediate polyelectrolyte layer and its high density in sites for enzyme binding.

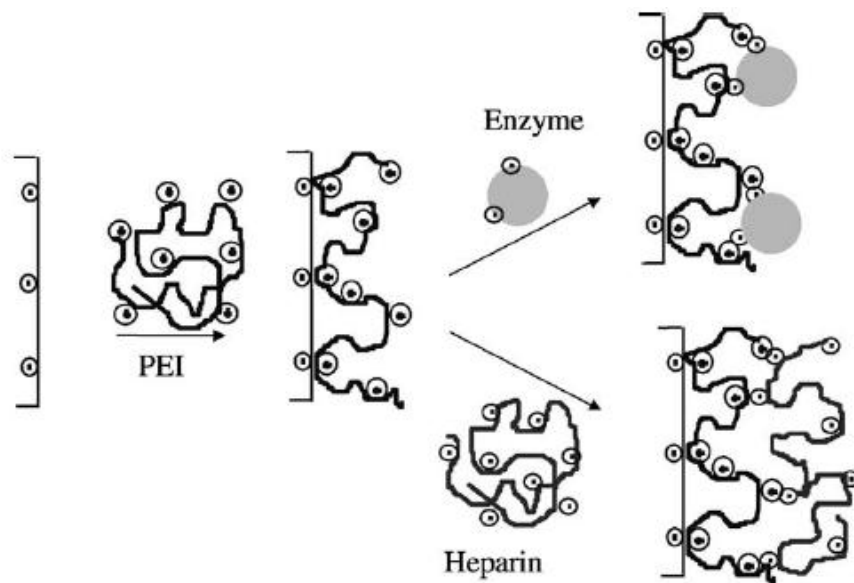


Figure 3.7. Schematic representation of the mechanism of adsorption of the PEI intermediate layer and immobilization of enzyme and heparin (Source: Nguyen et al., 2003).

In another study, Nguyen et al. (2004) investigated the mechanism of self-assembly immobilization of glucose oxidase onto the sulfonated polysulfone (SPSF).

Yu et al. (2007) studied the deposition of polysaccharide chitosan (CS)/dextran (DS) self-assembled multilayers on poly(tetramethylene adipate-co-terephthalate) (PTAT) membrane via LBL method for improving the hydrophilicity and hemocompatibility of PTAT membrane. They characterized the membranes by XPS, FE-SEM, AFM, contact angle measurements and human platelet adhesion, human plasma fibrinogen (HPF) adsorption and blood coagulation times. They found that chitosan/dextran sulfate polyelectrolyte multilayer has been successfully immobilized onto the aminolyzed PTAT membrane surface in a layer-by-layer assembly manner and



the membranes with DS as the outmost layer could resist the platelet adhesion and human plasma fibrinogen (HPF) adsorption, thereby prolonging effectively the blood coagulation times. However, PTAT membranes deposited with four bilayers of chitosan and dextran sulfate with dextran sulfate as the outermost layer cannot improve hydrophilicity.

In this study, the biomolecules were noncovalently attached by modifying the surface of the support membrane with a single or multilayer assembly of the polyelectrolytes. Although covalent attachment is the most commonly used method for immobilizing biomolecules on the blood contacting surfaces, modification with polyelectrolytes is a versatile, gentle and easy surface modification method for immobilization of functional molecules. Moreover, this method is conducted in an aqueous solution under mild ambient conditions which minimize the loss in the activity of biological agents. To construct the layer by layer self assembly of the polyelectrolytes, polyethyleneimine (PEI) and alginate (ALG) were chosen as positively and negatively charged polyelectrolytes due to their hydrophilic and biocompatible properties. Anticoagulant agent, heparin, was immobilized only on the outermost surface of the LBL assembly by blending with ALG. The intermediate layers were prepared with the alternate deposition of the PEI and heparin free ALG. Polyethyleneimine, was used as anchoring layer between other biomolecules ( $\alpha$ -lipoic acid (ALA) and superoxide dismutase (SOD)/catalase (CAT) enzyme couple) and negatively charged support membrane. This method is unique in that both antioxidants aren't attached on the membranes covalently through a complex chemistry which causes a significant decrease in the antioxidant activity due to their short half lives. In addition, the method allows site-specific binding of the carboxylic group of ALA to the amine group of PEI through electrostatic interactions, consequently, the active cyclic disulphide bond of ALA becomes available on the surface. For a comparison, SOD/CAT enzymes were also immobilized on plasma treated PSF membrane surface through covalent bonding. The influence of immobilization method on the conformation and activity of SOD-CAT enzymes has also been studied which has not been investigated previously.

## CHAPTER 4

### EXPERIMENTAL

#### 4.1. Materials

Polysulfone (PSF) with a molecular weight of 26000 g.mol<sup>-1</sup>, 1,2-Dichloroethane, chlorosulfonic acid, sodium dodecylsulfate (SDS) were purchased from Aldrich, 1-methyl-2-pyrrolidone (NMP) with a purity of >> 98% and micro BCA protein assay reagent kit were purchased from Fluka and Thermochemical, respectively. Heparin, bovine serum albumin (MW 65000), urea, vitamin B<sub>12</sub>, lysozyme, 2,2-diphenyl-1-picrylhydrazyl, alpha-lipoic acid, nitro blue tetrazolium, L-methionine, EDTA and riboflavin which are used for determining superoxide dismutase activity, and hydrogen peroxide which is used for measuring catalase activity and the enzymes that are superoxide dismutase and catalase were all supplied by Sigma. Cell viability kits, thiazole orange (TO) and propidium iodide (PI), and the monoclonal antibodies, PAC1, FITC and CD62 PE, used for determining of platelet activation were purchased from Becton Dickinson Immunocytometry Systems. H<sub>2</sub>NaPO<sub>4</sub> and Na<sub>2</sub>HPO<sub>4</sub> from Fluka and Riedel, respectively. Water used in the experiments was distilled ion-exchanged water. Branched polyethylenimine (PEI) (MW 750000) which contains 25% of tertiary amine groups, 50% of secondary amine groups, and 25% primary amine groups and sodium alginate were purchased from Aldrich-Sigma.

Phosphate buffer solution was prepared with 0.05 M H<sub>2</sub>NaPO<sub>4</sub> and Na<sub>2</sub>HPO<sub>4</sub>. It is buffered with saline for *in vitro* studies, which has a final concentration of 137 mM NaCl, 10 mM Phosphate, 2.7 mM KCl, and a pH of 7.4.

Whole blood was taken from a healthy single donor and the ethics committee approval for the experiments with blood was obtained.

## 4.2. Preparation of the Membranes

### 4.2.1. Preparation of Support Membranes

The conventional PSF has no functional groups and charges, thus, it was first modified by sulfonation to induce negatively charged groups ( $\text{SO}_3^-$ ) before preparing the support membrane as shown in Figure 4.1. For sulfonation, PSF was dissolved in dichloroethane (DCE) to obtain a 7.5 wt. % solution. Similarly, a solution of chlorosulfonic acid diluted in DCE (10 wt. %) was prepared and added drop-wise to the PSF solution. After mixing for 3 hours at 24 °C, modified polymer was recovered by precipitation in 50 ml of methanol. Ion exchange capacity (IEC) of sulfonated polysulfone (SPSF) was determined as  $0.9 \text{ meq.g}^{-1}$  using a method given in the study of Blanco et al. (2002).

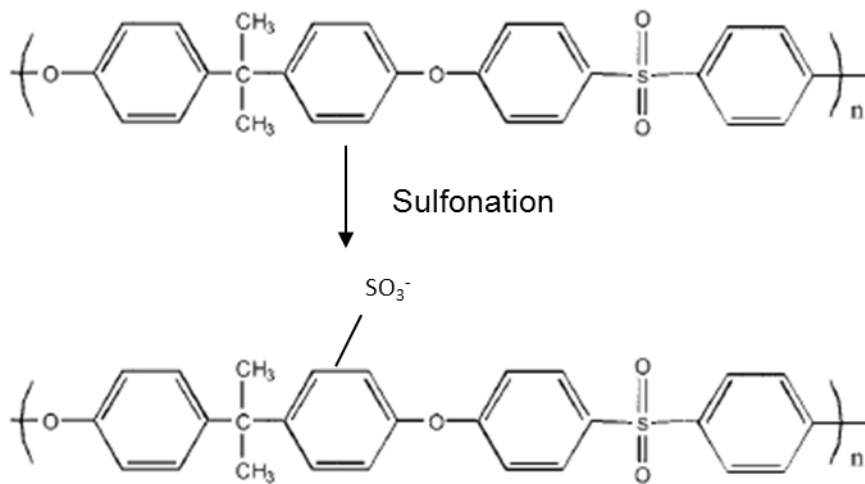


Figure 4.1. Sulfonation of polysulfone

(Source: Blanco et al., 2002) .

To prepare the PSF membranes, a solution of 20 wt.% of PSF N-methyl pyrrolidone was cast onto a 10cm x 24cm glass substrate with the aid of an automatic film applicator (Sheen Instrument Ltd., model number:1133N) at a speed of  $100 \text{ mm.s}^{-1}$ . The initial thickness of the cast film was adjusted by a four sided applicator with a gap size of  $150 \text{ }\mu\text{m}$ . Following casting, the support was transferred into an environmental chamber (Angelantoni Industrie, Italy, Challenge Series, model number:CH250) in which the solution was dried for 2 minutes under  $25 \text{ }^\circ\text{C}$  temperature

and 40 % relative humidity. Then, it was immediately immersed in a coagulation bath for 18 hour, and rinsed with pure water for 1 hour. The membranes were allowed to dry further for a period of 72 hours in a vacuum oven maintained at 100 °C. They were then kept in a desiccator until their use. The polysulfone-sulfonated polysulfone (PSF-SPSF) blend membranes were prepared from a solution at 10wt.% of PSF and 10wt.% of SPSF in NMP using the same protocol.

#### **4.2.2. Preparation of Heparin Immobilized Polysulfone Membrane**

Heparin immobilization was carried out by first depositing polyelectrolytes on the negatively charged PSF-SPSF blend membrane. First, the PSF-SPSF membrane was dipped in a 0.1 mg.ml<sup>-1</sup> of cationic macromolecule, polyethyleneimine (PEI) solution for 10 minutes. The pH of the branched PEI solution was adjusted by HCl to a value of 8, under its isoelectric point (8.8) (Erol et al., 2006), to obtain a sufficiently protonated form with 86% degree of ionization (calculated by Henderson-Hasselbalch equation), hence, to ensure its strong bonding on the negatively charged membrane surface through electrostatic attraction (Nguyen et al., 2004). To remove excessive PEI on the surface of the self-assembled layer, the membrane was rinsed with 500 ml water for 10 minutes and then immersed in a 1 mg.ml<sup>-1</sup> of ALG solution at pH 7.4 and 4 °C for 24 hours. Loosely-bound ALG was washed away under same conditions as described above. The dipping in alternating PEI and ALG solutions and rinsing after each removal were repeated 5 times to build multilayer assembly on the support membrane. Heparin immobilized membranes were prepared by blending HEP with ALG in the depositing solution where HEP concentration was varied as 15 wt.% and 45 wt.%. To minimize the use of heparin, it was immobilized only on the outermost layer of the 5 bilayer assembly, the intermediate layers were formed by alternating deposition of PEI and ALG layers. Amount of PEI released from the LBL assembly was determined spectrophotometrically by detecting the cuproammonium complex formed with copper (II) ion (Ungaro et al., 2003).

### 4.2.3. Preparation of Alpha-Lipoic Acid Immobilized Polysulfone Membrane

The method used for immobilizing ALA is based on initially adsorbing positively charged, hydrophilic polyelectrolyte, PEI, on the negatively charged membrane surface. For this purpose, the PSF-SPSF membrane was dipped in a 1 mg.ml<sup>-1</sup> of PEI solution (pH=8) for 10 minutes. To remove excessive PEI on the surface, the membrane was rinsed with 500 mL water for 10 minutes and then immersed in a 1 mg.ml<sup>-1</sup> or 5 mg.ml<sup>-1</sup> of ALA solution in 5% ethanol in PBS (pH:7.4) for 30 minutes at room temperature. The amount of ALA remained in the solution at the end of immobilization was determined using a UV spectrophotometer (Perkin Elmer Model No: Lambda 45). Figure 4.2 shows the site-specific binding of the carboxylic group of ALA to the protonated amine group of PEI through electrostatic interactions. This method allows the cyclic disulphide bond, which forms the active site of ALA, to become free on the surface of the membrane.

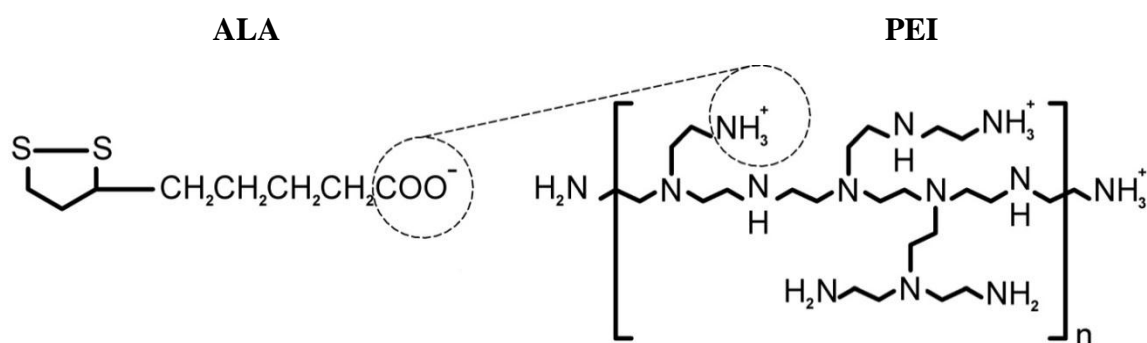


Figure 4.2. Structures of PEI and ALA and their possible ionic complexation

#### **4.2.4. Preparation of Superoxide Dismutase-Catalase Immobilized Polysulfone Membrane**

The SOD-CAT enzyme couple was immobilized either on a plasma treated PSF membrane or PEI deposited PSF-SPSF membrane. Immobilization of SOD and CAT onto plasma treated PSF membrane occurred with covalent bonding between amine groups on the surface and carboxylic groups of enzymes. On the other hand, the immobilization of enzymes onto PEI modified surface occurred via physical (ionic) bonding.

##### **4.2.4.1. SOD-CAT Immobilization onto the PEI Deposited PSF-SPSF Membranes**

In this method, enzymes (SOD, CAT or SOD/CAT) were immobilized onto the sulfonated polysulfone membrane via physical (ionic) bonding between negatively charged enzyme and positively charged PEI located on the sulfonated polysulfone membrane (PSF-SPSF). The PSF-SPSF support membrane was first dipped in a 0.1 wt. % PEI solution for 10 minutes. In order to obtain a sufficiently protonated form of PEI the pH of PEI solution was adjusted by hydrochloric acid (HCl) to a value of 8.0 that is under the pI of PEI (8.8) (Erol et al., 2006; Nguyen et al. 2004). After thorough washing to remove the excess polyelectrolytes, the membrane was immersed in a solution of 0.1-1.0 mg.ml<sup>-1</sup> of SOD and/or CAT at pH 7.4 for 24 hours at 4 °C. The isoelectric point of SOD and CAT enzymes are 4.95 and 5.4, respectively, and they are highly negatively charged at immobilization pH (pH 7.4). Therefore, ionic bonding occurs between the negatively charged carboxylic groups (carboxylate ions) of enzymes and protonated amine groups of polyethyleneimine (PEI) as shown in Figure 4.3.

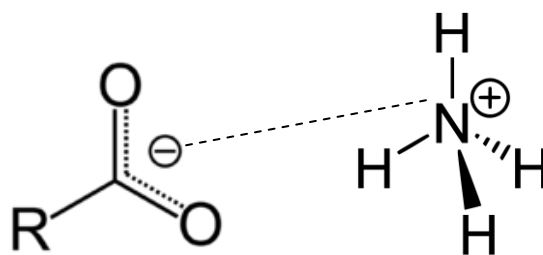


Figure 4.3. Schematic representation of ionic bonding between negatively charged carboxylic groups of enzymes and protonated amine groups of polyethyleneimine.

#### 4.2.4.2. SOD-CAT Immobilization onto the Plasma Treated PSF Membranes

The preparation of the membranes was completed in three steps: PSF membrane preparation, plasma treatment and immobilization of SOD and CAT enzymes. Polysulfone membranes were modified by means of plasma polymerization (PlzP) of ethylenediamine (EDA) under various conditions including plasma system (LF or RF), discharge power (25–150W) and exposure time (10–30 min). Experiments were conducted in Food Engineering Department at Hacettepe University, Ankara. PICO type LF and RF plasma equipments were supplied from Diener Electronics GmbH+ Co (Germany). The plasma chambers were stainless steel (150mm radius and 320mm length). A 40 kHz low-frequency generator (power range 0–200W) and a 13.6MHz radio-frequency generators (power range 0–100W) were used to sustain the plasmas in the reactors. Plasma polymerization was carried out in the fully closed and semi-automatic system. The plasma procedure was carried out in the same way for both LF and RF plasma systems. The membranes were placed on to the ground electrode in the middle of the reactor. At plasma generation, firstly low pressure was created in a recipient by means of a vacuum pump (Trivac, Germany). At a pressure of approximately 0.1 mbar, monomer EDA vapor was fed into the chamber and allowed to flow at a special rate from 0.1 mbar to 0.3 mbar. Then, plasma power was adjusted and the membranes were exposed to glow-discharge. At the end of the process, the plasma generator was turned off automatically and monomer inlet was closed manually. The plasma system was fed with argon gas for 10 min. and then placed in 0.1 mbar vacuum

pressure for 15 min. Argon feeding and vacuum applications were applied to deactivate free radicals in the plasma atmosphere.

For immobilization of enzymes, the plasma treated membranes were immersed directly in a solution of 0.1-1.0 mg.ml<sup>-1</sup> of SOD or CAT at pH 7.4 for 24 hours at room temperature. The amount of immobilized SOD and CAT were analyzed with Bradford method which utilizes the principle of protein-dye binding (Bradford, 1976). Enzymes (SOD, CAT or SOD/CAT) were covalently immobilized onto the polysulfone membrane with amide bonding between carboxylic groups of enzymes and amine groups of plasma treated polysulfone membrane without using any intermediate chemical linker groups (Figure 4.4). Complex, wet chemical steps are not required to achieve protein binding through linker-free immobilization (Bilek and McKenzie, 2010). Moreover, in some cases the reduction of stability of bioactive molecules due to usage of spacers may be prevented (Yin et al., 2009). Possible mechanism for the covalent binding of the enzymes is the strong binding sites of the lysine residues which is highly available in SOD and CAT (Bilek et al., 2010).

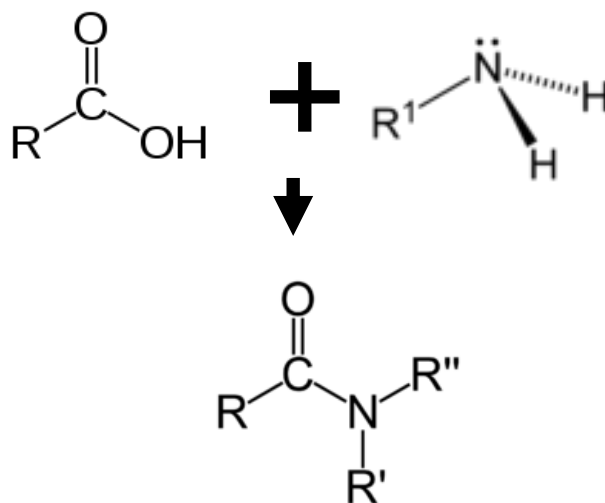


Figure 4.4. Schematic representation of amide bond between carboxylic groups of enzymes and amine groups of plasma treated polysulfone membrane.

### 4.3. Surface Characterization

Contact angle measurements for distilled water were carried out with Attension Optical tensiometer by means of a horizontal microscope, equipped with a video camera which is connected to a computer. The volume of liquid drop varied between 3 and 5  $\mu$ l.



The contact angle was calculated from the droplet screen image. Each reported contact angle measurement represents an average value of five separate drops on different areas of the membranes obtained from three different batches.

In order to identify the change in surface charge of the membrane due to polyelectrolyte deposition, the specific staining of the membrane was used. The negatively charged groups (carboxyl and sulfonate groups) on the membrane can form complexes with toluidine blue O dye at pH 10 and the positively charged groups (amine groups) with congo red at pH 7. The staining was performed by dipping the membranes in a 30 ppm solution of the dye dissolved in its associated solvent for ca. 30 min, followed by washing the sample with its solvent until the solvent became colorless (Yang and Lin, 2002). The amount of the charged groups on the membranes stained with toluidine blue O and congo red was determined spectrophotometrically in visible region (Aventes-Avemouse62). Intensity of each color resulting from adsorption of dyes on the membranes was reported as an average of 10 measurements.

The deposition of polyelectrolytes, HEP, ALA, SOD/CAT and conformation of proteins were followed by attenuated total reflectance Fourier transform infrared spectroscopy (ATR-FITR) (80 scans,  $4\text{ cm}^{-1}$  resolution, wavenumber range  $4000\text{-}650\text{ cm}^{-1}$ ) measurements. To show formation of multilayer self assembly, aqueous solutions of polyelectrolytes were prepared in the same manner as the multilayer dipping solutions and each solution was cast onto a ZnSe substrate and dried to leave a pure polymer film for FTIR characterization. The ALA or SOD/CAT immobilization and the conformation of the enzymes and adsorbed proteins were shown by directly analyzing the FTIR spectra of the membranes.

To determine the surface roughness of the membranes, a topographical map of the membrane surfaces was obtained with Atomic Force Microscopy (AFM) on a Digital Instruments MMSPM Nanoscope IV model.  $10\text{ }\mu\text{m} \times 10\text{ }\mu\text{m}$  surface was scanned with  $512 \times 512$  pixel resolution using a silicon tip attached to a cantilever, while maintaining a constant force between the tip and the sample.

The bulk morphology of the membranes was examined by scanning electron microscopy (SEM) on a FEI-Quanta 250 FEG model. The samples were coated with gold using a Magnetron Sputter Coating Instrument.

The XPS data were acquired with a X-ray Photoelectron Spectrometer PHI-5000 Versaprobe using an Al-monochromatic X-ray source (600 W). Survey spectra (0-1200 eV) were taken at a constant analyzer pass energy of 187.85 eV, and binding energy

windows for C1s, N1s, O1s and S2p were obtained at a pass energy of 93.90 eV. 1 cm x 1 cm sample was used and high-resolution spectra of C1s, N1s, O1s and S2p peaks were recorded at the takeoff angle of 45°. In order to predict which components are close to the surface, the takeoff angle between the film surface and the photoelectron energy analyzer was adjusted at 15° and 75°. Each peak was deconvoluted by assuming a Gaussian distribution and the area under the curve was calculated by using Microcal Origin software. Binding energy calibration was performed to ensure the peak position for the C 1s maximum located at 285.00 eV.

#### 4.4. Measurement of Alpha-Lipoic Acid Activity

Alpha-lipoic acid and its reduced metabolite, dihydrolipoic acid (DHLA) (Figure 4.5) form a redox couple and may scavenge a wide range of reactive oxygen species such as hydroxyl radicals, nitric oxide radicals, peroxyxynitrite, hydrogen peroxide and hypochlorite. The antioxidant activity of ALA was measured using the free-radical scavenging activity of DPPH radicals.

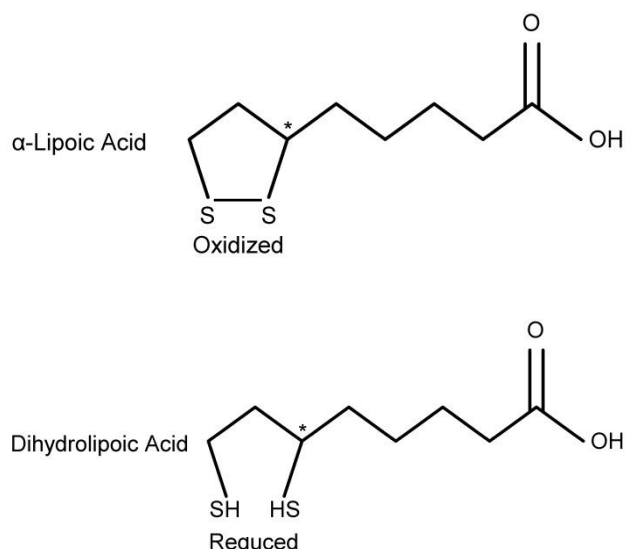


Figure 4.5. Chemical structure of alpha-lipoic acid (ALA) and dihydrolipoic acid (DHLA)

To measure free and immobilized antioxidant activities, ALA solutions freshly prepared in absolute ethanol were mixed with 0.1 mM ethanolic DPPH in a cuvette or the membranes were immersed into 3 ml of 0.1 mM ethanolic DPPH, respectively. As

the odd electron of DPPH becomes paired off, the absorption vanishes and resulting decolorization is stoichiometric with respect to the number of electrons taken up. Radical scavenging activity (RSA) was then determined by measuring the decrease in the absorption of DPPH solution at 516 nm as follows:

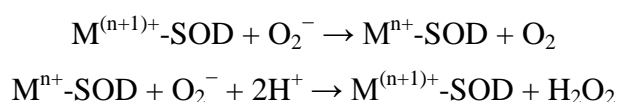
$$RSA\% = \left( \frac{Absorbance_0 - Absorbance_{eqb}}{Absorbance_0} \right) \times 100 \quad (4.1)$$

where,  $Absorbance_0$  and  $Absorbance_{eqb}$  represent absorbance measured at the beginning and at equilibrium, respectively.

To determine stability of immobilized ALA under typical hemodialysis conditions, 4 cm<sup>2</sup> of membranes were immersed into 10 ml of 0.05 M phosphate buffer solution at pH 7.4 and 37 °C. The solution was stirred thoroughly and the membrane samples were removed from the solution after 240 minutes. Then, the activity of the immobilized ALA and amount of released ALA were determined spectrophotometrically.

#### 4.5. Measurement of Superoxide Dismutase (SOD) Activity

The SOD catalysed dismutation of superoxide may be written with the following half-reactions:



where M = Cu (n=1) ; Mn (n=2) ; Fe (n=2) ; Ni (n=2).

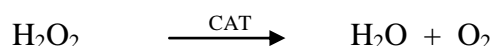
The antioxidant activities of free and immobilized SOD were determined by measuring the ability to inhibit the photochemical reduction of Nitrotetrazolium Blue Chloride (NBT). The experiments were conducted in 3 ml disposable cuvettes at 35°C. Each 3 ml mixture contains 2 ml Sodium phosphate buffer (PBS) of 50 mM at pH 7.4, 200 µl 75 µM NBT, 13 mM Methionine, 100 nM EDTA, 2µM Riboflavin solutions and SOD enzyme. SOD activity measurements were carried out with 30 µl of 0.025 mg.ml<sup>-1</sup> SOD. The riboflavin solution was added last and the cuvettes were shaken. The reaction was started under illumination of a 15 W fluorescent lamp. Each sample was kept under

the light for 10 minutes. After 10 minutes the fluorescent lamp was switched off in order to stop the reaction. Two absorbance data were collected for each sample: before adding the riboflavin solution into the cuvette and after 10 minute time period was completed. The absorbance of each sample was measured by a UV-Spectrophotometer (Perkin Elmer, mode no: Lambda 45) at 560 nm against a 3 ml PBS. Each measurement was repeated five times for each test. To determine immobilized SOD activity of the membranes, instead of free enzyme; 1 cm<sup>2</sup> membrane was immersed into 3 ml reaction mixture.

SOD activity is expressed as the percentage inhibition in reduction of NBT (inhibition of the formazan production) per g of SOD (or cm<sup>2</sup> membrane). The amount of superoxide dismutase required to inhibit the rate of formation of formazan by 50% is defined as 1 unit of activity.

#### 4.6. Measurement of Catalase (CAT) Activity

The antioxidant activities of free and immobilized CAT were determined by measuring the amount of hydrogen peroxide consumed enzymatically where hydrogen peroxide (H<sub>2</sub>O<sub>2</sub>) was used as a substrate. The reaction is as follows:



In order to determine the free activity of CAT, 25 µl of 0.01 mg.ml<sup>-1</sup> CAT was added into 2 ml H<sub>2</sub>O<sub>2</sub> solution. This reaction mixture was allowed to incubate for 10 minutes at 25 °C inside a container where no light existed. The absorbance of each cuvettes were measured before and after the reaction by a UV-spectrophotometer (Perkin Elmer, mode no: Lambda 45) at 240 nm against a 2.0 ml PBS. The immobilized CAT activity of the membranes was determined by immersing 1 cm<sup>2</sup> membrane into 2 ml H<sub>2</sub>O<sub>2</sub>.

The activity of free catalase was given as U/mg protein and immobilized catalase activities were expressed as U.mg<sup>-1</sup> protein or U.cm<sup>2</sup> membrane where 1U is defined as µmol H<sub>2</sub>O<sub>2</sub>.min<sup>-1</sup>.

## **4.7. Determination of Operational Stability of the Immobilized Enzymes**

To determine stability of immobilized SOD or CAT, membranes were immersed into 25 ml of 0.05 M phosphate buffer solution at pH 7.4 and 37 °C for 4 hours which corresponds to typical hemodialysis time. The solution was stirred thoroughly and the membrane samples were removed from the solution at the end of 240 minutes. The enzymatic activities were measured using same procedure described above.

## **4.8. *In vitro* Hemocompatibility**

### **4.8.1. Protein Adsorption Experiments**

Protein adsorption experiments were performed with (i) blood plasma proteins obtained from 50% platelet poor plasma (PPP) (ii) model protein, bovine serum albumin (BSA). The membranes (1.5 cm x 1.5 cm) equilibrated in 0.05 M, pH 7.4 phosphate buffer with saline at 37 °C for 15 hours, were first placed onto a 24-well plate. 1.0 ml of protein solution (platelet poor plasma (PPP) or BSA solution with a concentration of 4.5 mg.ml<sup>-1</sup> which is 10% dilution of the plasma level was poured onto membranes and allowed to remain at 37 °C for 1 h. After rinsing three times with PBS, they were removed from the well plate and rinsed again sufficiently with 50 ml of PBS in order to remove loosely-bond protein. Each membrane sample was placed into a glass bottle containing 1 wt.% aqueous solution of sodium dodecylsulfate (SDS) and shaken (150 rpm) in a shaking bath for 3 h at room temperature to detach the adsorbed protein on the surface. In order to take into account an interference which may be caused by SDS, membrane samples not treated with protein was used as a proper control. A protein analysis kit (Micro BCA protein assay reagent kit, #23235, Pierce, Rockford, IL, USA) based on the bicinchoninic acid (BCA) method was used to determine the protein concentration in the SDS solution. (Ishihara et al. 1999)

The absorbance of the solution at 562 nm was measured by a spectrophotometer (Perkin Elmer Model No: Lambda 45). The fresh blood collected in citrated tubes from healthy volunteer was centrifuged at 2800 rpm for 15 minutes at room temperature to obtain platelet poor plasma.

#### **4.8.2. Platelet and Blood Cell Adhesion and Activation**

In order to analyze the platelet activation, unmodified and modified PSF membranes were incubated with acid citrate dextrose (ACD)-whole blood at 37 °C for 25 min. 5 µL of whole blood suspension was carefully added to the bottom of all tubes and platelet activation-dependent monoclonal antibodies of PAC1, FITC and CD62 PE were added. Specificity of PAC1 binding is demonstrated by staining in the presence of RGDS (Arg-Gly-Asp-Ser) peptide (a competitive inhibitor) as the negative control tube and adenosine diphosphate (ADP) as the positive control. Without vortex mixing, the tubes were gently mixed and incubated in the dark for 15 to 20 minutes at room temperature. Following the incubation period, 1 ml of cold 1 % paraformaldehyde was added to each tube and they were finally stored at 2–8 °C in the dark for at least 2 hours. The percentage of activated platelets was counted by Flow Cytometer (BD FACS Canto).

The platelets and blood cell adhesion on the membrane surfaces was determined by incubating the samples at 37 °C with platelet rich plasma (PRP) and heparinized fresh human blood for 25 and 15 minutes, respectively. After incubation, the samples were gently washed to remove loosely bound platelets and blood cells, fixed with glutaraldehyde (2.5 % in 0.1M sodium cacodylate buffer, pH 7.2) for 30 min at 4 °C, and rinsed three times with PBS buffer with saline. The samples were then dehydrated in graded ethanol series (30, 50, 70, 90, and 100 %, 500 ml each) for 10 min each and air dried. Finally, they were sputtered with gold and analyzed with SEM (FEI-Quanta 250 FEG).

#### **4.8.3. Blood Coagulation Time**

Blood coagulation time was measured by activated partial thromboplastin time (APTT). The sample membrane (1×1 cm<sup>2</sup>) was put in a glass tube, 100 µl of actin activated cephaloplastin reagent (Dade Behring Inc., USA) was added, and the tube was incubated at 37 °C for 1 min. Then, 100 µl of PPP solution was added to the sample solution at 37 °C, it was incubated for 30 min, and finally 100 µl of 0.025 M CaCl<sub>2</sub> solution was added. The clotting time of the plasma solution was recorded at the first sign of fibrin formation (Yang and Lin, 2002).

To determine stability of immobilized HEP under typical hemodialysis conditions, blood coagulation time (APTT) was measured in the same manner, after the membranes were immersed into 10 ml of 0.05 M phosphate buffer solution at pH 7.4 and 37 °C. The solution was stirred thoroughly and the membrane samples were removed from the solution after 240 minutes.

#### **4.8.4. ROS Levels in Plasma**

Chemiluminescence (CL) method was used to measure the production of ROS in the samples using a chemiluminescence analyzer. Heparinized blood samples collected from healthy, non-smoking donor were wrapped with aluminum foil to prevent light exposure until testing for ROS levels. 2 ml whole blood was incubated both with 2 cm<sup>2</sup> modified and unmodified membranes for 4 hours at 37 °C. Then, 50 µl of blood sample was immediately placed in a 96-well plate, an aliquot of 125 µl of luminol was added to the blood sample and after 5 minutes incubation, 50µl of HOCl was added. Luminol (1 mg.ml<sup>-1</sup>) was used as an amplifier. The photon emission from the sample was counted at 20-sec intervals at room temperature under atmospheric conditions. For each sample, the assay was performed in triplicate, and the ROS levels were expressed as CL counts.

#### **4.8.5. Cell Viability Assay**

To determine toxic effects of the membranes, peripheral blood mononuclear cells (PBMCs) were isolated from the sample of healthy human blood by using ficol hypec gradient centrifugation. The membranes (1.5 cm×1.5 cm) were placed in 96 well-plate with 200 µl PBMCs sample and maintained at 37 °C for 4 and 48 hours. The number of live and dead cells were determined with Flow cytometer (BD FacsCanto). For labeling live and dead cells; Thiazole Orange (TO) and Propidium Iodide (PI) were used, respectively. The broth media that contains TO and PI but no cells were used as the negative control.

## 4.9. Permeation Experiments

Permeation experiments were carried out in a side by side diffusion cell (Permegear Membrane Transport Systems) using urea, vitamin B<sub>12</sub>, lysozyme and salt as model solutes. Samples were removed from each chamber at given time intervals and concentration of myoglobin and vitamin B<sub>12</sub> were determined by directly measuring their natural absorbance at 409 and 360 nm, respectively. The concentration of urea was determined by first adding an enzymatic reagent (BT Product, Turkey) and then reading the absorbance of this mixture at 340 nm while the salt concentration was measured with a conductivimeter (WTW-Cond340i). The overall mass transfer coefficient which has contributions both from the bulk fluid and the membrane was evaluated from the solute concentration data. The effective permeability of the solute was determined from the overall and individual mass transfer coefficients (Langsdorf and Zydney, 1994).

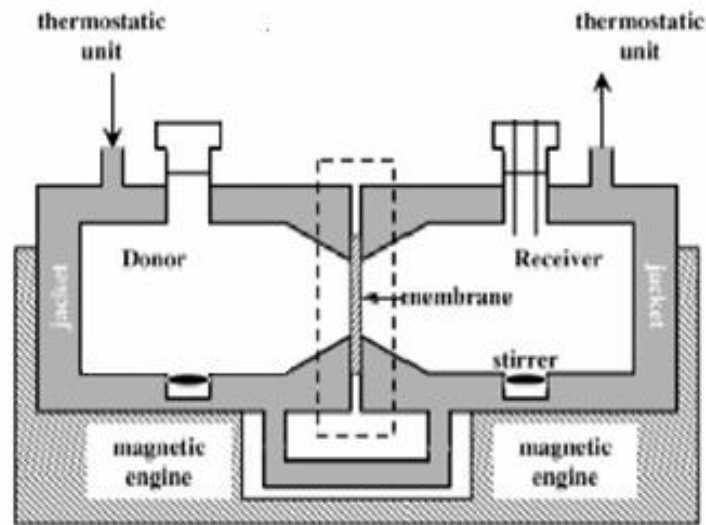


Figure 4.6. Experimental set-up used for permeation experiments.

In order to calculate effective permeation coefficient ( $P_m$ ); the overall mass transfer coefficient,  $k_o$ , was evaluated directly from the solute concentration data using the integrated form of the solute mass balance:

$$\ln \left[ \frac{C_1(t_f) - C_2(t_f)}{C_1(t_0) - C_2(t_0)} \right] = k_o \times A \left[ \frac{1}{V_1} - \frac{1}{V_2} \right] x (t_f - t_0) \quad (4.2)$$



where  $V_1$  and  $V_2$  are the volumes of the chambers, and  $C_1$  and  $C_2$  are the concentrations at times  $t_o$  and  $t_f$ . The overall mass transfer coefficient ( $k_o$ ) has contributions from both the bulk fluid and the membrane:

$$\frac{1}{k_o} = \frac{1}{P_m} + \frac{2}{k_b} \quad (4.3)$$

$$\frac{k_b r}{D_\infty} = \alpha x \text{Re}^{0.567} x \text{Sc}^{0.33} \quad (4.4)$$

where the factor of two in the second term of the right-hand side of Equation 4.3 reflects the presence of boundary layers in the two chambers. The bulk mass transfer coefficient ( $k_b$ ) was evaluated from Equation 4.4 with  $\alpha = 0.27$  based on the specific geometry of the diffusion cell.

#### 4.10. Mechanical Analysis

The tensile strength of the membranes is measured using a Shimadzu AG-I-250 KN testing machine. The membranes are strained at constant rates of  $0.25 \text{ mm}\cdot\text{min}^{-1}$  and  $0.5 \text{ mm}\cdot\text{min}^{-1}$  until failure. The test method and sample preparation is in accordance with ASTM D 882-02 standard. At least five test coupons with a 10 mm in width and 5 cm in length are used for measurements.

#### 4.11. Data Analysis

The data was analyzed with the statistical software Minitab 15. Statistical evaluation of the data was performed using Student's paired t test. The probability (P) values  $P < 0.05$  were considered to be statistically significant differences. The results were expressed as mean  $\pm$  standard error. The propagation of error was taken into account and calculated from the total derivative of the function.

## CHAPTER 5

### RESULTS AND DISCUSSION

#### **5.1. Surface Modification of Polysulfone Based Hemodialysis Membranes with Layer by Layer Self Assembly of Polyethyleneimine/Alginate-Heparin**

The studies in the first part of this thesis aim to improve biocompatibility of hemodialysis membranes through generating i) nonthrombogenic surfaces by binding anticoagulant heparin ii) nonfouling surfaces by increasing the hydrophilicity. To achieve this task, 2 control membranes, PSF and PSF-SPSF, and 6 modified membranes (1 and 5 bilayer PEI/ALG and PEI/ALG-HEP coated membranes) were prepared. Heparin was immobilized only on the last layer of the assembly and its concentration in the coating solution was changed from 15% (wt.%) to 100 % (wt.%). Table 5.1 lists the codes of the unmodified and modified membranes.

Table 5.1. Codes of the unmodified and modified PSF membranes with layer by layer self assembly of polyethyleneimine/alginate-heparin.

<b>Membrane Code</b>	<b># of Bilayer</b>	<b>Polyanion Type in the Middle Layers</b>	<b>Polyanion Type in the Outermost Layer</b>	<b>Heparin Concentration in ALG-HEP Mixture( wt. %)</b>
PSF	0	-	-	-
PSF-SPSF	0	-	-	-
PSF-SPSF-PEI-ALG-1b	1	-	ALG	0
PSF-SPSF-PEI-ALG-5b	5	ALG	ALG	0
PSF-SPSF-PEI-ALG/HEP-15-1b	1	-	ALG-HEP	15
PSF-SPSF-PEI-ALG/HEP-15-5b	5	ALG	ALG-HEP	15
PSF-SPSF-PEI/ALG-HEP-45-1b	1	-	ALG-HEP	45
PSF-SPSF-PEI-ALG/HEP-45-5b	5	ALG	ALG-HEP	45
PSF-SPSF-PEI-ALG/HEP-100-1b	1	-	HEP	100
PSF-SPSF-PEI-ALG/HEP-100-5b	5	ALG	HEP	100

### **5.1.1. Surface Characterization of the Heparin Immobilized Membranes**

The first surface characteristic of the membranes investigated was their hydrophilicity since it plays an important role in thrombogenesis (Spijker et al., 2002). The hydrophilicity was determined through contact angle measurements and the results are shown in Figure 5.1. It is seen that the hydrophilic character of the PSF membrane was remarkably improved by blending PSF with SPSF and depositing polyelectrolyte layers on the PSF-SPSF membrane as observed by a decrease in the contact angle values. Increasing the number of polyelectrolyte layer or the HEP concentration in the ALG-HEP blend solution did not change the contact angles.

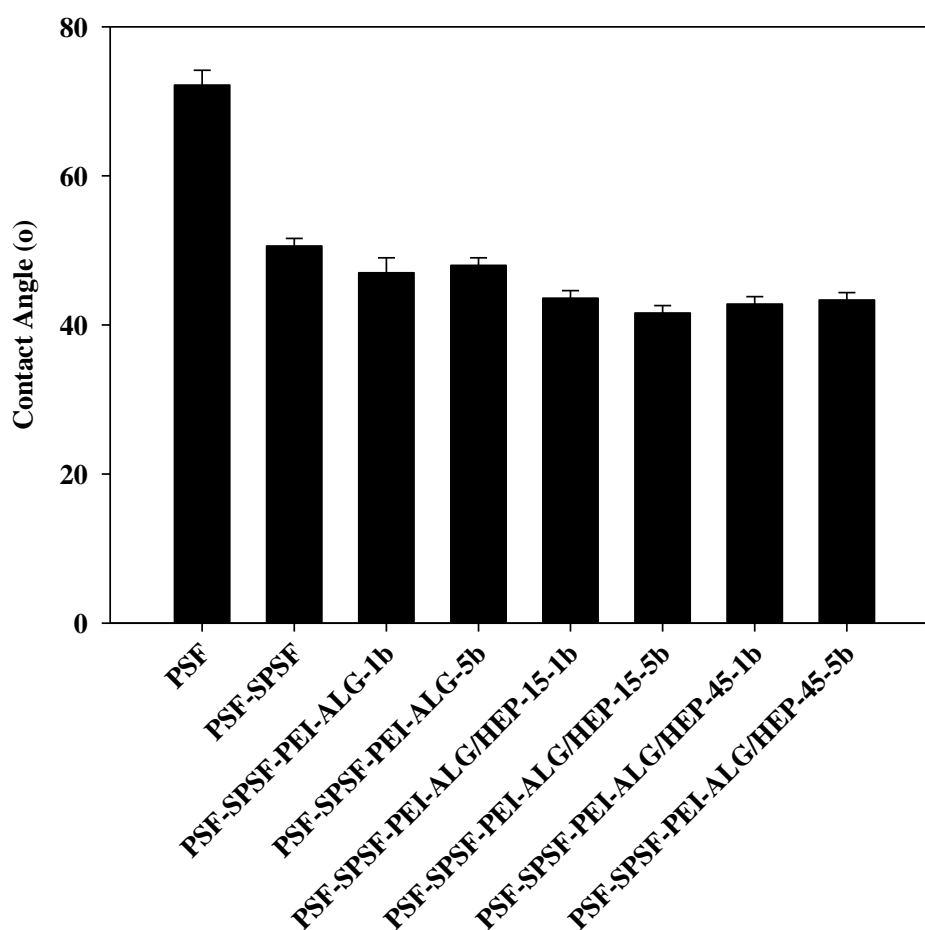


Figure 5.1. Water contact angles of the unmodified and modified PSF membranes layer by layer self assembly of polyethyleneimine/alginate-heparin.

The surface charge of the membranes was determined by the staining technique. The results in Figure 5.2 illustrate that all the PEI/ALG or PEI/ALG-HEP coated membranes were significantly stained with basic toluidine blue o dye. The intensity of blue colour compared to that of red colour was found much higher. This simply indicates that the net charges of the PSF-SPSF and all the polyelectrolyte deposited membranes are negative. The result for positively charged PSF-SPSF-PEI (where PEI is on the outermost layer) membrane was used as a positive control for acidic congo red staining while staining of uncharged PSF with both basic and acidic dyes indicates the nonspecific staining of dyes.

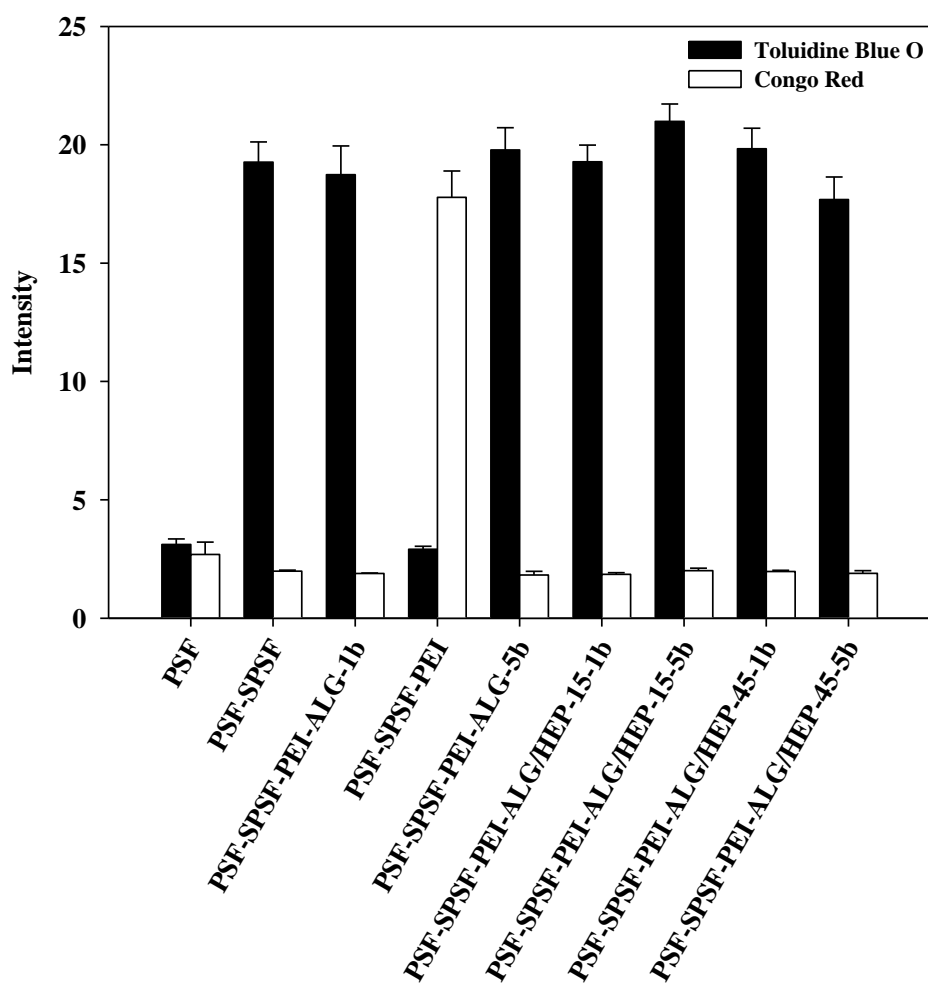
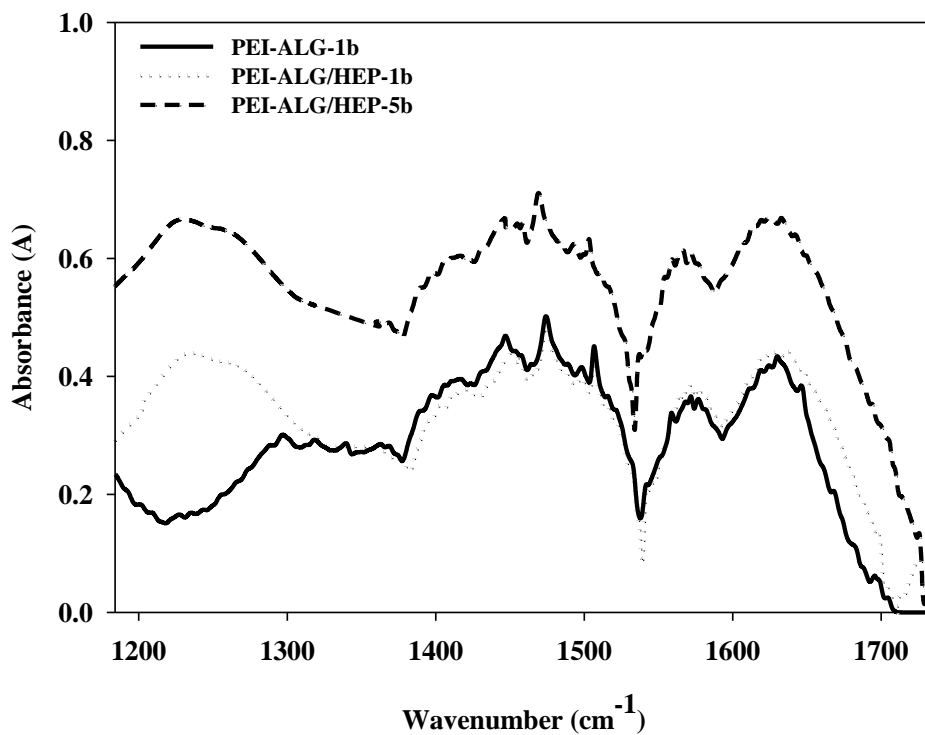


Figure 5.2. Intensity of colours of Toluidine Blue O and Congo Red dyes adsorbed on the unmodified and modified PSF membranes with layer by layer self assembly of polyethyleneimine/alginate-heparin.

Figure 5.3a shows the FTIR spectra of ALG and ALG-HEP in the form of the multilayer films. ALG layer consists of two distinct adsorption bands of the carboxylic acid functional groups;  $\nu = 1565-1542 \text{ cm}^{-1}$  (asymmetric stretching band of  $\text{COO}^-$ ) and  $\nu = 1710-1700 \text{ cm}^{-1}$  (C=O stretching of COOH). In the case of ALG-HEP layer, S–O stretching modes of  $\text{SO}_3$  groups in HEP was also seen centered at  $1230 \text{ cm}^{-1}$ . Asymmetric  $\text{NH}_3^+$  bending band of PEI at  $1630 \text{ cm}^{-1}$  overlaps with the adsorption bands of the carboxylic acid functional groups in ALG-HEP layer. To solve this problem, each band of ALG-HEP and PEI was deconvoluted by assuming a Gaussian distribution and using Microcal Origin software (Figure 5.3b). The degree of ionization of ALG-HEP layer in 1 and 5 bilayer multilayer formation was calculated from

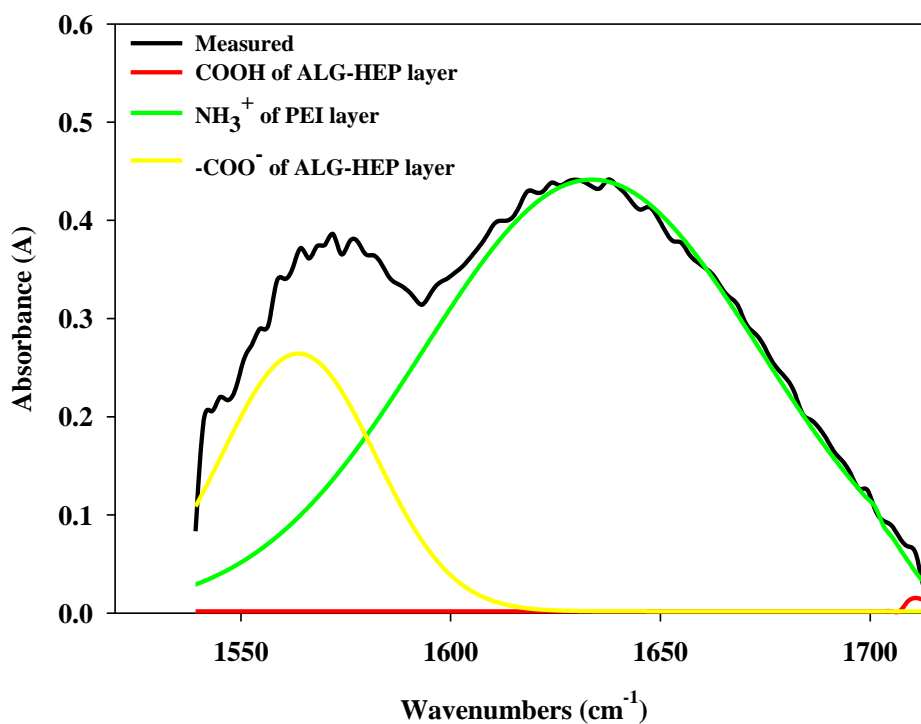
$\alpha = \frac{Area_{COO^-}}{[Area_{COO^-} + Area_{COOH}]}$  (Choi and Rubner, 2005). As can be seen from Figure 5.3b, almost all of the COOH groups were transformed into COO<sup>-</sup> form, hence, the degree of ionization was calculated as 0.99 and 0.97 for 1 and 5 bilayer formation, respectively. The degree of ionization of ALG and HEP in the solution has also a similar value (0.99) which indicates that there is no change in the ionizable groups during adsorption of these polyelectrolytes. The presence of S–O stretching modes of SO<sub>3</sub> groups at around 1230 cm<sup>-1</sup>, moreover, the increase of the signal intensity for the 5-bilayer coating compared to the 1-bilayer one shown in Figure 5. 3a are clear evidences of the multilayer film formation.



(a)

Figure 5.3. Representative FTIR-ATR spectra of (a) PEI/ALG-HEP or PEI/ALG multilayers on the ZnSe substrate and (b) an example of a peak fitting result for the 1 bilayer PEI/ALG-HEP multilayers.

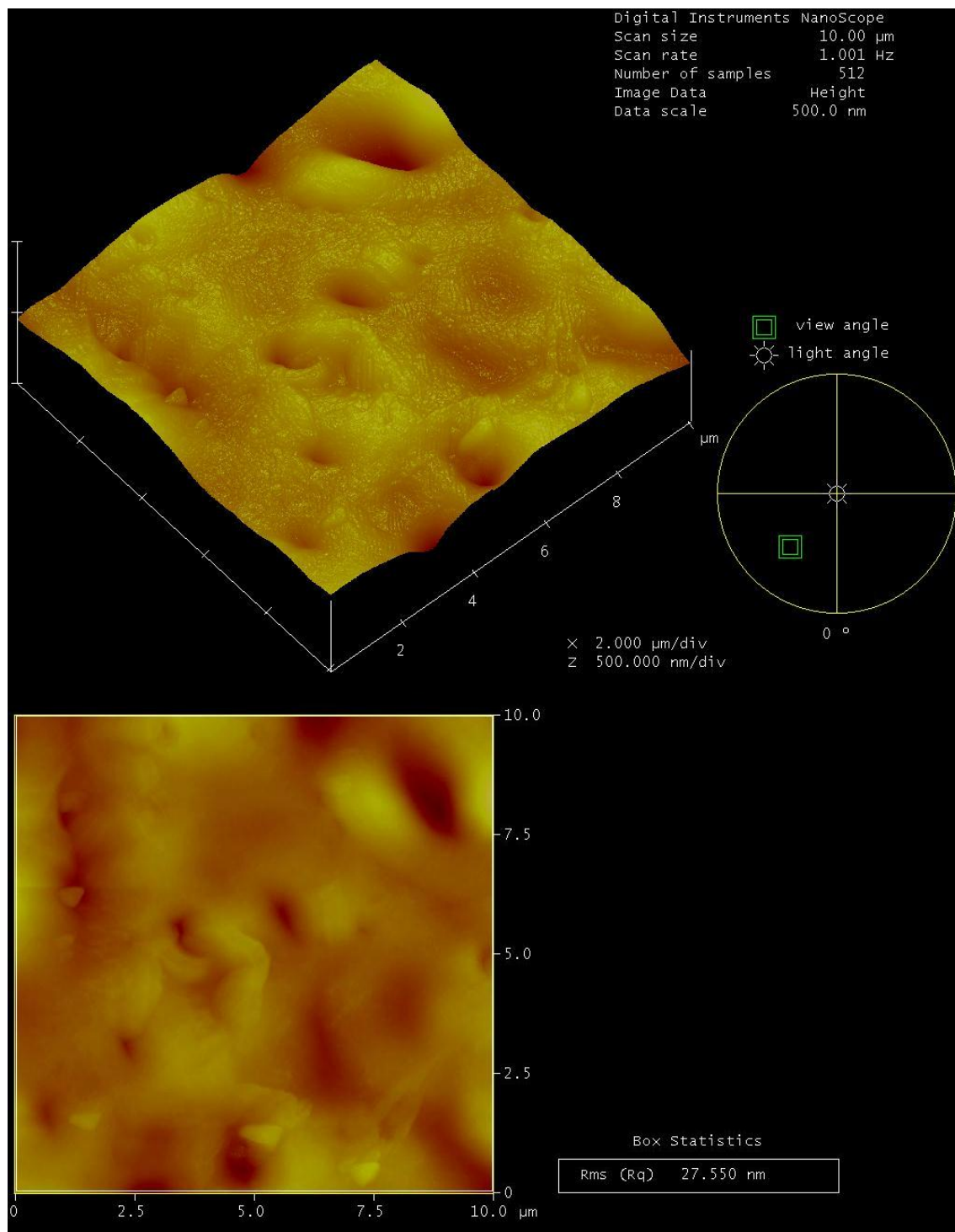
(cont. on next page)



(b)

Figure 5.3. (cont.)

The average surface roughness of the membranes was obtained from the analysis of AFM images shown in Figure 5.4. The unmodified PSF membrane had the smoothest surface while sulfonation significantly increased the surface roughness. On the other hand, the layer by layer deposition of PEI/ALG or PEI/ALG-HEP on the surface of PSF-SPSF improved the smoothness of the surface (Figure 5.5). This can be attributed to the energy-minimization process taken place on the surface of the deposited film, where PEI undergoes conformational change to minimize the surface area as a result of diffusional mobility of PEI chains.

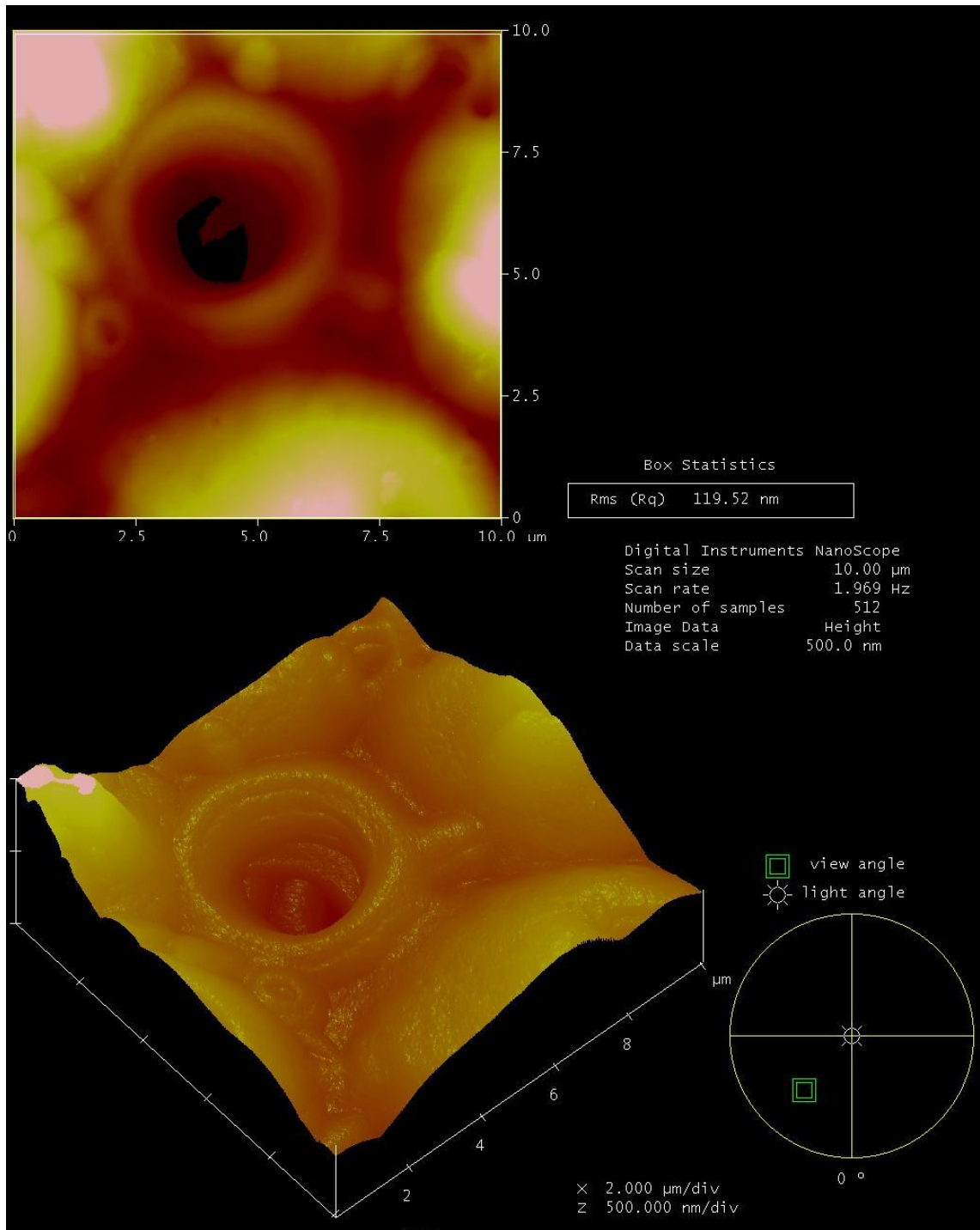


(a)

Figure 5.4. AFM images of (a) PSF (b) PSF-SPSF and (c) PSF-SPSF-PEI-ALG/HEP-15-1b membranes.

(cont. on next page)

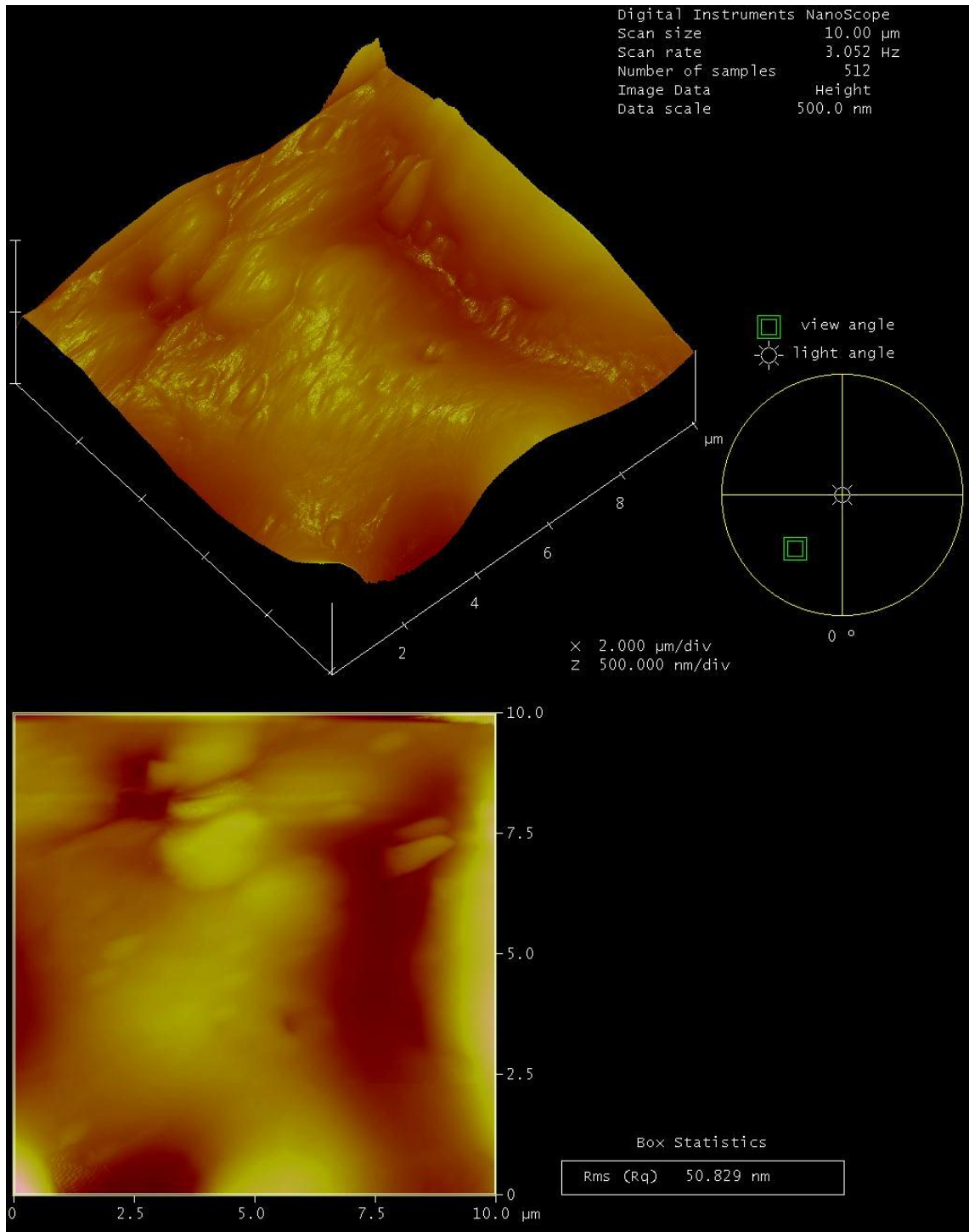




(b)

Figure 5.4. (cont.)

(cont. on next page)



(c)

Figure 5.4. (cont.)

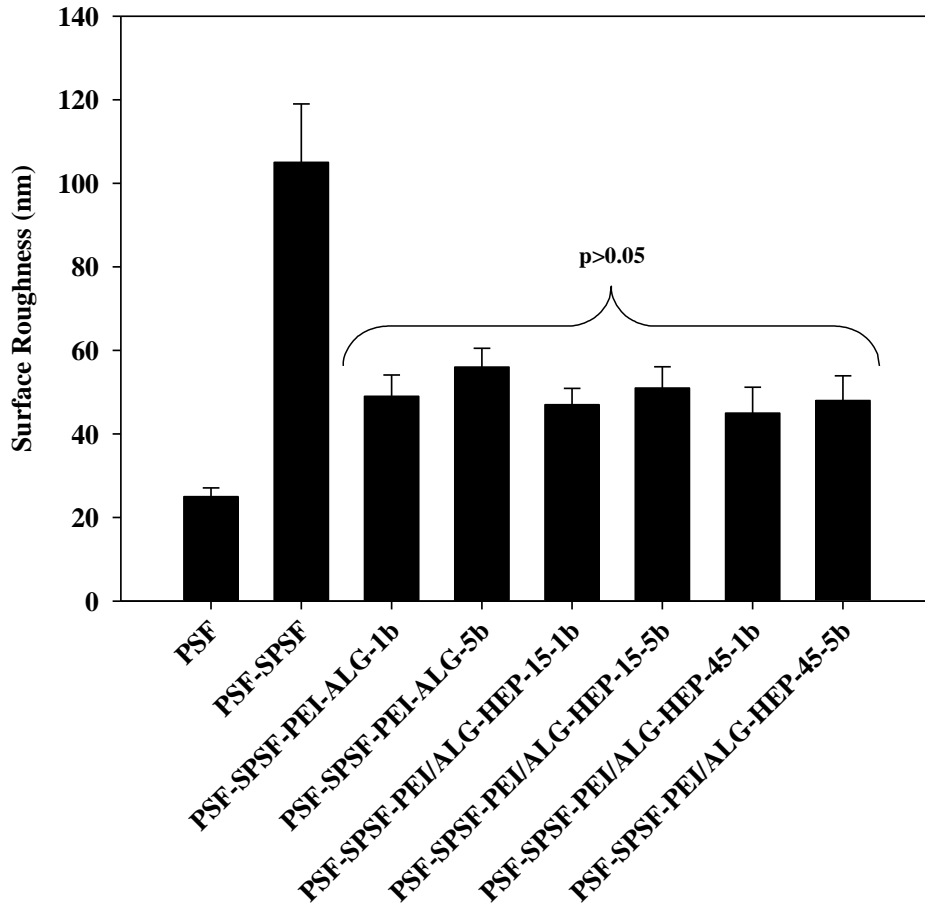


Figure 5.5. Surface roughness of unmodified and modified PSF membranes with layer by layer self assembly of polyethyleneimine/alginate-heparin.

The change in the bulk structure of the PSF membrane through blending with SPSF and polyelectrolyte deposition was observed with the SEM pictures. Figure 5.6 shows that native (PSF) and modified membranes have an asymmetric structure. The PSF-SPSF membrane is more porous than the PSF membrane, however, these pores were blocked with polyelectrolytes, therefore, the bulk structures of the PSF and the 1 and 5-bilayer PEI/ALG-HEP coated membranes are similar. The presence of PEI/ALG-HEP coatings on the surface of the uncoated membranes can not be seen in Figures 5.6c and 5.6d since the increase in the total thickness of the membrane with the coating is on the order of 10 nm. It was possible to detect the polyelectrolyte coatings when the thickness was increased to about 1  $\mu\text{m}$  by changing the concentration of each polyelectrolyte to 10  $\text{mg}\cdot\text{ml}^{-1}$  and adding 1 M NaCl into the coating solution (Figures 5.6e and 5.6f).

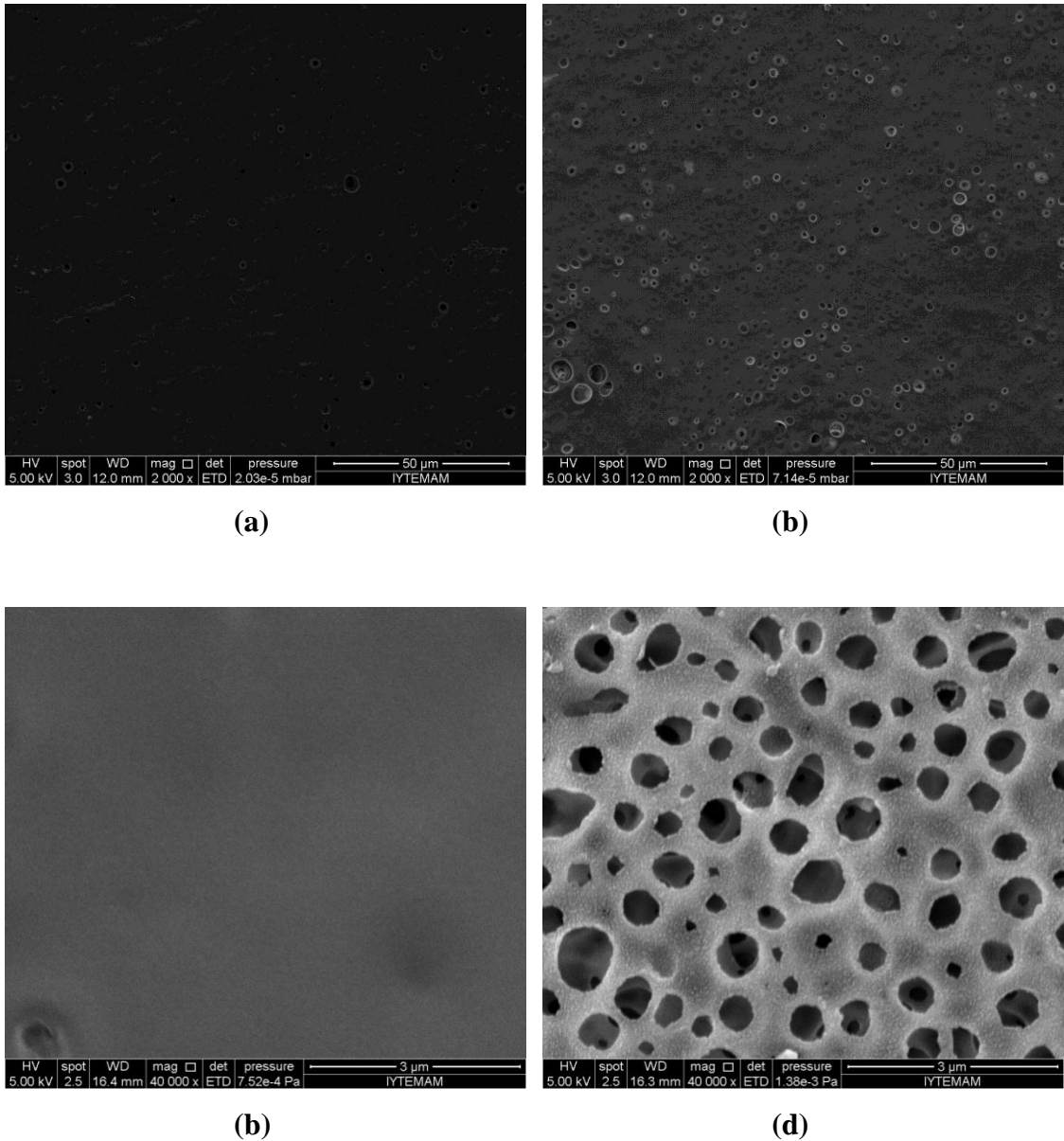
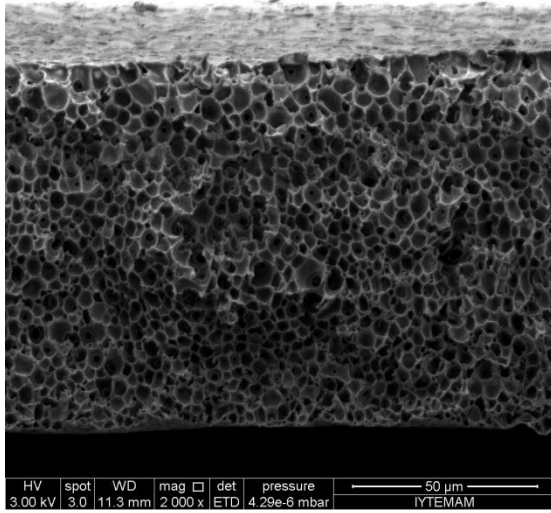
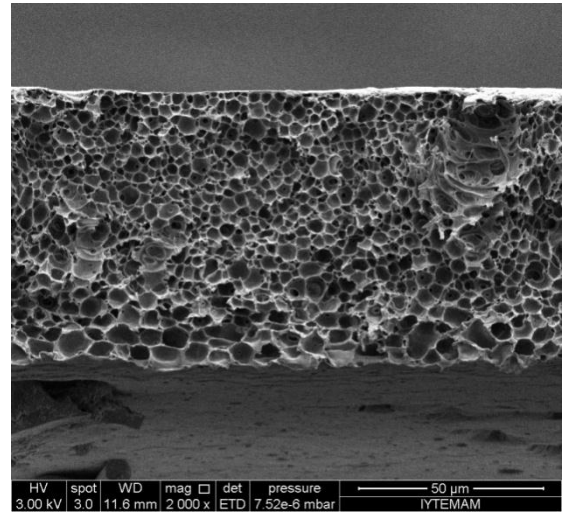


Figure 5.6. Surface SEM pictures of (a-c) dense skin (b-d) porous layer of PSF. Cross section SEM pictures of (e) PSF (f) PSF-SPSF (g) PSF-SPSF-PEI-ALG/HEP-15-1b (h) PSF-SPSF-PEI-ALG/HEP-45-5b membranes. Magnification x 2000 (a-b; e-f); x 40000 (c-d). \*PSF-SPSF-PEI/ALG-5b magnification x 5000 (i) 10000 (j). \* 5 bilayer PEI/ALG coating was prepared from a polyelectrolyte solution with a concentration of  $10 \text{ mg.ml}^{-1}$  containing 1 M NaCl.

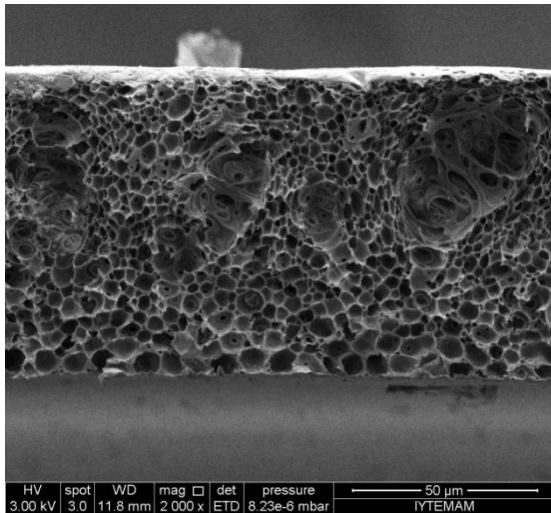
(cont. on next page)



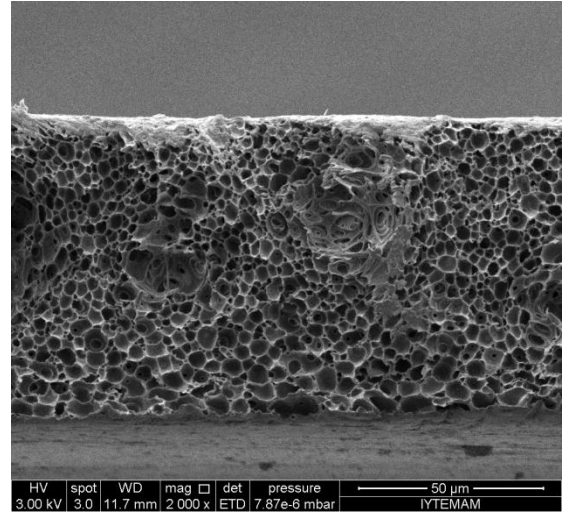
(e)



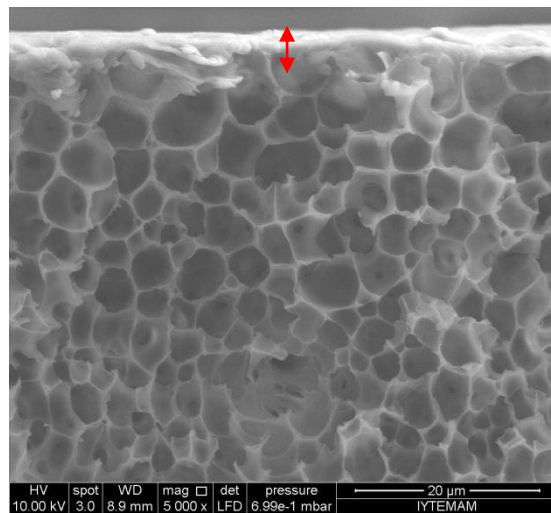
(f)



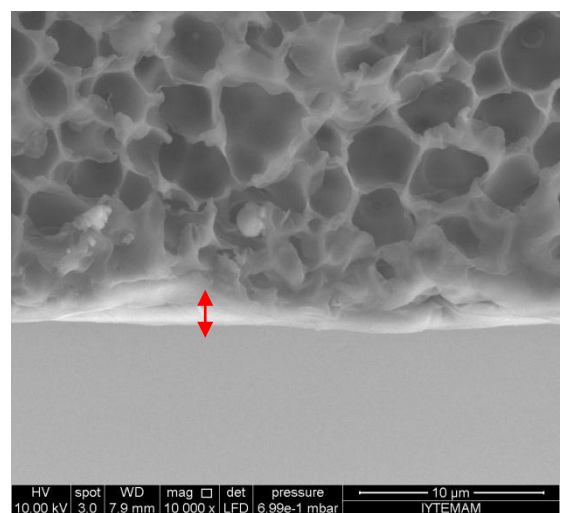
(g)



(h)



(i)



(j)

Figure 5.6. (cont.)



## 5.1.2. *In vitro* Hemocompatibility of Heparin Immobilized Membranes

### 5.1.2.1. Protein Adsorption Capacity

Plasma protein adsorption on the membrane is the key phenomena during thrombogenic formation (Deeisch et al., 1998), therefore, protein adsorption capacities of all the membranes were determined. The experiments were first performed with a negatively charged BSA, to represent most of the negatively charged proteins in blood. It is seen from Figure 5.7 that the highest BSA adsorption occurred on most hydrophobic PSF membrane. Blending PSF with SPSF and depositing polyelectrolytes on the PSF-SPSF blend membrane reduced protein adsorption by 30 % and 51 %, respectively. Although the PSF membrane has the smoothest surface, the strong protein binding affinity of this membrane is due to hydrophobic groups on the surface while less protein binding to the blend and polyelectrolyte deposited membranes is related to their more hydrophilic character compared to the PSF membrane as shown in Figure 5.1. In addition to hydrophobic interactions, electrostatic interactions are also effective on the protein adsorption. During protein adsorption experiments, BSA was negatively charged since its isoelectric point, pI:4.9, is lower than the pH of the solution adjusted to physiological pH 7.4. The PSF membrane has no charged group on the surface, on the other hand, the PSF-SPSF and the 1 and 5-bilayer PEI/ALG and PEI/ALG-HEP coated membranes carry negatively charged  $-\text{OSO}_3^-$  and  $-\text{COO}^-$  groups that can repel BSA due to electrostatic interactions. The PEI/ALG or PEI/ALG-HEP coated membranes adsorb less protein than the PSF-SPSF membrane since their surfaces are much more smooth than the PSF-SPSF membrane. Not only BSA but also blood plasma proteins adsorbed on the membranes were determined and the results are shown in Figure 5.8. The decrease in the adsorption of plasma proteins on the membranes due to PEI/ALG or PEI/ALG-HEP immobilization (appr. 42 %) is not as high as in the case of BSA adsorption (appr. 51 %). This is expected since human plasma proteins are a mixture of approximately 200 kinds with different charge, hydrophobicity and structure, consequently, their adsorption mechanism is quite complicated. The results in Figures 5.7 and 5.8 show that all the polyelectrolyte deposited membranes have similar BSA and plasma protein adsorption capacities ( $p > 0.05$ ). This could be attributed to similar hydrophilicity, surface charge and surface roughnesses of these membranes as shown in

Figures 5.1, 5.2 and 5.5, respectively.

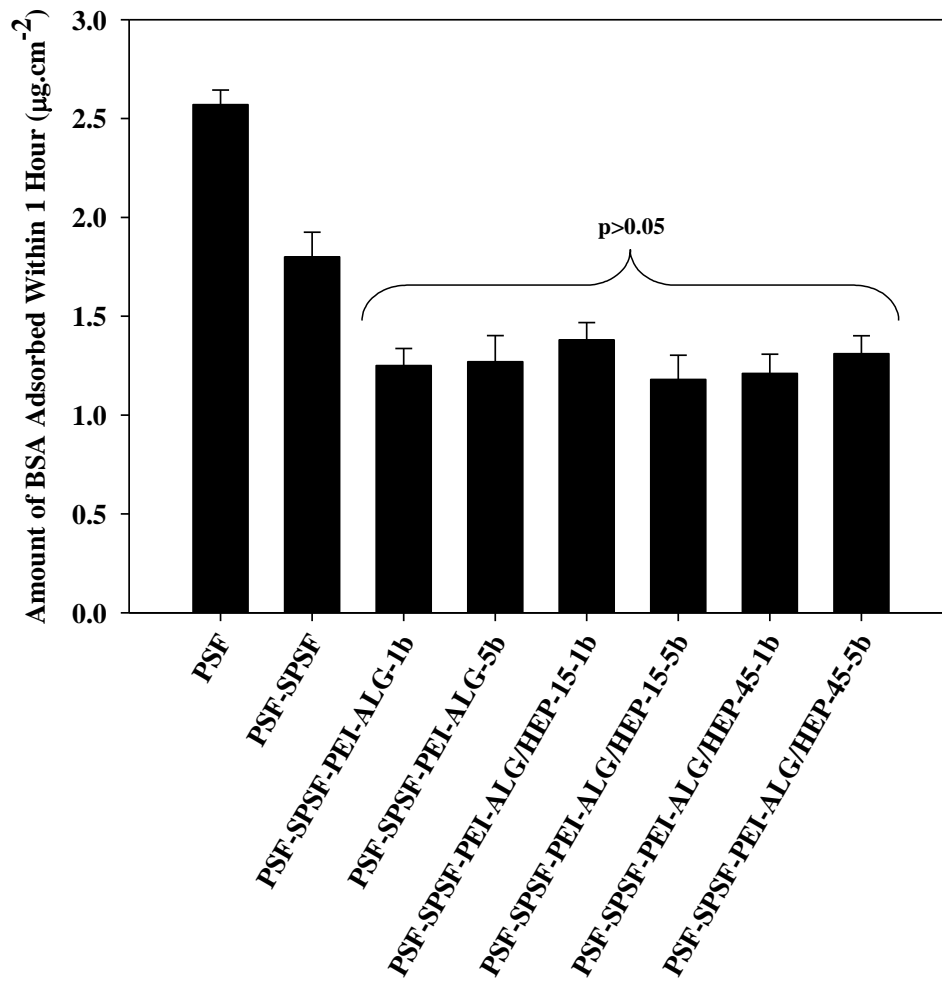


Figure 5.7. Amount of BSA adsorbed onto the unmodified and modified PSF membranes with layer by layer self assembly of polyethyleneimine/alginate-heparin.

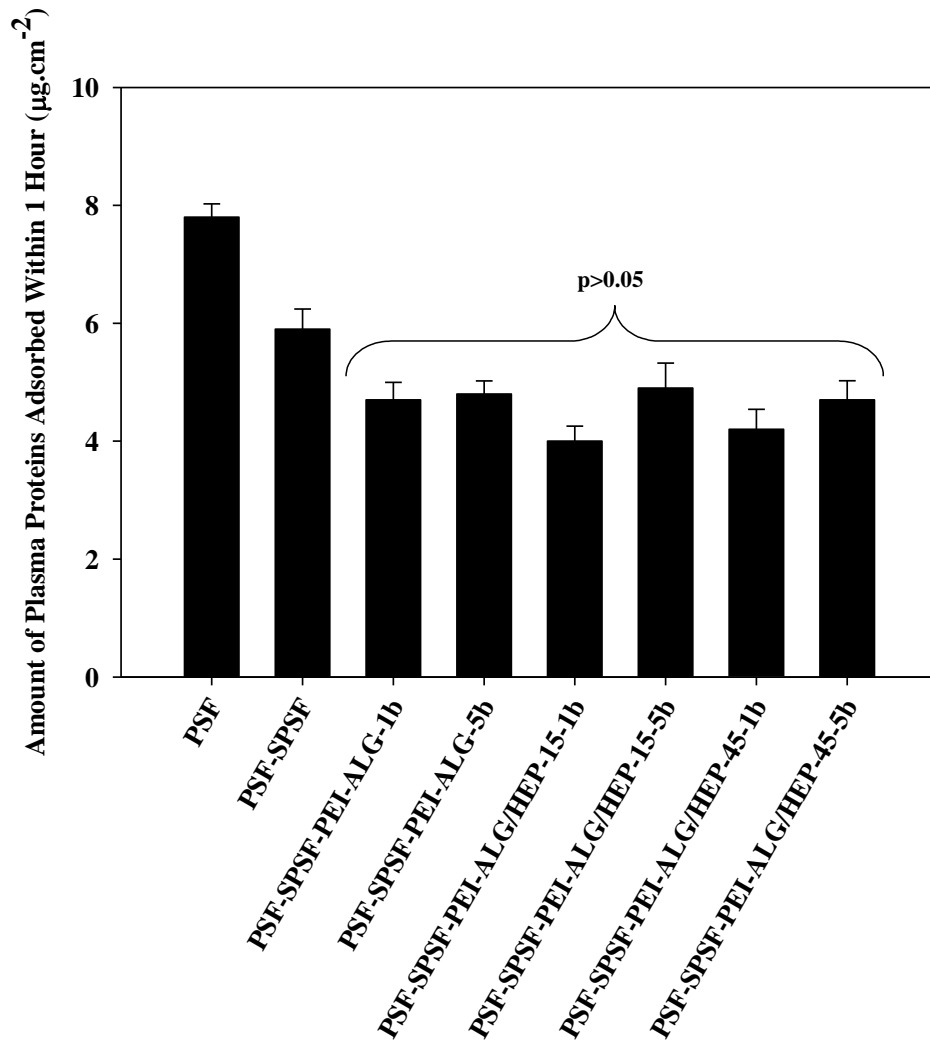


Figure 5.8. Amount of blood plasma proteins adsorbed on the unmodified and modified PSF membranes with layer by layer self assembly of polyethyleneimine/alginate-heparin.

### 5.1.2.2. Platelet and Blood Cell Activation

Platelets play a crucial role in the coagulation by secreting or releasing prothrombotic factors, therefore, platelet activation on different membranes was determined. Figure 5.9 shows that the highest platelet activation occurred on the PSF and PSF-SPSF membranes, on the other hand, polyelectrolyte deposition remarkably decreased the activation ( $p < 0.05$ ). All the PEI/ALG and PEI/ALG-HEP coated membranes did not show significantly different activation ( $p > 0.05$ ). The reduction of platelet activation on the polyelectrolyte deposited membranes can be attributed to



decreased plasma protein adsorption capacities of these membranes. Adsorption and conformational change of proteins in blood is known to regulate the adhesion and activation of platelets (Edmunds et al., 2003). The conformation of adsorbed plasma proteins was examined through analyzing the secondary structure of proteins with FTIR-ATR (Figure 5.10). When a protein adsorbs on the surface of any bioincompatible material, its secondary structure strongly changes, while the alpha-helix content is decreasing, the unordered structure and/or beta-structure increases, in turn denaturation occurs. The secondary structure of adsorbed proteins was determined by calculating the contents of alpha-helix, beta structure (sheet and turn) and unordered structure through integrating the amide I band (region 1620-1700  $\text{cm}^{-1}$ ) as seen in Figure 5.10 b-d. The results were tabulated in Table 5.2. Although the amount of adsorbed plasma proteins on the PSF-SPSF membrane is lower than that on PSF membrane, they caused similar platelet activation since the decrease in alpha-helix content of PSF-SPSF is higher than that of PSF. Consequently, denaturation of the adsorbed protein on the PSF-SPSF surface induced the platelet adhesion. As for the ALG/HEP coated surface, the conformation of the adsorbed protein is close to the native protein (alpha-helix content of human serum albumin is 51%) which minimize the adhesion of platelets.

The FTIR-ATR results in Figure 5.10 also confirmed that among 3 types of membranes the amount of adsorbed protein on the PSF membranes is the highest, while that on the PEI/ALG-HEP is the lowest.

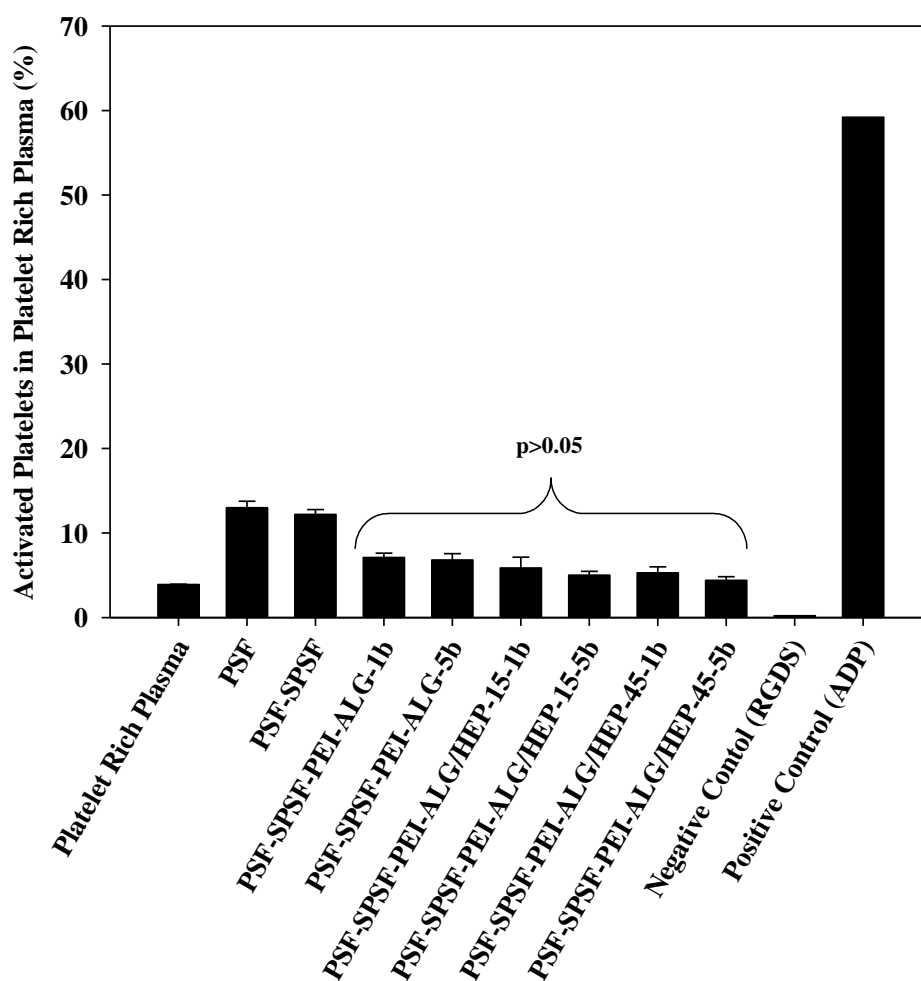
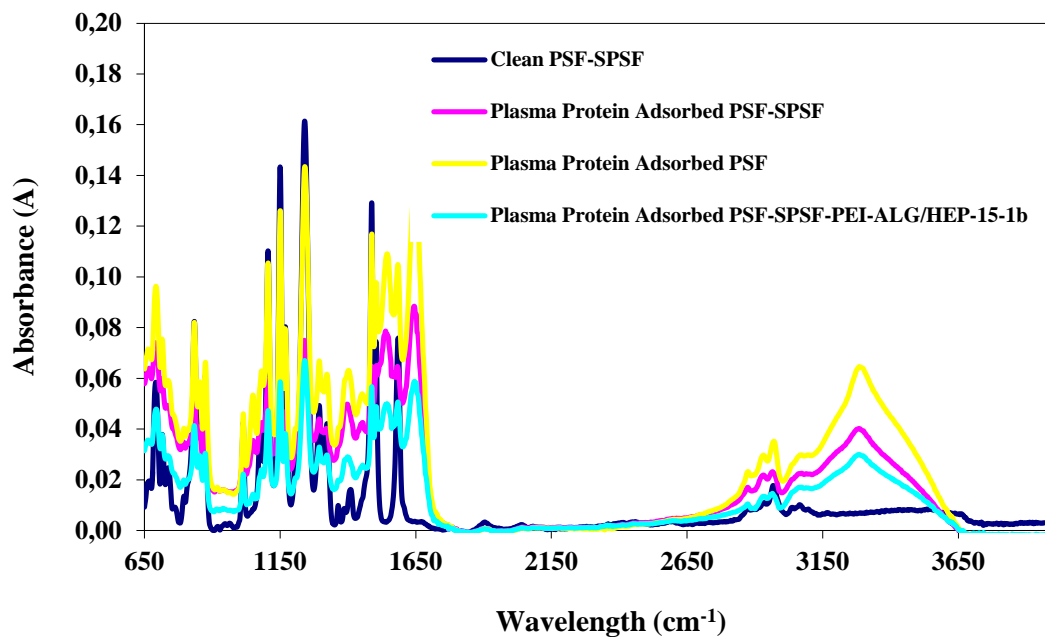


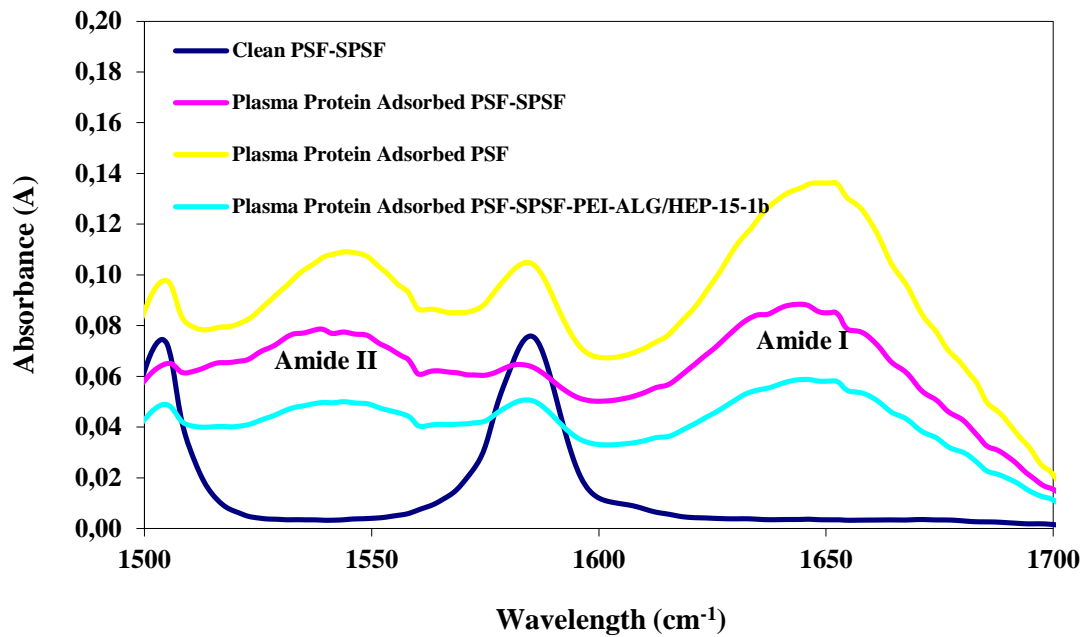
Figure 5.9. Amount of platelet activation on the unmodified and modified PSF membranes with layer by layer self assembly of polyethyleneimine/alginate-heparin.



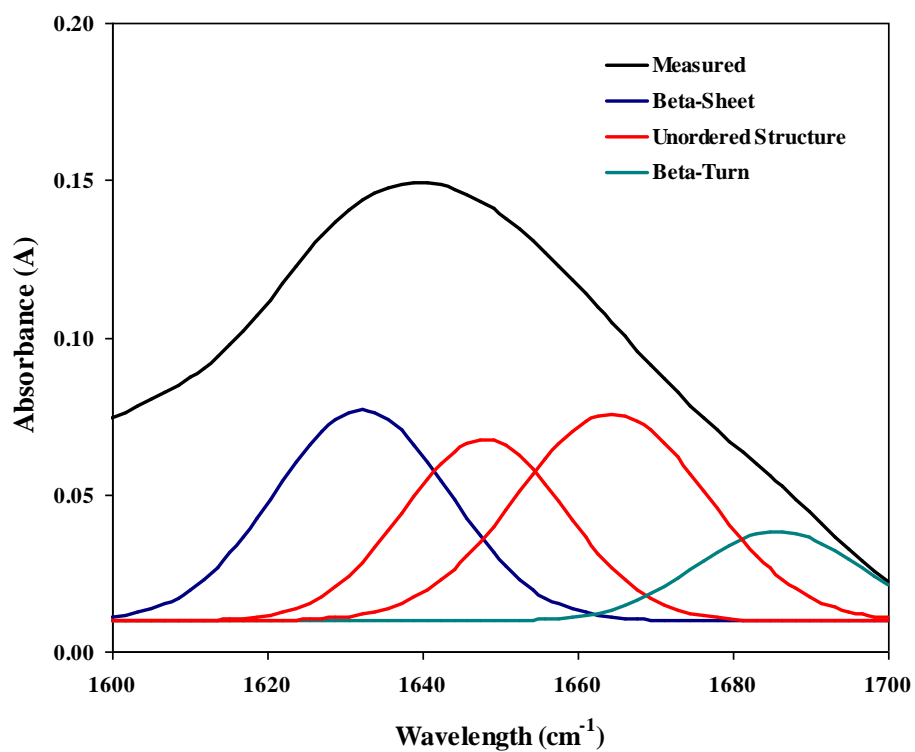
(a)

Figure 5.10. FTIR-ATR spectra of PSF-SPSF membrane before blood plasma protein adsorption and PSF, PSF-SPSF and PSF-SPSF-PEI-ALG/HEP-15-1b membranes after blood plasma protein adsorption in a region (a) 650-4000  $\text{cm}^{-1}$  (b) 1500-1700  $\text{cm}^{-1}$ . Deconvoluted spectra in the chosen band (1600-1700  $\text{cm}^{-1}$ ) of blood plasma protein adsorbed (c) PSF (d) PSF-SPSF (e) PSF-SPSF-PEI-ALG/HEP-15-1b membranes.

(cont. on next page)



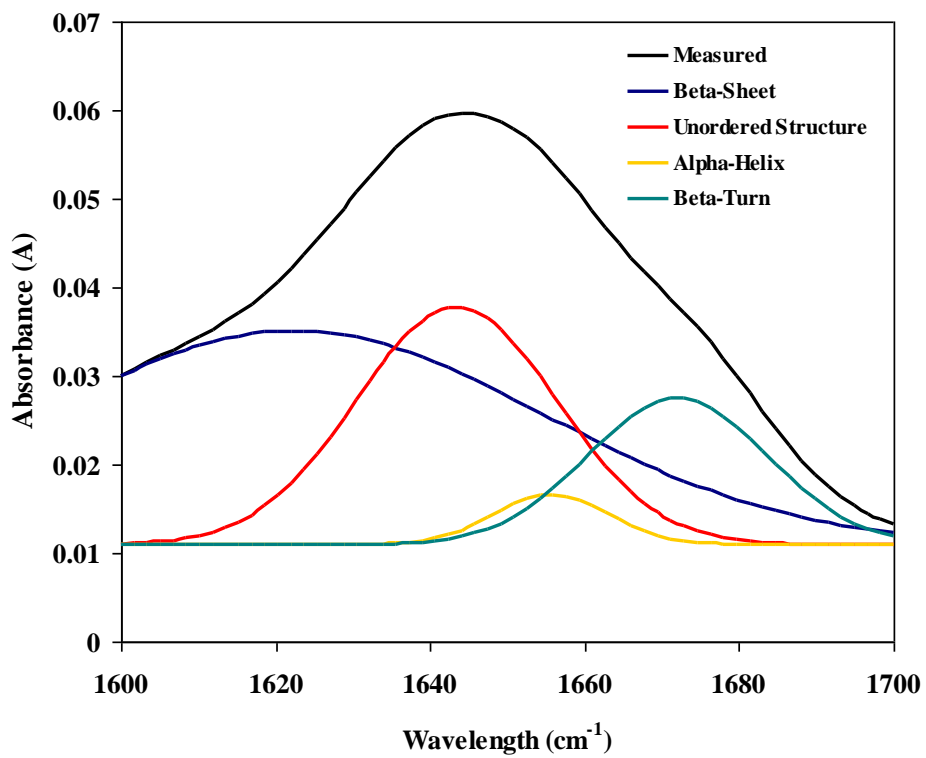
(b)



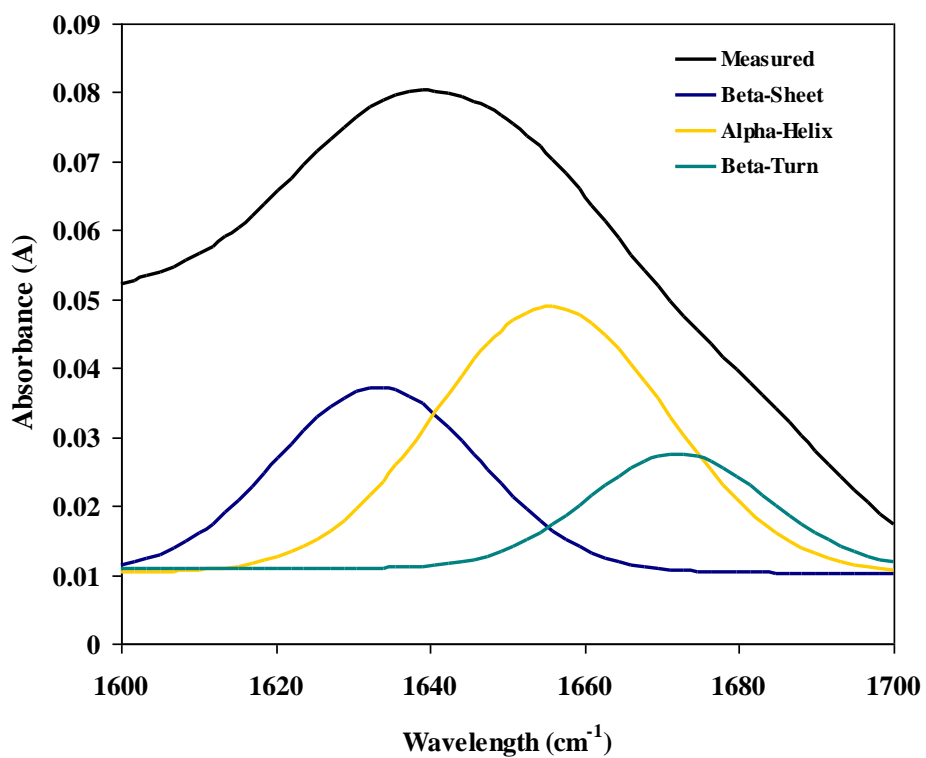
(c)

Figure 5.10. (cont.)

(cont. on next page)



(d)



(e)

Figure 5.10. (cont.)

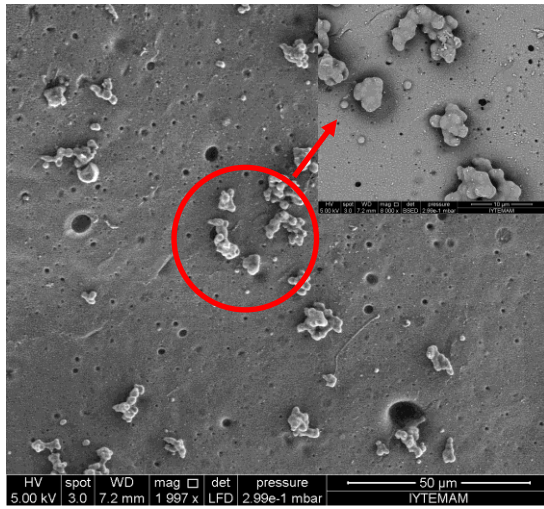
Table 5.2. Secondary structure of adsorbed blood plasma proteins on the unmodified and modified PSF membranes estimated from the deconvoluted FTIR spectra

Membrane Code		$\beta$ -sheet (1620-1640 $\text{cm}^{-1}$ )	Unordered structure (1641-1649 $\text{cm}^{-1}$ )	$\alpha$ -helix (1650-1658 $\text{cm}^{-1}$ )	Unordered structure (1658-1665 $\text{cm}^{-1}$ )	$\beta$ -turn (1665-1688 $\text{cm}^{-1}$ )
PSF	Assigned Frequency ( $\text{cm}^{-1}$ )	1632	1648	-	1664	1686
	Content (%)	31	24	-	33	12
PSF-SPSF	Assigned Frequency ( $\text{cm}^{-1}$ )	1622	1643	1656	-	1672
	Content (%)	57	26	3	-	14
PSF-SPSF-PEI-ALG/HEP-15-1b	Assigned Frequency ( $\text{cm}^{-1}$ )	1633	-	1656	-	1683
	Content (%)	32	-	52	-	16

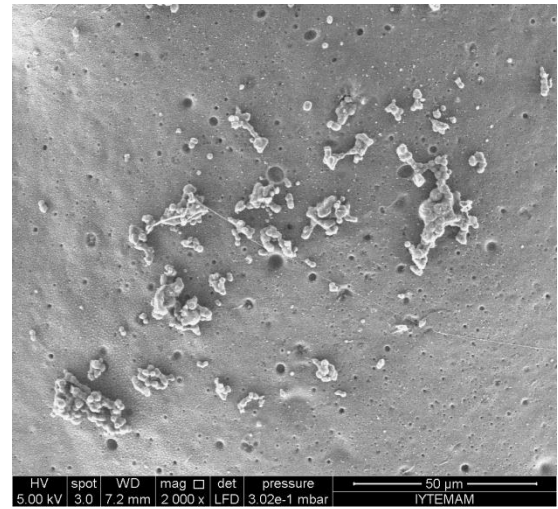
To identify the adherent platelets on the membranes, scanning electron microscope pictures were also used. When activation starts, multiple prothrombotic factors are released and the platelets change from disc to varying degrees of dendritic

shape. Figure 5.11 shows that more platelets adhered on the PSF and PSF-SPSF ones than the PEI/ALG-HEP coated membranes and they had mainly dendritic shape indicating the beginning of the platelet activation (Massa et al., 2005).

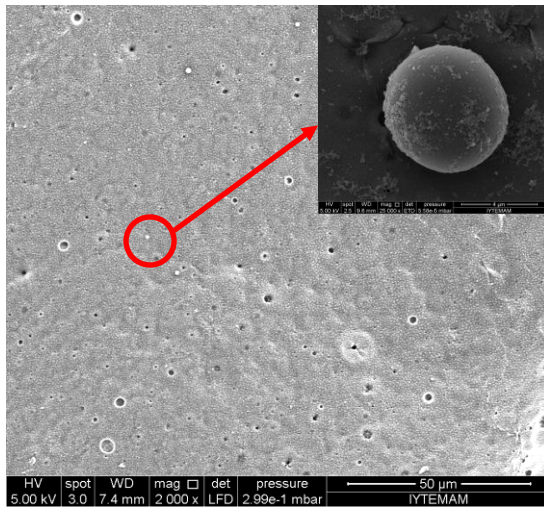
Figures 5.12a and 5.12b show that not only platelets but also mononuclear cells attached to the uncoated PSF-SPSF surface and changed their morphology which is a clear sign of activation. In contrast, fewer adhered cells were detected on the PEI/ALG-HEP coated membranes and no signs of morphology change were observed (Figures 5.11c and 5.11d) primarily due to much more smooth surfaces of these membranes and presence of an anticoagulant agent which is in contact with blood cells.



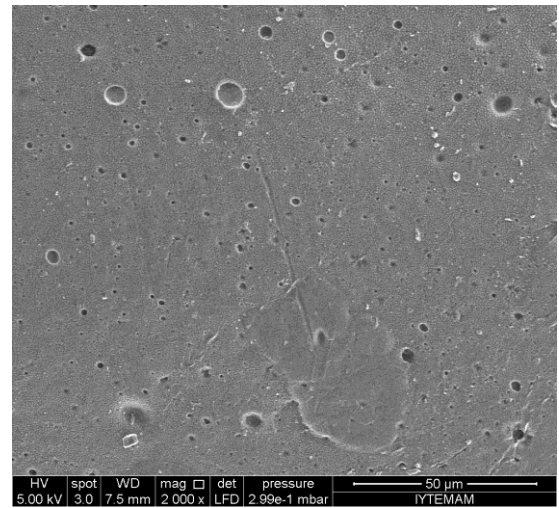
(a)



(b)



(c)



(d)

Figure 5.11. The SEM pictures of unmodified and modified PSF membranes after incubating with PRP for 25 minutes (a) PSF (b) PSF-SPSF (c) PSF-SPSF-PEI-ALG/HEP-15-1b (d) PSF-SPSF-PEI-ALG/HEP-45-5b, magnification x2000.



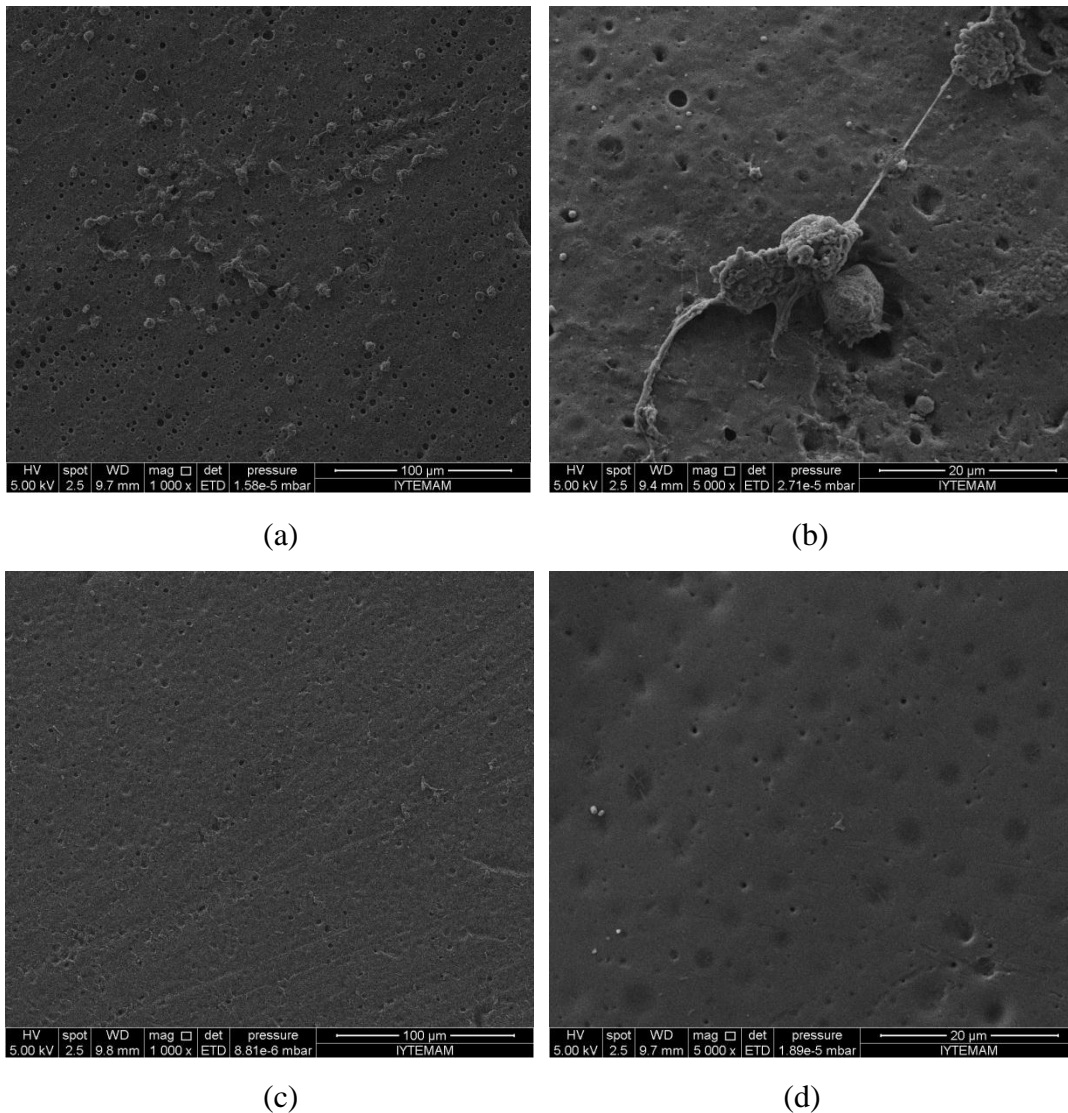


Figure 5.12. The SEM pictures of (a-b) PSF-SPSF and (c-d) PSF-SPSF-PEI-ALG/HEP-15-1b membranes after incubating in whole blood for 15 minutes. Magnification (a-c) x1000 and (b-d) x 5000.

### 5.1.2.3. Activated Partial Thromboplastin Time (APTT)

The anticoagulant property of the heparin immobilized membranes was determined by means of activated partial thromboplastin time (APTT). The unmodified PSF, PSF-SPSF and PEI/ALG deposited membranes were used as reference samples. The APTT values for the samples are listed in Table 5.3. All heparin immobilized membranes displayed significantly longer APTT values than other membranes and the control. In the absence of heparin, improvement in the APTT values of the PEI/ALG coated membranes compared with those of PSF and PSF-SPSF membranes is due to

their decreased protein adsorption capacities and platelet activation. Increasing the number of polyelectrolyte coated layers did not change the blood coagulation time ( $p>0.05$ ) since protein adsorption capacities of these membranes were similar and heparin mixed with ALG was coated only on the outermost layer of the assembly. In addition, no significant improvement in the APTT values was observed by increasing the initial concentration of heparin in the depositing solution first from 15 % to 45 % and further to 100 % ( $p>0.05$ ). This simply proves that diluting HEP with ALG does not cause a decrease in its biological activity. When HEP is blended with ALG, the surface of PEI is partly covered by long chained ALG. Therefore, most of the active sites of heparin,  $-\text{OSO}_3^-$ , which forms an ionic bond with the positively charged  $\text{NH}_2$  groups in PEI can become free, and its biological activity is preserved. The proposed strategy can be an economical alternative for the modification of hemodialysis membranes since HEP is an expensive compound compared to ALG. In previous studies, the LBL deposition of HEP with different polyelectrolytes such as chitosan, collagen, dextrin sulfate and albumin on different blood-contacting surfaces has been carried out (Sperling et al., 2006; Houska et al., 2008; Liu et al., 2009; Chen et al., 2009; Shu et al., 2011; Lin et al., 2011). In these studies, HEP was used alone not only in the last layer of the assembly but also in each alternating layer to provide charge reversal of the polycation layer. Consequently, it is obvious that amount of HEP used in such assemblies is more than that required in the assembly proposed in this study.

Table 5.3. APTT values of the unmodified and modified PSF membranes with layer by later self assembly of polyethyleneimine/alginate-heparin.

Membrane Code	APTT (sec)	
	Before stored in PBS	After stored in PBS
Control (Blood Plasma)	35±3	35±3
PSF-SPSF	37±2	35±5
PSF-SPSF-PEI-ALG-1b	63±5	59±3
PSF-SPSF-PEI-ALG-5b	57±7	52±9
PSF-SPSF-PEI-ALG/HEP-15-1b	195±43	142±43
PSF-SPSF-PEI-ALG/HEP-15-5b	195±43	115±40
PSF-SPSF-PEI-ALG/HEP-45-1b	247±35	195±43
PSF-SPSF-PEI-ALG/HEP-45-5b	221±40	195±43
PSF-SPSF-PEI-ALG/HEP-100-1b	195±43	169±44
PSF-SPSF-PEI-ALG/HEP-100-5b	221±40	142±43

The APTT values for the membranes after stored in pH 7.4 PBS at 37 °C for a period of 4 hours were not found significantly different from those for the freshly prepared membranes ( $p>0.05$ ). This result suggests that ionic bonding of heparin to the surface is sufficiently strong that can provide to retain most of its anticoagulant activity is stable under typical hemodialysis conditions.

#### 5.1.2.4. Cytotoxicities

Cytotoxicities of the unmodified and modified PSF membranes were examined with peripheral blood mononuclear cells (PMBCs) isolated from the sample of healthy human blood. Figure 5.13 shows live and dead cells labeled with thiazole orange (TO) and propidium iodide (PI), respectively and Table 5.4 lists the percentage of live cells. The results demonstrated that toxic effects of all the membranes on the PMBCs are similar ( $p>0.05$ ) and proposed modification technique does not cause a negative effect on the nontoxic property of PSF.

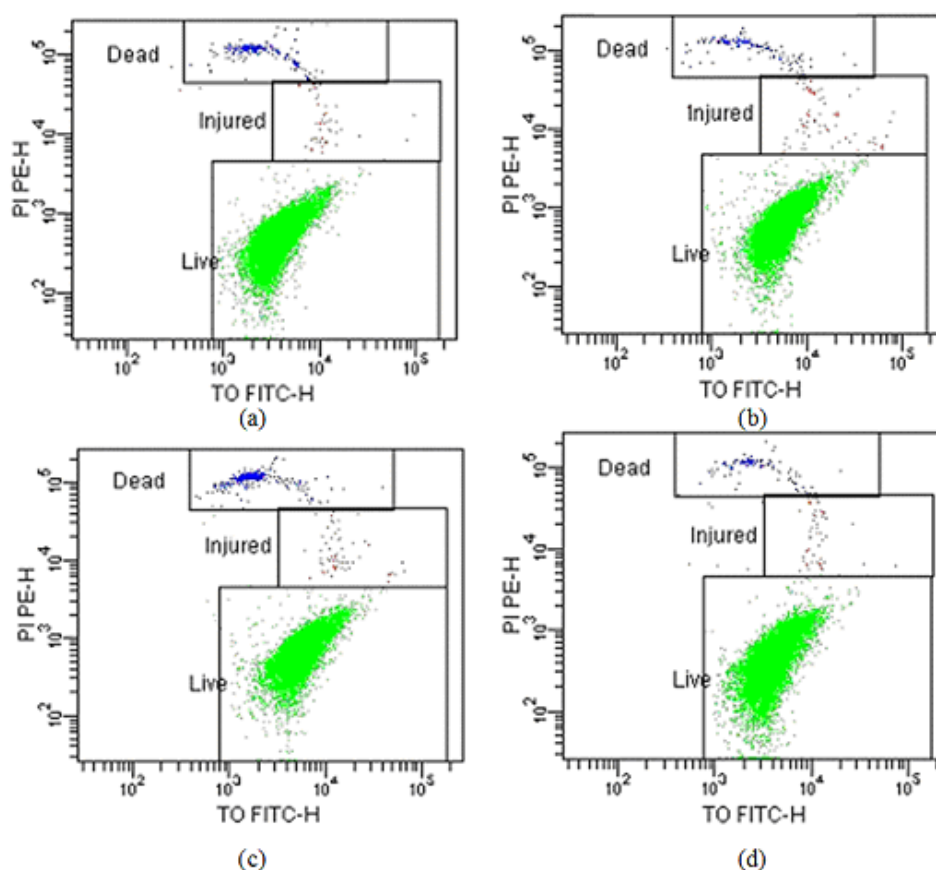


Figure 5.13. Live and dead cells labeled with TO and PI after incubating PMBCs with  
 (a) Control (PMBCs without membrane) (b) PSF (c) PSF-SPSF (d) PSF-SPSF-PEI-ALG/HEP-15-1b membranes.

Table 5.4. % of live cells after incubating PMBCs with the unmodified and modified PSF membranes for 4 hours.

Membrane Code	Live Cell %
Control (PMBCs)	99.3±0.5
PSF-SPSF	99.6±0.3
PSF-SPSF-PEI-ALG-1b	98.8±0.2
PSF-SPSF-PEI-ALG-5b	99.8±0.7
PSF-SPSF-PEI-ALG/HEP-15-1b	98.1±0.3
PSF-SPSF-PEI-ALG/HEP-15-5b	98.7±0.5
PSF-SPSF-PEI-ALG/HEP-45-1b	97.9±0.9
PSF-SPSF-PEI-ALG/HEP-45-5b	97.6±1.1

The positively charged PEI is known to be toxic, therefore, the amount of PEI released during 4 hours in PBS with salt at pH 7.4 and 37 °C was determined. The results indicated that the released amount which is about 3.3 µg per ml blood (1 µg/cm<sup>2</sup> membrane) is the lower than the toxic dosage of branched PEI (10 µg/ml cell) (Wen et al., 2012). The differences in the toxicities caused by the support PSF membrane and the PEI coated membranes on the PMBCs were also found insignificant at the end of 24 and 48 hours incubation. The result confirms that the amount of PEI leached from the membrane into the blood is in the nontoxic limits.

### **5.1.3. Transport and Mechanical Properties of the Heparin Immobilized Membranes**

The results of permeation experiments showed that the differences in transport rates of all solutes through bare PSF membrane, PSF-SPSF blend membrane and PEI/ALG-HEP coated membranes are statistically insignificant ( $p > 0.05$ ) (Figure 5.14). Transport properties of asymmetric membranes are mainly affected by the porosity and pore size of dense skin layer and also thickness of the dense skin layer. The layer by layer deposition of polyelectrolytes occurs on the surface, thus, this technique does not change the bulk structure of the membrane as shown in Figure 5.6. Furthermore, depositing PEI/ALG-HEP layers onto the surface of the membranes caused only a few nanometer increase in thickness of the membranes. Therefore, neither bulk structure, nor thickness of dense skin layer are affected by polyelectrolyte deposition.

The clearing performance of the unmodified and modified membranes for lysozyme and vitamin B12 are comparable with those of the industrial hemodialysis membranes AN69 ( $1.5 \times 10^{-12} \text{ m}^2 \cdot \text{s}^{-1}$  for MW=15000;  $4.0 \times 10^{-11} \text{ m}^2 \cdot \text{s}^{-1}$  for MW=1700) and Cuprophan ( $1.0 \times 10^{-13} \text{ m}^2 \cdot \text{s}^{-1}$  MW=15000;  $1.5 \times 10^{-11} \text{ m}^2 \cdot \text{s}^{-1}$  MW=1700), reported by Langsdorf and Zydney (1994).

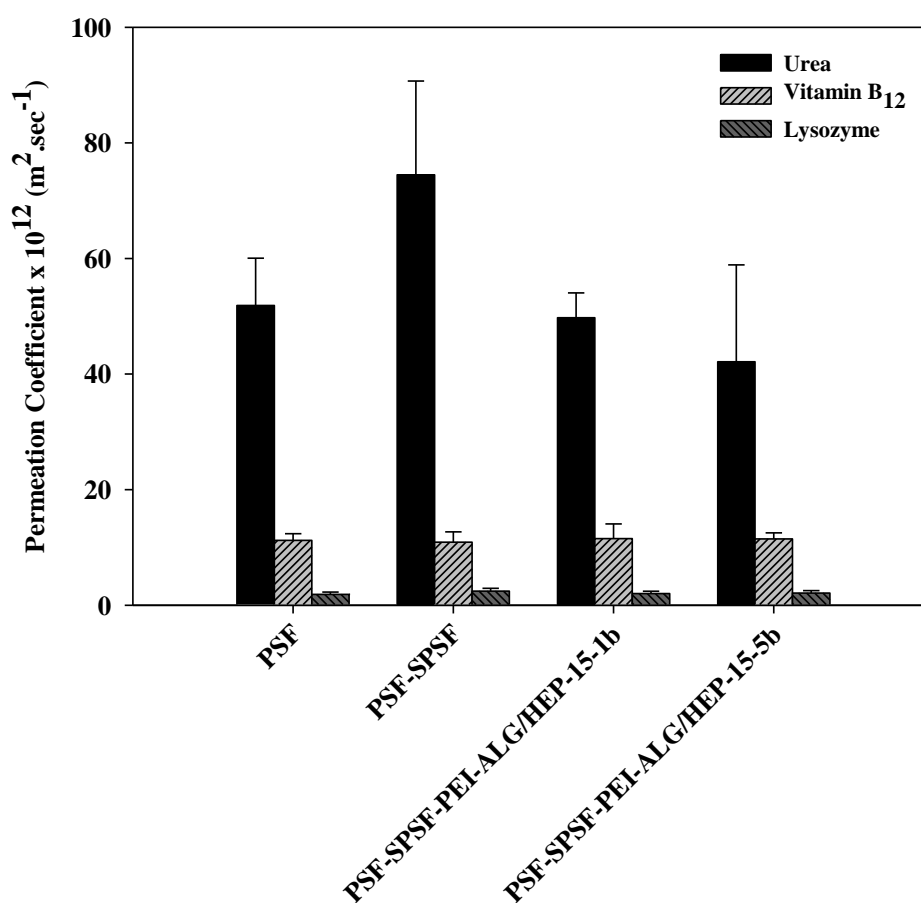


Figure 5.14. The permeation coefficient of urea, vitamin B<sub>12</sub> and lysozyme through the unmodified and modified PSF membranes with layer by layer self assembly of polyethyleneimine/alginate-heparin.

Permeation of NaCl through membranes was also investigated to show the effect of polyelectrolyte deposition on the transport properties of salt. The salt permeability through unmodified PSF membrane was enhanced by blending with SPSF from  $5.60 \times 10^{-11} \text{ m}^2.\text{sec}^{-1}$  to  $7.72 \times 10^{-11} \text{ m}^2.\text{sec}^{-1}$ . This improvement was resulted from the introducing charged groups on the surface by blending SPSF. On the other hand, it was not changed with the 1 bilayer polyelectrolyte deposition (PSF-SPSF-PEI-ALG-1b) since the surface charge densities of PSF-SPSF and polyelectrolyte deposited PSF-SPSF membranes were found similar.

Mechanical properties of the membranes were evaluated in terms of maximum tensile strength and Young's modulus values and the results are listed in Table 5.5. As expected, blending PSF with SPSF caused slight decrease in maximum tensile strength

of the PSF membrane. While deposition of 1 bilayer polyelectrolyte on the PSF-SPSF membrane does not significantly change the mechanical properties ( $p>0.05$ ), the maximum tensile strength of the 5 bilayer polyelectrolyte coated membrane (PSF-SPSF-PEI-ALG/HEP-15-5b) is higher than both the PSF-SPSF and the 1 bilayer polyelectrolyte coated membrane (PSF-SPSF-PEI-ALG/HEP-15-1b). This can be attributed to elimination of defects on the surface of the membrane after 5 bilayer coating. The mechanical strength of the unmodified and modified membranes are much higher than the required tensile strength for the maximum pressure of 500 mm Hg ( $60.6 \times 10^{-3}$  MPa) (Leber et al., 1978).

Table 5.5. Mechanical properties of the unmodified and modified PSF membranes with layer by layer self assembly of polyethyleneimine/alginate-heparin.

Membrane Code	Maximum Tensile Stress (MPa)	Young Modulus (MPa)
PSF	2.78±0.22	39.82 ±5.97
PSF-SPSF	2.25 ±0.18	50.25 ±7.54
PSF-SPSF-PEI-ALG/HEP-15-1b	2.04 ±0.16	43.17 ±6.48
PSF-SPSF-PEI-ALG/HEP-15-5b	2.96 ±0.24	45.71 ±6.86

## 5.2. Immobilization of Alpha Lipoic Acid onto Polysulfone Membranes to Suppress Hemodialysis Induced Oxidative Stress

In the second part of the thesis, it is aimed to develop functional PSF membranes through  $\alpha$ -lipoic acid (ALA) immobilization and investigate the *in vitro* effects of this modification on blood compatibility of the membranes, especially on the inhibition of reactive oxygen species in blood plasma. To achieve this task, 2 uncoated (PSF and PSF-SPSF) and 3 coated membranes (PSF-SPSF-PEI-ALA-I, PSF-SPSF-PEI-ALA-II, PSF-SPSF-PEI-ALA-III) were prepared as listed in Table 5.6. The coated membranes were manufactured by first adsorbing a positively charged, hydrophilic polyelectrolyte PEI on the negatively charged PSF-SPSF membrane surface and then binding ALA to PEI through electrostatic interactions. In the case of PSF-SPSF-PEI-ALA-II membrane,

ALA was sandwiched between two PEI layers while it is forming the outermost layer of the PSF-SPSF-PEI-ALA-I and PSF-SPSF-PEI-ALA-III membranes.

Table 5.6. Codes of the unmodified and modified PSF membranes with ALA immobilization

Membrane Code	Weight percentages (wt.%)			Molecule Type on the Last Layer	ALA Concentration (mg.ml <sup>-1</sup> )
	PSF	SPSF	NMP		
PSF	20	0	80	-	-
PSF-SPSF	10	10	80	-	-
PSF-SPSF-PEI-ALA-I	10	10	80	ALA	1
PSF-SPSF-PEI-ALA-II	10	10	80	PEI	1
PSF-SPSF-PEI-ALA-III	10	10	80	ALA	5

### 5.2.1. Quantification of Amount of ALA in the Membrane and Release of ALA from the Membranes

It is crucial to determine the amount of ALA immobilized in the membrane and the potential loss of ALA during typical hemodialysis period. The absorption band of alpha-lipoic acid at around 330 nm starts to disappear which corresponds to the rupture of S-S bond of the 1,2-dithiolane ring in lipoic acid (Matsugo et al., 1996). The shift around 270 nm observed in the UV-VIS spectra can be considered as an indication of the formation of thyl radical (Manoj et al., 2011). Thus, all measurements were taken by scanning between 200-500 nm as shown in Figure 5.15a. The obtained result in Figure 5.15b shows that at low ALA concentration (1 mg.ml<sup>-1</sup>), more than 50% of ALA added to the coating solution was retained in the final membrane. Upon increase in ALA concentration in the solution to 5 mg.ml<sup>-1</sup> the ALA loading of the final membrane, PSF-SPSF-PEI-ALA-III, slightly increased compared with the amount immobilized in PSF-SPSF-PEI-ALA-I membrane.

The amount of ALA leached into PBS solution at the end of 4 hour incubation is also shown in Figure 5.15. As expected, the lowest amount of ALA release occurred from the PSF-SPSF-PEI-ALA-II membrane since ALA was sandwiched between two PEI layers. Compared with this membrane, the fraction of ALA leached out from the



PSF-SPSF-PEI-ALA-I and PSF-SPSF-PEI-ALA-III membranes relative to the amount immobilized into these membranes initially is higher due to direct contact of ALA with the solution. For all cases most of the loaded ALA retained within the membranes after incubating with PBS for 4 hours, implying a sufficiently strong PEI-ALA complex formation. This results because at pH 7.4 PEI is highly positively charged (isoelectric point=8.8) while ALA is highly negatively charged (pKa=5.2) (Ruixia et al., 2004) with degree of ionization of 96% and 99% (calculated by Henderson-Hasselbalch equation), respectively. It should be noted that the ALA released from the membranes does not necessarily hinder the use of these membranes in hemodialysis, because the maximum amount released into the blood from a 2 m<sup>2</sup>-membrane area (0.097 mg.ml<sup>-1</sup>) is comparable to the amount orally administrated (0.100 mg.ml<sup>-1</sup>) to the patients in clinical studies (Teichert et al., 2005; Chang et al., 2007).

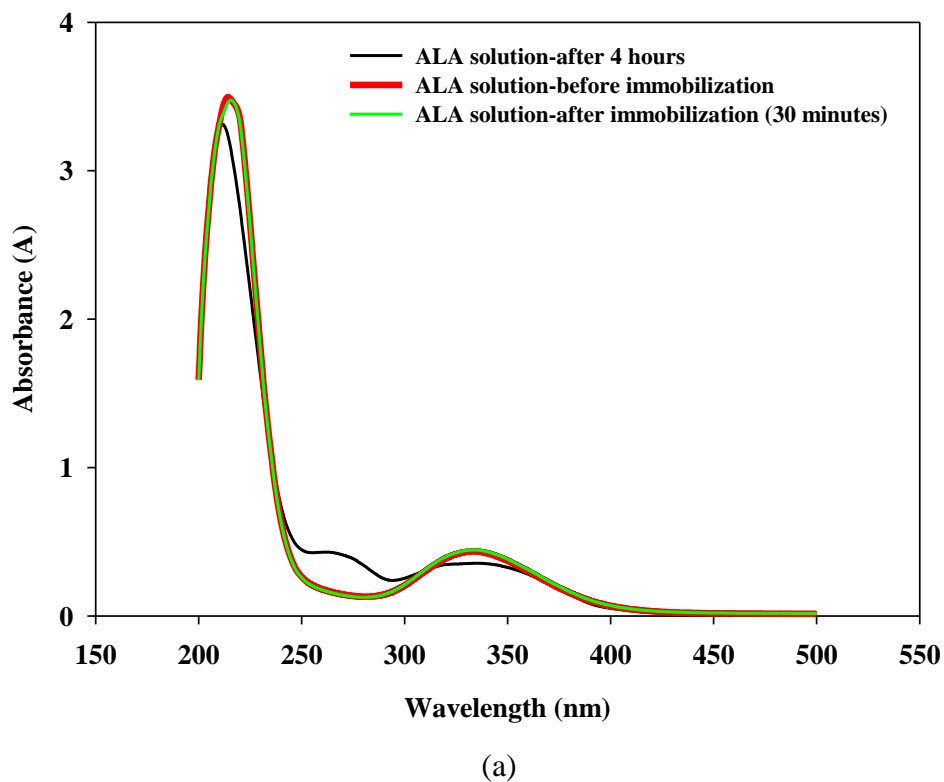
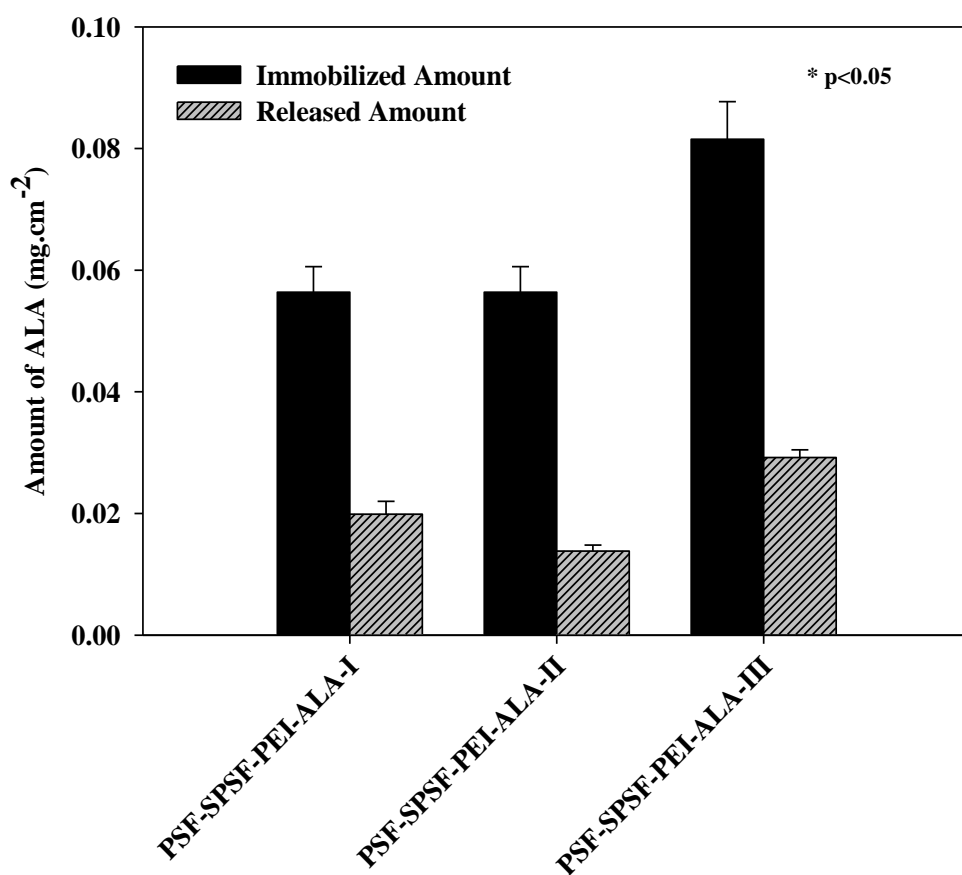


Figure 5.15. (a) UV-Spectrum of ALA (b) Amount of immobilized and released ALA. Immobilized amount of ALA for PSF-SPSF-PEI-ALA-III membrane is significantly different from that of PSF-SPSF-PEI-ALA-I and PSF-SPSF-PEI-ALA-II membranes ( $p < 0.05$ ). Released amounts of ALA for each membrane are statistically different from each other ( $p < 0.05$ ).

(cont. on next page)



(b)

Figure 5.15. (cont.)

### 5.2.2. Surface Characterization of ALA Immobilized Membranes

Figure 5.16 shows that blending PSF with SPSF improved its hydrophilic character as confirmed by the drop in the water contact angle values. No significant decrease in the contact angle values was observed through ALA immobilization on the surface of the blend membrane due to presence of hydrophobic groups in addition to hydrophilic groups in the structure of ALA. On the other hand, the contact angle of the PSF-SPSF-PEI-ALA-II membrane was found significantly lower ( $p < 0.05$ ) than that of the PSF-SPSF blend membrane since hydrophilic polyelectrolyte PEI, forms the last layer of this membrane.

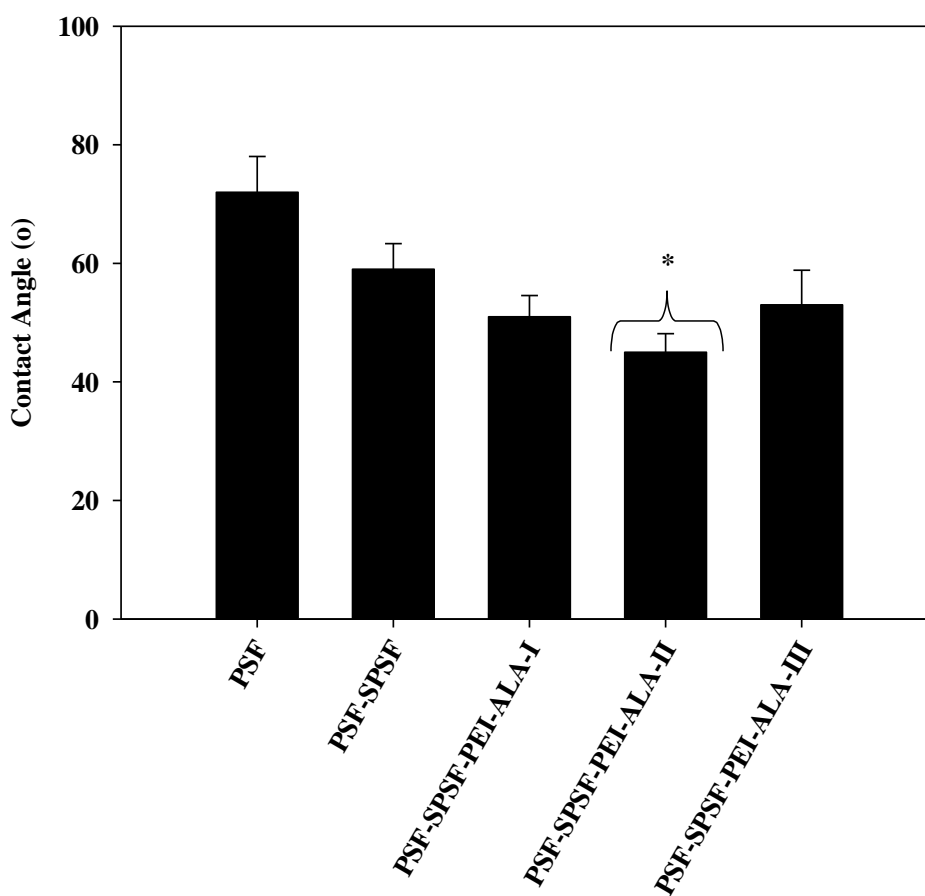


Figure 5.16. Water contact angles of PSF membranes. \*Contact angle of PEI-ALA-II membrane is statistically different from that of PSF-SPSF membrane ( $p < 0.05$ )

XPS evaluation spectra of two different ALA coated PSF membranes are shown in Figure 5.17. In order to determine which component is located close to the surface, the low angle ( $15^\circ$ ) measurements were performed. The ratio of the areas under the deconvoluted S and N peaks to C peaks were calculated. The calculated values for PSF-SPSF-PEI-ALA-I membrane were compared with those of the PSF-SPSF-PEI-ALA-II membranes in order to investigate the surface groups.

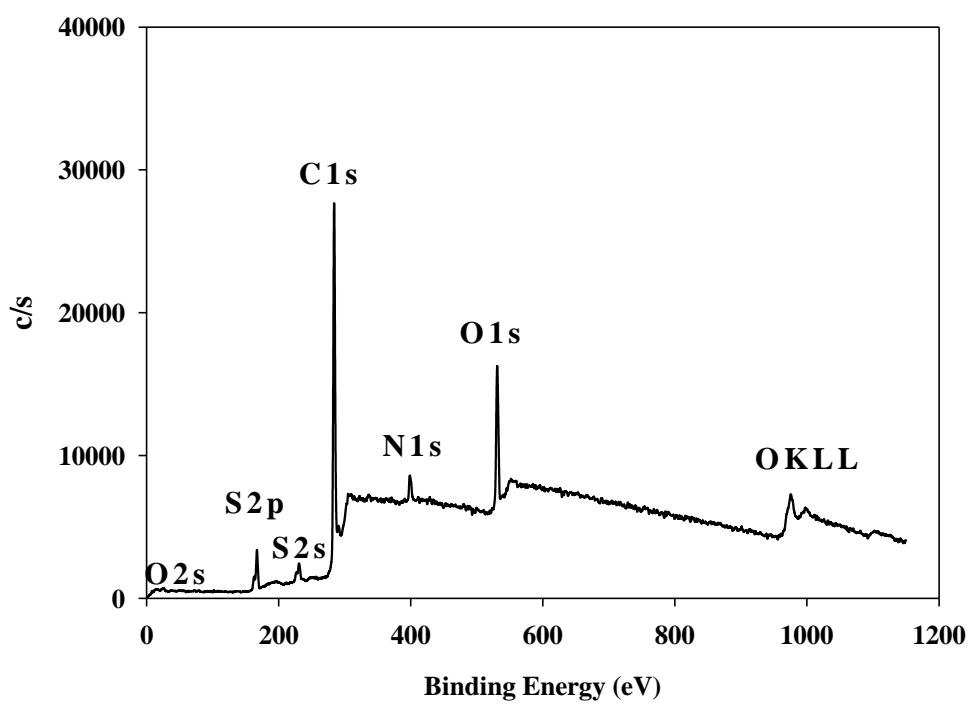
N1s high-resolution spectra, gives mainly charged amine group nitrogen ( $-\text{NH}_3^+$ ) peak at 400.7 eV as shown in Figure 5.17b. The peak for uncharged amine group ( $-\text{NH}_2$ ) was not observed since 96 % of the amine groups of PEI are protonated. It is seen from Table 5.7 that the area for N1s peak obtained at both  $15^\circ$  and  $75^\circ$  with PEI-ALA-II membrane is higher than that for the PEI-ALA-I membrane. The result at  $15^\circ$  simply indicates the presence of more  $-\text{NH}_3^+$  groups near the surface of the PSF-SPSF-

PEI-ALA-II membrane, hence, proving that PEI forms the last layer of this membrane. The higher value of the area at  $75^\circ$  for the PSF-SPSF-PEI-ALA-II membrane results from the presence of two PEI layers where ALA is sandwiched between these layers.

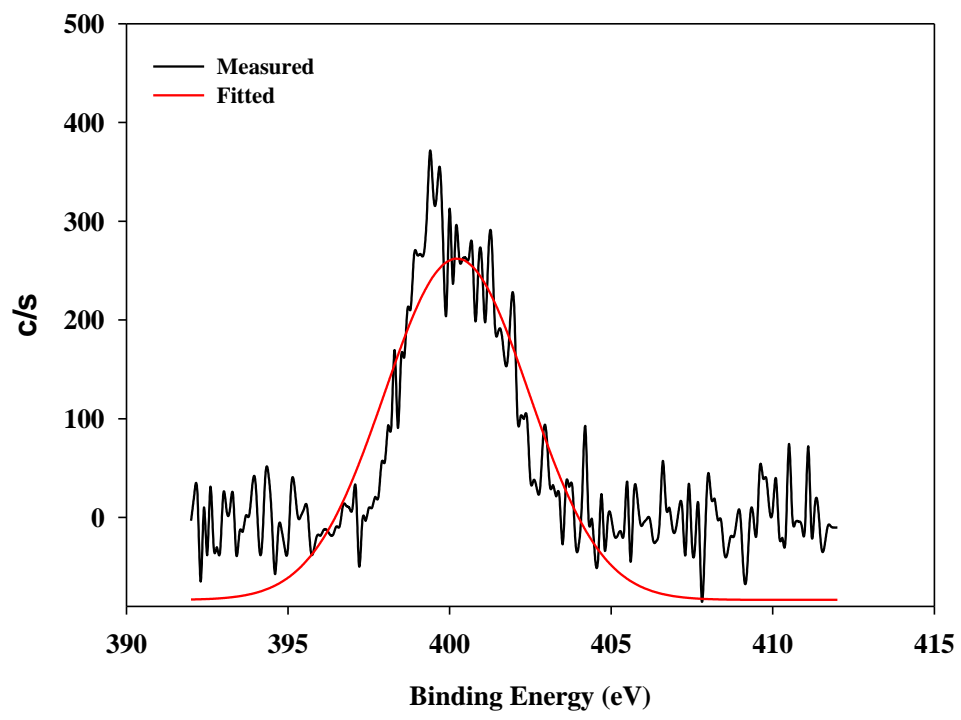
The S2p signal consists of three deconvoluted peaks (Figure 5.17c). The first peak situated at 162.7 eV, is the signal of the sulphur bonded to carbon or hydrogen (-S-C or -S-H), the second peak situated at 164.1 eV, is the signal of the elemental S (-S-S), and the signal at higher binding energy (167.1 eV) represents the oxidized sulfur species ( $-\text{SO}_3^{-2}$  or  $-\text{SO}_2$ ). Larger area of the peak at 162.7 eV and 164.1 eV, recorded at  $15^\circ$  for the PEI-ALA-I membrane compared with the PEI-ALA-II (Table 5.7) confirms the presence of ALA as the last layer of this membrane since -S-S, -S-H or -S-C exists only in the structure of ALA. This result also confirms that the cyclic disulphide bond, the active site of ALA, is available on the surface as proposed at the beginning of this study. The ratio of the peak areas at 167.1 eV is close to 1 since these peaks result from  $\text{SO}_3^{-2}$  groups in the support membrane common to both PSF-SPSF-PEI-ALA-I and PSF-SPSF-PEI-ALA-II membranes.

The high-resolution C1s spectrum (Figure 5.17d) shows four deconvoluted peaks as follows: the aliphatic carbon (-C-C- or -C-H at 285.1 eV), carbon bonded to the amine groups (-HC-NR<sub>2</sub>, where R is C or H, at 286.5 eV), the carboxyl carbon (-COO- at 288.1 eV) and carbon bonded to sulfur (-C-S- at 284.1 eV).

The O1s signal consists of two deconvoluted peaks (Figure 5.17e). The first peak situated at 532.4 eV represents the ( $\text{SO}_3^{-2}$ ), and the second peak situated at 530.4 eV represents the carboxylic oxygen atom (COO<sup>-</sup>).



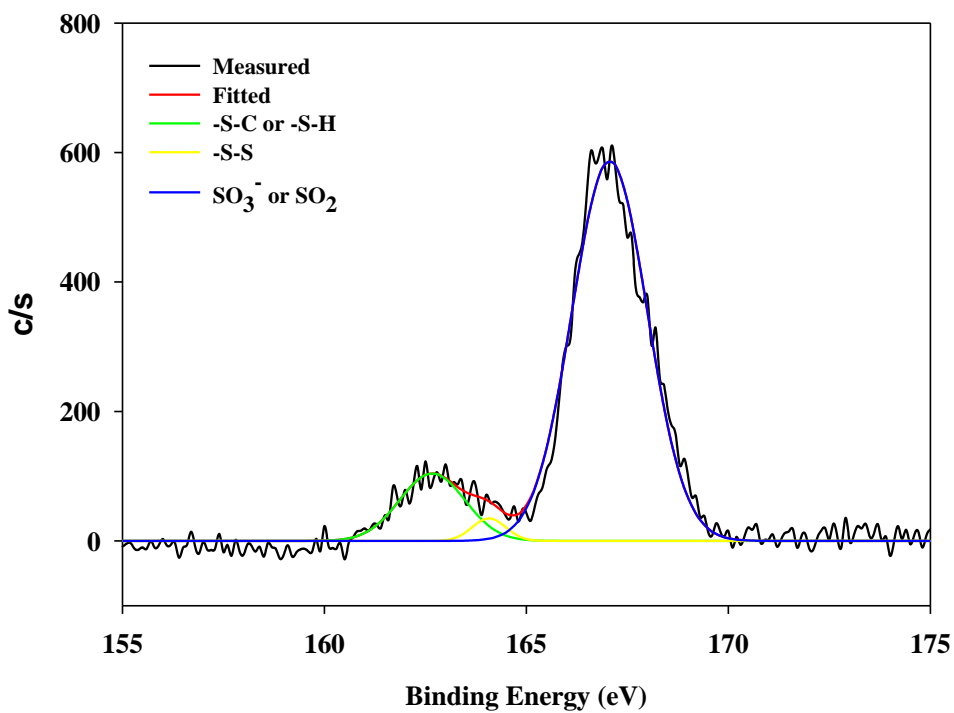
(a)



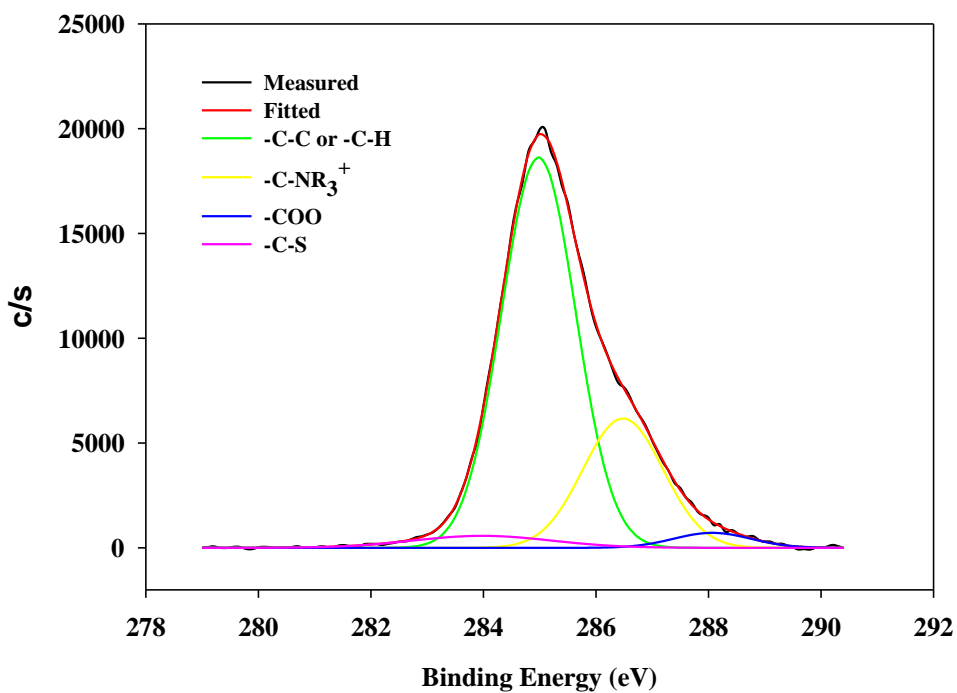
(b)

Figure 5.17. XPS Spectra of PSF-SPSF-PEI-ALA-I membrane for (a) survey at 45° (b) N 1s (c) S 2p (d) C 1s and (e) O 1s peaks at 15°.

(cont. on next page)



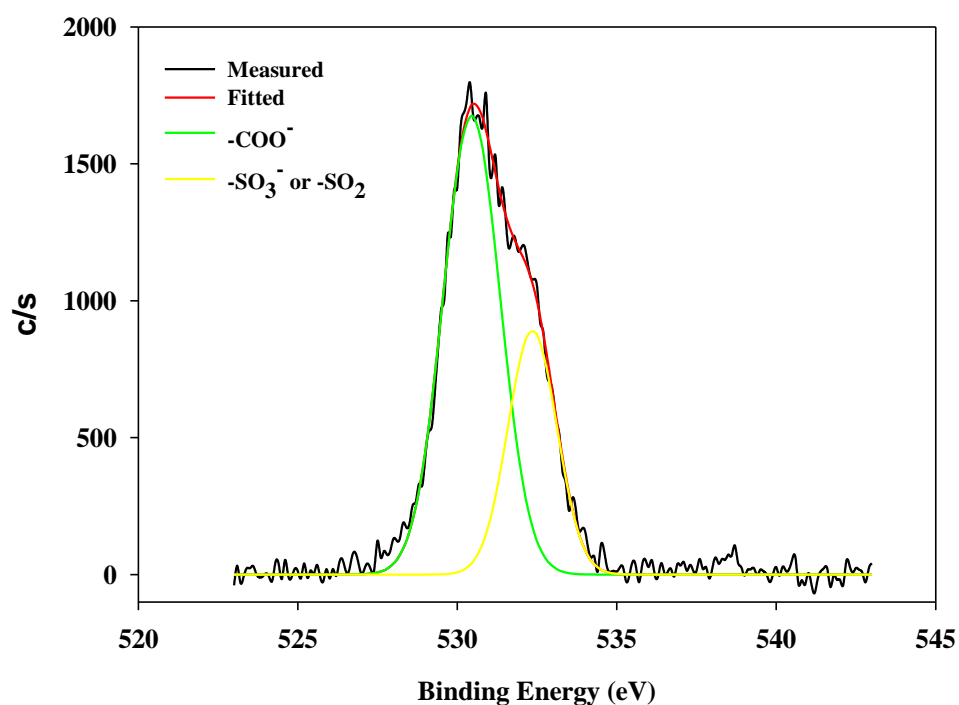
(c)



(d)

Figure 5.17. (cont.)

(cont. on next page)



(e)

Figure 5.17. (cont.)

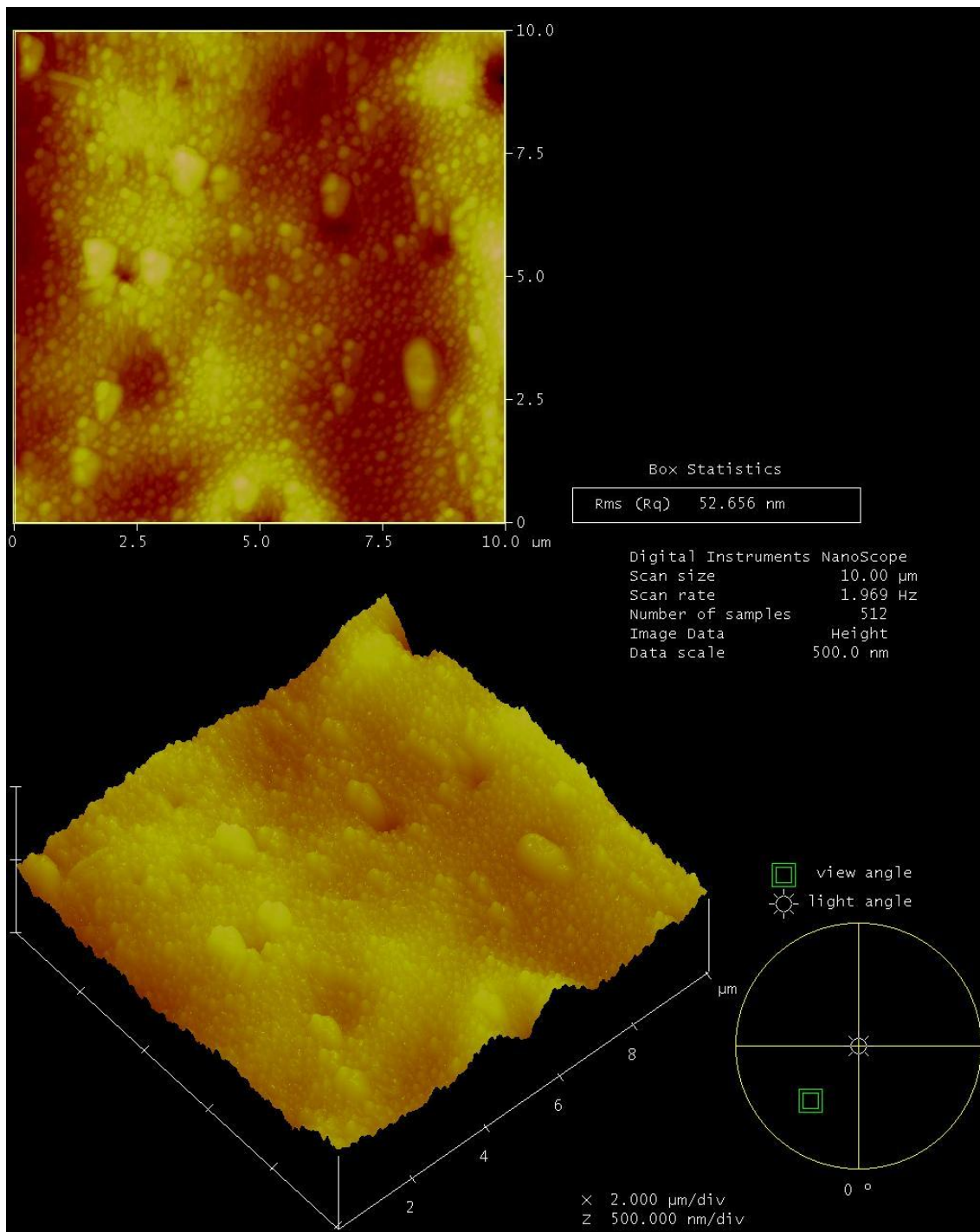
Table 5.7. The ratio of calculated peak areas of the PSF-SPSF-PEI-ALA-I membrane to those of PSF-SPSF-PEI-ALA-II membrane

Main peaks	N1s	S2p		
Deconvoluted peaks	$-\text{NH}_3^+$	$-\text{S-C}$ or $-\text{S-H}$	$-\text{S-S}$	$-\text{S-O}$
Core level (eve)	400.7	162.7	164.1	167.1
Takeoff angle				
$15^\circ$	0.90	2.20	3.33	1.14
$75^\circ$	0.84	1.48	1.66	1.15

The surface roughness of the membranes was obtained from the analysis of AFM images shown in Figure 5.18. As shown previously, the unmodified PSF

membrane had the smoothest surface and sulfonation significantly increased the surface roughness. The layer by layer deposition of PEI-ALA (52 nm) or PEI-ALA-PEI (48 nm) on the surface of PSF-SPSF improved the smoothness of the surface (Figure 5.19). This can be explained by the enhanced diffusional mobility of PEI chains allowing deformation on the surface of the PSF-SPSF membrane to minimize the surface area as a result of the energy-minimization process. Similar roughnesses of coated membranes which have either PEI or ALA on the outermost layer originated from the small size of ALA.

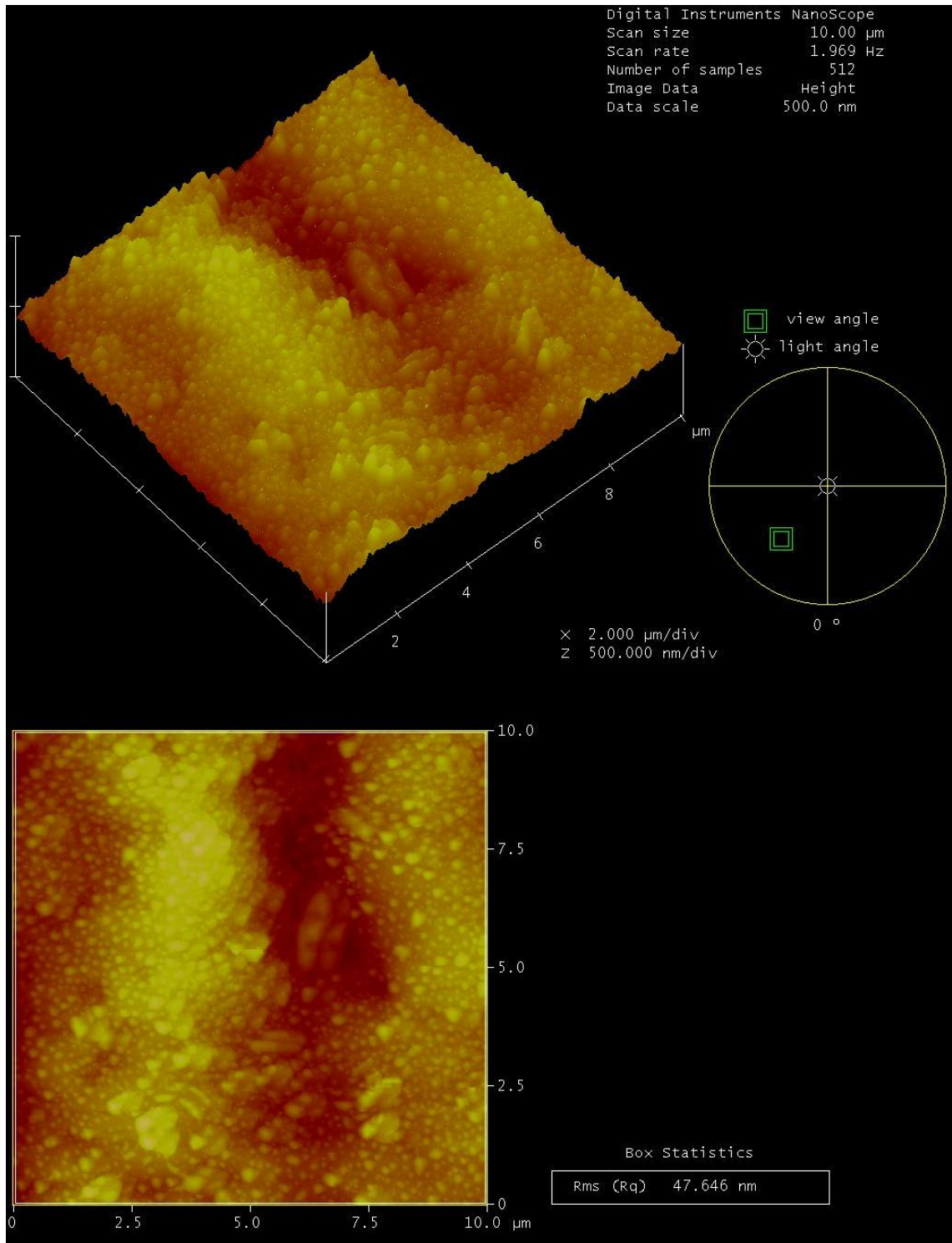




(a)

Figure 5.18. AFM images of (a) PSF-SPSF-PEI-ALA-I (b) PSF-SPSF-PEI-ALA-II membranes.

(cont. on next page)



(b)

Figure 5.18. (cont.)

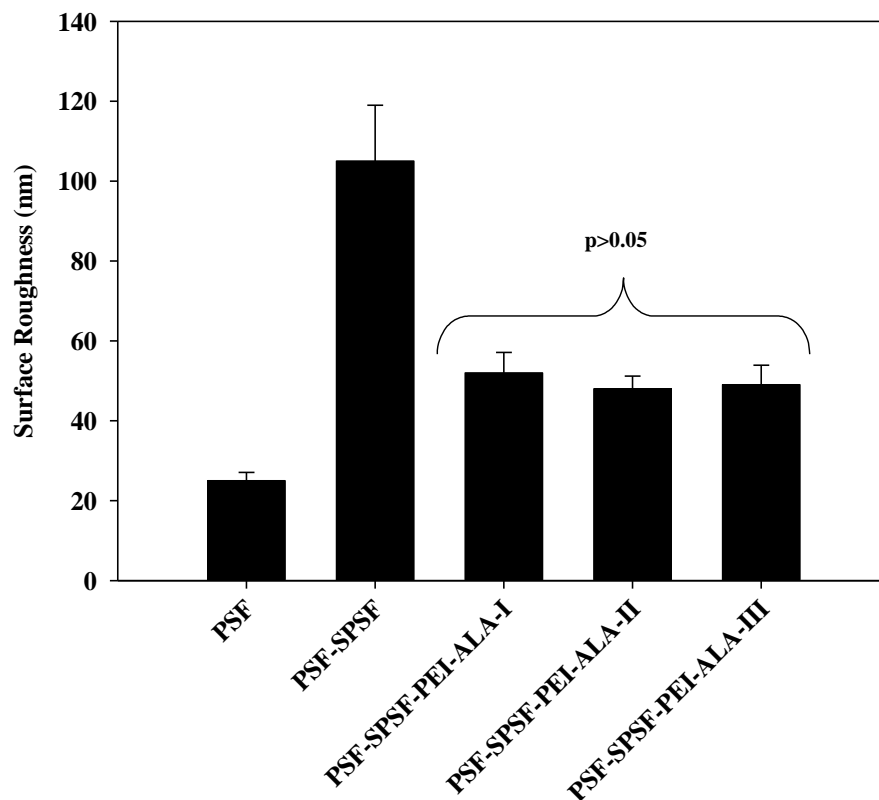


Figure 5.19. Surface roughness of unmodified and modified PSF membranes with ALA immobilization.

Figure 5.20 illustrates that the PEI/ALA coating did not cause any change in bulk structure of the PSF-SPSF membrane. Despite ALA is a small molecule, it could not penetrate inside the pores due to the presence of PEI layer due to its strong binding to PEI.

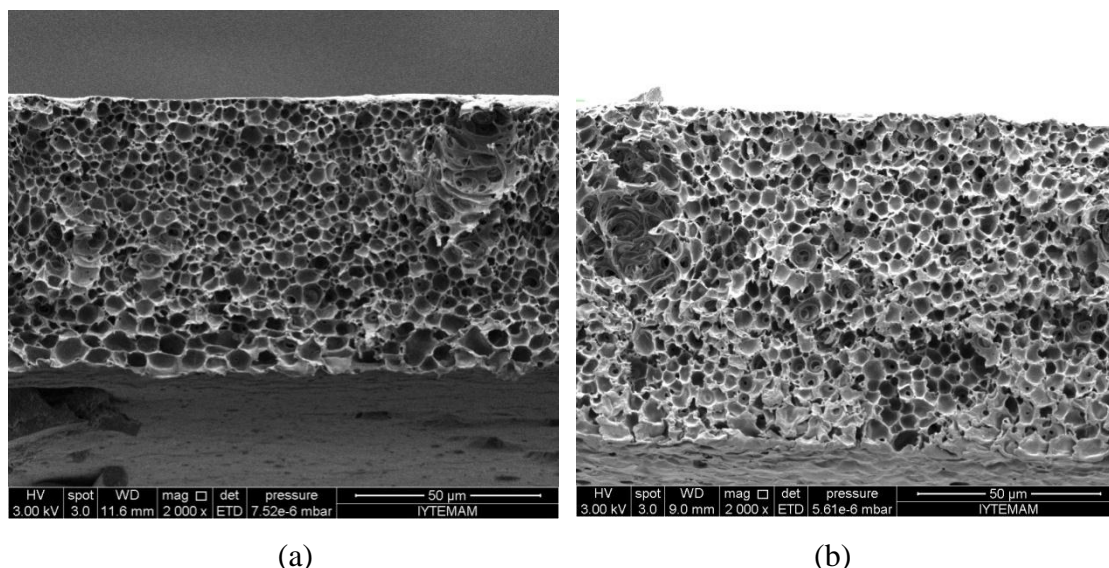


Figure 5.20. SEM pictures of (a) PSF-SPSF and (b) PSF-SPSF-PEI-ALA-I membranes. Magnificationx2000.

### 5.2.3. The Antioxidant Activity of Free $\alpha$ -Lipoic Acid and $\alpha$ -Lipoic Acid Immobilized Membranes

The radical scavenging activities (RSA) of free and immobilized ALA were calculated with Equation 4.1. and the results are plotted in Figure 5.21. The initial antioxidant activities (10<sup>th</sup> minute) of immobilized ALA are lower than that of the free ALA due to increased mass transfer resistance for the DPPH radical to reach active sites and limited accessibility to these sites. On the other hand, at the end of 4 hours, immobilized ALA has higher activities since the antioxidant activity of free ALA is stable for only 10 minutes (data not shown). Instability of ALA under light and heat and its short biological half-life has also been reported by other studies (Kofuji et al., 2008; 2009). The highest antioxidant activity was obtained with the PSF-SPSF-PEI-ALA-II membrane. This is not only due to conserving activity of ALA between two PEI layers, but also due to fewer ALA leached out from this membrane during 4 hours. Although the initial antioxidant activity of the PSF-SPSF-PEI-ALA-III membrane is higher than that of the PSF-SPSF-PEI-ALA-I membrane due to higher ALA loading in this membrane, their activities are almost the same at the end of 4 hours. The results in Figure 5.21 indicate that ALA can maintain its antioxidant activity during typical hemodialysis time by immobilizing onto the membrane, especially between two hydrophilic polyelectrolyte layers.

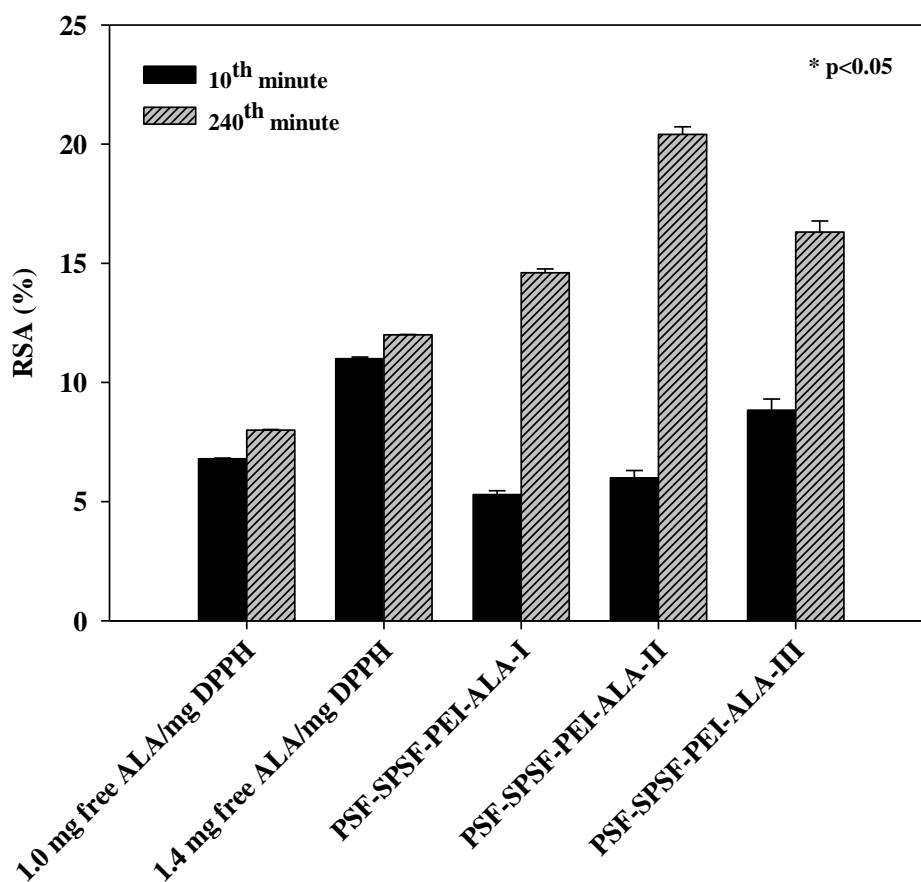


Figure 5.21. % RSA of free and immobilized ALA. \*RSA (%) values of free ALA and all ALA immobilized membranes at 240<sup>th</sup> minute are statistically different from each other ( $p < 0.05$ )

#### 5.2.4. Determination of Immobilized ALA Stability in Buffer

The stability of immobilized ALA was determined by storing the membranes in pH 7.4 PBS buffer at 37 °C for a period of 4 hours. The retained antioxidant activities of the two membranes, PSF-SPSF-PEI-ALA-I and PSF-SPSF-PEI-ALA-III, are similar since they include almost the same amount of ALA at the end of storage period in PBS (Figure 5.22). As expected immobilization of ALA between two PEI layers caused less activity loss during storage compared to the case that ALA was on the outermost layer of the assembly.

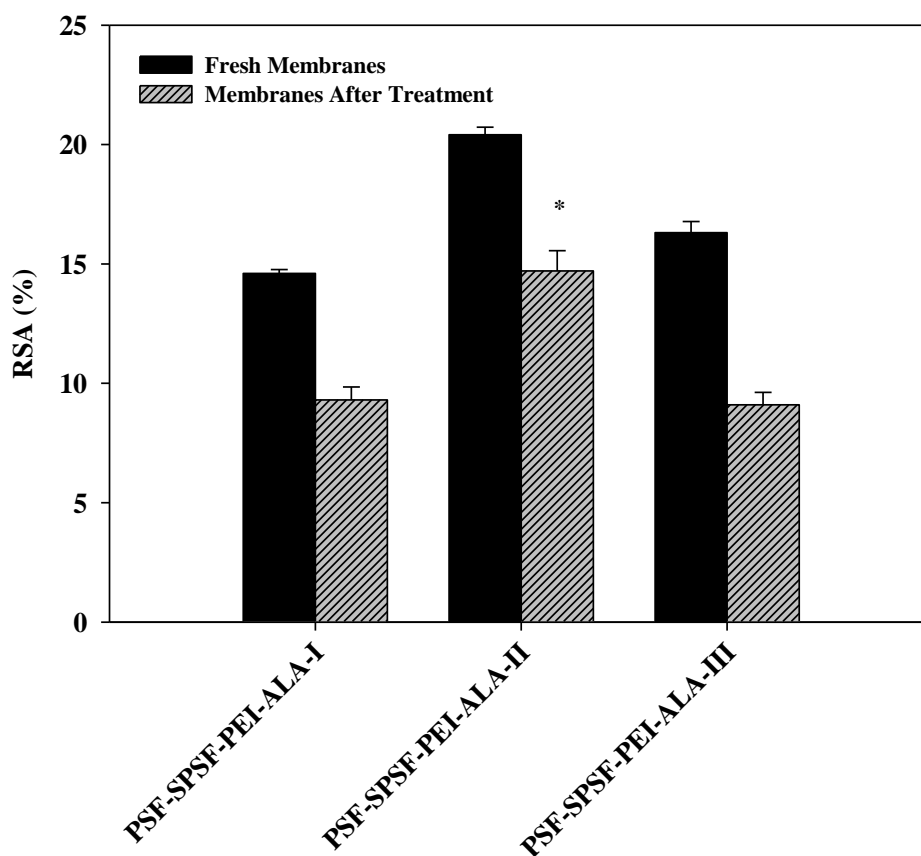


Figure 5.22. The effect of storing time on the relative antioxidant activity of  $\alpha$ -lipoic acid immobilized on PSF membranes. Membranes were stored in phosphate buffer solution at pH=7.4, T=37°C for 4 hours. \*After treatment, RSA (%) value of the PSF-SPSF-PEI-ALA-II membrane is statistically different from those of the PSF-SPSF-PEI-ALA-I and PSF-SPSF-PEI-ALA-III membranes. (p<0.05)

## 5.2.5. *In vitro* Hemocompatibility of ALA Immobilized PSF Membranes

### 5.2.5.1. Protein Adsorption Capacity

The amount of plasma protein adsorbed on the membranes was determined since it is the initial reaction of blood-material interactions followed by an increase in the levels of reactive oxygen species (ROS) in addition to thrombogenic formation. The

highest plasma protein adsorption occurred on the most hydrophobic PSF membranes, whereas blending PSF with SPSF and coating this blend membrane with PEI-ALA layer reduced protein adsorption by 24% and approximately 40%, respectively, as seen in Figure 5.23. Although the PSF membrane has the smoothest surface among all modified and unmodified membranes, less protein binding to the PSF-SPSF and PEI-ALA deposited membranes is related to their more hydrophilic character. In addition, the blend membrane (PSF-SPSF) and the membranes containing ALA in the outermost layer (PSF-SPSF-PEI-ALA-I and PSF-SPSF-PEI-ALA-III) carry negatively charged groups on their surfaces that can repel similarly charged blood proteins. The lower protein adsorption capacity of the ALA immobilized membranes is attributed to their much more smooth surfaces compared with that of the PSF-SPSF membrane.

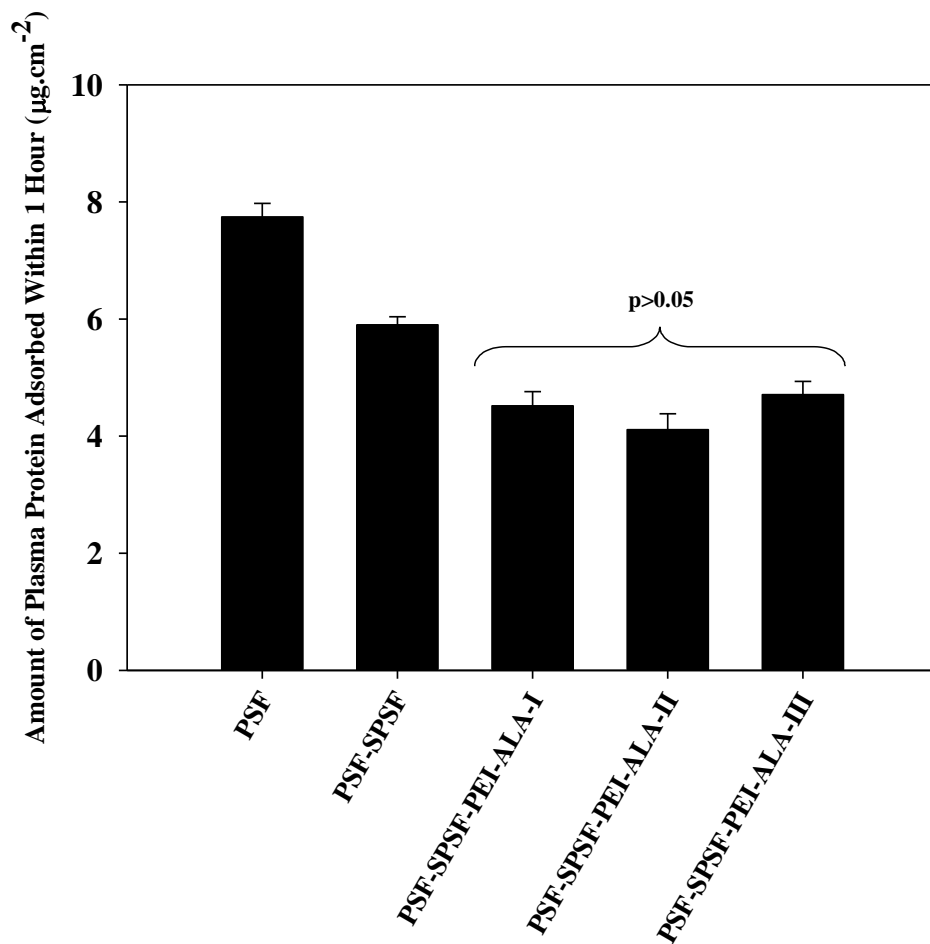


Figure 5.23. The amount of blood plasma proteins adsorbed onto ALA coated PSF membranes

### **5.2.5.2. Platelet Adhesion and Activation**

Platelet activation on ALA coated membranes was determined since the researchers demonstrated that the adhesion of platelets to hemodialysis membranes is of primary importance to the ROS production process. It is suggested that the membranes induce platelet activation, resulting in the formation of platelet–neutrophil microaggregates and the adhesion of activated platelets to neutrophils causes the neutrophils to produce ROS. Several studies have also suggested that ROS can significantly modify platelet functions including platelet surface markers expression, as well as platelet aggregation (Itoh et al., 2006) Figure 5.24 shows that the ALA immobilization remarkably decreased the activation ( $p < 0.05$ ). Similar to the ALG or ALG-HEP coated PSF membranes, the suppression of platelet activation on the modified membranes upon ALA immobilization can be attributed to their lower protein adsorption capacities since the activation of intrinsic coagulation, platelet adhesion and aggregation may depend on the composition and conformation of the protein layer adsorbed onto the surface. The differences in the platelet activation on the PEI-ALA deposited membranes were found insignificant ( $p > 0.05$ ) even though ALA was not in direct contact with blood in the case of the PSF-SPSF-PEI-ALA-II membrane. The result suggests that not only the presence of ALA on the surface but also the hydrophilic character of the surface determines the platelet activation.



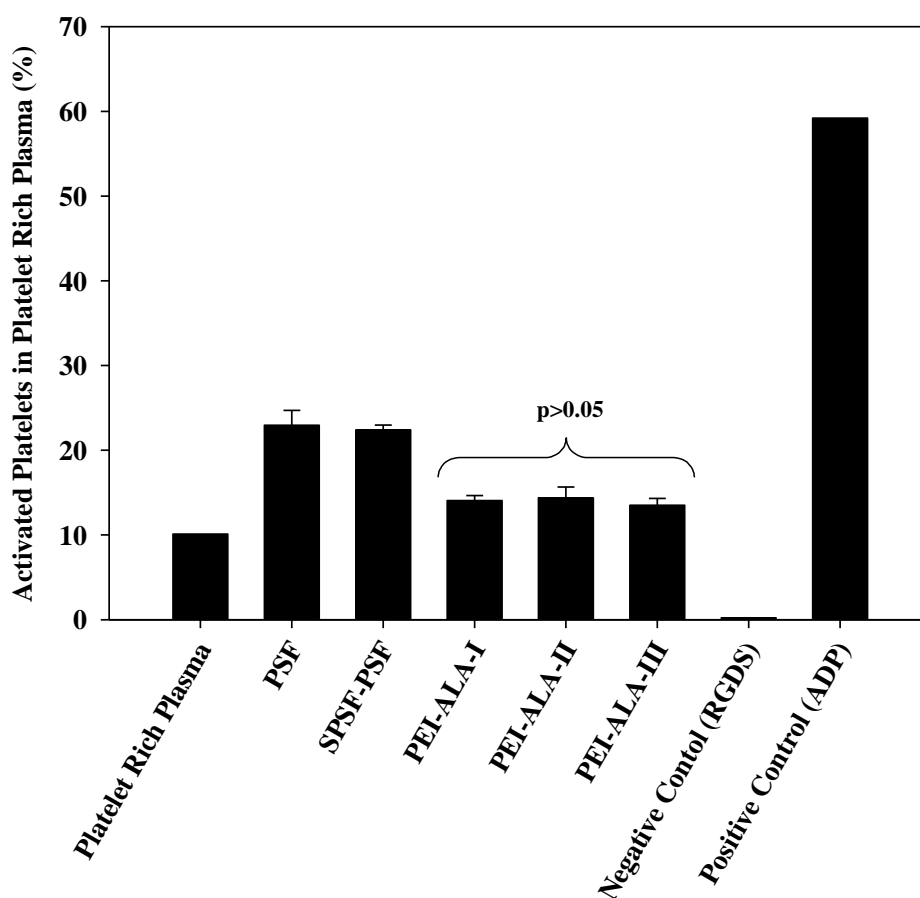


Figure 5.24. Amount of platelet activation on the unmodified and modified PSF membranes with ALA immobilization.

The morphology and activation of adhered platelet and cells in blood on the coated surfaces after incubation with PRP were also examined by SEM analysis. Figures 5.25 and 5.26 show that adhered and activated platelets and other blood cells observed on the SPSF-PSF blend membrane were not seen with the PEI-ALA coated membranes. ALA immobilization prevents the platelet activation not only by reducing the protein adsorption capacity of the membranes but also by inhibiting the ROS production in blood as discussed above. In a clinical study by Chang et al. (2007) ALA administration in end-stage renal disease patients reduced the asymmetric dimethylarginine (ADMA) level in blood, which is an indicator of decreased platelet aggregation.

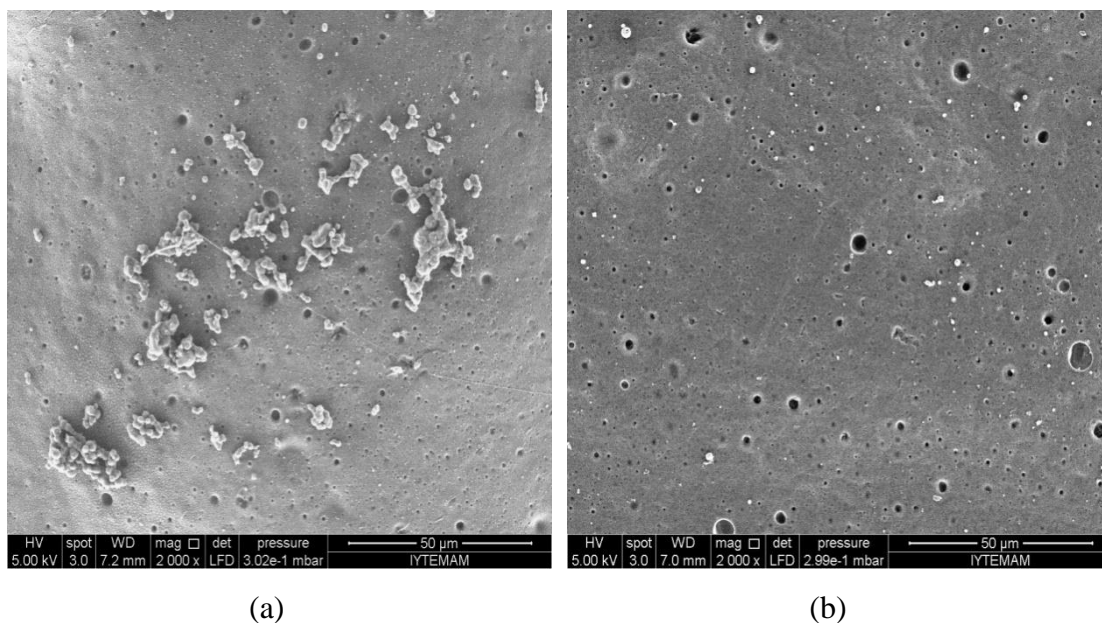


Figure 5.25. The SEM pictures of (a) PSF-SPSF (b) PSF-SPSF-PEI-ALA-I membranes after incubating with PRP for 25 minutes, magnification x2000.

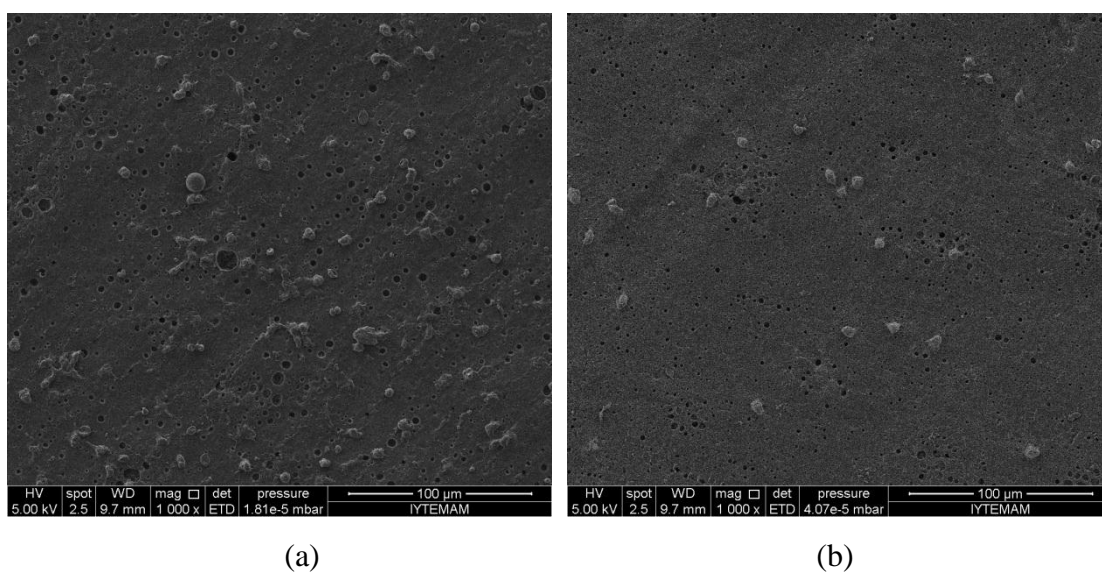


Figure 5.26. The SEM pictures of (a) PSF-SPSF (b) PSF-SPSF-PEI-ALA-I membranes after incubating with whole blood for 15 minutes, magnification x1000.

### 5.2.5.3. Activated Partial Thromboplastin Time

All ALA immobilized membranes displayed significantly longer APTT values than the PSF, PSF-SPSF membranes and the control (Table 5.8). This can be explained by decreased adsorption of blood proteins and platelet activation on these membranes. In

addition, as will be discussed in the next section, the production of ROS is suppressed when blood is in contact with ALA deposited membranes, which helps to prolong the APTT through inhibition of intrinsic pathway. The results in Table 5.8 suggest that the ALA immobilization on the PSF membrane may allow to decrease the amount of anticoagulant injected to the patient during hemodialysis.

Table 5.8. The APTT values for unmodified and modified PSF membranes with ALA immobilization

<b>Membrane Code</b>	<b>APTT (sec.)</b>
Control (Blood Plasma)	39±2
PSF	37±3
PSF-SPSF	38±3
PSF-SPSF-PEI-ALA-I	61±5
PSF-SPSF-PEI-ALA-II	57±2
PSF-SPSF-PEI-ALA-III	64±7

#### **5.2.5.4. Inhibition of Reactive Oxidant Species in Plasma**

The ability of uncoted and ALA coated PSF membranes in the inhibition of ROS in whole blood are shown in Figure 5.27 where the ROS level was expressed as CL counts of HOCl. The results show that the ALA immobilized on the SPSF-PSF membrane significantly suppressed the ROS formation in blood. The difference in the CL counts of HOCl obtained with the ALA loaded membranes and the control (blood incubated without any membrane) was found statistically insignificant ( $p>0.05$ ). Clinical studies showed that administration of ALA could decrease the biomarkers of hemodialysis induced oxidative stress in end-stage renal disease patients (Chang et al., 2007). ALA is possibly rapidly converted to DHLA in many tissues after administrated. ALA and its reduced form DHLA redox couple effectively scavenge a number of free radicals, such as  $H_2O_2$ , HOCl, and  $O_2^-$  in both lipid and aqueous domains. On the other hand, other antioxidants used to modify hemodialysis membranes in previous studies are effective either in aqueous medium (vitamin C) or lipid environment (vitamin E). It has been noted that ALA is one of the most powerful antioxidant and also prooxidant

for the other antioxidants in blood. The prooxidative property of ALA has been shown in (*in vitro* and *in vivo*) studies by regeneration of variety antioxidants including glutathione, vitamin C, vitamin E and coenzyme Q10 (Packer et al., 1995).

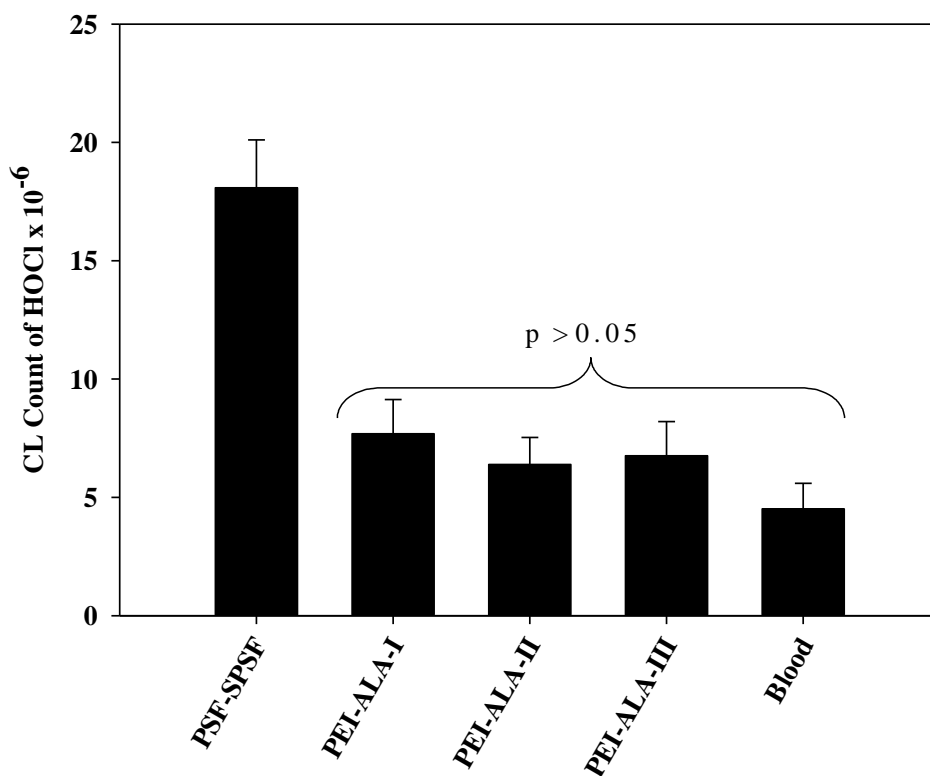


Figure 5.27. The inhibition HOCl in blood by unmodified and modified PSF membranes with ALA immobilization.

### 5.2.5.5. Cytotoxicity

A functional agent intended for biomedical applications should be nontoxic in its pure form. In this study, the cytotoxicity of pure ALA was not measured since it is administrated to hemodialysis patients to reduce complications caused by oxidative stress. As pointed out earlier, the maximum amount of ALA released from the membranes is lower than the amount orally taken by the hemodialysis patients. Cytotoxicity studies conducted with the membranes have shown that the viability of peripheral mononuclear blood cells (PMBC) after 4 hours treatment with unmodified and modified membranes is close to 100% (Table 5.9). The excellent cell viability of the modified membranes confirms that the method proposed for ALA immobilization

does not have a significant negative effect on the nontoxic property of the unmodified PSF membrane.

Table 5.9. % live peripheral mononuclear blood cells after 4 hours treatment with modified and unmodified PSF membranes

<b>Membrane Code</b>	<b>Live Cell %</b>
Control (PMBCs)	100
PSF	99.6±0.2
PSF-SPSF	98.1±0.3
PSF-SPSF-PEI-ALA-I	99.2±0.1
PSF-SPSF-PEI-ALA-II	98.6±0.5
PSF-SPSF-PEI-ALA-III	97.4±0.2

### **5.2.6. Transport and Mechanical Properties of the ALA Immobilized Membranes**

To illustrate the influence of ALA immobilization on the transport properties of PSF membranes, permeation experiments were performed with the uncoated and two coated membranes using urea, vitamin B<sub>12</sub> and lysozyme as model solutes. Figure 5.28 shows that the difference in the transport characteristics of the uncoated and ALA loaded membranes was found statistically insignificant ( $p>0.05$ ). This was expected since only the surface of the membrane was modified, bulk structure remained unchanged. Moreover, additional mass transfer resistance due to polyelectrolyte and ALA deposition is rather small since the increase in the total thickness is negligible as in the case of PEI-HEP/ALG coated membranes.

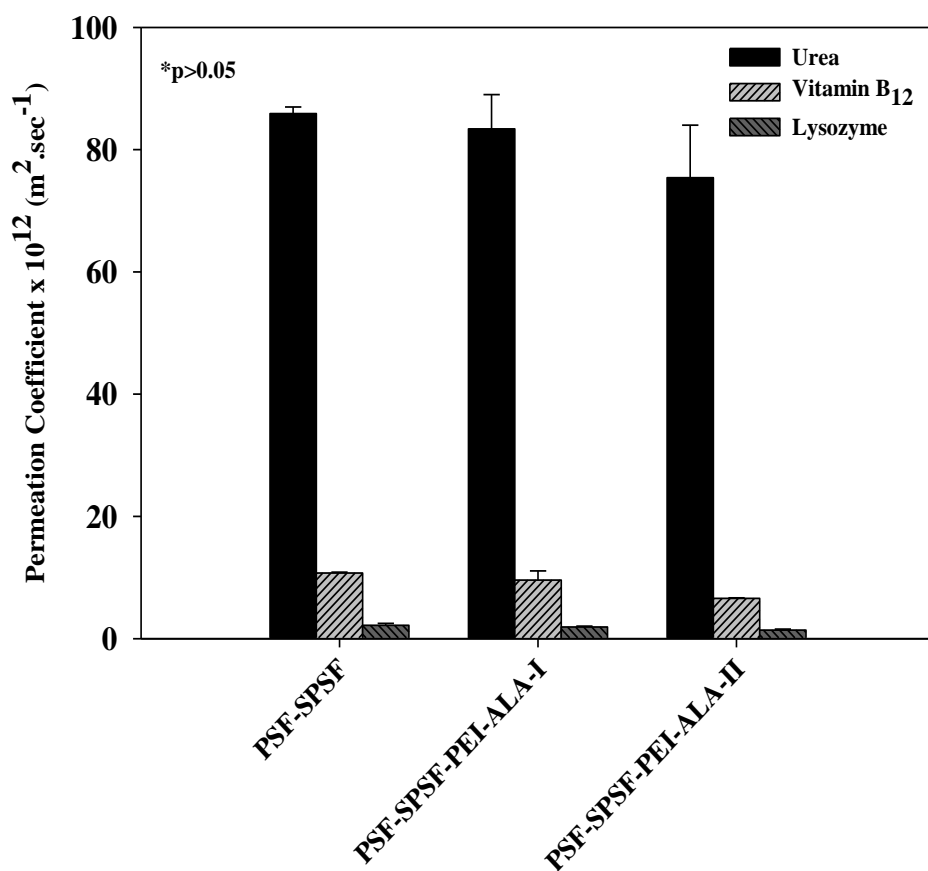


Figure 5.28. The permeation coefficient of urea, vitamin B<sub>12</sub> and lysozyme through unmodified and modified PSF membranes with ALA immobilization. \*Permeation coefficients of all the solutes through each membrane are not statistically different ( $p > 0.05$ )

The mechanical properties of unmodified PSF-SPSF membrane did not change significantly with PEI-ALA coating (Table 5.10).

Table 5.10. Mechanical properties of the unmodified and modified PSF membranes with ALA immobilization

<b>Membrane Code</b>	<b>Maximum Tensile Stress (MPa)</b>	<b>Young Modulus (MPa)</b>
PSF	2.78±0.22	39.82±5.97
PSF-SPSF	2.25±0.18	50.25±7.54
PSF-SPSF-PEI-ALA-I	2.41 ±0.37	53.17 ±9.11
PSF-SPSF-PEI-ALA-II	2.39 ±0.26	49.67 ±7.93

### **5.3. Immobilization of Superoxide Dismutase and Catalase onto Polysulfone Membranes to Suppress Hemodialysis Induced Oxidative Stress**

In the third part of the thesis, superoxide dismutase (SOD)-catalase (CAT) mixture was immobilized onto the polysulfone membranes by modifying and activating the surface with PEI deposition or plasma treatment. To compare kinetic parameters, both enzymes were also immobilized individually thus total of 6 membranes were prepared as listed in Table 5.11. In the following section first free and immobilized enzyme kinetics then the biocompatibility, transport and mechanical properties of the modified membranes are discussed.

Table 5.11. Codes of the unmodified and modified PSF membranes with SOD/CAT immobilization.

Membrane Code	Weight percentages %			Molecule Type on the Last Layer	Immobilization Method
	PSF	SPSF	NMP		
PSF-PLS	20	0	80	-	-
PSF-PLS-CAT	20	0	80	CAT	Covalent bonding through plasma treated surface
PSF-PLS-SOD	20	0	80	SOD	
PSF-PLS-SOD/CAT	20	0	80	SOD/CAT	
PSF-SPSF-PEI-CAT	10	10	80	CAT	Ionic bonding through PEI coated surface
PSF-SPSF-PEI-SOD	10	10	80	SOD	
PSF-SPSF-PEI-SOD/CAT	10	10	80	SOD/CAT	

### 5.3.1. Optimization Conditions for SOD/CAT Immobilization

It is well known that the activity of an enzyme is influenced by pH, temperature, concentration of the enzyme solution and immobilization time. In previous studies, optimum immobilization time and temperature were reported as 24 h and 5 °C considering the amount of bound catalase and the activity of immobilized catalase together (Alptekin et al., 2009, 2010). Based on these studies, the SOD and CAT enzymes immobilizations were carried out at 4 °C and physiological pH 7.4 within 24 hours by varying the initial enzyme and PEI concentrations. Figure 5.29 shows that there is no statistically significant difference between the activities of both SOD and CAT enzymes adsorbed on the PEI layer which was prepared from a 0.1 mg.ml<sup>-1</sup> or 1 mg.ml<sup>-1</sup> of PEI solution. The result simply indicates that 0.1 mg.ml<sup>-1</sup> concentration is sufficient to cover the negatively charged surface of the support membrane with a positively charged, linear chained cationic polyelectrolyte, PEI.

The influence of enzyme concentration on the immobilized amount and the activity is shown in Figure 5.30. As the concentration of CAT was increased from 0.1 to 1 mg.ml<sup>-1</sup>, its activity when immobilized either on PEI modified or plasma treated surface did not change significantly (p<0.05) although the immobilized amount especially on the plasma treated surface increased significantly. Similar trend was also



observed in the case of SOD immobilization (Figure 5.31). It appears that both PEI modified and plasma treated surfaces were not saturated with SOD or CAT enzymes even at  $1 \text{ mg.ml}^{-1}$  concentration. On the other hand, due to enzyme-enzyme interaction on the immobilized state, the active side of the enzyme might have been blocked or the conformation of the enzyme might have changed both of which limit increase in the activity with the increase in immobilized amount.

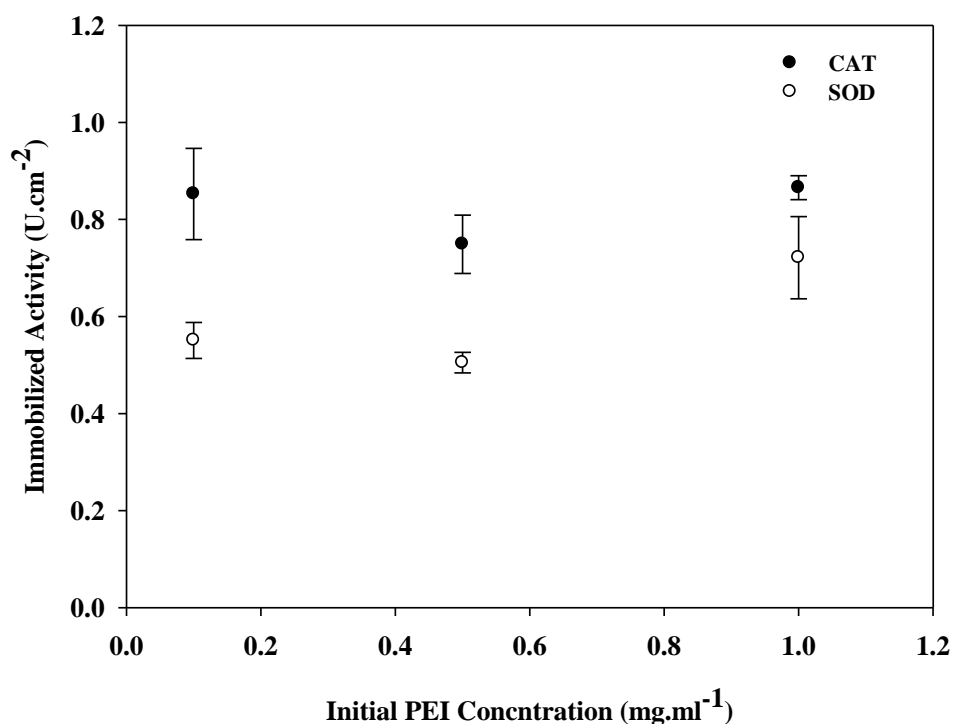
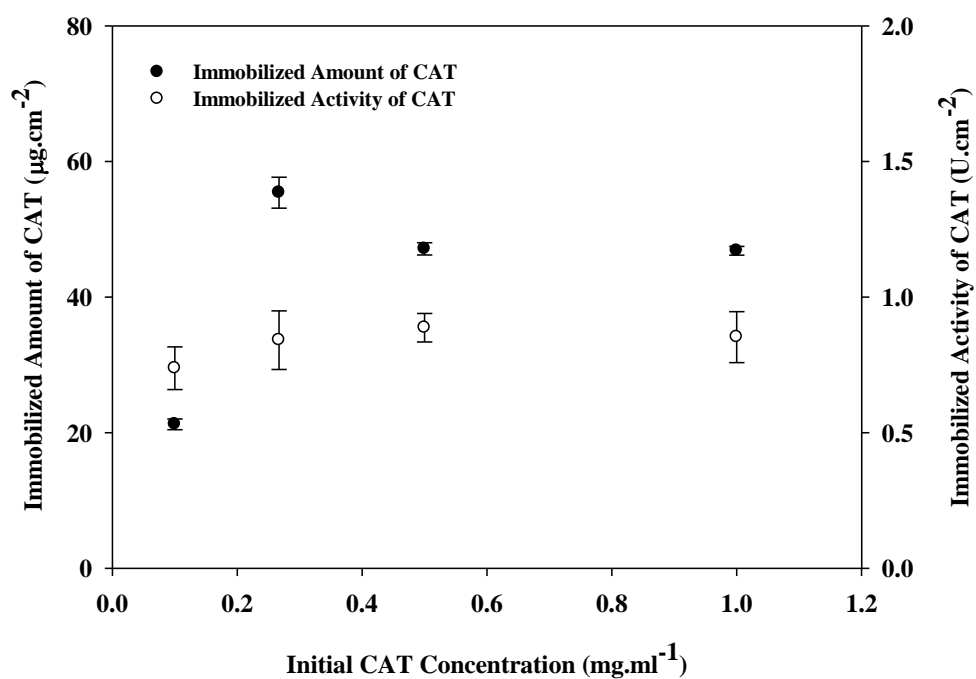
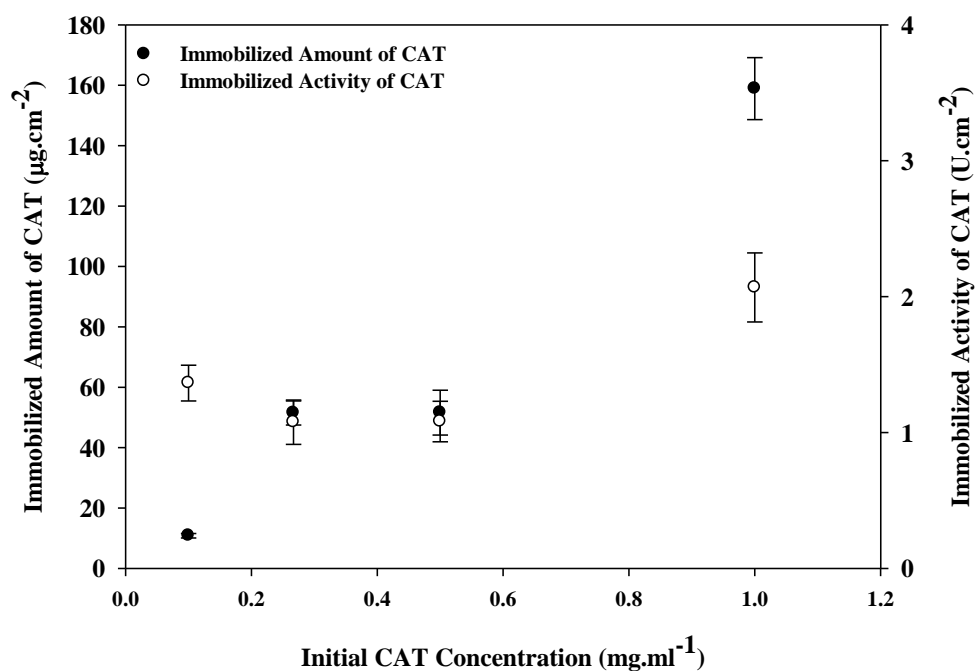


Figure 5.29. Immobilized activities of SOD and CAT vs initial PEI concentration. Experiments were conducted with  $C_{\text{CAT-initial}}: 0.25 \text{ mg.ml}^{-1}$  and  $C_{\text{H}_2\text{O}_2}: 30 \text{ mM}$ ,  $C_{\text{SOD-initial}}: 0.25 \text{ mg.ml}^{-1}$  and  $C_{\text{Riboflavin}}: 2\mu\text{M}$ .

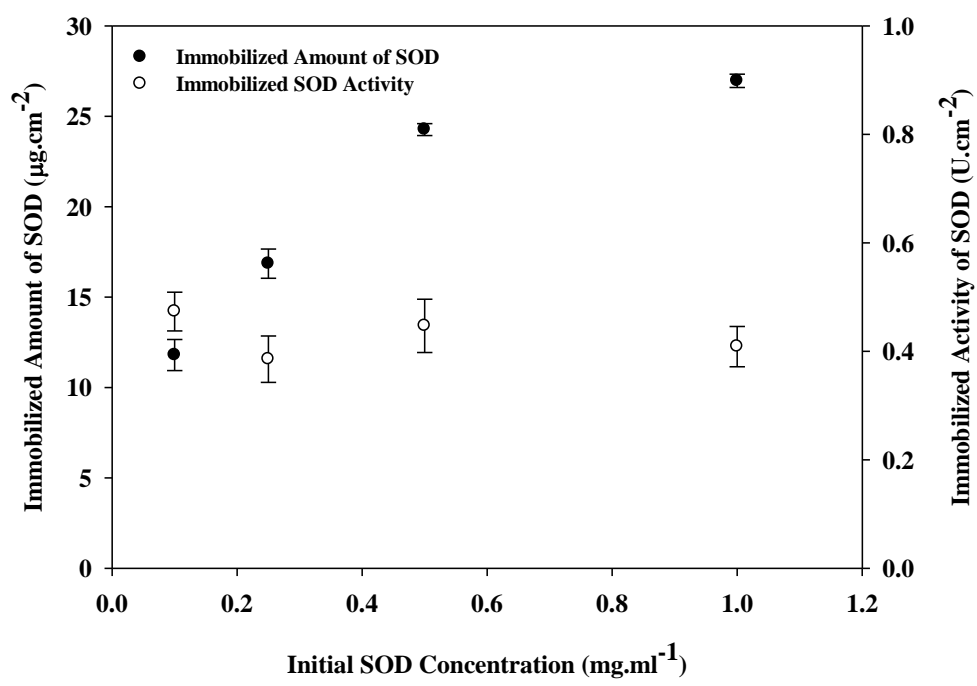


(a)

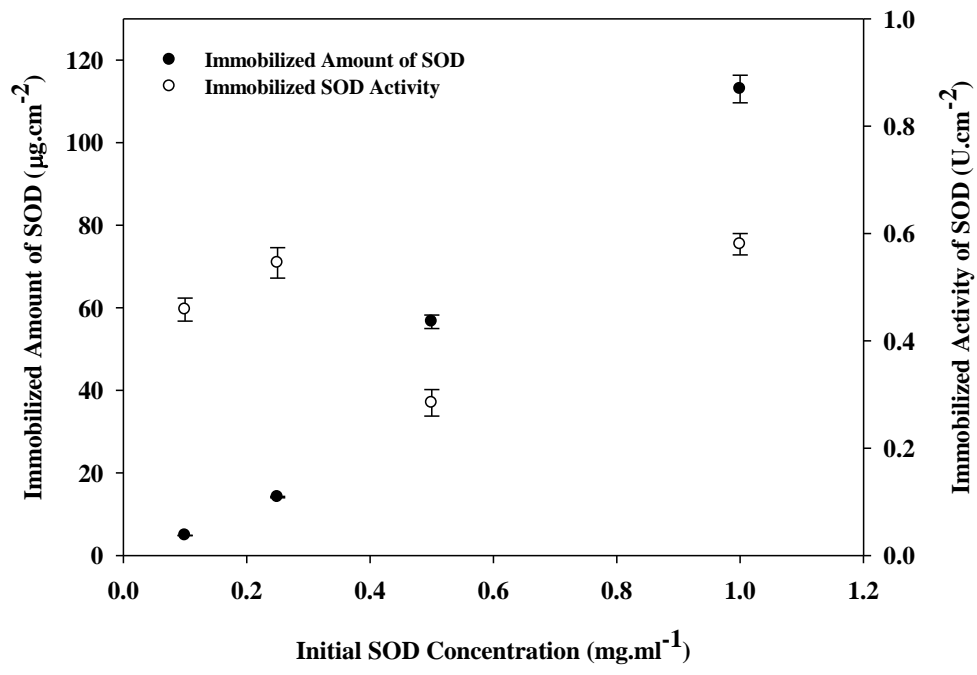


(b)

Figure 5.30. Amount of CAT and the activity of CAT immobilized on the PEI modified (a) and plasma treated b) surfaces. Experiments were conducted with  $C_{\text{PEI-initial}}: 0.1 \text{ mg.ml}^{-1}$  and  $C_{\text{H}_2\text{O}_2}: 30 \text{ mM}$ .



(a)



(b)

Figure 5.31. Amount of SOD and the activity of SOD immobilized on the PEI modified (a) and plasma treated b) surfaces. Experiments were conducted with  $C_{PEI-initial}: 0.1 \text{ mg.ml}^{-1}$  and  $C_{Riboflavin}: 2\mu\text{M}$ .

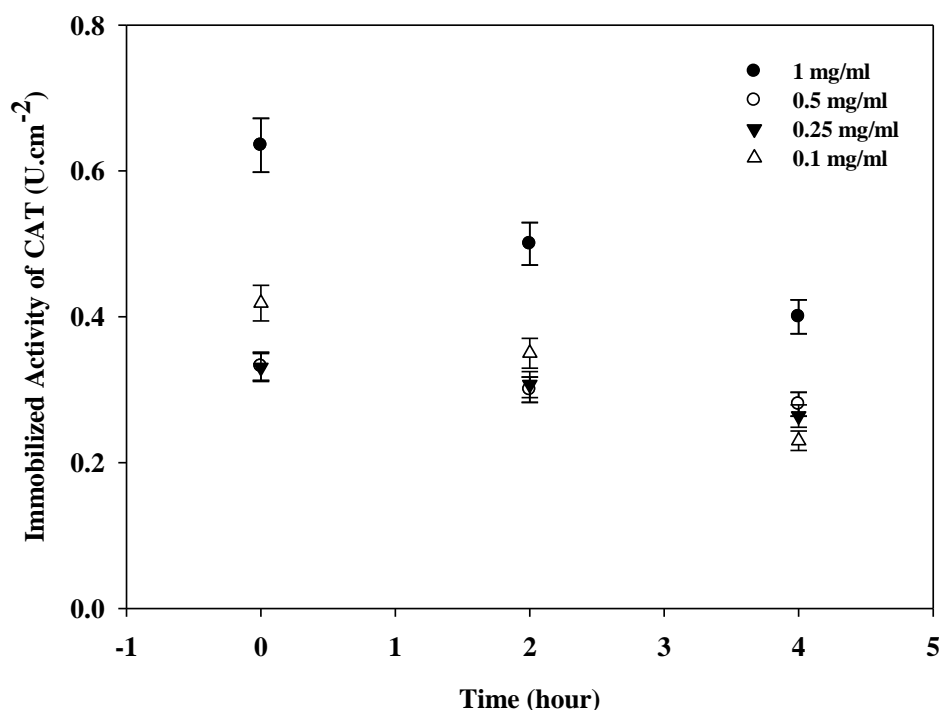


Figure 5.32. Stability of immobilized CAT of PSF-SPSF-PEI-CAT membrane vs time.

Table 5.12 lists specific activities ( $\text{U} \cdot \text{mg enzyme}^{-1}$ ) calculated from the data in Figure 5.30 and 5.31. The highest enzyme activity per mg of immobilized enzyme was obtained with the lowest initial concentration for both SOD and CAT enzymes. At high enzyme concentration, due to over-saturation of the membrane surface, substrate diffusion limitation occurs. In addition, the presence of protein-protein interactions between the loaded enzyme molecules becomes more important and these hinder the substrate conversion. To decide on the optimum enzyme concentration, the change in enzyme activity during 4 hour period was also followed (Figure 5.32). The highest immobilized activity loss was observed with an initial enzyme concentration of  $0.1 \text{ mg} \cdot \text{ml}^{-1}$  ( $45\% \pm 8.2\%$ ). The loss in the activity when immobilized from the solution containing either  $0.25 \text{ mg} \cdot \text{ml}^{-1}$  ( $20\% \pm 3.9$ ) or  $0.5 \text{ mg} \cdot \text{ml}^{-1}$  ( $16\% \pm 3.1\%$ ) was found similar. Thus, considering the activities initially and of the end of 4 hour storage, the optimum enzyme concentration for immobilization was determined as  $0.25 \text{ mg} \cdot \text{ml}^{-1}$ .

Table 5.12. Specific activities of immobilized SOD and CAT enzymes

Initial Enzyme Concentration (mg.ml <sup>-1</sup> )	Specific Activity (U.mg <sup>-1</sup> )			
	PEI Adsorption		Plasma Treatment	
	SOD	CAT	SOD	CAT
0.1	40 ± 3	35 ± 3	283 ± 17	126 ± 1
0.25	23 ± 5	15 ± 9	116 ± 5	21 ± 8
0.5	18 ± 6	19 ± 3	15 ± 6	21 ± 10
1	15 ± 6	18 ± 6	15 ± 3	13 ± 11

### 5.3.2. Surface Characterization of SOD/CAT Immobilized Membranes

The water contact angle values shown in Figure 5.33 illustrated the enhanced hydrophilic character of the PSF surface after plasma treatment. The hydrophilicities of PSF-SPSF blend membrane or PEI modified and plasma activated PSF membranes were found similar ( $p > 0.05$ ). Immobilization of SOD/CAT enzymes either covalently on plasma treated or ionically on PEI adsorbed surfaces significantly decreased the hydrophobicity of the starting PSF membrane.

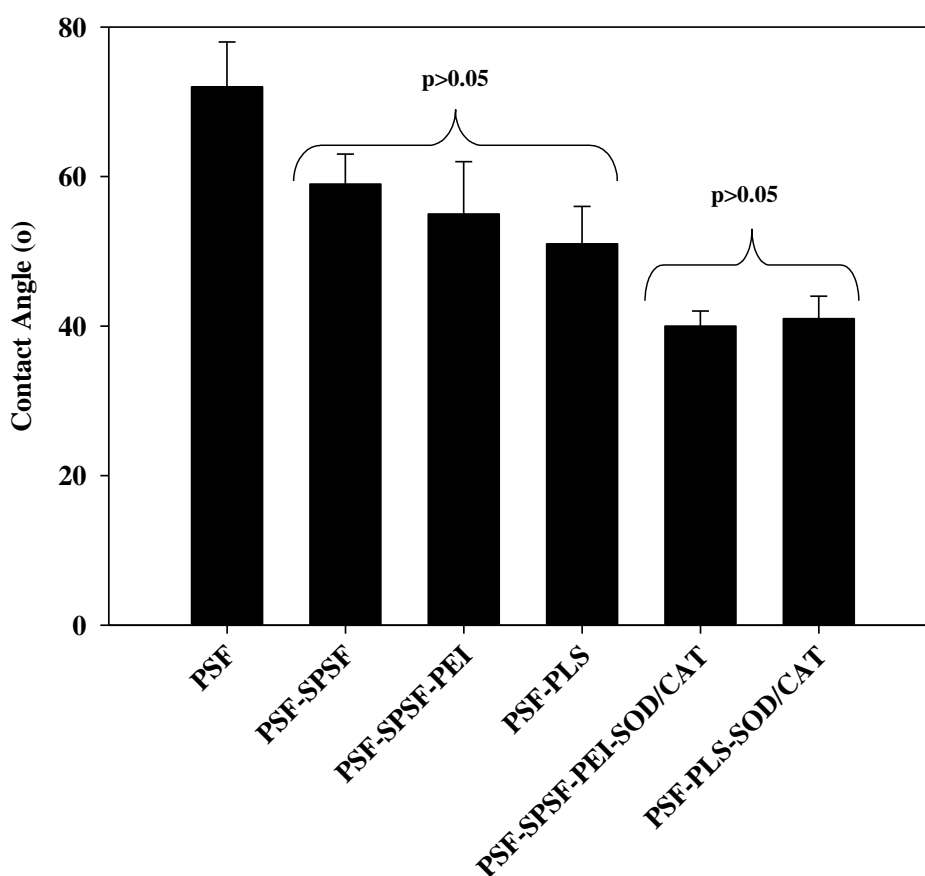
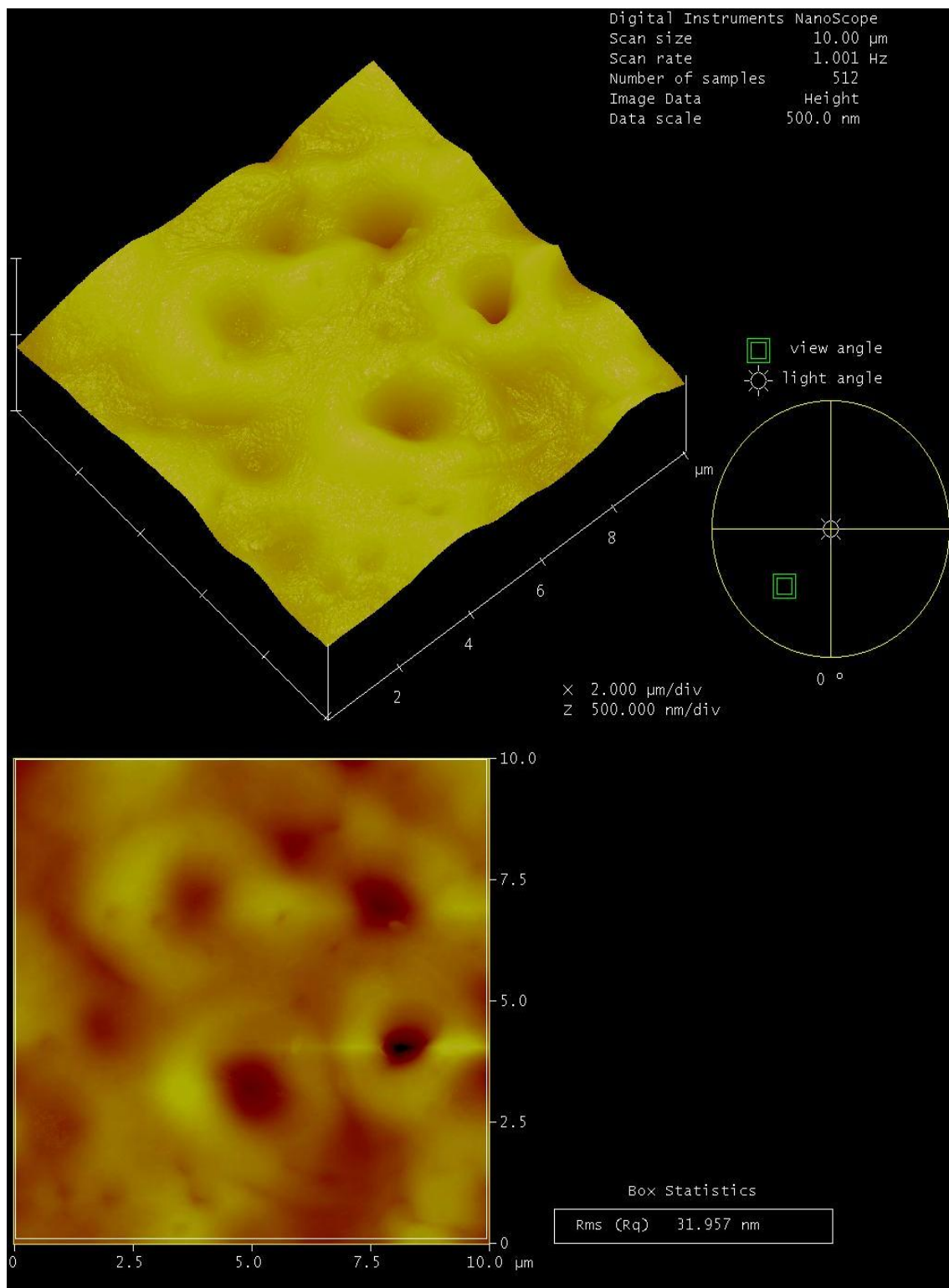


Figure 5.33. Water contact angle of unmodified and modified PSF membranes with SOD/CAT immobilization.

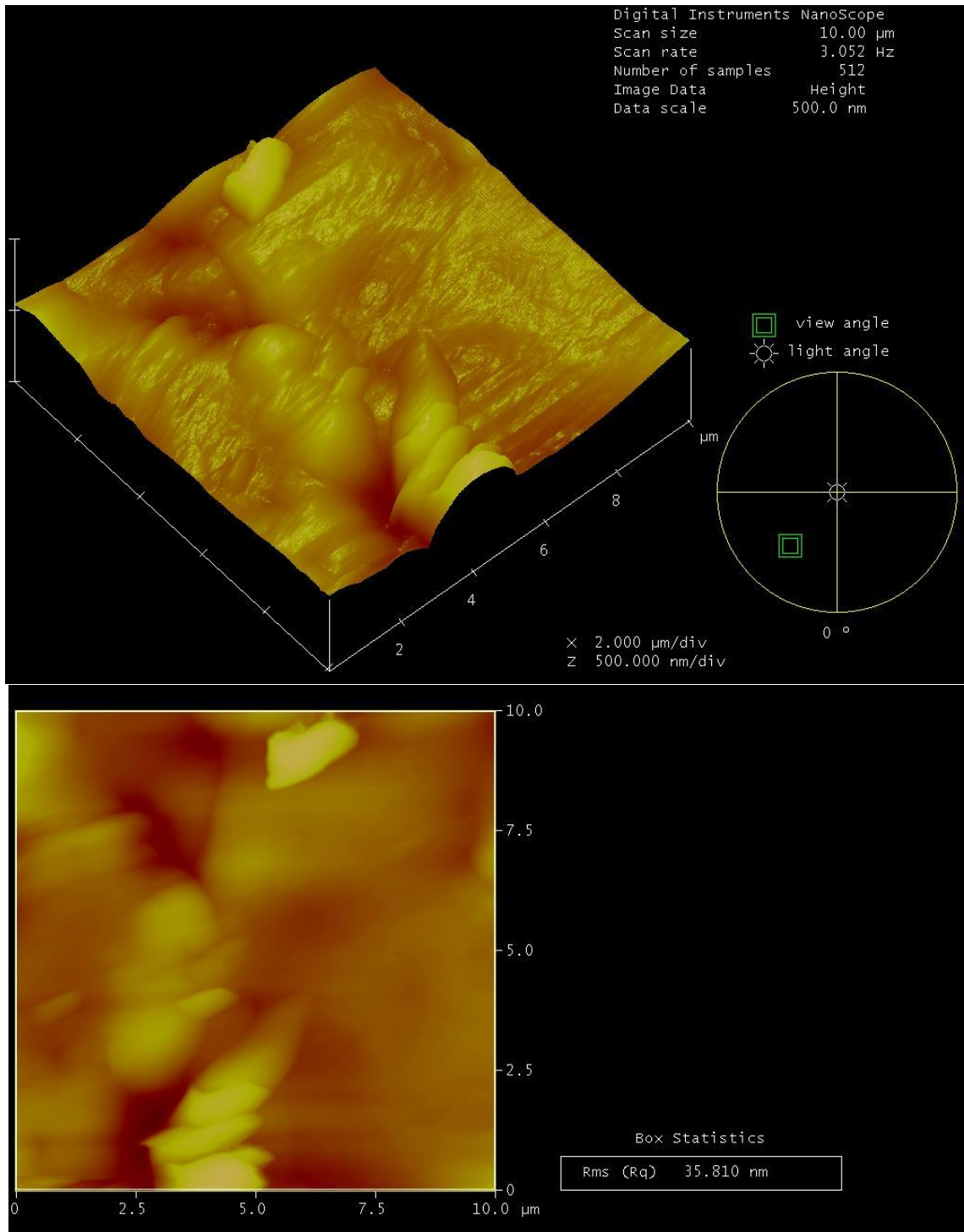
The surface roughnesses of the plasma treated and SOD/CAT coated membranes were obtained from the analysis of AFM images shown in Figure 5.34. The smoothness of the PSF membrane did not change significantly after plasma treatment and enzyme immobilization on the plasma treated surface (Figure 5.35) The enzyme immobilization on the PEI modified PSF-SPSF membrane decreased the roughness significantly, however, the value is still higher than that of the plasma treated one. This is due to restricted motion of the enzyme molecules on the plasma treated surface as a result of the strong and rigid covalent bonding.



(a)

Figure 5.34. AFM images of (a) PSF-PLS (b) PSF-PLS-SOD/CAT and (c) PSF-SPSF-PEI-SOD/CAT membranes.

(cont. on next page)

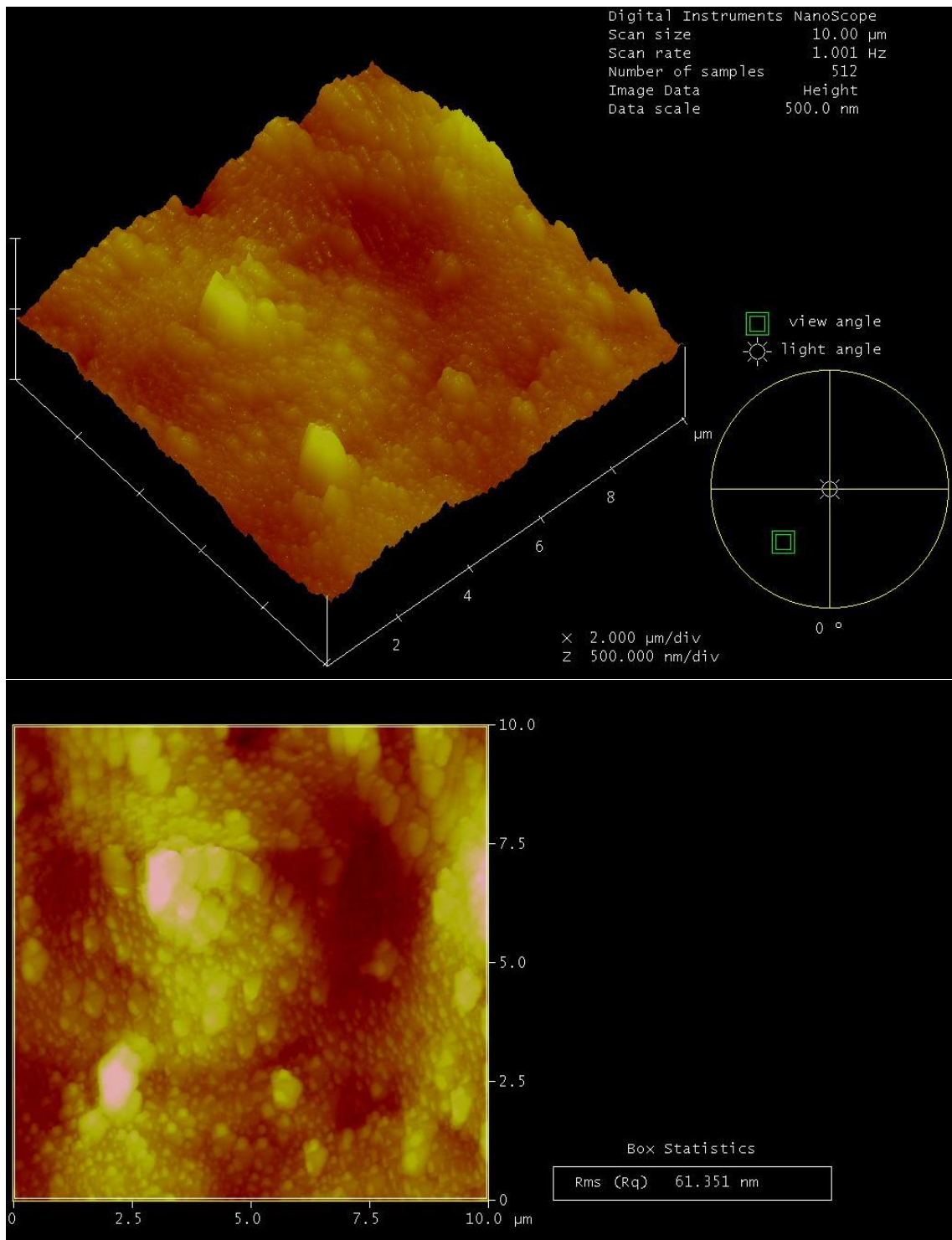


(b)

Figure 5.34. (cont.)

(cont. on next page)





(c)

Figure 5.34. (cont.)

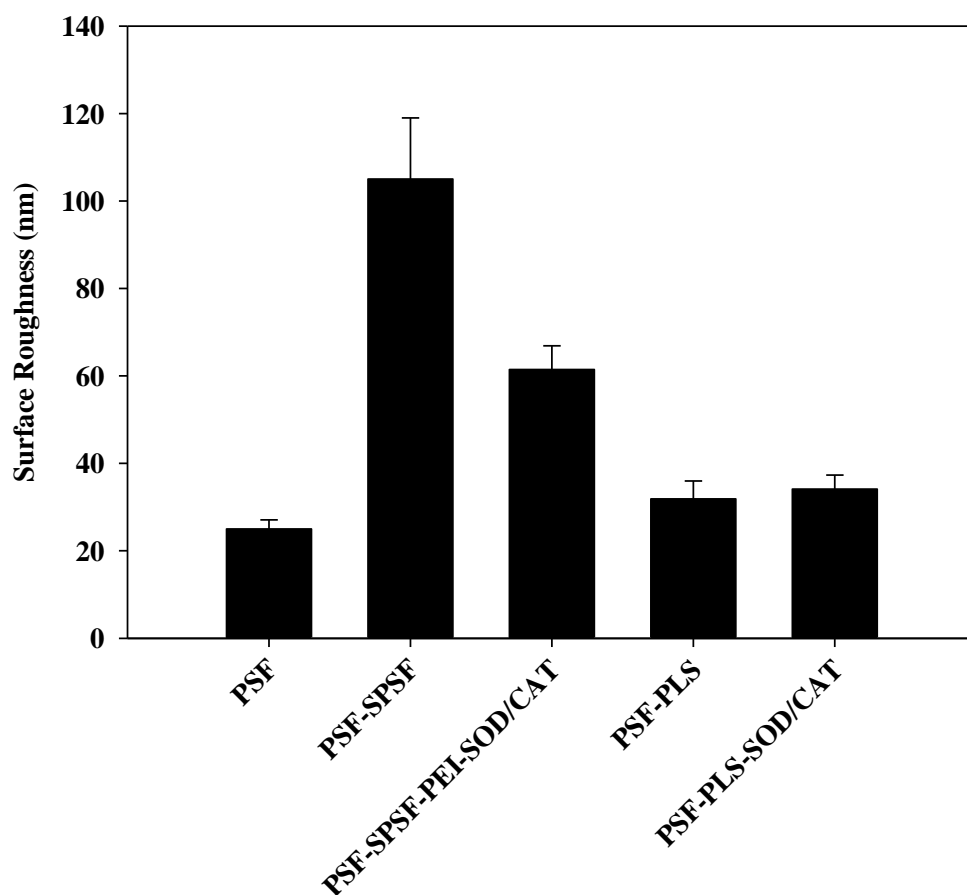
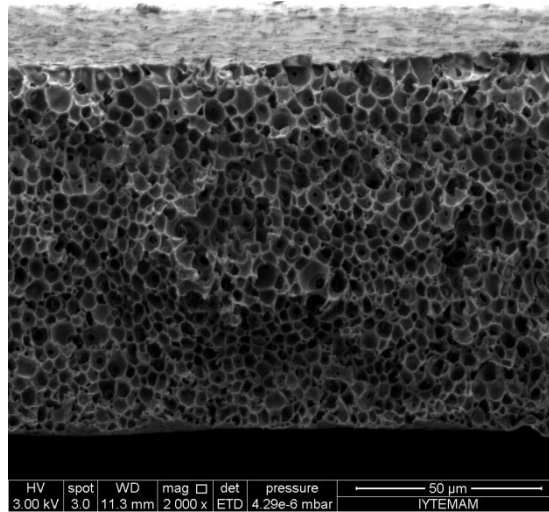
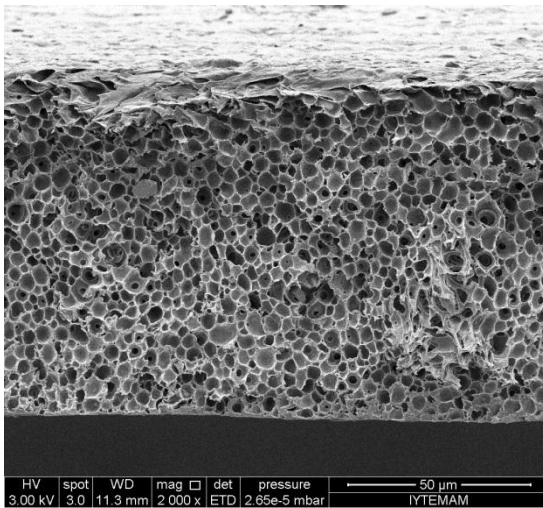


Figure 5.35. Surface roughness of unmodified and modified PSF membranes with SOD/CAT immobilization

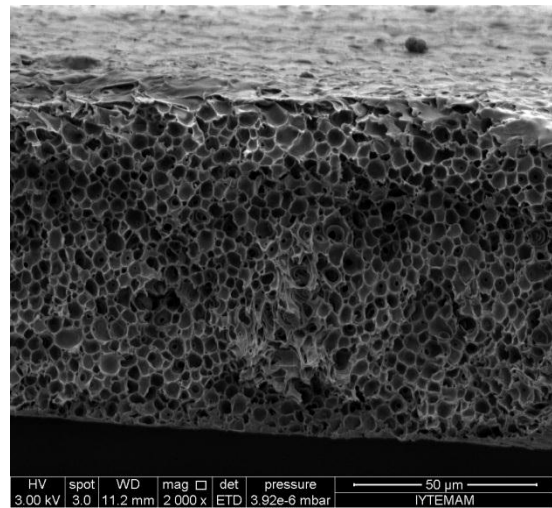
The SEM pictures shown in Figure 5.36 illustrated that neither plasma treatment nor enzyme immobilization on the plasma treated surface changed the bulk structure of the unmodified PSF membrane. Similarly, the SOD/CAT immobilization on the PEI deposited surface had no effect on the bulk structure of the support membrane.



(a)



(b)



(c)

Figure 5.36. Cross section SEM pictures of (a) PSF (b) PSF-PLS (c) PSF-PLS-SOD/CAT membranes.

Figure 5.37a illustrates the FTIR-ATR spectrum of native SOD/CAT enzyme couple. In the spectrum, the amide I, amide II and amide III bands are located around  $1650\text{ cm}^{-1}$ ,  $1550\text{ cm}^{-1}$  and  $1290\text{ cm}^{-1}$ . The amide I band is a strong and broad band containing several spectral contributions arising from different types of protein secondary structures. Additional vibrational bands which are not assigned to structured features but originate from the various side chains were also observed. The strongest ones are:  $1082$ ,  $1455$  and  $1467\text{ cm}^{-1}$ . The bands centred at  $1467\text{ cm}^{-1}$  and  $1455\text{ cm}^{-1}$  belong to protein side chain deformation vibrations ( $\text{CH}_3$  and  $\text{CH}_2$ , respectively), while the strong band at  $1082\text{ cm}^{-1}$  can be attributed to C-C and C-O vibrations (David et al., 2012). The broad  $\text{NH}_2$  band centred around  $3200\text{ cm}^{-1}$  is usually overlapped with

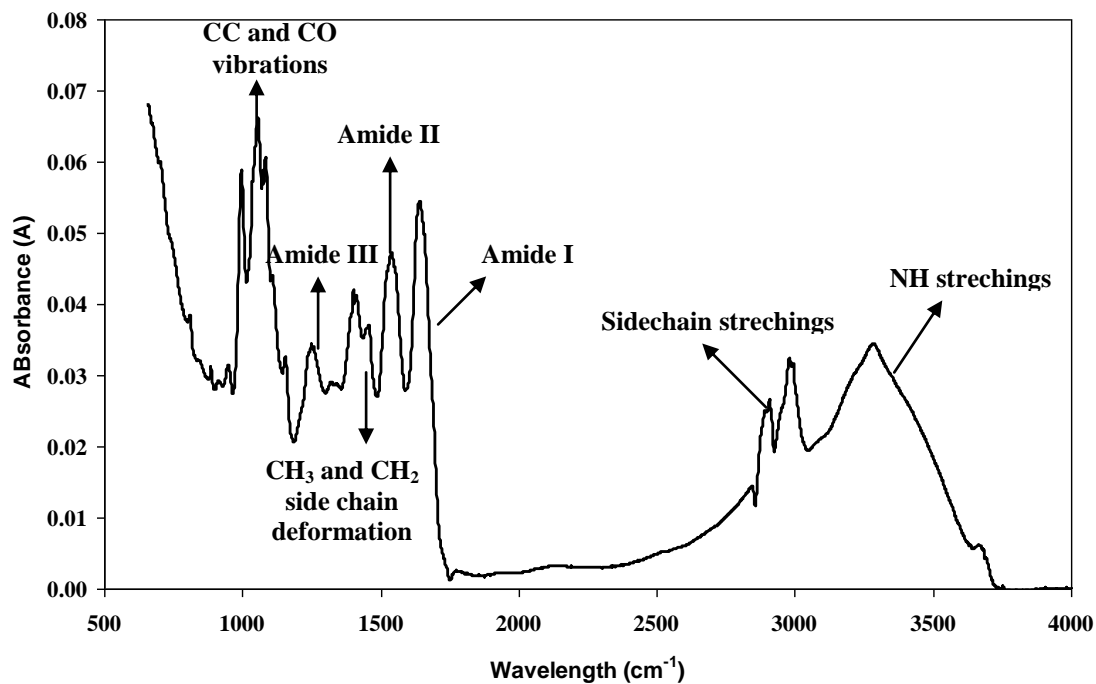
the OH-stretching band of hydrating H<sub>2</sub>O molecules. The FTIR-ATR spectrum of SOD/CAT couple immobilized on PEI modified and plasma activated surfaces are shown in Figures 5.37b and 5.37c, respectively. This method gives an insight into the outer few hundred nanometers of surface which is much deeper than the thickness of the enzyme immobilized layer. The presence of the most characteristic amide I and amide II bands in the range of 1700-1500 cm<sup>-1</sup> confirms successful immobilization of the enzymes. The higher peak intensity of amide bonds for PSF-PLS-SOD/CAT membrane also clearly reveals the amide bond formed by enzyme immobilization.

FTIR-ATR analysis was also used to investigate how the surface properties of the membranes affect the conformation of immobilized enzymes and the resulting enzymatic activity. Little conformational information can be obtained directly from the original IR spectra of the enzymes (Figure 5.37 a-c). Since the assignment of amide I absorbance components gives more detailed information of the secondary structures, in turn the conformation integrity of enzymes, the FTIR spectra in the 1600 to 1700 cm<sup>-1</sup> region was deconvoluted (Figure 5.37 d-f). The contents of each band in the total amide I absorbance were obtained by integrating the each component and the results were summarized in Table 5.13. It is known that the secondary structure of Cu-Zn-SOD (determined by x-ray crystallographic structural analysis) contains more than 50% beta-strands and turns and about 40% unordered structures but small fraction of  $\alpha$ -helix (Sun et al., 1997). The major feature of Cu-Zn-SOD secondary structure is that the enzyme contains 8-stranded beta-barrel, with the active site held between the barrel and two surface loops (Tainer et al. 1983).  $\beta$ -strand structure is an important determinant in stability of the Cu-Zn-SOD. On the other hand, the secondary structure of CAT has 30%  $\alpha$ -helical, 34%  $\beta$ -sheet, 17%  $\beta$ -turn and 19% unordered structures (Houli et al., 1996). In this case,  $\alpha$ -helix is the preferred determinant of the CAT structural integrity (Griebenow and Klibanov, 1996). In the context of protein structure, the term stability is usually defined as the tendency to maintain a native conformation (Lehninger et al., 1993). Hence, the change in the content of beta strand and  $\alpha$ -helix of immobilized SOD-CAT with respect to native SOD-CAT was used to determine the stability of immobilized enzymes and the results are shown in Table 5.13.

SOD immobilized onto plasma treated or PEI modified surfaces have similar  $\beta$ -sheet content with the native enzyme indicating no significant conformational change upon immobilization. On the other hand, the CAT enzyme lost its native conformation when immobilized onto both PEI modified and plasma treated surfaces as confirmed by

a decrease in  $\alpha$ -helix content from 30% to 16% and 13%, respectively. CAT (MW: 250000) is a larger molecule compared to SOD (MW:32500) and is preferentially adsorbed on the membrane surface. In addition, adsorption of SOD on the CAT, hence, consequent interactions between CAT and SOD molecules may have influenced the conformation of CAT.

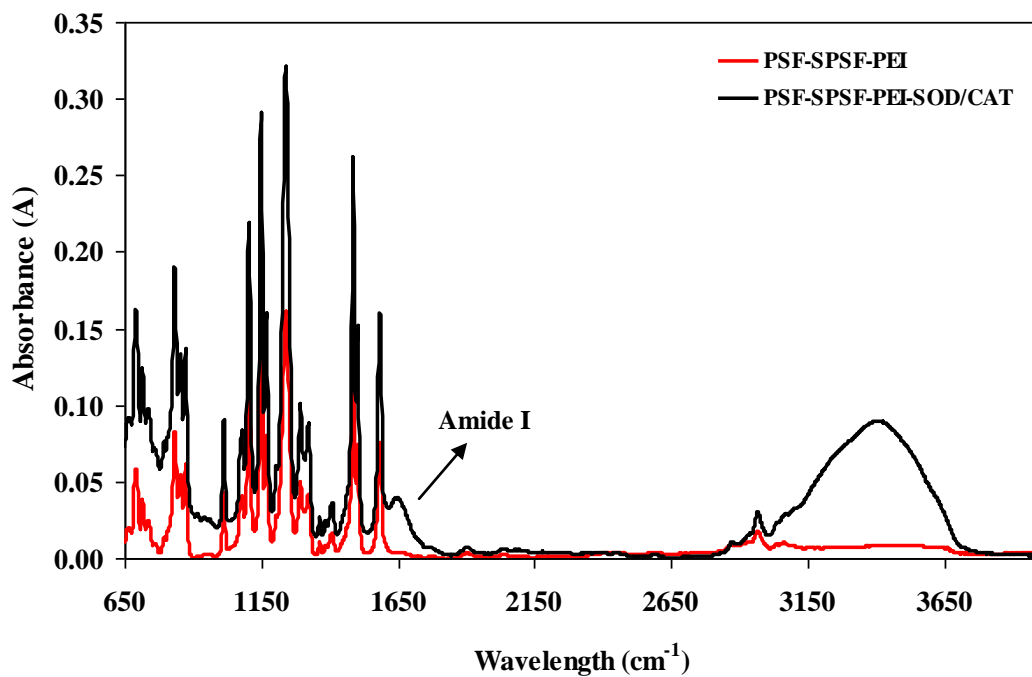
$H_2O_2$ , the product of the reaction catalysed by SOD and the substrate of the reaction catalysed by CAT, is known as denaturant. Therefore, FTIR-ATR analyses were repeated after the immobilized enzymes were incubated for 10 minutes (reaction time) in 30 mM  $H_2O_2$  solution. The results indicated that the  $\beta$ -sheet content of SOD decreased from 39 % to 23% and from 37 % to 13 % when it was immobilized onto plasma treated and PEI modified surfaces, respectively. The surface characteristics of the membranes, hence, the interaction forces (electrostatic interactions, hydrogen bonding, hydrophobic and van der Waals interactions) between the surface of the membrane and the enzymes affect the conformation of an adsorbed enzyme. Since the hydrophilicity of the PEI modified and plasma treated surfaces are similar, the difference in the surface roughness and surface charge may be the reasons of the difference in stabilities of the enzymes immobilized onto two different modified surfaces.  $\alpha$ -helix content of the CAT enzyme did not change after immobilization onto both surfaces and incubation in  $H_2O_2$  suggesting that  $H_2O_2$  with that dosage (30mM) is not denaturant against CAT enzyme.



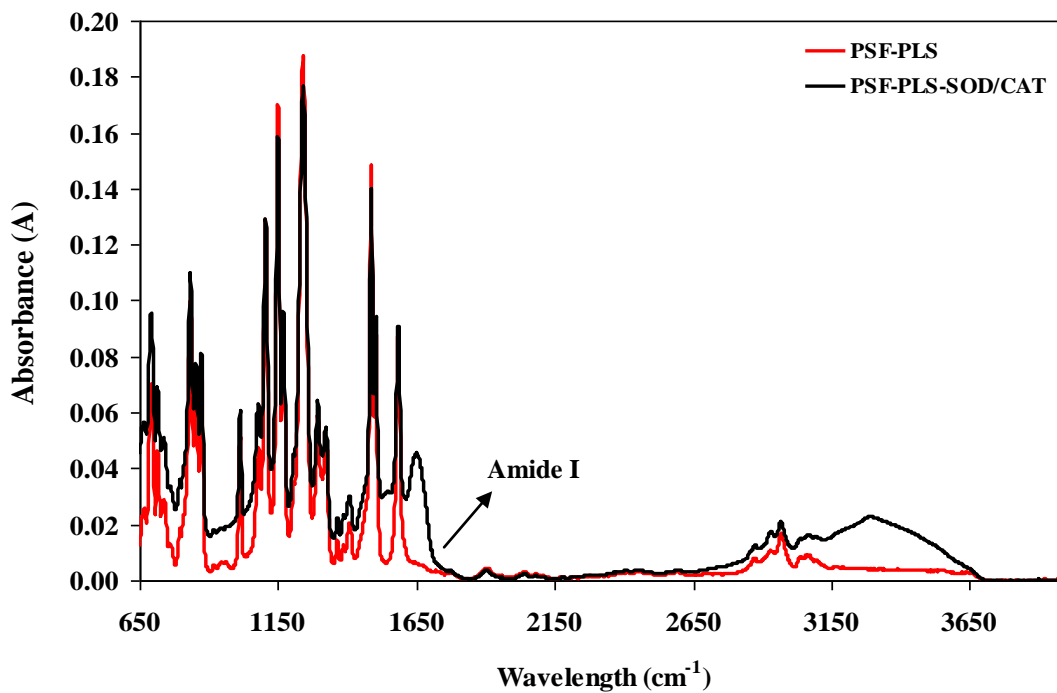
(a)

Figure 5.37. FTIR-ATR spectra of (a) native SOD/CAT (b) PSF-SPSF-PEI and PSF-SPSF-PEI-SOD/CAT (c) PSF-PLS and PSF-PLS-SOD/CAT membranes. Deconvoluted spectra in the chosen band ( $1600\text{-}1700\text{ cm}^{-1}$ ) of (d) native SOD/CAT (e) PSF-SPSF-PEI-SOD/CAT (f) PSF-PLS-SOD/CAT membranes.

(cont. on next page)



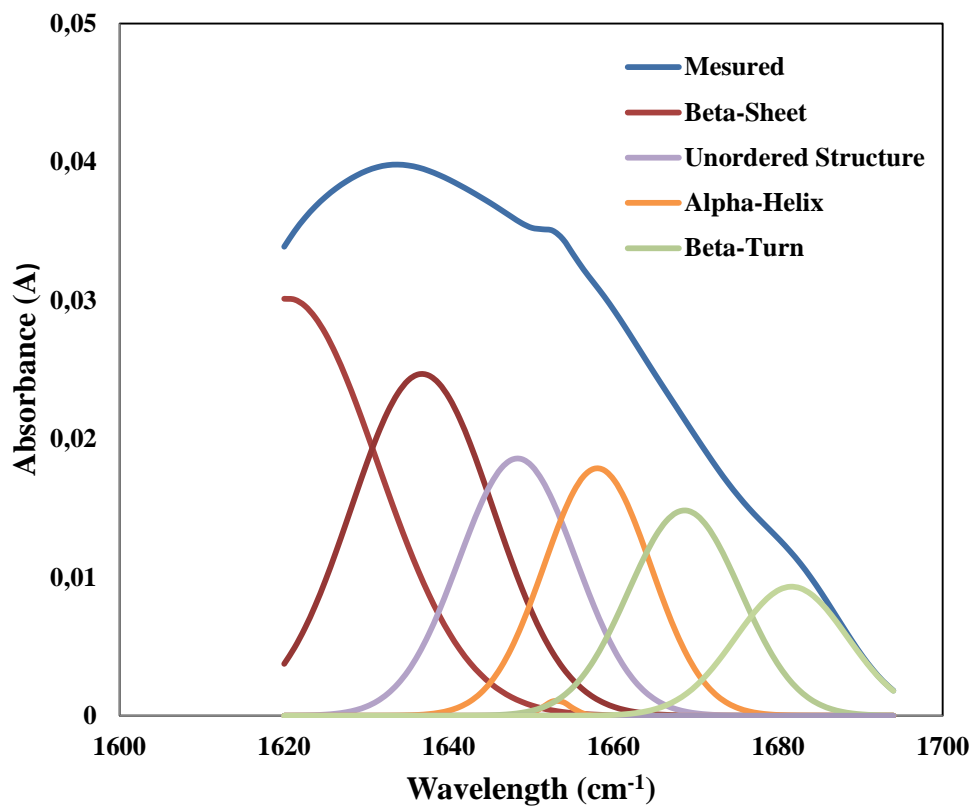
(b)



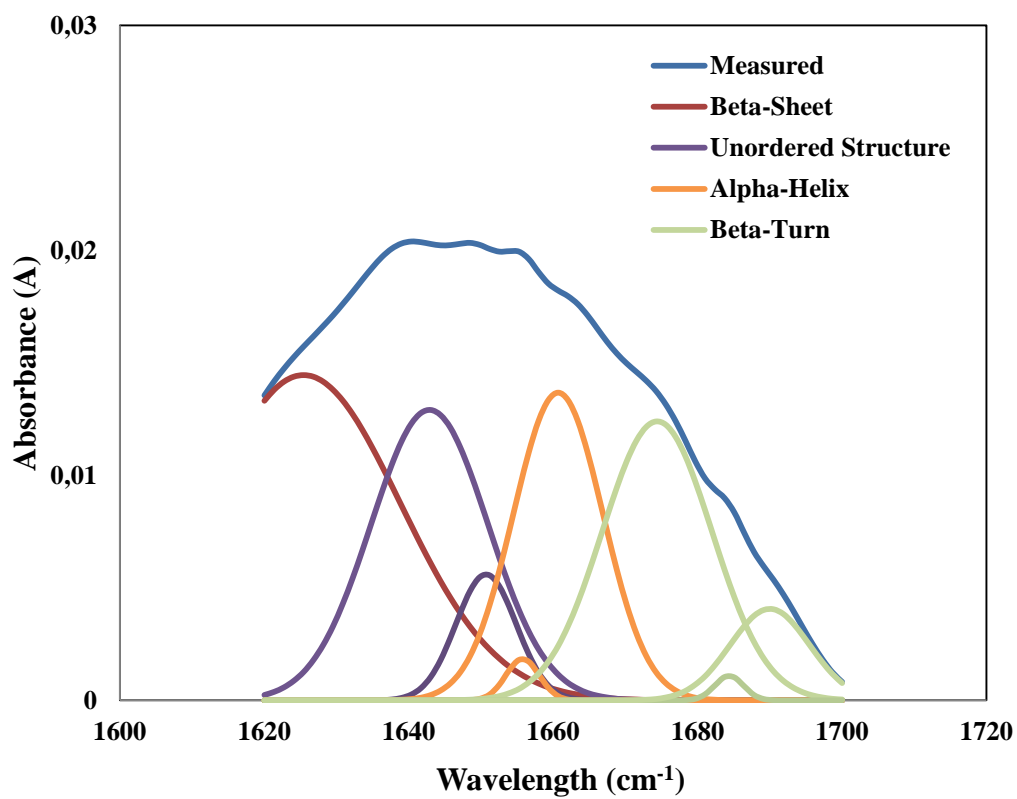
(c)

Figure 5.37. (cont.)

(cont. on next page)



(d)

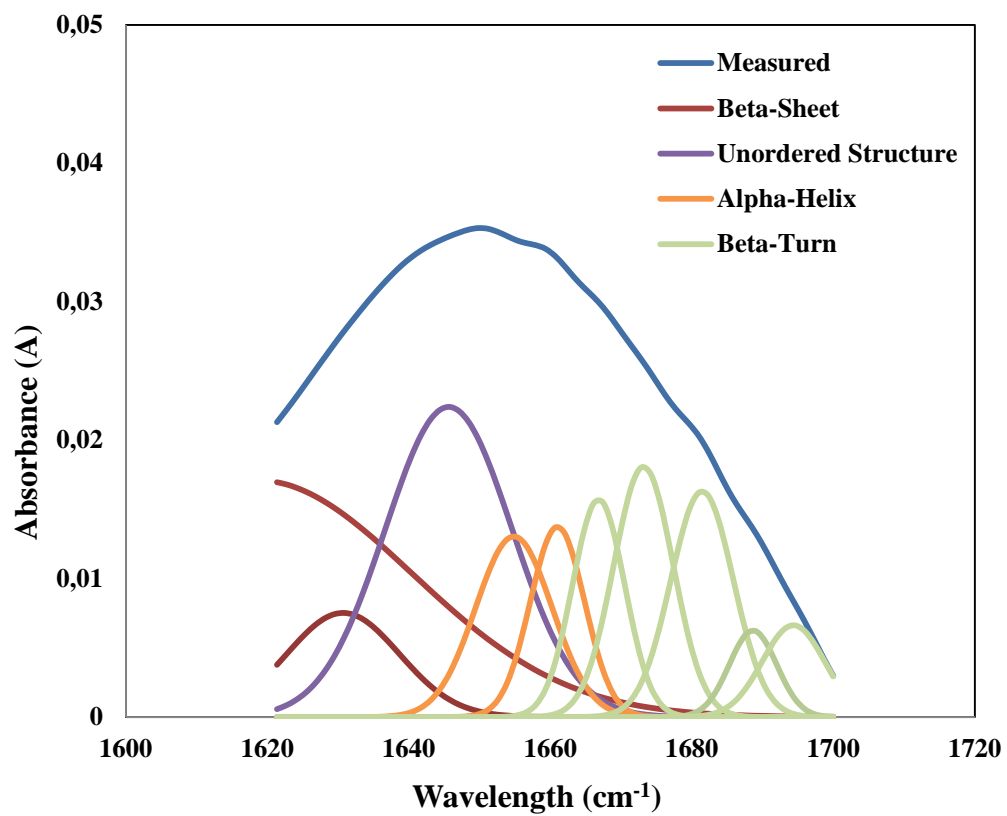


(e)

Figure 5.37. (cont.)

(cont. on next page)





(f)

Figure 5.37. (cont.)

Table 5.13. Secondary structure of native and immobilized SOD and CAT estimated from the deconvoluted FTIR Spectra

	<b>Secondary Structure</b>	<b>B-sheet</b>	<b>Unordered structure</b>	<b><math>\alpha</math>-helix</b>	<b>B-turn</b>
	<b>Assigned Frequency (cm<sup>-1</sup>)</b>	1620-1635	1641-1649	1652-1658	1660-1700
<b>Native Zn-Cu-SOD (Sun et al., 1997)</b>	<b>% Content</b>	34	49	-	17
<b>Native-CAT (Houli et al., 1996)</b>		34	19	30	17
<b>Native SOD/CAT</b>		44	18	16	22
<b>PSF-PLS-SOD/CAT</b>		39	21	13	27
<b>PSF-SPSF-PEI-SOD/CAT</b>		37	24	16	23

### **5.3.3. Stability of Immobilized SOD/CAT**

The stabilities of immobilized SOD and CAT enzymes were determined under typical hemodialysis conditions. Figure 5.38 and 5.39 shows the change in the activities when the membranes were stored at 37 °C in pH 7.4 phosphate buffer solution for 4 hours. The losses in the initial CAT and SOD activities correspond to 21% and 32% versus 23% and 37% when the SOD/CAT enzyme couple was immobilized on the plasma treated and PEI modified surfaces, respectively. It can be seen from Figure 5.40 that after storing in PBS buffer for 4 hours the amount of both enzymes remaining on the plasma treated surface was found higher than that on the PEI modified surface. This occurs due to stronger attachment with covalent bonding between the enzymes and plasma treated surface. The differences in the residual catalytic activities of the plasma treated and PEI modified surfaces can be explained by the differences in the strength of the binding, consequently, the conformation of the enzymes on the surfaces. Simply, the conformation as a result of interactions between enzyme-enzyme molecules or enzyme ionic components in PBS buffer solution during 4 hour storage is more restricted with a covalent bond on the plasma treated surface.

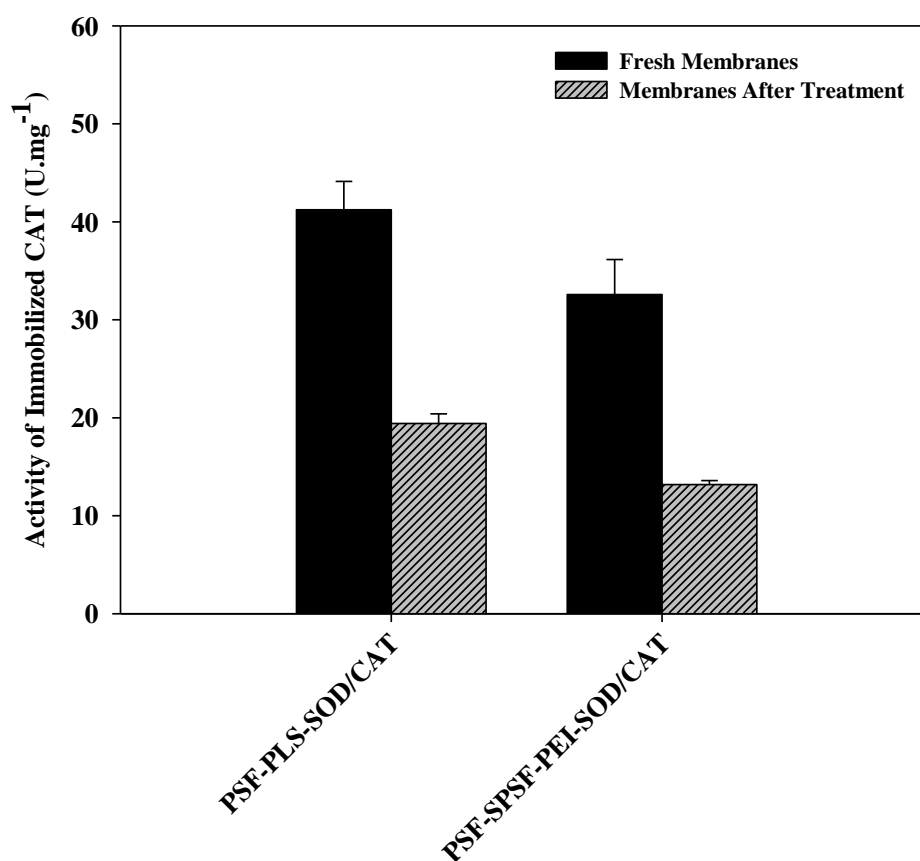


Figure 5.38. Stability of immobilized CAT at operating conditions ( $T=37\text{ }^{\circ}\text{C}$  and  $\text{pH}:7.4$ ). CAT was immobilized by layer by layer self-assembly of polyelectrolytes and plasma treatment method. Analyses were conducted with  $C_{\text{PEI-initial}}: 0.1\text{ mg.ml}^{-1}$ ;  $C_{\text{CAT-initial}}: 0.25\text{ mg.ml}^{-1}$ ;  $C_{\text{H}_2\text{O}_2}: 30\text{ mM}$ .

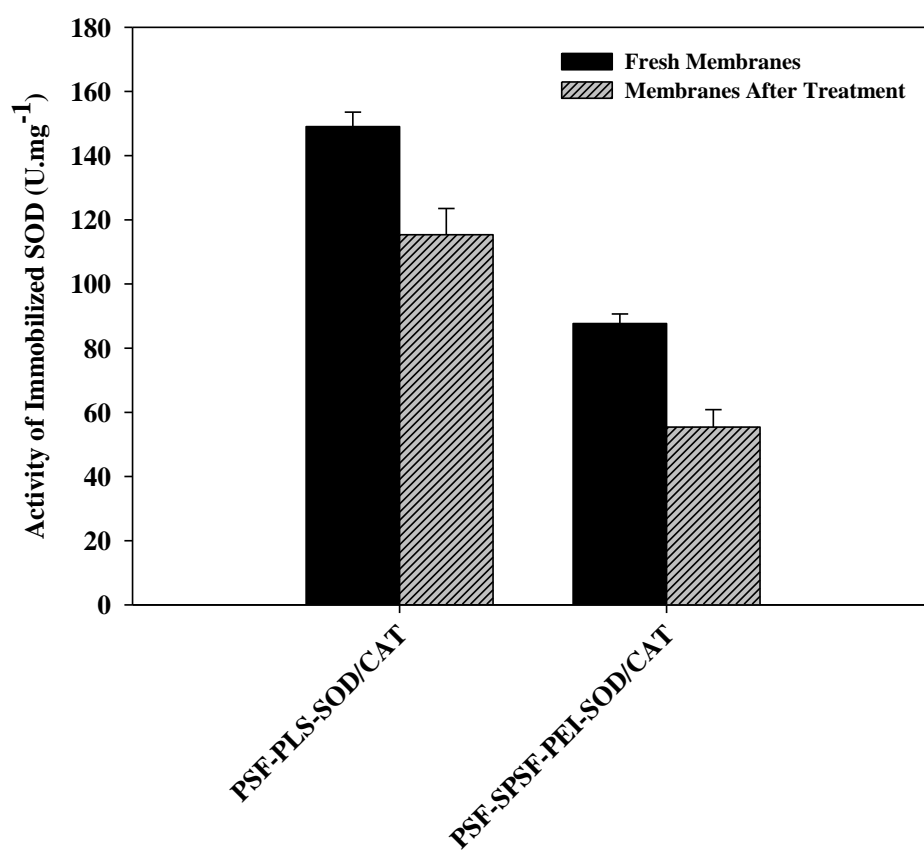


Figure 5.39. Stability of immobilized SOD at typical operating conditions ( $T=37\text{ }^{\circ}\text{C}$  and  $\text{pH}=7.4$ ). Experiments were conducted with  $C_{\text{PEI-initial}}: 0.1\text{ mg.ml}^{-1}$ ;  $C_{\text{enzyme-initial}}: 0.25\text{ mg.ml}^{-1}$ ;  $C_{\text{Riboflavin}}: 2\text{ }\mu\text{M}$ .

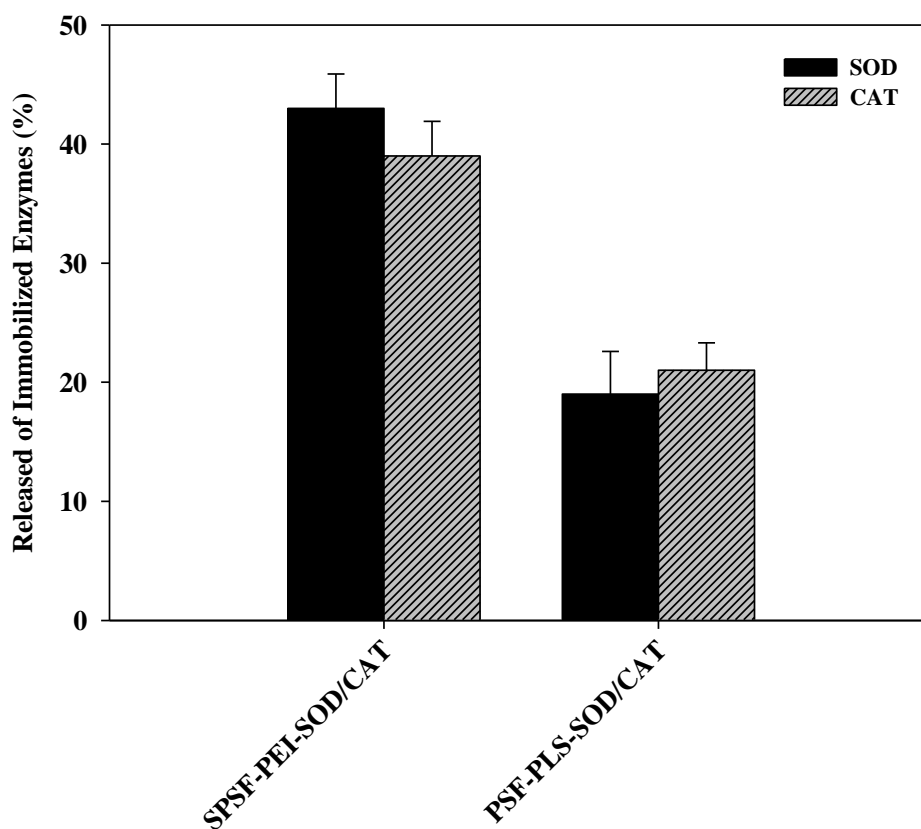
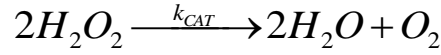
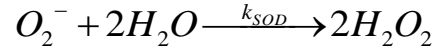


Figure 5.40. Amount of released SOD and CAT at typical operating conditions ( $T=37^{\circ}\text{C}$  and  $\text{pH}:7.4$ ).

### 5.3.4. Kinetic Study of Immobilized SOD/CAT

The enzyme-catalyzed reactions are successfully described with the Michaelis-Menten equation in the case one substrate involved in the reaction. Two kinetic parameters that appear in this equation are useful to characterize an enzyme in either free or immobilized form. The first parameter,  $V_{\text{max}}$ , represents the maximum reaction rate, while the Michaelis constant  $K_m$  is a measure of the tightness of binding of the substrate to the enzyme. To measure kinetic parameters,  $\text{H}_2\text{O}_2$  concentration was adjusted below the limit that causes inhibition of CAT enzyme.

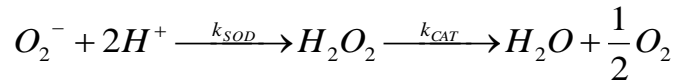
When SOD and CAT are immobilized separately, the Michaelis-Menten rate expressions are given in Equation 5.1 and 5.2:



$$r_{O_2^-} = \frac{V_{\max,SOD} \times C_{O_2^-}}{K_{M,SOD} + C_{O_2^-}} \quad (5.1)$$

$$r_{H_2O_2} = \frac{V_{\max,CAT} \times C_{H_2O_2}}{K_{M,CAT} + C_{H_2O_2}} \quad (5.2)$$

However, when they are coimmobilized, each intrinsic step in the reaction sequence follows Michaelis-Menten kinetics and the rate expressions are given by;



$$r_{O_2^-} = \frac{V_{\max,SOD} \times C_{O_2^-}}{K_{M,SOD} + C_{O_2^-}} \quad (5.3)$$

$$r_{H_2O_2} = -\frac{V_{\max,CAT} \times C_{H_2O_2}}{K_{M,CAT} + C_{H_2O_2}} + \frac{V_{\max,SOD} \times C_{O_2^-}}{K_{M,SOD} + C_{O_2^-}} \quad (5.4)$$

Based on kinetic parameters determined for native SOD and CAT enzymes, it was found that  $\left(\frac{V_{\max}}{K_m}\right)_{SOD} \gg \left(\frac{V_{\max}}{K_m}\right)_{CAT}$  ( $1.1 \times 10^9 \gg 5.1 \times 10^2$ ). This result simply indicates that overall reaction is controlled by the second one.

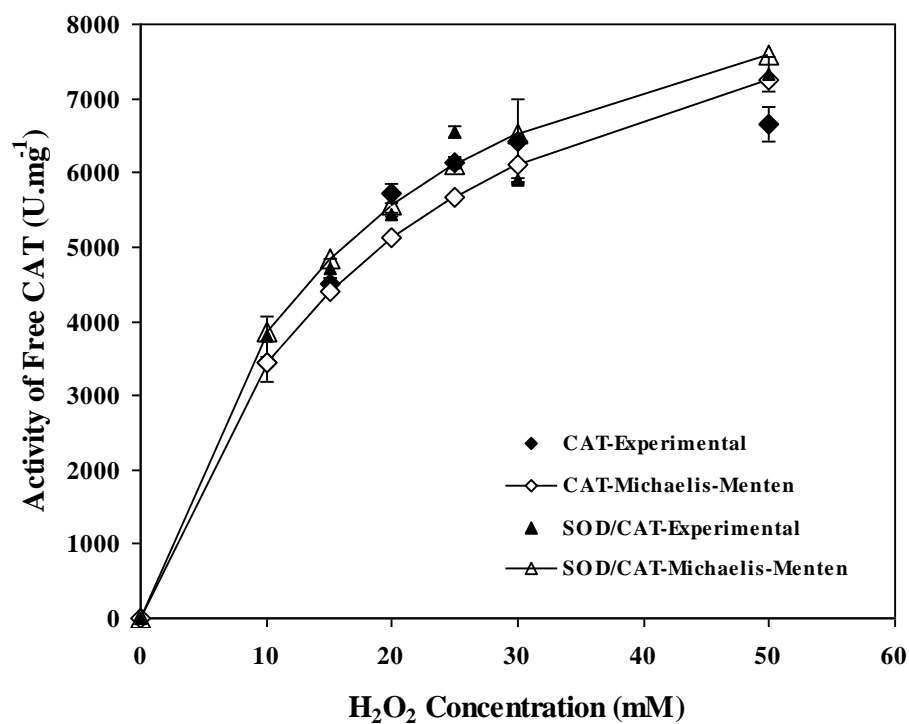
Kinetics parameters,  $K_m$  and  $V_{\max}$ , for free catalase (Figure 5.41a) and immobilized catalase without (Figure 5.41b) or with SOD (Figure 5.41c) were determined by obtaining rates of  $H_2O_2$  decomposition for various levels of  $H_2O_2$ . Figure 5.41 demonstrates that the decomposition of  $H_2O_2$  by either native or immobilized catalase follows the Michaelis-Menten type kinetics. Kinetic parameters calculated from

this figure are listed in Table 5.14. The value of  $K_m$  was found to be 22.7 mM whereas the  $V_{max}$  was calculated as 11579 ( $U \cdot mg \text{ enzyme}^{-1}$ ) for free catalase. The kinetic parameters of free CAT did not change significantly.

The  $K_m$  and  $V_{max}$  values of CAT upon immobilization onto either PEI modified or plasma treated surface changed dramatically. This occurs as a result of the structural changes in the enzyme during immobilization or lower accessibility of the substrate to the active site of the enzyme. The  $K_m$  values of immobilized catalase were found higher than that of free catalase indicating the decrease in the affinity of the enzyme to its substrate. This may be probably as a result of conformational change of CAT enzyme causing the steric hindrance of the active site by the support, the loss of enzyme flexibility necessary for binding to substrate or diffusional resistance to substrate molecules. Change in kinetic parameters of CAT after immobilization has been reported by other authors (Akkus Cetinus et al., 2000, 2009). For example, Çetinus and Öztop (2000) studied the immobilization of catalase on chitosan film and found that  $V_{max}$  value of the free catalase was 24,042  $U \cdot mg \text{ enzyme}^{-1}$  whereas, upon immobilization, it was decreased about 24-fold ( $1022 U \cdot mg \text{ enzyme}^{-1}$ ). They also (2009) reported that the  $V_{max}$  value of catalase was decreased 262-fold upon immobilization on the chitosan beads.

The  $V_{max}/K_m$  ratio reflects both affinity and catalytic ability of an enzyme, thus, it was calculated for both free and immobilized form of the enzymes. As seen in Table 5.14, the  $V_{max}/K_m$  values for CAT immobilized on the plasma treated and PEI deposited surfaces are similar. The change in the conformation of the CAT enzyme upon immobilization by ionic binding onto PEI modified surface occurred in a smaller extent as reported earlier. However, the covalent bonding onto the plasma treated surface provides a stronger attachment of the enzyme on the membrane surface and higher resistance to denaturant,  $H_2O_2$ . Consequently, CAT enzyme immobilized on the surfaces modified either with plasma or polyelectrolyte deposition gives similar catalytic performance. The activity of CAT enzyme slightly increased when immobilized with SOD.

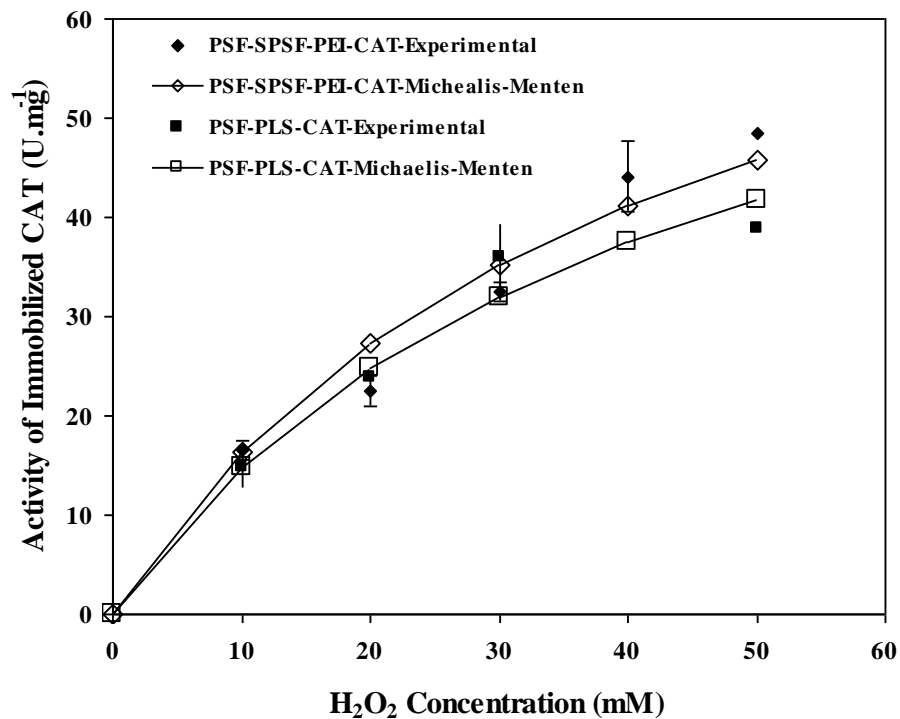




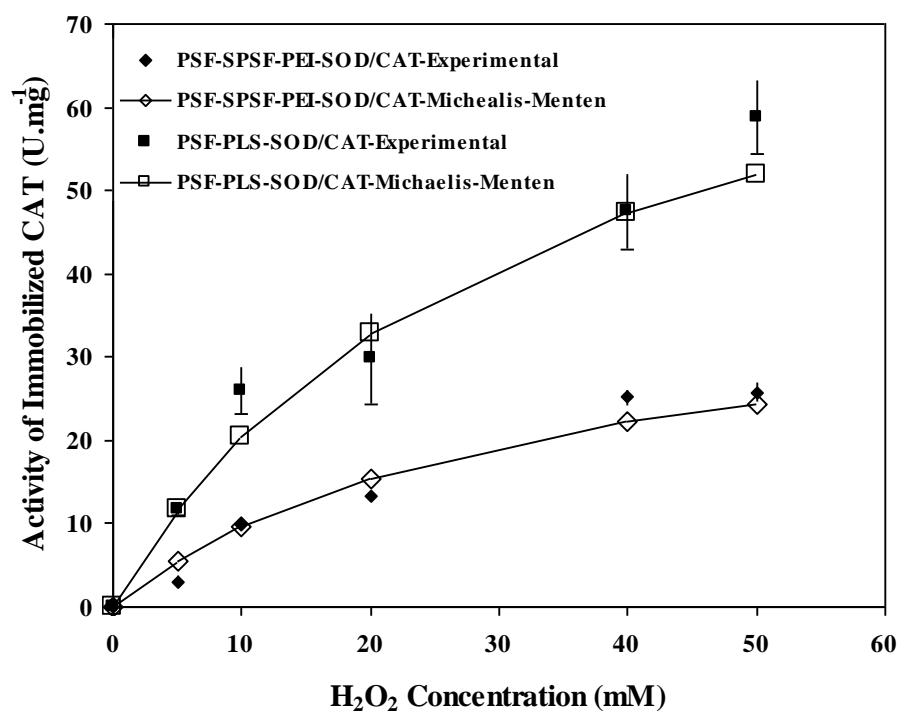
(a)

Figure 5.41. Substrate concentration vs. activity of free CAT (a), immobilized CAT on the PEI modified (b) and plasma treatment (c) surfaces. Experiments were conducted with  $C_{\text{PEI}}^{\text{initial}}$ :  $0.1 \text{ mg.ml}^{-1}$ ;  $C_{\text{enzyme}}^{\text{initial}}$ :  $0.25 \text{ mg.ml}^{-1}$  and  $C_{\text{H}_2\text{O}_2}$ :  $30 \text{ mM}$ .

(cont. on next page)



(b)



(c)

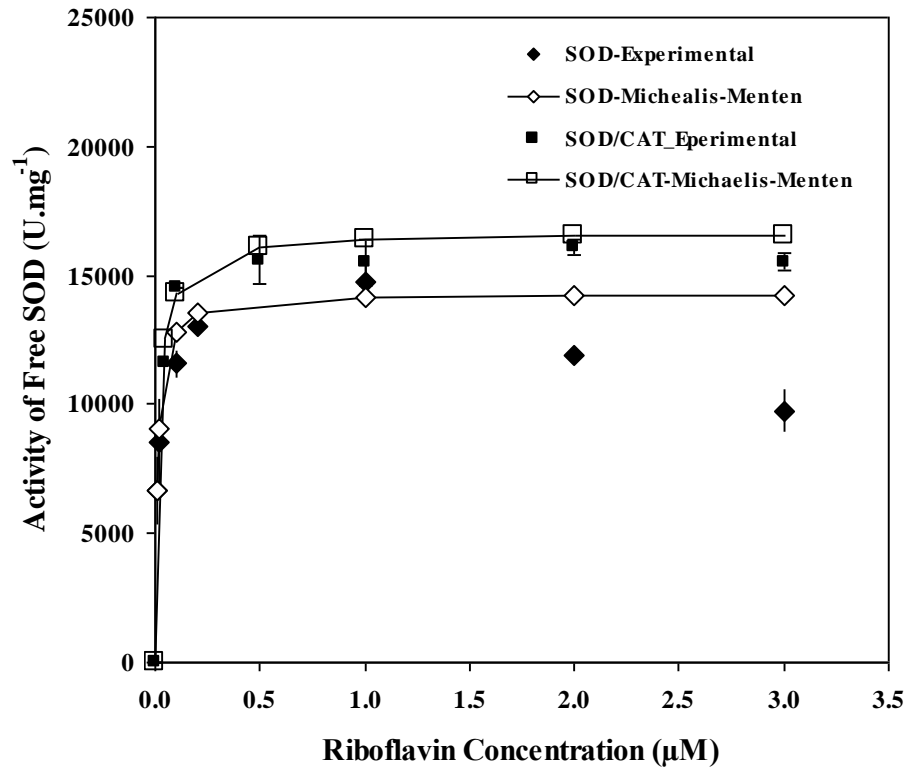
Figure 5.41. (cont.)

Table 5.14. Michealis-Menten kinetic parameters of native and immobilized CAT

Membrane Code	$V_{max}$ (U.mg <sup>-1</sup> )	$K_M$ (mM)	$V_{max}/K_M$ (U.mg <sup>-1</sup> .mM <sup>-1</sup> )
Native CAT	11579 ± 1168	22.7 ± 4.4	510 ± 111
PSF-SPSF-PEI-CAT	83.8 ± 10.1	49.1 ± 10.2	1.71 ± 0.41
PSF-PLS-CAT	80.9 ± 5.8	38.7 ± 5.2	2.09 ± 0.32
Native SOD-CAT	13238 ± 1354	25.9 ± 4.5	511 ± 103
PSF-SPSF-PEI-SOD/CAT	91.7 ± 16.1	45.9 ± 14.2	1.99 ± 0.71
PSF-PLS-SOD/CAT	117.3 ± 16.0	33.9 ± 9.9	3.46 ± 1.11

Kinetic parameters, for free SOD (Figure 5.42a) and immobilized SOD without (Figure 5.42b) or with CAT (Figure 5.42c) were determined using riboflavin as superoxide (O<sub>2</sub><sup>-</sup>) source and listed in Table 5.15. For the free enzyme the  $K_m$  was found to be  $1.3 \times 10^{-5}$  mM, whereas  $V_{max}$  value was calculated as 14080 U.mg enzyme<sup>-1</sup>. Figure 5.42a also illustrates that H<sub>2</sub>O<sub>2</sub> inactivation of SOD is prevented by the presence of catalase, since CAT consumes H<sub>2</sub>O<sub>2</sub> as soon as it forms.

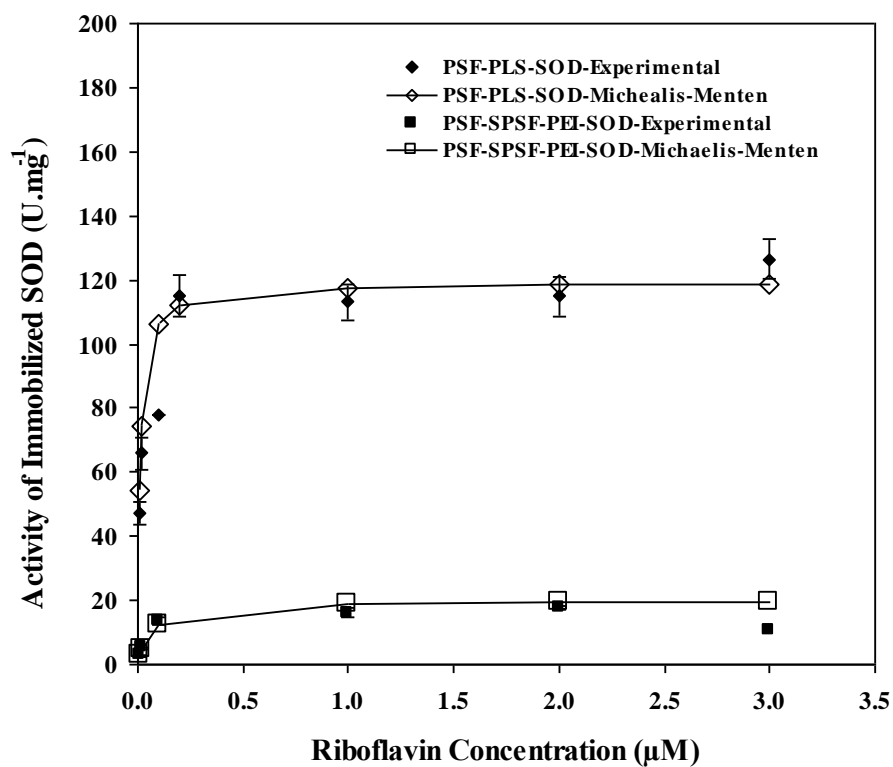
The catalytic activity of SOD immobilized on the plasma treated surface was found higher than that on the PEI modified surface as confirmed by higher  $V_{max}/K_m$  values. This can be explained by the fact that covalent attachment of SOD provides higher resistance to the H<sub>2</sub>O<sub>2</sub> inhibition than that of ionic binding on the PEI modified surface. The presence of CAT enzyme enhanced the activity of SOD by a factor of two when immobilized on the PEI modified surface. This is due to improved resistance against inactivation with H<sub>2</sub>O<sub>2</sub> in the presence of CAT. The same effect was not observed when the enzymes were coimmobilized on the plasma treated surfaces since covalent bonding itself already provides sufficient resistance to the H<sub>2</sub>O<sub>2</sub> inhibition.



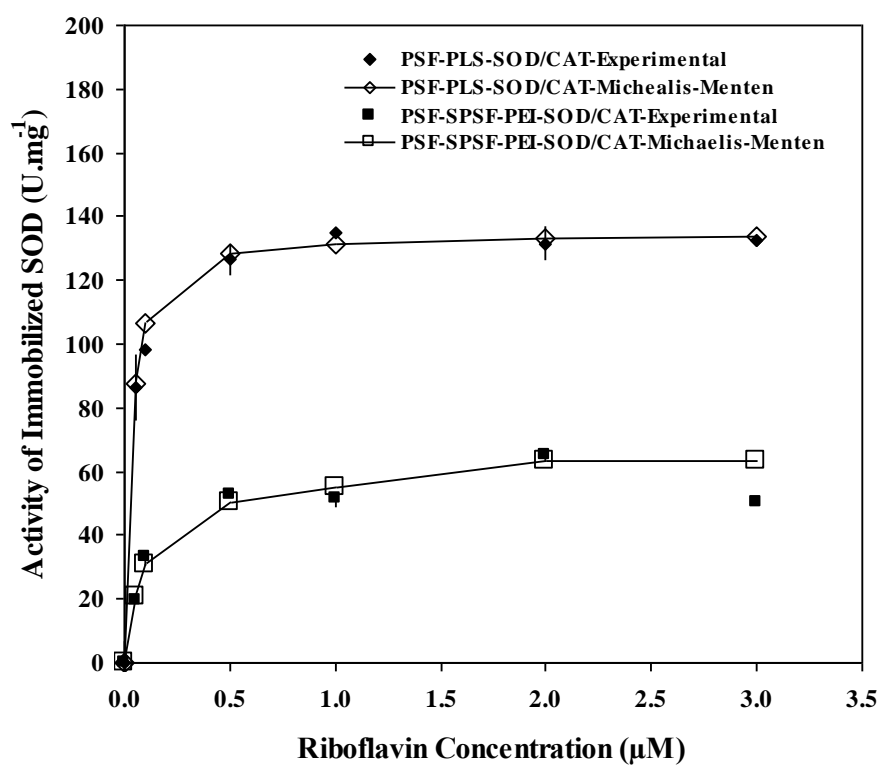
(a)

Figure 5.42. Substrate concentration vs activity of free SOD (a), immobilized on the PEI modified (b) and plasma treated (c) surfaces. Experiments were conducted with  $C_{PEI}^{initial}$ :  $0.1 \text{ mg.ml}^{-1}$ ;  $C_{enzyme}^{initial}$ :  $0.25 \text{ mg.ml}^{-1}$  and  $C_{Riboflavin}$ :  $2 \text{ μM}$ .

(cont. on next page)



(b)



(c)

Figure 5.42. (cont.)

Table 5.15. Michealis-Menten kinetic parameters for native and immobilized SOD

Membrane Code	$V_{max}$ (U.mg <sup>-1</sup> )	$K_M$ (mM)x 10 <sup>5</sup>	$V_{max}/K_M$ (U.mg <sup>-1</sup> .mM <sup>-1</sup> ) x 10 <sup>-5</sup>
Native SOD	14080 ± 489	1.3 ± 0.2	10839 ± 1708
PSF-SPSF-PEI-SOD	18.1 ± 0.8	4.7 ± 1.0	3.85 ± 0.84
PSF-PLS-SOD	117.3 ± 5.5	1.8 ± 0.5	65.17 ± 18.36
Native SOD-CAT	15983 ± 250	1.6 ± 0.3	9989 ± 1880
PSF-SPSF-PEI-SOD/CAT	70.9 ± 3.8	10.3 ± 2.4	6.88 ± 1.65
PSF-PLS-SOD/CAT	142.2 ± 6.3	3.1 ± 0.3	45.87 ± 4.88

The enzymatic reaction rates determined are defined as observed reaction rate due to the presence of mass transfer resistance. In the immobilized enzymes, substrate conversion takes place in three steps; substrate transport from the bulk medium to the surface of enzyme, enzymatic conversion into product and product transport back from the surface to the bulk medium. To determine the influence of external mass transfer resistance on the observed reaction rates and the relative importance of the mass transfer compared to the enzymatic reaction is determined by a dimensionless number called Damköhler number,  $Da_{II}$ . The Damköhler number is defined as the ratio of the maximum reaction rate to the maximum mass transfer rate.

$$Da_{II} = \frac{V_{max}}{K_L \times C_S} \quad (5.6)$$

Where  $V_{max}$  (mmol.cm<sup>-2</sup>.sec<sup>-1</sup>) is the maximum reaction rate;  $K_L$  is the liquid phase mass transfer coefficient of substrate (cm.sec<sup>-1</sup>),  $C_S$  (mmol.ml<sup>-1</sup>) is the concentration of substrate at the surface of the enzyme.

The change in Damköhler number with respect to stirring rate for native and immobilized CAT is shown in Table 5.16. Experimentally, the same activities for immobilized CAT were measured when the stirring rate was increased from 600 rpm to 800 rpm. Consistent with this observation, Damköhler numbers at these stirring rates were calculated similar, and, the values are much smaller than 1 indicating that mass transfer limitations are negligible.

SOD is known as the diffusion-controlled enzyme which is defined as an superefficient enzyme with  $k_{cat}/K_M$  of  $1.7 \times 10^{10} \text{ M}^{-1} \text{ s}^{-1}$  ( $k_{cat}=[E] \times V_{max}$ ) the highest catalytic rate ever reported for any enzyme (Stroppolo et al., 2001). Such enzymes are considered to be perfect, since their rate-limiting step is not due to the their enzymatic efficiencies. As seen in Table 5.16, the Damköhler numbers for all types of the membranes and the native enzyme are much higher than 1 for both stirring rates (600 rpm and 800 rpm). This simply indicates that the stirring rate is not sufficient to eliminate external mass transfer resistance. Infact, sharp increase in the activity of immobilized SOD to the maximum reaction rate at low substrate concentration shown in Figures 5.42a and 5.42b illustrates that the reaction takes place in the “mass transfer limited” region. In addition, the degree of conversion which is about 0.9 for all cases provides a quick estimate of the fact that the reaction is in the mass transfer limited region. Mass transfer resistance is usually minimized by high stirring rates, on the other hand, this might cause partial or complete denaturation of enzyme and the loss of enzyme. To decrease Damköhler number to a value of 0.1 so that the external mass transfer effects are negligible, required stirring rate was calculated as  $2.5 \times 10^{10}$  rpm. It is clear that practically SOD enzyme either in free or immobilized form cannot work in reaction-limited regime. Knowing this fact, the kinetic parameters of free and immobilized SOD were still calculated from the observed reaction rates to investigate how the surface treatment method influences the immobilized activities.

Table 5.16. The change in Damköhler numbers with respect to stirring rate for the native and immobilized CAT.

Stirring Rate Sample	600 rpm	800 rpm
Native CAT	0.02	0.02
PSF-SPSF-PEI-CAT	0.06	0.05
PSF-PLS-CAT	0.06	0.05
Native SOD-CAT	0.02	0.02
PSF-SPSF-PEI-SOD/CAT	0.04	0.03
PSF-PLS-SOD/CAT	0.07	0.06

Table 5.17. The change in Damköhler numbers with respect to stirring rate for the native and immobilized SOD.

Sample	Stirring Rate	
	600 rpm	800 rpm
Native SOD	328	279
SPSF-PEI-SOD	62	52
PSF-PLS-SOD	336	285
Native SOD-CAT	308	262
SPSF-PEI-SOD/CAT	313	266
PSF-PLS-SOD/CAT	336	285

### 5.3.5. *In vitro* Hemocompatibility of SOD/CAT Immobilized PSF Membranes

#### 5.3.5.1. Protein Adsorption Capacity

Figure 5.43 shows that the PSF-PLS membrane generated through plasma polymerization of PSF with allylamine reduced protein adsorption by 53% with respect to PSF membrane. In many studies, it is reported that plasma polymerization of hydrophilic monomeric gases carried out at low temperature reduced protein fouling due to formation of polar groups on the surface. (Belfort and Ulbricht, 1996) The water contact angle values (Figure 5.33) illustrated the enhanced hydrophilic character of the PSF surface after plasma treatment. Although their hydrophobic characters are similar, the amount of proteins adsorbed onto the plasma treated PSF surface is lower than that on the PSF-SPSF membrane due to smoother surface of this membrane. Moreover, the PSF-SPSF membrane is significantly negatively charged with  $\text{SO}_3^-$  groups which favors protein adsorption by electrostatic interactions. (Ostuni et al., 2001) On the other hand, plasma treated membranes which are appr. neutral due to nonprotonated  $\text{NH}_2$  groups are more suitable as nonfouling surface. Immobilization of SOD/CAT enzyme couple on the PEI modified and plasma treated membranes remarkably reduced protein adsorption capacities of these membranes. Although SOD and CAT enzymes have



hydrophobic patches, it is well known that the amino acid sequence 194-222 in the carboxyl-terminal end of SOD is strongly hydrophilic (Hjalmarsson et al., 1987). The improvement of the membrane hydrophilicity by SOD/CAT immobilization weakened the protein-PSF surface hydrophobic interactions and thus, significantly decreased the protein adsorption. There are also many studies in the literature that indicate reduced protein fouling as a consequence of modification of the hydrophobic surfaces through protein immobilization (Ulbricht and Riedel, 1998; Fang et al., 2009). The protein adsorption capacities of the SOD/CAT immobilized membranes were found lower than other PSF membranes modified with either ALA or HEP/ALG coating. This occurs as a result of the chain movement of the immobilized enzyme on the surface that might affect the surrounding area, thus, prevent the deposition of more protein on the surface of the membrane (Fang et al., 2009). SOD/CAT immobilization on the plasma treated membrane created a surface which shows slightly higher resistance to protein adsorption compared with the surface generated by immobilizing some enzymes on the PEI adsorbed PSF-SPSF membrane (Figure 5.43). This result can be explained by much more smooth surface of the plasma treated membrane. In addition, the plasma treated surface (PSF-PLS) underneath the enzyme layer has also lower protein adsorption capacity than PSF-SPSF-PEI surface.

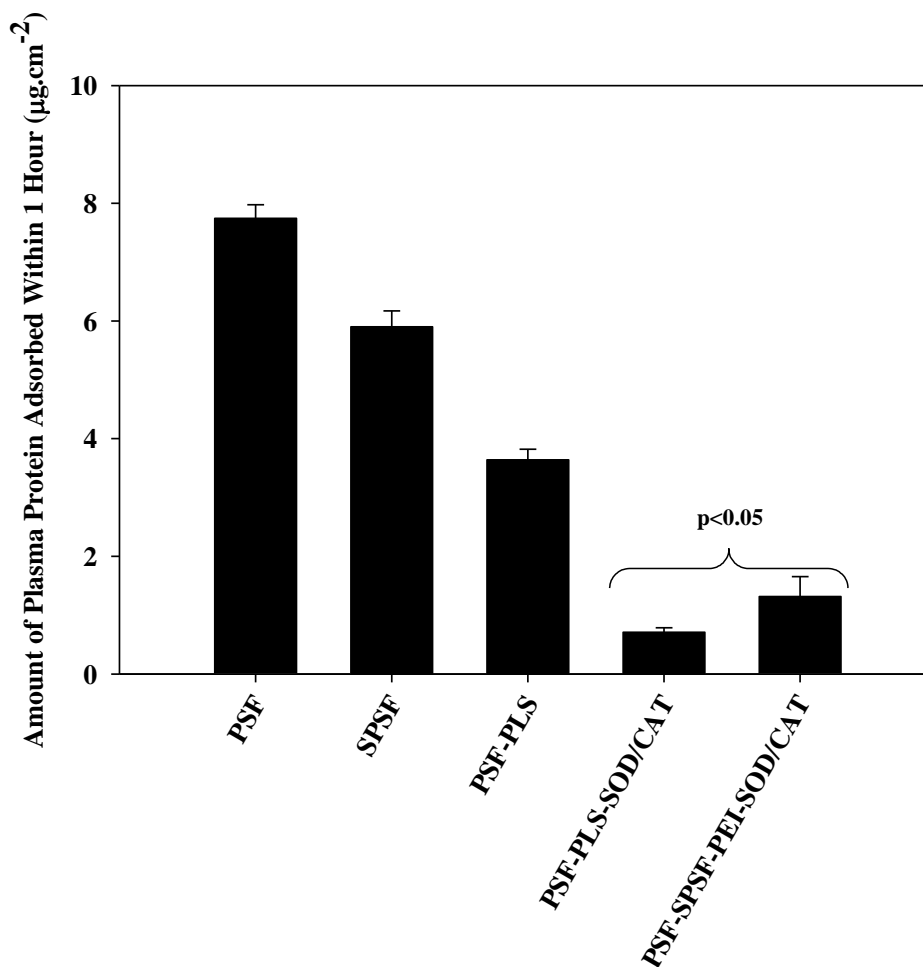


Figure 5.43. The amount of blood plasma proteins adsorbed onto unmodified and modified PSF membranes with SOD/CAT immobilization.

### 5.3.5.2. Platelet Adhesion and Activation

Figure 5.44 shows that the plasma treatment and SOD/CAT immobilization remarkably decreased the platelet activation to the level of control. It was also noticed that the SOD/CAT immobilization resulted higher reduction of platelet activation than that of ALA immobilization ( $p < 0.05$ ). The suppression of platelet activation on all of the modified membranes prepared in this thesis is believed to stem from diminished protein adsorption. The platelet adhesion, aggregation and activation of intrinsic coagulation depend on the amount and conformation of the protein layer adsorbed onto the surface. Consequently, lower activation of platelets on the SOD/CAT immobilized membranes compared to the ALA immobilized ones is due to lower protein adsorption capacities of these membranes. In addition, it was reported that when SOD induces the

platelet activation, CAT fully prevents SOD-dependent platelet activation (Krötz et al, 2002; Ryszawa et al., 2006). Platelet adhesion and cell activation was also investigated by SEM pictures. Figure 5.45 and 5.46 illustrated that adhered and activated platelets and blood cells observed on the SPSF-PSF membrane were not seen on the plasma treated PSF membrane and SOD/CAT coated membranes.

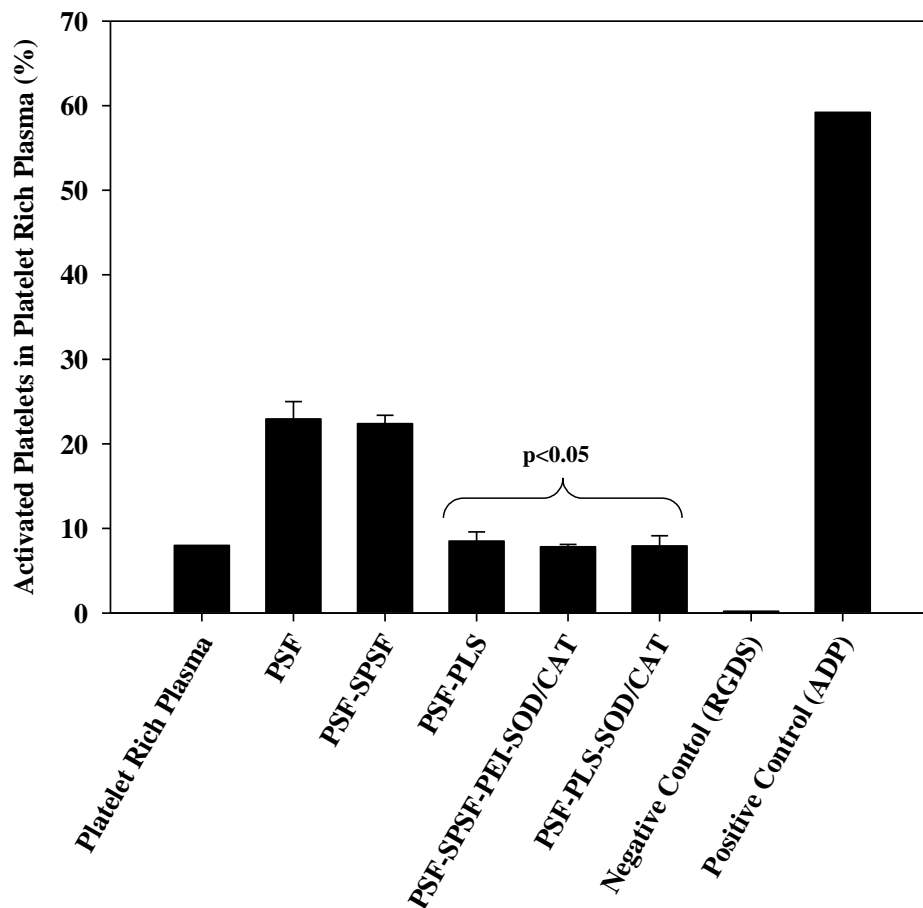


Figure 5.44. Amount of platelet activation on the unmodified and modified PSF membranes with SOD/CAT immobilization.

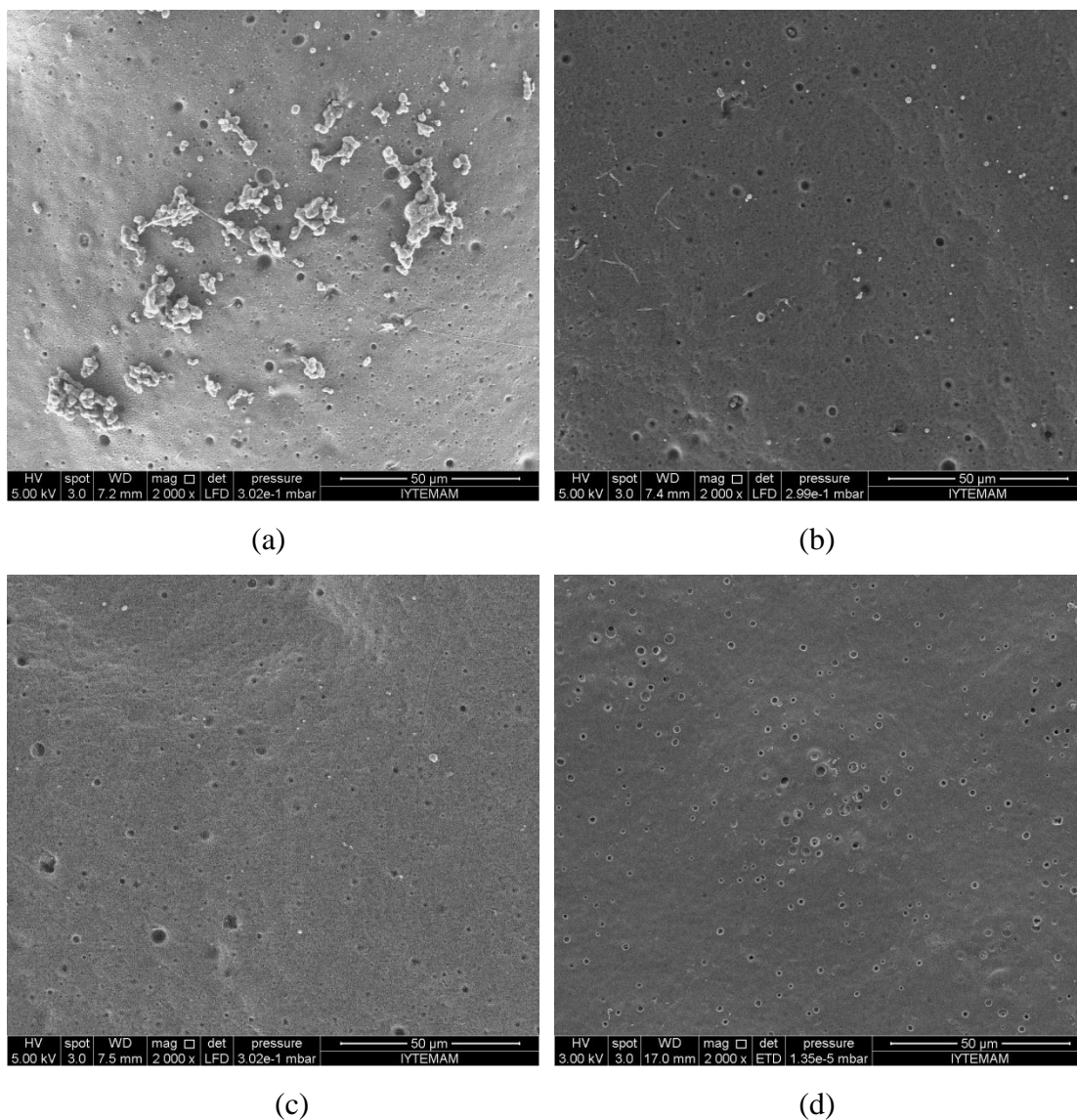


Figure 5.45. The SEM pictures of (a) PSF-SPSF-PEI-SOD/CAT and (b) PSF-PLS-SOD/CAT membranes after incubating with PRP for 25 minutes, magnification x 2000.

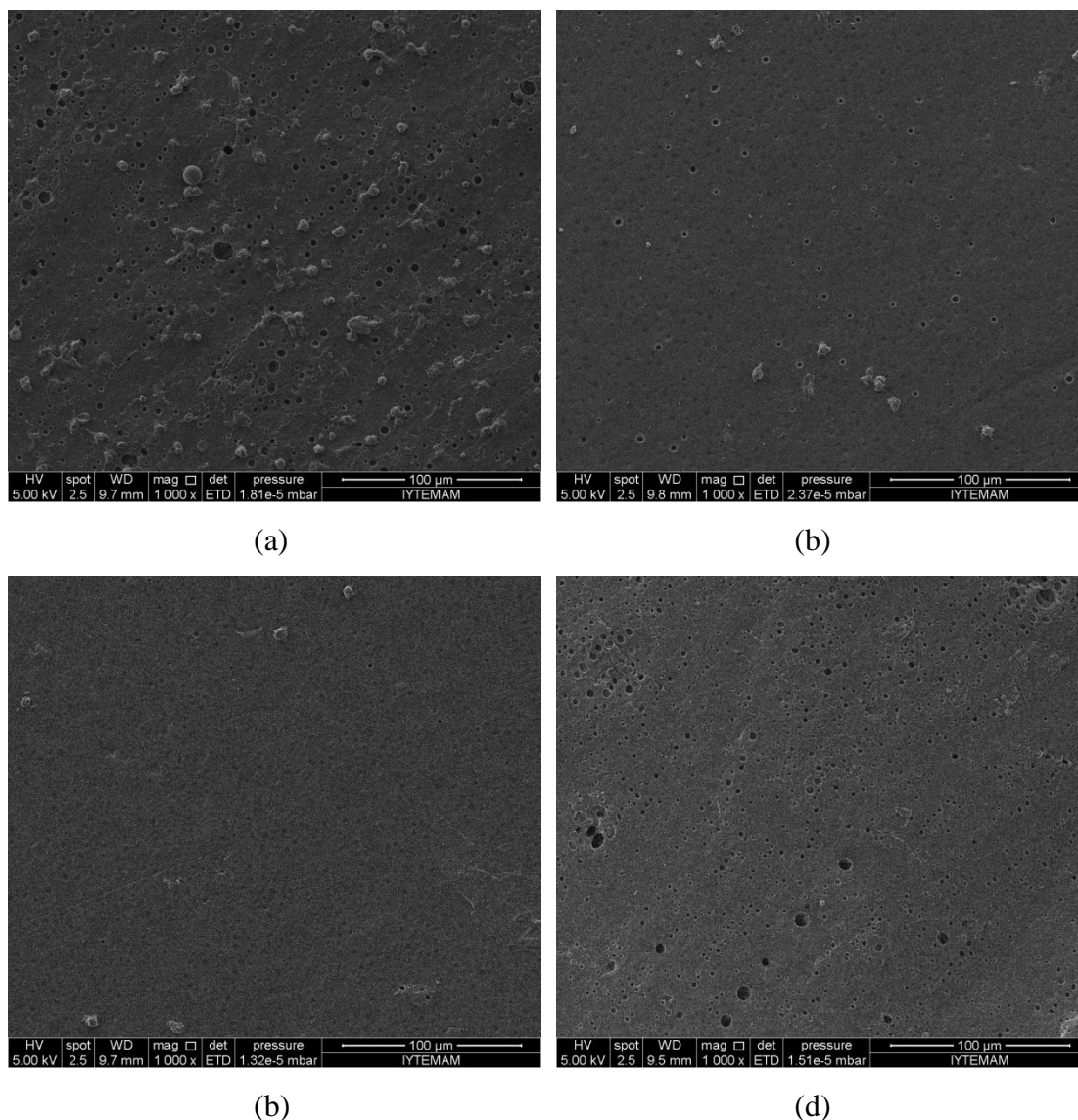
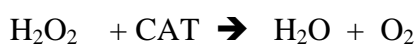
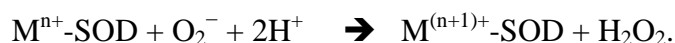
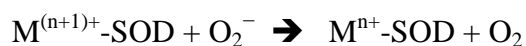


Figure 5.46. SEM pictures of (a) PSF-SPSF (b) PSF-PLS (c) PSF-PLS-SOD/CAT and (d) PSF-SPSF-PEI-SOD/CAT membranes after incubating with whole blood for 15 minutes, magnification x 1000

### 5.3.5.3. Inhibition of Reactive Oxidant Species in Plasma

The *in vitro* antioxidant activity of SOD/CAT coated membranes was investigated in relevance to the inhibition of ROS in the blood. Figure 5.47 shows that the SOD/CAT immobilized on the membranes significantly suppressed the ROS formation (expressed as CL counts of HOCl) in blood. The difference in the CL counts of HOCl obtained with the SOD/CAT immobilized on either PEI modified or plasma treated surfaces was found statistically insignificant ( $p > 0.05$ ).

SOD/CAT immobilized membranes displayed similar reduction in HOCl level with ALA immobilized ones. The enzyme couple catalyzed the conversion of superoxide anion which is the most effective radical in the biological system to water and oxygen as follows:



where M = Cu (n=1) ; Mn (n=2) ; Fe (n=2) ; Ni (n=2).

As a result of the reduction in the  $O_2^-$  and  $H_2O_2$  level in blood, oxidative balance is reformed in favor of the antioxidants in blood. Consequently, the increased antioxidants can dissipate the other ROS in blood such as HOCl. Although ALA can directly scavenge the HOCl radical in blood, ALA or SOD/CAT modified membranes were capable of reducing reactive oxygen species level in blood at similar rates.

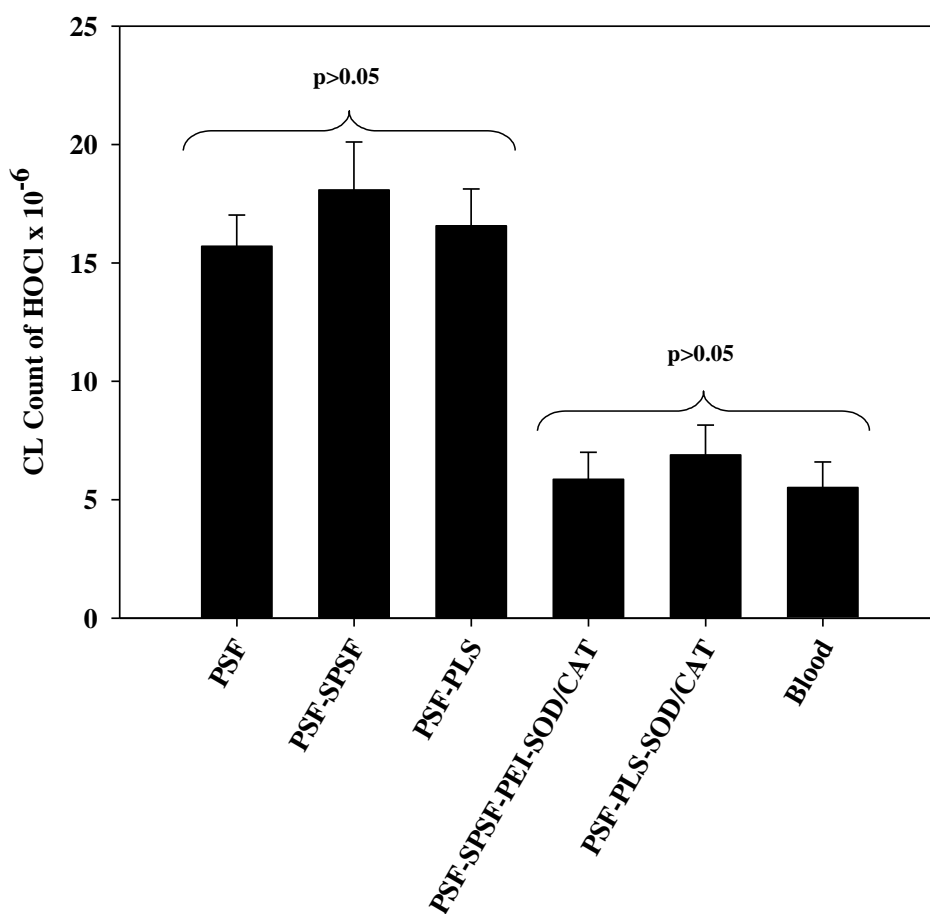


Figure 5.47. The inhibition HOCl in blood by unmodified and modified membranes with SOD/CAT immobilization.

#### 5.3.5.4. Activated Partial Thromboplastin Time

The APTT values for SOD/CAT immobilized membranes were analyzed since the decreased adsorption of blood proteins and platelet activation on these membranes and inhibition of ROS production raise an expectation for these membranes to prolong the coagulation time (APTT). The results show that SOD/CAT immobilization provided significantly longer APTT values than the PSF, PSF-SPSF membranes and the control regardless of the immobilization method (Table 5.18). The capacity of SOD/CAT immobilized membranes in inhibiting ROS was found similar although the immobilization on the plasma treated surface caused lower protein adsorption and platelet activation on the surface. The result suggests that the ROS inhibition is more

effective than improved antifouling property to prolong the coagulation time by SOD/CAT immobilization. This result also was confirmed by the observation that the improvement in APTT value for plasma treated PSF membrane in the absence of SOD/CAT was found smaller. In addition, the PSF membranes modified with  $\alpha$ -lipoic acid and SOD/CAT immobilization were also able to prolong the blood coagulation time, although coagulation was observed earlier than heparin containing membranes.

Table 5.18. APTT Values for SOD/CAT Immobilized Membranes

Membrane Code	APTT (s)
Control (Blood Plasma)	39±2
PSF	36±3
PSF-SPSF	37±4
PSF-PLS	49±3
PSF-SPSF- PEI-SOD/CAT	67±4
PSF-PLS-SOD/CAT	62±3

### 5.3.5.5. Cytotoxicity

The cytotoxicities of pure SOD and CAT were not measured since they are the most important blood antioxidants with a concentration of  $548 \mu\text{g.l}^{-1}$  in blood serum ( $240 \text{ mg.l}^{-1}$  in erythrocytes in blood) (Sun et al., 1988). While SOD can be very toxic in the presence of iron in blood, it is nontoxic in combination with CAT or another peroxidase (Maop et al., 1993). Cytotoxicity studies conducted with the SOD/CAT immobilized membranes have shown that the viability of peripheral mononuclear blood cells (PMBC) after 4 hours treatment with unmodified and modified membranes is close to 100% (Table 5.19). The excellent cell viability of the modified membranes confirms that the SOD/CAT immobilization does not have a significant negative effect on the nontoxic property of the unmodified PSF membrane.



Table 5.19. % Live peripheral mononuclear blood cells after 4 hours treatment with unmodified and modified PSF membranes with SOD/CAT immobilization.

<b>Membrane Code</b>	<b>Live Cell %</b>
Control (PMBCs)	100
PSF	98.7±1.1
PSF-SPSF	97.9±0.9
PSF-PLS	98.1±0.7
PSF-SPSF-PEI-SOD/CAT	98.3±1.2
PSF-PLS-SOD/CAT	99.4±0.2

### **5.3.6. Transport and Mechanical Properties of the SOD/CAT Immobilized Membranes**

It is known that plasma treatment may cause etching on the surface of the membrane (Favia and d'Agostino, 1998). This may result in the disruption of the dense skin layer and the semi-permeable character of the membrane. It is seen from the Figure 5.48 that after plasma treatment, permeabilities of the solutes did not change significantly within the statistical confidence limits ( $p>0.05$ ). The result indicates that there is no etching on the PSF-PLS membrane, which is also proven by SEM and AFM pictures (Figure 5.34-5.36). The permeation coefficients of the solutes through SOD/CAT immobilized membranes were found similar ( $p>0.05$ ). In addition, SOD/CAT immobilization did not change the permeation characteristics of the unmodified PSF membranes since the increase in the total thickness of the membrane with the enzyme layer is on the order of a few nanometers. Neither the bulk structure of the support membrane nor the thickness of dense skin layer was affected by enzyme immobilization, consequently, high permeation rates of toxic solutes through PSF membranes did not change.

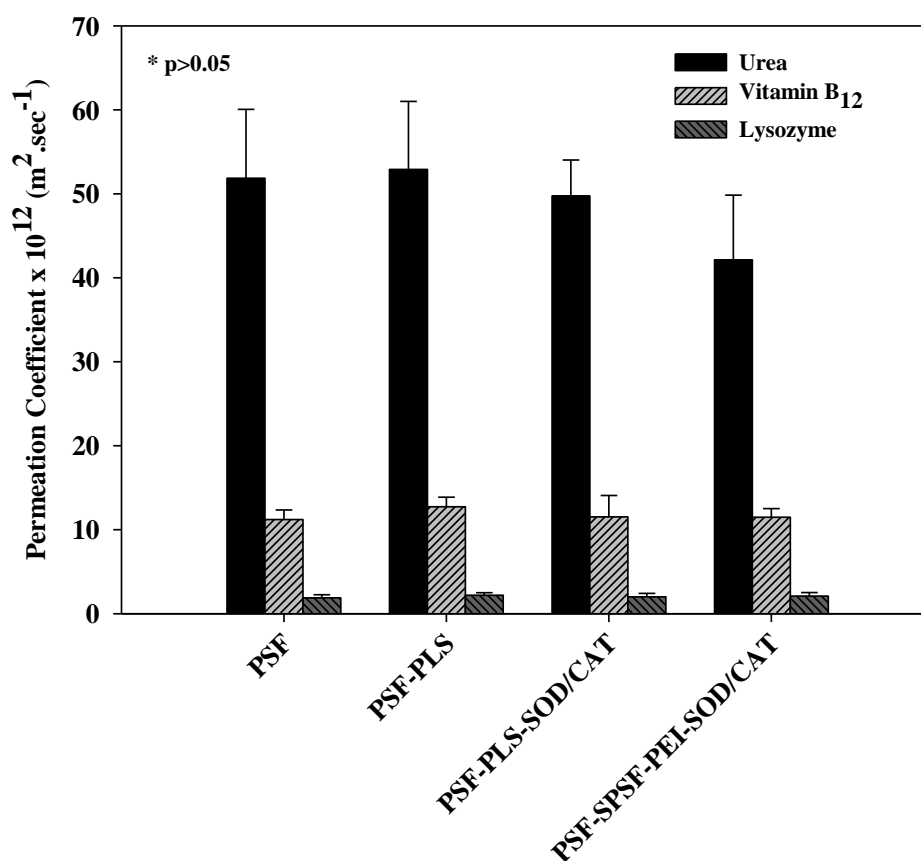


Figure 5.48. The permeation coefficient of urea, vitamin B<sub>12</sub>, lysozyme through unmodified and modified PSF membranes with SOD/CAT immobilization. \* Permeation coefficients of each membrane are not statistically different from each other for each solute (p>0.05)

Mechanical properties of the unmodified and modified membranes are listed in Table 5.20. As expected, plasma treatment of PSF caused slight decrease in maximum tensile strength of the PSF membrane, while deposition of SOD/CAT on either plasma treated or PEI modified membranes did not significantly change the mechanical properties (p>0.05).

Table 5.20. Mechanical properties of the unmodified and modified PSF membranes with SOD/CAT immobilization.

<b>Membrane Code</b>	<b>Maximum Tensile Stress (MPa)</b>	<b>Young Modulus(MPa)</b>
PSF	2.78±0.22	39.82±5.97
PSF-SPSF	2.25±0.18	50.25±7.54
PSF-PLS	2.39±0.21	49.72±5.51
PSF-PLS-SOD/CAT	2.26 ±0.17	51.19±7.73
PSF-SPSF-PEI-SOD/CAT	2.31 ±0.19	43.27±4.11

## CHAPTER 6

### CONCLUSION

In this thesis, it was aimed to improve the blood compatibility of PSF based hemodialysis membranes through generating antithrombogenic and antioxidative surfaces. A commonly used approach to provide antithrombogenic properties is to immobilize anticoagulant heparin onto the surface of these materials. In this study, the same approach was adopted, and heparin was immobilized ionically by layer by layer (LBL) self assembly of polyelectrolytes. In particular, the feasibility of using a blend of heparin and alginate in the outermost layer of the LBL assembly was tested. The results revealed that diluting heparin with alginate did not cause a decrease in its biological activity, moreover, most of its anticoagulant activity was stable under typical hemodialysis conditions. In most of the previous studies, the biomaterial was first activated by a bi- or trifunctional agent and then heparin was coupled covalently to the biomaterial. This two-step procedure is complicated and time consuming, in addition, the functional agents may cause crosslinking which may reduce the permeability of the membrane. The LBL technique used in this study is an easy method and can be conducted in an aqueous solution under mild ambient conditions which minimize the loss in the activity of heparin due to attachment on the membrane surface. Although heparin was immobilized by LBL method in a limited number of previous studies, it was used alone as a polyanion not only in the outermost layer but also in the intermediate layers as well. The strategy proposed in this study which corresponds to attaching heparin only on the terminating layer of the assembly by blending with alginate can be an economical alternative approach for the modification of hemodialysis membranes since heparin is an expensive compound.

Alpha-lipoic acid and SOD/CAT enzyme couple, were chosen as modifying agents to create a surface with an antioxidative property. It was hypothesized that ALA can be site-specifically attached on the PEI modified support membrane through an electrostatic interaction. This hypothesis was confirmed by XPS analysis that the cyclide disulphide bond which forms the active site of ALA was available on the surface. The instability of ALA under light or heat and its short biological half-life was

improved through immobilization and the greatest enhancement was achieved when it was sandwiched between two PEI layers. SOD/CAT enzyme couple were immobilized both ionically and covalently on the PEI modified and plasma treated surfaces, respectively. The loss of enzymes from PEI modified surface was found larger during storage in PBS buffer at pH 7.4 and the enzymes on the plasma treated surface were more stable at the end of 4 hours. The inactivation of SOD by H<sub>2</sub>O<sub>2</sub> was prevented in the presence of CAT, on the other hand, the catalytic activities of CAT were similar in the presence or absence of SOD. The CAT enzyme was shown to operate in the reaction-limited region while SOD catalyzed the reaction in the diffusion-limited regime at all substrate concentrations. The calculations indicated that it is practically not possible to eliminate external mass transfer resistance to function SOD enzyme in the reaction limited regime.

*In vitro* hemocompatibility results indicated that the immobilization of all biomolecules (heparin, alpha-lipoic acid or SOD/CAT enzyme couple) reduced the protein adsorption, platelet adhesion and activation on the PSF membranes. Although coagulation was observed earlier than heparin containing membranes, the PSF membranes modified with  $\alpha$ -lipoic acid and SOD/CAT immobilization were also able to prolong the blood coagulation time. In addition, they were capable of reducing reactive oxygen species level in blood at similar rates. The surface characterization studies demonstrated that the hydrophilicity, the surface charge and roughnesses have significant influence on the biocompatibility of the membranes as they change the protein adsorption level and conformation of the adsorbed proteins on the surface of the membranes. While improving the blood compatibility of the PSF membranes, their desired properties such as nontoxicity, high permeation rates for toxic compounds and high mechanical strength were protected after biomolecule immobilization.

The results obtained in this thesis suggest that the ALA or SOD/CAT immobilized PSF membrane could be an alternative to prevent hemodialysis induced oxidative stress and may allow decreasing the amount of anticoagulant injected to the patient during hemodialysis. On the other hand, the cost-effective modification of the hemodialysis membranes is critical since their reuse is forbidden in most countries. Therefore, it is suggested to use ALA as a modifying agent since it is much cheaper than SOD/CAT enzyme couple.

It is worth of continuing the efforts in this field for future studies. First of all, clinical studies for PSF membranes modified with ALA immobilization can be carried

out. In addition, the use of a polyelectrolyte biomolecule blend can be extended to other expensive and highly functional biomolecules to immobilize on different blood-contacting devices. Furthermore, the developed SOD/CAT immobilized PSF membranes could be evaluated for biosensor applications.

## REFERENCES

- Akkus, Ç.S., Nursevin, Ö.H. (2000). Immobilization of catalase on chitosan film. *Enzyme and Microbial Technology*, 26, 497–501
- Akkus, Ç.S., Sahin, E., Saraydin, D. (2009). Preparation of Cu(II) adsorbed chitosan beads for catalase immobilization. *Food Chemistry*, 114, 962–969
- Alptekin, O., Tukul, S.S., Yıldırım, D., Alagoz, D. (2009). Characterization and properties of catalase immobilized onto controlled pore glass and its application in batch and plug-flow type reactors. *Journal of Molecular Catalysis B: Enzymatic*, 58, 124–131.
- Alptekin, O., Tukul, S.S., Yıldırım, D., Alagoz, D. (2010). Immobilization of catalase onto Eupergit C and its characterization. *Journal of Molecular Catalysis B: Enzymatic*, 64, 177–183.
- Bailey, J.E., Ollis, D.F. (1986). *Biochemical Engineering Fundamentals*. 2.edition, Mcraw-Hill International Editions.
- Baumann, H., Kokott, A. (2000). Surface modification of the polymers present in a polysulfone hollow fiber hemodialyser by covalent binding of heparin or endothelial cell surface heparan sulfate: Flow characteristics and platelet adhesion. *J. Biomater. Sci. Polym. Ed.*, 11, 245-272.
- Bilek, M.M., McKenzie, D.R. (2010) Plasma modified surfaces for covalent immobilization of functional biomolecules in the absence of chemical linkers: towards better biosensors and a new generation of medical implants. *Biophys Rev.*, 2, 55–65.
- Blitz, J.P., Guniko, V.M. (2006). Surface modifications to influence adhesion of biological cells and adsorption of globular proteins. *Surface Chemistry in Biomedical and Environmental Science*, 159, 176-181.
- Blanco, J.F., Nguyen, Q.T., Scaetzel, P. (2002). Sulfonation of polysulfones: Suitability of the sulfonated materials for asymmetric membrane preparation. *J. Appl. Polym. Sci.*, 84, 2461-2473.
- Bradford, M.M. 1976., A Rapid and Sensitive Method for the Quantitation of Microgram Quantities of Protein Utilizing the Principle of Protein-Dye Binding. *Analytical Biochemistry*, 72, 248-254.
- Brink, L.E.S., Elbers, S.J.G., Robbertsen, T., Both, P. (1993). The anti-fouling action of polymers preadsorbed on ultrafiltration and microfiltration membranes. *J. Membr. Sci.*, 76, 281.
- Candan, F., Gültekin, F., Candan, F. (2002) Effect of vitamin C and zinc on osmotic fragility and lipid peroxidation in zinc-deficient hemodialysis patients. *Cell*

- Chanard, J., Lavaud, S., Paris, B., Toure, F., Rieu, P., Renaux, J.L., Thomas, M. (2005). Assessment of heparin binding to the AN69 ST hemodialysis membrane: I. Preclinical studies. *Asaio J.*, 51, 342-347.
- Chanard, J., Lavaud, S., Maheut, H., Kazes, I., Vitry, F., Rieu, P. (2008). The clinical evaluation of low-dose heparin in haemodialysis: a prospective study using the heparin-coated AN69 ST membrane. *Nephrol. Dial. Transplant.*, 23, 2003-2009.
- Chang, J.W., Lee, E.K., Kim, T.H., Min, W.K., Chun, S., Lee, K.U., Kim, S.B., Park, J.S. (2007). Effects of alpha-lipoic acid on the plasma levels of asymmetric dimethylarginine in diabetic end-stage renal disease patients on hemodialysis: a pilot study. *American Journal of Nephrology*, 27, 70-74.
- Chen, V., Fane, A.G., Fell, C.J.D. (1992). The use of anionic surfactants for reducing fouling of ultrafiltration membranes: their effects and optimization. *J. Membr. Sci.*, 67, 249-261.
- Chen, J.L., Li, Q.L., Chen, J.Y., Chen, C., Huang, N. (2009). Improving blood-compatibility of titanium by coating collagen-heparin multilayers. *Appl. Surf. Sci.*, 255, 6894-6900.
- Cheung, A.K., Parker, C.J., Janatova, J., Brynda, E. (1992). Modulation of complement activation on hemodialysis membranes by immobilized heparin. *J. Am. Soc. Nephrol.*, 2, 1328-1337.
- Choi, J., Rubner, M.F. (2005). Influence of the Degree of Ionization on Weak Polyelectrolyte Multilayer Assembly. *Macromolecules*, 38, 116-124
- Clermont, G., Sandrine, L.S., Cabanne, J.F.C., Motte, G., Guillard, J.C., Chevet, D., Rochette, L. (2001). Vitamin E-Coated Dialyzer Reduces Oxidative Stress in Hemodialysis Patient. *Free Radical Biology & Medicine*, 31, 233-241.
- Çelik, Ö., Akbuğa, J. (2007). Preparation of superoxidase dismutase loaded chitosan microspheres: Characterization and Release Study. *European Journal of Pharmaceutics and Biopharmaceutics*, 66, 42-47.
- David, C., d'Andrea, C., Lancelota, E., Bochterle, J., Guillot, N., Fazio, B., Maragò, O.M., Sutton, A., Charnaux, N., Neubrech, F., Pucci, A., Gucciardi, P.G., de la Chapelle, M.L. (2012). Raman and IR spectroscopy of manganese superoxide dismutase, a pathology biomarker. *Vibrational Spectroscopy*, 62, 50– 58.
- Decher, G. (1997). Fuzzy Nanoassemblies: Toward Layered Polymeric Multicomposites. *Science*, 277, 1232–1237.
- Delfino, V.D.A., Vianna, A.C.A., Mocelin, A.J., Barbosa, D.S., Mise, R.A., Matsuo, T. (2007). Folic acid therapy reduces plasma homocysteine levels and improves plasma antioxidant capacity in hemodialysis patients. *Applied Nutritional*



*Investigation*, 23, 242-247.

- Deppisch, R., Storr, M., Buck, R., Gohl, H. (1998). Blood material interactions at the surfaces of membranes in medical applications. *Sep. Purif. Technol.*, 14, 241-254.
- Edmunds, L.H., Jr., Hessel, E.A., II, Colman, R.W., Menasche, P, Hammon, J.W., Jr. (2003). Extracorporeal Circulation. 315–387. *Cardiac Surgery In The Adult*, 11. Second Edition. McGraw-Hill Companies
- Erol, M, Du, H, Sukhishvili, S. (2006). Control of specific attachment of proteins by adsorption of polymer layers. *Langmuir*, 19 22(26), 11329-11336.
- Favia, P., d'Agostino, R. (1998). Plasma treatments and plasma deposition of polymers for biomedical applications, *Surface and Coatings Technology*, 98, 1102-1106.
- Fang, B., Ling, Q., Zhao, W., Ma, Y., Bai, P., Wei, Q., Li, H., Zhao, C. (2009). Modification of polyethersulfone membrane by grafting bovine serum albumin on the surface of polyethersulfone/poly(acrylonitrile-co-acrylic acid) blended membrane. *Journal of Membrane Science*, 329, 46–55.
- Ferretti, G., Bacchetti, T., Masciangelo, S., Pallotta, G. (2008). Lipid peroxidation in hemodialysis patients: Effect of vitamin C supplementation. *Clinical Biochemistry*, 41, 381-386.
- Floccari, F., Aloisi, C., Crascy, E., Sofi, T., Campo, S., Tripodo, D., Criseo, M., Frisina, N., Buemi, M. (2005). Oxidative Stress and Uremia. *Medicinal Research Reviews*, 25, 473-486.
- Ford, I., Cotter, M.A., Cameron, N.E., Greaves, M. (2001). The effects of treatment with  $\alpha$ -lipoic acid or evening primrose oil on vascular hemostatic and lipid risk factors, blood flow, and peripheral nerve conduction in the streptozotocin-diabetic rat. *Metabolism*, 50, 868-875.
- Giovagnoli, S., Blasi, P., Ricci, M., Rossi, C. (2004). Biodegradable microspheres as carriers for native superoxide dismutase and catalase delivery. *AAPS Pharm. Sci. Tech.*, 5, 1-9.
- Gong, M., Wang, Y.B., Li, M., Hu, B.H., Gong, Y.K. (2011). Fabrication and hemocompatibility of cell outer membrane mimetic surfaces on chitosan by layer by layer assembly with polyanion bearing phosphorylcholine groups. *Colloids and Surfaces B: Biointerfaces*, 85, 48–55.
- Griebenow, K., Klibanov, A.M. (1995). Lyophilization-induced changes in the secondary structure of proteins. *Proc. Natl. Acad.*, 92, 10969-10976.
- Guzey, D., McClements, D.J. (2006). Formation, stability and properties of multilayer emulsions for application in the food industry. *Advances in Colloid and Interface Science*, 128–130, 227–248.

- Hasegawa, T., Iwasaki, Y., Ishihara, K. (2011). Preparation and performance of protein-adsorption-resistant asymmetric porous membrane composed of polysulfone/phospholipid polymer blend, *Biomaterials*, 22, 243-.
- Higuchi, A., Nakagawa, T. (1990). Surface-modified polysulfone hollow fibers. III. Fibers having a hydroxide group. *J. Appl. Polym. Sci.*, 41, 1973-.
- Hjalmarsson, K., Marklund, S.L., Engstrom, A., Edlund, T. (1987). Isolation and sequence of complementary DNA encoding human extracellular superoxide dismutase (placental cDNA expression library/nucleotide sequence/amino acid sequence/molecular evolution/oxygen radicals). *Proc. Natl. Acad. Sci.*, 84, 6340-6344.
- Houli, J., Changling, L., Zhanjun, S., Sun, M, Zehan, D. (1996). FTIR study of the catalytic mechanism of catalase on the hydrolysis of soman. *Acta Biophysica Sinica*, 12, 200-220
- Houska, M., Brynda, E., Solovyev, A., Broucková, A., Krízová, P., Vanícková, M., Dyr, J.E. (2008). Hemocompatible albumin-heparin coatings prepared by the layer-by-layer technique. The effect of layer ordering on thrombin inhibition and platelet adhesion. *J. Biomed. Mater. Res. A.*, 86, 769-778.
- Ishihara, K., Fukumoto, K, Iwasaki, Y, Nakabayashi, N. (1999). Modification of polysulfone with phospholipid polymer for improvement of the blood compatibility. Part 1. Surface characterization. *Biomaterials*, 20, 1545-1551
- Itoh, S., Susuki, C., Tsuji, T. (2006). Platelet activation through interaction with hemodialysis membranes induces neutrophils to produce reactive oxygen species. *Journal of Biomedical Materials Research Part A*. 77A, 294 - 303.
- Jahnig, F. (1983). Thermodynamics and kinetics of protein incorporation into membranes (hydrophobic effect/protein immobilization/lipid-protein interaction/hydrogen bonds/conformational entropy). *Biophysics*, 80, 3691-3695.
- Kofuji, K., Nakamura, M., Isobe, T., Murata, Y., Kawashima, S. (2008). Stabilization of  $\alpha$ -lipoic acid by complex formation with chitosan. *Food Chemistry*, 109, 167-171.
- Kofuji, K., Isobe, T., Murata, Y. (2009). Controlled release of  $\alpha$ -lipoic acid through incorporation into natural polysaccharide-based gel beads. *Food Chemistry*, 115, 483-487.
- Krötz, F., Sohn, H.Y., Gloe, T., Zahler, S., Riexinger, T., Schiele, T.M., Becker, B.F., Theisen, K., Klauss, V., Pohl, U. (2002). NAD(P)H oxidase-dependent platelet superoxide anion release increases platelet recruitment. *Blood*, 100, 917-924.
- Kung, F.C., Yang, M.C. (2006-a). Effect of conjugated linoleic acid grafting on the hemocompatibility of polyacrylonitrile membrane. *Polymers for Advanced Technologies*, 17, 419-425.

- Kung, F.C., Yang, M.C. (2006-b). The effect of covalently bonded conjugated linoleic acid on the reduction of oxidative stress and blood coagulation for polysulfone hemodialyzer membrane. *International Journal of Biological Macromolecules*, 38, 157-164.
- Kung, F.C., Yang, M.C. (2006-c). Effect of conjugated linoleic acid immobilization on the hemocompatibility of cellulose acetate membrane. *Colloids and Surfaces B: Biointerfaces*, 47, 36-42.
- Kung, F.C., Yang, M.C. (2007). The reduction of oxidative stress, anticoagulation of platelets, and inhibition of lipopolysaccharide by conjugated linoleic acid bonded on a polysulfone membrane. *Polymers for Advanced Technologies*, 18, 286-291.
- Langsdorf, L.J., Zydney, A.L. (1994). Diffusive and convective solute transport through hemodialysis membranes: A hydrodynamic analysis. *J. Biomed. Mater. Res.*, 28, 573-582.
- Lavaud, S., Canivet, E., Wuillai, A., Maheut, H., Randoux, C., Bonnet, J.M., Renaux, J.L., Chanard, J. (2003). Optimal anticoagulation strategy in hemodialysis with heparin-coated polyacrylonitrile membrane. *Nephrol. Dial. Transplant*, 18, 2097-2104.
- Lavaud, S., Paris, B., Maheut, H., Randoux, C., Renaux, J.L., Rieu, P., Chanard, J. [http://apps.webofknowledge.com/DaisyOneClickSearch.do?product=WOS&search\\_mode=DaisyOneClickSearch&colName=WOS&SID=S2GkkkhM4I@cK8847Eo&author\\_name=Chanard,%20J&dais\\_id=3768698](http://apps.webofknowledge.com/DaisyOneClickSearch.do?product=WOS&search_mode=DaisyOneClickSearch&colName=WOS&SID=S2GkkkhM4I@cK8847Eo&author_name=Chanard,%20J&dais_id=3768698) (2005). Assessment of the heparin-binding AN69 ST hemodialysis membrane: II. Clinical studies without heparin administration. *Asaio J.*, 51, 348-351.
- Leber, H.W., Wizemann, V., Goubeaud, G., Rawer, P., Schütterle, G. (1978). Hemodiafiltration: a new alternative to hemofiltration and conventional hemodialysis. *Artif Organs.*, 2(2), 150-153.
- Lee, K.B., Kim, B., Lee, Y.H., Yoon, S.J., Kang, W.H., Huh, W., Kim, D.J., Oh, H.Y., Kim, Y.G. (2004). Hemodialysis using heparin-bound Hemophan in patients at risk of bleeding. *Nephron. Clin. Pract.*, 97, 5-10.
- Lehninger, A.L., Nelson, D.L., Cox, M.M. (1993). *Principles of Biochemistry*, 2nd edition, p: 111-133 New York: Worth Publishers, U.S.A.
- Lin, W.C., Liu, T.Y., Yang, M.C. (2004). Hemocompatibility of polyacrylonitrile dialysis membrane immobilized with chitosan and heparin conjugate. *Biomaterials*, 25, 1947-1957.
- Lin, Q., Yan, J., Qiu, F., Song, X., Fu, G., Ji, J. (2011). Heparin/collagen multilayer as a thromboresistant and endothelial favorable coating for intravascular stent. *J. Biomed. Mater. Res. A.*, 96, 132-141.

- Liu, M., Yue, X.L., Dai, Z.F., Ma, Y., Xing, L., Zha, Z.B., Liu, S.Q., Li Y. (2009). Novel Thrombo-resistant coating based on iron-polysaccharide complex multilayers. *ACS Appl. Mater. Interfaces*, *1*, 113-123.
- Mahlicli, F.Y., Altinkaya, S.A. (2009). The effects of urease immobilization on the transport characteristics and protein adsorption capacity of cellulose acetate based hemodialysis membranes. *J Mater Sci: Mater Med.*, *20*, 2167-2179.
- Manoj, V.M., Aravind, U.K., Mohan, H., Aravindakumar, C.T. (2011). Reaction of hydroxyl radicals with S-nitrosothiols: Formation of thiyl radical (RS•) as the intermediate. *Res. Chem. Intermed.*, *37*, 1113–1122.
- Mao, G.D., Thomas, P.D., Lopaschuk, G.D., Poznansky, M.J. (1993). Superoxide dismutase (SOD)-catalase conjugates. Role of hydrogen peroxide and the Fenton reaction in SOD toxicity. *Journal of Biological Chemistry*, *268*, 416-420.
- Marsh, S.A., Coombes, J.S. (2006). Vitamin E and  $\alpha$ -lipoic acid supplementation increase bleeding tendency via an intrinsic coagulation pathway. *Clinical Applied Thrombosis/Hemostasis*, *12*, 169-173.
- Massa, T.M., Yang, M.L., Hod, J.Y.C., Brashe, J.L., Santerrea, J.P. (2005). Fibrinogen surface distribution correlates to platelet adhesion pattern on fluorinated surface-modified polyetherurethane. *Biomaterials*, *26*, 7367–7376
- Matsugo, S., Han, D., Tritschler, H.J., Packer, L. (1996). Decomposition of  $\alpha$ -lipoic acid derivatives by photoirradiation-formation of dihydrolipoic acid from  $\alpha$ -lipoic acid. *Biochem Mol Biol Int.*, *38(1)*, 51-59.
- Miyata, T., Jikihara, A., Nakamae, K. (1997). Permeation Decomposition of Urea Through Asymmetrically Urease-Immobilized Ethylene-Vinyl Alcohol Copolymer Membranes. *Journal of Applied Polymer Science*, *63*, 1579-1588.
- Morena, M., Jaussent, I., Chalabi, L., Bergnoux, A.S., Dupuy, A.M., Badiou, S., Rakic, C., Thomas, M., Canoud, B., Cristol, J.P. (2010). Biocompatibility of heparin-grafted hemodialysis membranes: Impact on monocyte chemoattractant protein-1 circulating level and oxidative status. *Hemodial. Int.*, *14*, 403-410.
- Morti, S., Shao, J., Zydney, A. L. (2003). Importance of asymmetric structure in determining mass transport characteristics of hollow fiber hemodialyzers. *Journal of Membrane Science*, *224*, p: 39.
- Mydlik, M., Derzsiova, K., Racz, O., Sipulova, A., Lovasova, E., Petrovicova, J. (2001). A modified dialyzer with vitamin E and antioxidant defense parameters. *Kidney International*, *59*, 144-147.
- Neelakandan, C., Chang, T., Alexander, T., Define, L., Evancho-Chapman, M., Kyu, T. (2011). In vitro evaluation of antioxidant and anti-inflammatory properties of genistein-modified hemodialysis membranes. *Biomacromolecules*, *12*, 2447-2455.

- Nguyen, Q. T., Ping, Z., Nguyen, T., Rigal, P. (2003). Simple method for immobilization of bio-macromolecules onto membranes of different types. *Journal of Membrane Science*, 213, 85–95.
- Nguyen, Q.T., Glinel, K., Pontie, M., Ping, Z. (2004). Immobilization of biomacromolecules onto membranes via an adsorbed monolayer: An insight into the mechanism. *Journal of Membrane Science*, 232, 123-132.
- Nie, F.Q., Xu, Z.K., Ye, P., Wu, J., Seta, P. (2004). Acrylonitrile-based copolymer membranes containing reactive groups: effects of surface-immobilized poly(ethylene glycol)s on anti-fouling properties and blood compatibility. *Polymer*, 45, 399-407.
- Ostuni, E., Chapman, R.G., Holmlin, R.E., Takayama, S., Whitesides, G.M. (2001). A Survey of Structure–Property Relationships of Surfaces that Resist the Adsorption of Protein. *Langmuir*, 17, 5605-5620.
- Packer, L., Witt, E.H., Tritschler, H.J. (1995). Alpha-lipoic acid as a biological antioxidant. *Free Radical Biology & Medicine*, 19, 227-250.
- Park, J.Y., Acar, M.H., Akthakul, A., Kuhlman, W., Mayes, A.M. (2006). Polysulfone-graft-poly(ethylene glycol) graft copolymers for surface modification of polysulfone membranes. *Biomaterials*, 27(6), 856-865.
- Pastor, I., Salinas-Castillo, A., Esquembre, R., Mallavia, R., Mateo, C.R. (2010). Multienzymatic system immobilization in sol–gel slides: Fluorescent superoxide biosensors development. *Biosensors and Bioelectronics*, 25, 1526–1529.
- Quinn, J.F, Johnston, A.P.R., Such, G.K., Zelikin, A.N., Caruso, F. (2007). Next generation, sequentially assembled ultrathin films: beyond electrostatics. *Chem. Soc. Rev.*, 36, 707-718.
- Renò, F, Lombardi, F., Cannas, M. (2004). Polystyrene surface coated with vitamin E modulates human granulocyte adhesion and MMP-9 release. *Biomolecular Engineering*, 21(2), 73–80
- Reno, F., Aina, V., Gatti, S., Cannas, M. 2005. Effect of vitamin E addition to poly(D,L)-lactic acid on surface properties and osteoblast behaviour, *Biomaterials*, 26, 5594–5599.
- Ruixia, W., Jinlong, C., Lianlong, C., Zheng-hao, F., Ai-min, L., Quanxing, Z. (2004). Study of adsorption of lipoic acid on three types of resin. *Reactive & Functional Polymers*, 59, 243-252.
- Ryszawa, N., Kawczynska, A., Pryjma, J., Czesnikiewicz-Guziki, M., Adamek-Guziki, T., Naruszewicz, M., Korbut, R., Guziki, T. J. (2006). Effects of novel plant antioxidants on platelet superoxide production and aggregation in atherosclerosis. *Journal of Physiology and Pharmacology*, 57, 611.626.

- Sagedal, S., Witczak, B.J., Osnes, K., Hartmann, A., Os, I., Eikvar, L., Klingenberg, O., Brosstad, F. (2011). A Heparin-Coated Dialysis Filter (AN69 ST) Does Not Reduce Clotting during Hemodialysis when Compared to a Conventional Polysulfone Filter (F x 8). *Blood Purificat.*, 32, 151-155.
- Shu, Y., Ou, G., Wang, L., Zou, J., Li, Q. (2011). Surface modification of titanium with heparin-chitosan multilayers via layer-by-layer self-assembly technique. *J. Nanomater*, 2011, 1-8.
- Sperling, C., Houska, M., Brynda, E., Streller, U., Werner, C. (2006). In vitro hemocompatibility of albumin-heparin multilayer coatings on polyethersulfone prepared by the layer-by-layer technique. *J. Biomed. Mater. Res. A.*, 76A, 681-689.
- Sperling, C., Fischer, M., Maitz, M.F., Werner, C. (2009). Blood coagulation on biomaterials requires the combination of distinct activation processes. *Biomaterials*, 30, 1-10.
- Spijker, H.T., Bos, R., Busscher, H.J., van Kooten, T.G., van Oeveren, W. (2002). Platelet adhesion and activation on a shielded plasma gradient prepared on polyethylene. *Biomaterials*, 23, 757-766.
- Stamatialis, D.F., Papenburg, B.J., Giron'es, M., Saiful, S., Bettahalli, S.N.M., Schmitmeier, S., Wessling, M. (2008). Medical applications of membranes: Drug delivery, artificial organs and tissue engineering. *Journal of Membrane Science*, 308, 1-34.
- Stepniewska, J., Dolegowska, B., Ciechanowski, K., Kwiatkowska, E., Millo, B., Chlubek, D. (2006). Erythrocyte Antioxidant Defense System in Patients with Chronic Renal Failure According to the Hemodialysis Conditions. *Archives of Medical Research*, 37, 353-359
- Sun, S., Yue, Y., Huang, X., Meng, D. (2003) Protein adsorption on blood-contact membranes. *Journal of Membrane Science*, 222, 3-18.
- Sun, W.Y., Fang, J.L., Chen, M., Xia, P.Y., Tang, W.X. (1997). Secondary structure of copper, zinc superoxide dismutase dependent on metal ions investigated by fourier transform IR spectroscopy. *Inc. Biopoly.*, 42, 297-303.
- Sun, Y., Oberley, L.W., Li, Y. (1988). A simple method for clinical assay of superoxide dismutase. *Clinical Chemistry*, 34/3, 497-500.
- Tainer, J.A., Getzoff, E.D., Richardson, J.S., Richardson, D.C. (1983). Structure and mechanism of copper, zinc superoxide dismutase. *Nature*, 306, 284-287.
- Teichert, J., Tuemmers, T., Achenbach, H., Preiss, C., Hermann, R., Ruus, P., Preiss, R. (2005). Pharmacokinetics of alpha-lipoic acid in subjects with severe kidney damage and end-stage renal disease. *Journal of Clinical Pharmacology*, 45, 313-328.

- Thierry, B., Winnik, F.M., Merhi, Y., Silver, J., Tabrizian, M. (2003). Bioactive Coatings of Endovascular Stents Based on Polyelectrolyte Multilayers. *Biomacromolecules*, 4, 1564-1571.
- Ulbricht, M., Belfort, G. (1996). Surface modification of ultrafiltration membranes by low temperature plasma II. Graft polymerization onto polyacrylonitrile and polysulfone. *Journal of Membrane Science*, 111, 193-215.
- Ulbricht, M., Riedel, M., Marx, U. (1996). Novel photochemical surface functionalization of polysulfone ultrafiltration membranes for covalent immobilization of biomolecules. *Journal of Membrane Science*, 120(2), 239-259.
- Ulbricht, M., Riedel, M. (1998). Ultrafiltration membrane surfaces with grafted polymer 'tentacles': preparation, characterization and application for covalent protein binding. *Biomaterials*, 19, 1229.
- Ungaro, F., De, Rosa, G., Miro, A., Quaglia, F. (2003). Spectrophotometric determination of polyethylenimine in the presence of an oligonucleotide for the characterization of controlled release formulations. *Journal of Pharm Biomed Anal.*, 5;31(1), 143-149.
- Villalong, R., Cao, R., Fragoso, A., Damiao, A.E., Pedro, D., Caballero J.O. (2005). Supramolecular assembly of cyclodextrin-modified gold nanoparticles and Cu, Zn-superoxide dismutase on catalase. *Journal of Molecular Catalysis B: Enzymatic*, 35, 79-85.
- Wang, Z.G., Wan, L.S., Xu, Z.K. (2007). Surface engineerings of polyacrylonitrile-based asymmetric membranes towards biomedical applications: An overview. *Journal of Membrane Science*, 304, 8-23.
- Ward, R.A., Klein, E., Harding, G.B., Murchison, K.E. (1998). Response of complement and neutrophils to hydrophilized synthetic membranes. *Trans. Am. Soc. Artif. Intern. Organs*, 34, 334.
- Wen, S., Zheng, F., Shen, M., Shi, X. (2012). Surface modification and PEGylation of branched polyethyleneimine for improved biocompatibility. *Journal of Applied Polymer Science*, DOI: 10.1002/app.38444.
- Woffinfin, C., Hoenich, N.A. (1988). Blood-membrane interactions during haemodialysis with cellulose and synthetic membranes. *Biomaterials*, 9, 53.
- Yamamoto, K.I., Matsuda, M., Okuoka, M., Yakushiji, T., Fukuda, M., Miyasaka, T., Matsumoto, Y., Sakai, K. (2007). Antioxidation property of vitamin E-coated polysulfone dialysis membrane and recovery of oxidized vitamin E by vitamin C treatment. *Journal of Membrane Science*, 302/15, 115-118.
- Yang, M.C., Lin, C.C. 2001. Urea permeation and hydrolysis through hollow fiber dialyzer immobilized with urease. *Biomaterials*, 22, 891-896.

- Yang, M.C., Lin, W.C. (2002). Surface modification and blood compatibility of polyacrylonitrile membrane with immobilized chitosan–heparin conjugate. *J. Polym. Res.*, 9, 201-206.
- Yang, M.C., Lin, W.C. (2003). Protein adsorption and platelet adhesion of polysulfone membrane immobilized with chitosan and heparin conjugate. *Polym. Advan. Technol.*, 14, 103-113.
- Ye, S.H., Watanabe, J., Iwasaki, Y., Ishihara, K. (2002). Novel cellulose acetate membrane blended with phospholipid polymer for hemocompatible filtration system. *J. Membr. Sci.*, 210, p: 411.
- Ye, S.H., Watanabe, J., Iwasaki, Y., Ishihara, K. (2005). In situ modification on cellulose acetate hollow fiber membrane modified with phospholipid polymer for biomedical application. *Journal of Membrane Science*, 249, 133-141.
- Yin, Y., Nosworthy, N.J., Gong, B., Bax, D., Kondyurin, A., McKenzie, D.R., Bilek, M. M. (2009). Plasma Polymer Surfaces Compatible with a CMOS Process for Direct Covalent Enzyme Immobilization. *Plasma Process. Polym.*, 6, 68–75
- Yu, D.G., Jou, C.H., Lin, W.C., Yang, M.C. (2007). Surface modification of poly(tetramethylene adipate-co-terephthalate) membrane via layer-by-layer assembly of chitosan and dextran sulfate polyelectrolyte multilayer. *Colloids and Surfaces B: Biointerfaces*, 54, 222–229.
- Zhang, Z., Zhang, M., Chen, S., Horbett, T.A., Ratner, B.D., Jiang, S. (2008). Blood compatibility of surfaces with superlow protein adsorption. *Biomaterials*, 29, 4285–4291.



## APPENDIX A

### CALIBRATION CURVES and EXTINCTION COEFFICIENTS

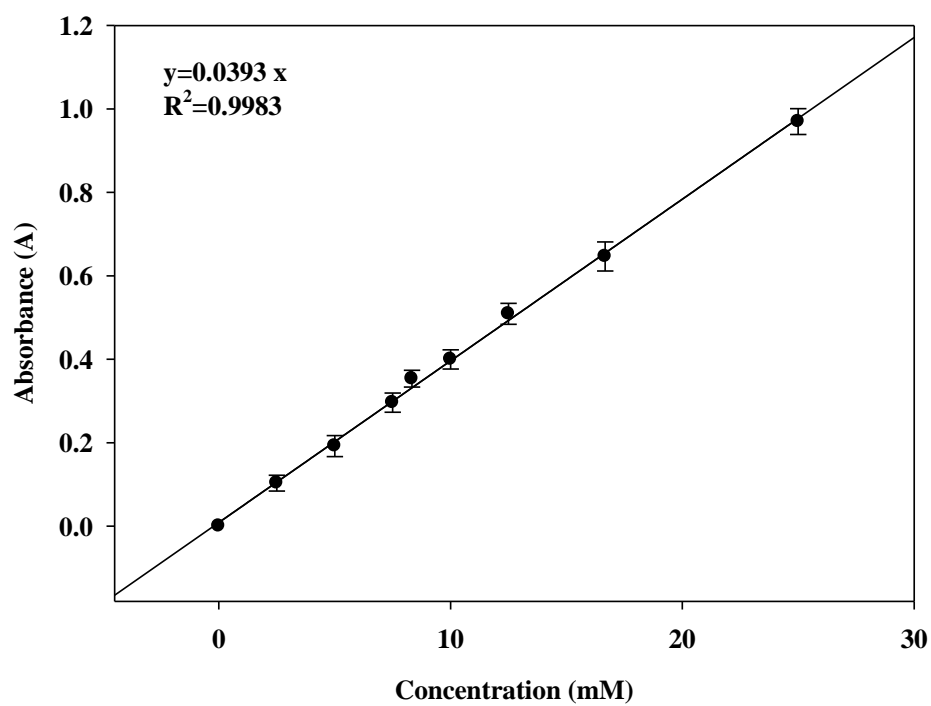


Figure A. 1. Calibration curve for H<sub>2</sub>O<sub>2</sub>

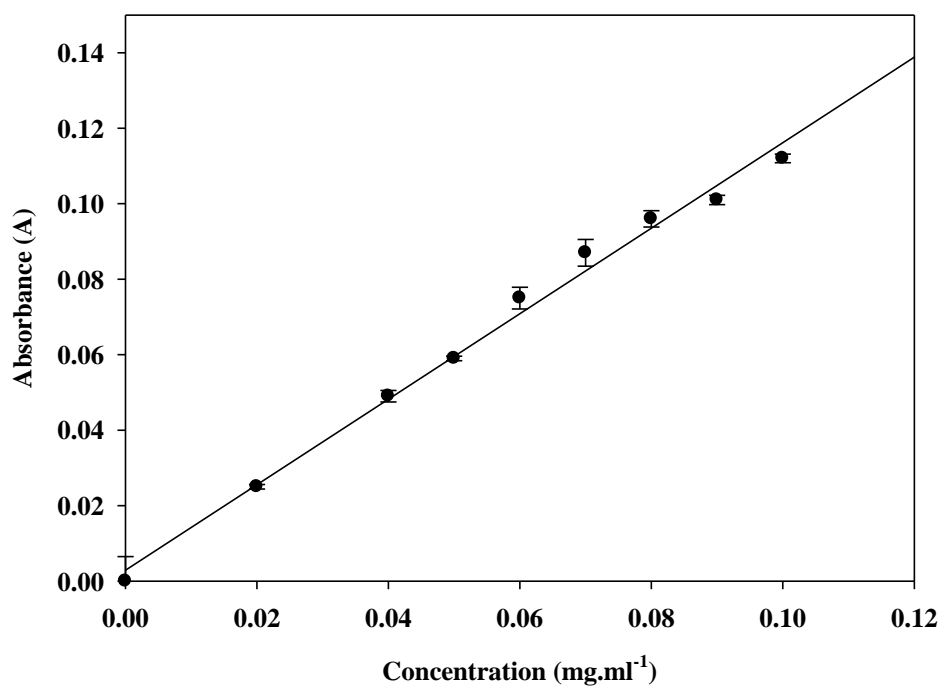


Figure A. 2. Calibration curve for ALA

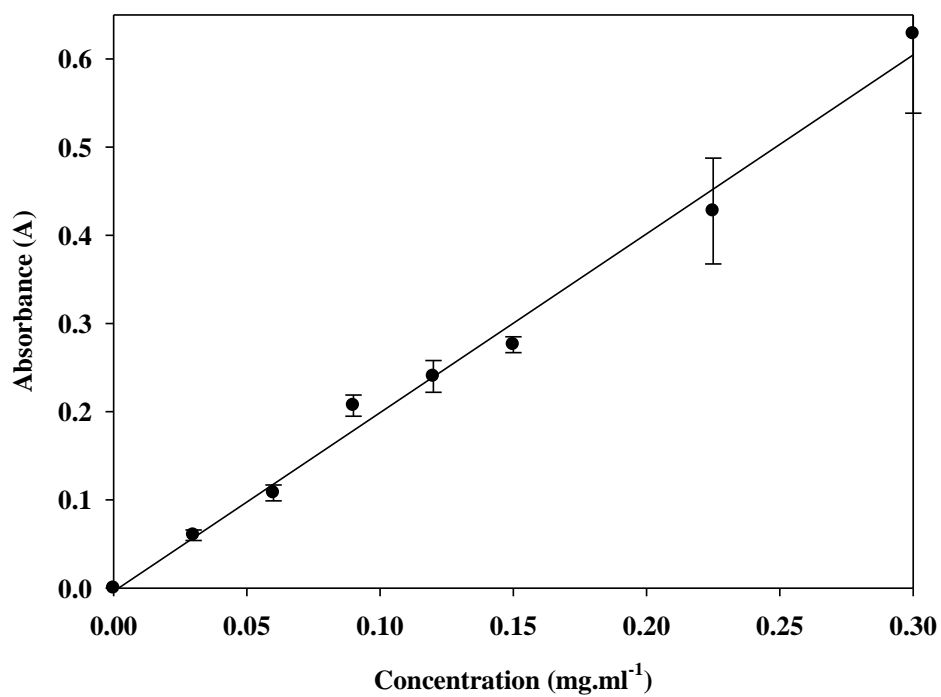


Figure A.3. Calibration curve for BSA

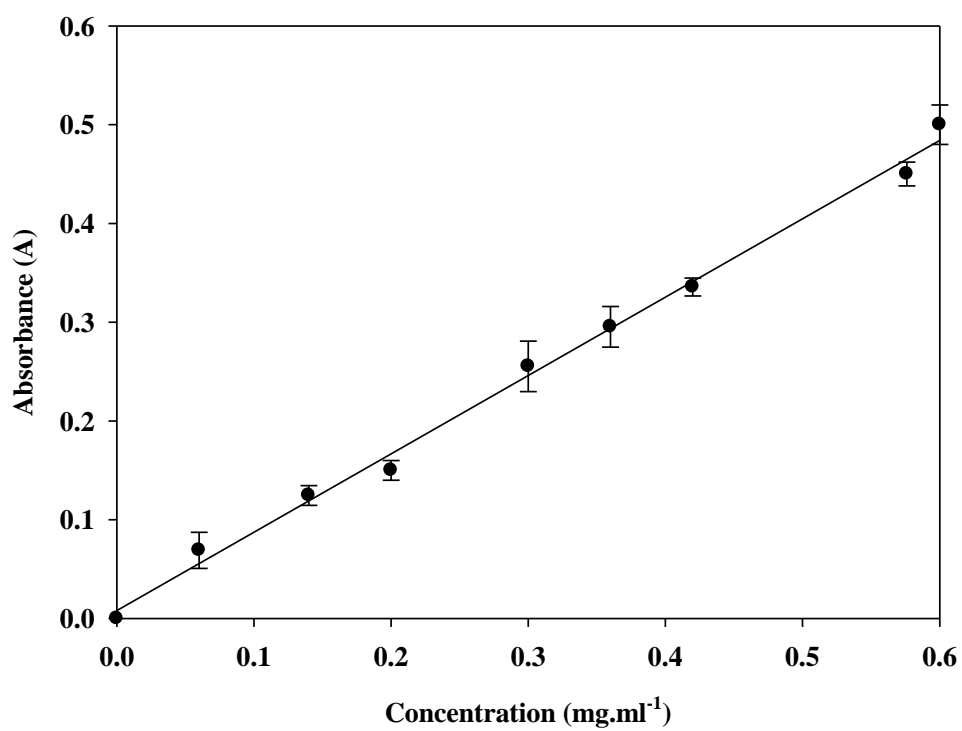


Figure A.4. Calibration curve for vitamin B<sub>12</sub>

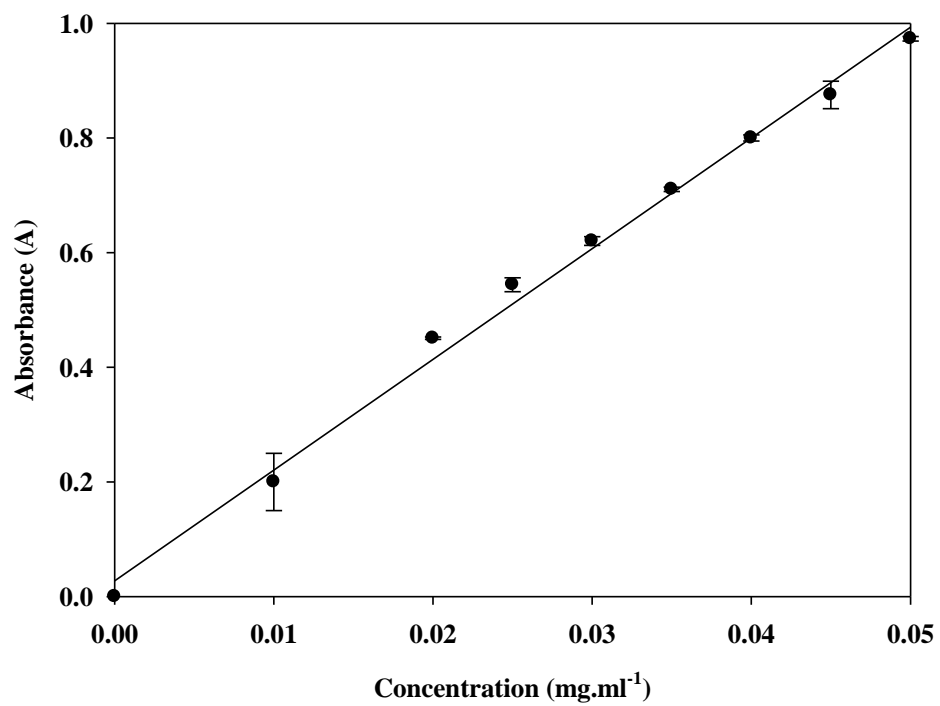


Figure A.5. Calibration curve for lysozyme

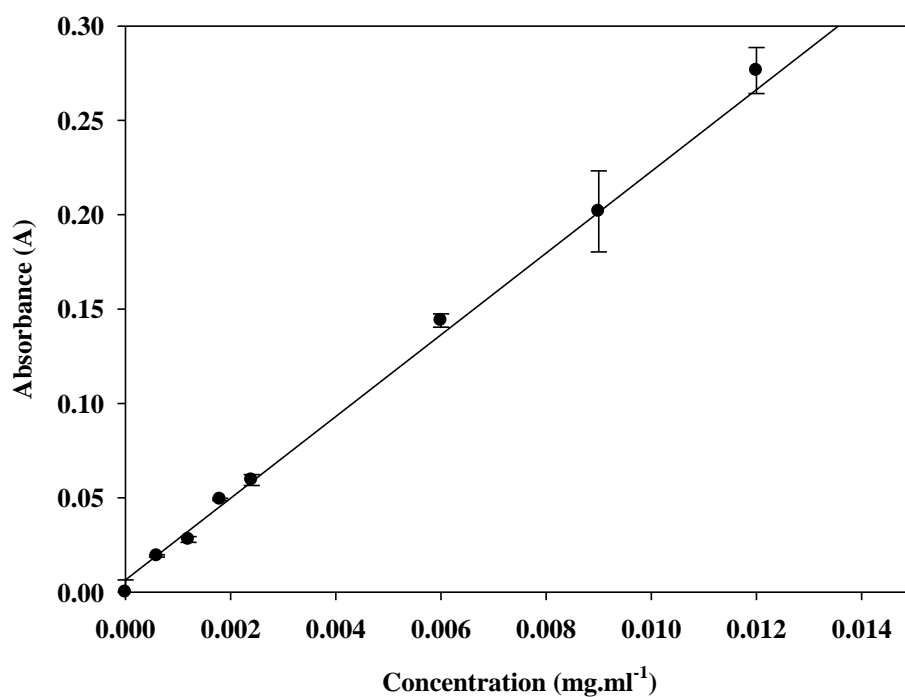


Figure A.6. Calibration curve for urea

Table A.1. Extinction coefficients of SOD and CAT

<b>Enzyme Type</b>	<b>Wavelength (nm)</b>	<b>Extinction Coefficient (mM<sup>-1</sup>.cm<sup>-1</sup>)</b>
SOD	258	12.79
	276	9.31
	407	1.84
CAT	258	166.76
	276	200.45
	407	139.41

# CURRICULUM VITAE

## 1. Education

M. Sc. (2003-2007) : Chemical Engineering, İzmir Institute of Technology, İZMİR  
Thesis Topic: “Preparation and characterization of hemodialysis membranes”

B.Sc (1998-2003) : Chemical Engineering, Hacettepe University, ANKARA

## 2. Publications

### 2.1. SCI Expanded Journal Papers

YAŞAR MAHLIÇLI F., ALSOY ALTINKAYA S. (2009). “The Effects of Urease Immobilization on the Transport Characteristics and Protein Adsorption Capacity of Cellulose Acetate Based Hemodialysis Membranes”, *Journal of Materials Science: Materials in Medicine*: 20. p. 2167-2179.

ŞAHİN E., YAŞAR MAHLIÇLI F., YETGİN S., BALKÖSE D. (2011). “Preparation and Characterization of Flexible Poly(vinyl chloride) Foam Films”, *Journal of Applied Polymer Science*: 125-2. p. 1448-1455.

YAŞAR MAHLIÇLI F., ALSOY ALTINKAYA S., YÜREKLİ Y. (2012). “Preparation and Characterization of Polyacrylonitrile Membranes Modified with Polyelectrolyte Deposition For Separating Similar Sized Proteins”, *Journal of Membrane Science*: 415–416. p. 383-390

YAŞAR MAHLIÇLI F., ALSOY ALTINKAYA S. (2012). “Surface Modification of Polysulfone Based Hemodialysis Membranes with Layer by Layer Self Assembly of Polyethyleneimine/Alginate-Heparin: A Simple Polyelectrolyte Blend Approach for Heparin Immobilization”, *Journal of Materials Science: Materials in Medicine*: doi 10.1007/s10856-012-4804-2.

### 2.2. International Conference Papers

YAŞAR MAHLIÇLI F., ALSOY ALTINKAYA S. (2009). “The Influences of the Layer by Layer Deposition of Polyethylenimine and Alginate on the Transport Rates and Hemocompatibility of PSf Membranes”, Euromembrane Conference, Montpellier, France.

YAŞAR MAHLIÇLI F., UZ M., BÜYÜKÖZ M., ALSOY ALTINKAYA S. (2011). “Asymmetric Cellulose Acetate Membranes Containing Chitosan Nanoparticles for Wound Healing”, International Congress on Membranes and Membrane Processes, University of Twente, Amsterdam, Netherlands.

YAŞAR MAHLIÇLI F., ALSOY ALTINKAYA S. (2012) “Preparation and Characterization of Polysulfone based Hemodialysis Membranes with Improved Biocompatibility Through Alpha-lipoic Acid Immobilization” Euromembrane Conference, London, UK.

YAŞAR MAHLIÇLI F., ALSOY ALTINKAYA S. (2011). “Asymmetric Cellulose Acetate Membranes Containing Silver Nanoparticles for Wound Healing”, Nanoscience& Nanotechnology Conference, Sabancı University, İstanbul, Türkiye.